# Sources and Fluxes of Water and Salt Below a Regional Groundwater Discharge Complex, South-Eastern Australia.

submitted by
Nikki Michelle Howes, B.Sc. (Hons.)

as a requirement in full for the degree of
Doctor of Philosophy
in the
School of Chemistry, Physics and Earth Sciences
Flinders University of South Australia

February 2003

# Table of Contents

## CHAPTER 5 A NUMERICAL MODEL OF GROUNDWATER FLOW BELOW A REGIONAL GROUNDWATER DISCHARGE COMPLEX 153

## CHAPTER 6 ISOTOPIC TRACERS TO CONSTRAIN THE CONCEPTUAL MODEL OF A GROUNDWATER DISCHARGE COMPLEX 185

# Abstract

Regional groundwater discharge zones accumulate large quantities of salt as hypersaline subsurface brines in arid and semi-arid environments. However, relatively little is known about the links between hydraulic and hydrochemical processes affecting water and solutes below the large complexes of playa lakes that are common throughout Australia and many other parts of the world. This thesis has investigated, using a combination of hydraulic, hydrochemical and isotopic methods, variability in hydrochemical and hydraulic processes at a range of scales ($10^{-2}$–$10^{3}$ m) in the Raak Plain groundwater discharge complex of south-eastern Australia.

The study found that subsurface brine compositions below the playas at Raak Plain are essentially evapo-concentrated versions of the seawater-like inflow, despite variations in physical playa characteristics such as size, shape, and the presence / absence of surface water bodies and salt crusts. Small differences in ionic ratios in the top 5 cm of sediment pore waters occur due to seasonal precipitation and dissolution of surface salt efflorescences, and fractionation due to different rates of diffusive transport of ions across steep concentration gradients. Chemical and isotopic data and hydraulic modelling suggest that variability in playa physical characteristics is due to different vertical hydraulic gradients across a 30 m thick aquitard separating the regional aquifer from the local dune recharge areas. This results in locally recharged groundwater either flowing directly onto the playa surface, forming surface water bodies and salt crusts, or circulating through the deeper aquifer system before being discharged. The hydraulic modelling, in particular, highlighted the delicate balance between local and regional flow systems in groundwater discharge complexes.

Despite the importance of local flow systems, and separation of the playas from the regional aquifer by a 30 m thick aquitard, $^{36}Cl$ data and playa-scale solute balances suggested that regional groundwater is still the major source of solutes to the playas at Raak Plain, with groundwater and solute residence times in the discharge complex of less than 50 k yrs, and about 2 k yrs required for accumulation of the present brines. Such short accumulation times support brine leakage by some mechanism, and increases in regional groundwater salinity below Raak Plain also appear to be due to mixing with brine. However, [$Cl^-$] vs depth profiles below the playas suggest that the subsurface brine bodies are currently confined within the top 10 m of the aquitard, and density-driven convection below the playas has been ruled out due to the strong upward hydraulic gradients there. One mechanism for brine leakage, suggested by the hydraulic modelling, is via lateral movement in the aquitard along sandy layers into the local recharge zones where downward hydraulic gradients allow advection or diffusion into the regional aquifer. Time scales for salinization by this process would be of the order of $10^3$ to $10^6$ yrs.

The possibiility of brine leakage over the history of the discharge complex, caused by ponding of water at the surfaces of playa lakes, was investigated at one of the playas currently used for salt harvesting. Here, pore water ion and stable isotope vs depth profiles indicated (1) downward displacement of the original brine body by up to 5 m over 20 years of periodically pumping regional groundwater onto the playa surface, and (2) enhanced downward diffusion of salt through the 30 m thick aquitard, with a time scale of the order of $10^4$ yrs. This has implications for long-term management of playa lakes used as evaporation basins, as well as suggesting a possible mechanism for re-distribution of salt in natural groundwater systems that alternate between aridity and higher rainfall conditions.

# Declaration

I certify that this thesis does not incorporate without acknowledgement any material previously submitted for a degree or diploma in any university; and that to the best of my knowledge and belief it does not contain any material previously published or written by another person except where due reference is made in the text.

Nikki M. Howes

# Publications Associated With This Thesis

## Conference Papers

Howes, N.M., Le Gal La Salle, C. and Herczeg, A.L., 2000, **The use of environmental tracers to determine brine leakage from natural groundwater discharge zones and artificial evaporation basins.**, *Proceedings, 4th Environmental Engineering Research Event, Victor Harbor, South Australia, November 21-24, 2000.*

Howes, N.M., Le Gal La Salle, C. and Herczeg, A.L., 2001, **Evidence for brine circulation in a groundwater discharge zone.**, *Proceedings, Water-Rock Interaction 2001, Sardinia, Italy, June 10-15, 2001*, Swets and Zeitlinger, Lisse, Netherlands.

Howes, N.M., Le Gal La Salle, C. and Herczeg, A.L., 2001, **Evidence for brine leakage from a groundwater discharge zone, Raak Plains, Victoria.**, 8th Murray Darling Basin Groundwater Workshop, Victor Harbor, SA, September 2001.

# Acknowledgements

The research described in this thesis was carried out collaboratively through the Centre for Groundwater Studies, between the Flinders University of South Australia and CSIRO Land and Water, Adelaide. I would like to thank my supervisors Dr Andrew Herczeg (CSIRO) and Dr Corinne Le Gal La Salle (Flinders) for their continual support, patience, inspiration and technical advice. Thanks also to Andrew and Corinne for the many hours spent reading the chapters of this thesis and the invaluable suggestions for their improvement. I would also like to thank Dr Craig Simmons (Flinders) for his advice and discussions on the hydraulic aspects of the project, as well as for his words of encouragement along the way.

Thanks to John Dighton (CSIRO) for his hard work, support and technical advice in both the field and laboratory, to Leslie McCluskey, Glenn Harrington, Andrew Holub and Martin Wood for their assistance in the field and Megan Lefournour (CSIRO) for her advice to and patience with the numerous students in the laboratory. Thanks to Glenn Harrington (DWLBC) for proofreading chapters and providing useful feedback, and to Andrew Love (DWLBC) for his understanding as I combined finishing a thesis with a new job.

I gratefully acknowledge the financial support of an Australian Postgraduate Award, provided by the Flinders University of South Australia and a supplementary stipend from the Centre for Groundwater Studies. Thanks also to the Centre for Groundwater Studies for assistance with travel costs to attend the 10th International Symposium on Water-Rock Interaction in Villasimius, Italy.

Finally, thanks to my parents Sue and Fred, sister Sally and all those close to me for their encouragement and constant support throughout my studies.

# Chapter 1 Introduction

## 1.1 Scope and Objectives of Thesis

Salinization of surface and groundwater is an increasing problem in arid and semi-arid parts of the world. An increasing population, and the associated expansion of agriculture and industry into arid and semi-arid areas, has placed huge demands on water resources. Schemes that divert water to regions previously adapted to very dry conditions are becoming more and more common, and such interference in these delicate hydrological balances has, in many cases, had disastrous consequences (e.g. Hillel, 1991; Williams, 2001; Vengosh, 2002). For example, rising water tables caused by intensive irrigation and clearing of native vegetation can mobilize salt previously stored in unsaturated zones over many thousands of years, leading to surface and groundwater salinization, and land and infrastructure degradation (Allison et al., 1990).

Salt lakes and playa lakes (a type of dry or episodically filled salt lake) in arid and semi-arid regions can be points of regional evaporative discharge of groundwater and/or surface water. By evapo-concentration of their inflow waters, they also accumulate large quantities of salt in the form of surface and subsurface brines and evaporite mineral deposits. The hypersaline brines can then sink into the underlying sediments, to be stored there or released into the underlying groundwater system, with the potential to further salinize the aquifer (Teller et al., 1982; Duffy and Al-Hassan, 1988; Fan et al., 1997; Wooding et al., 1997 (a&b)). The predominantly groundwater-fed playa lakes (groundwater discharge zones) (Fig. 1.1) are surface expressions of highly saline groundwater systems. Here, water tables are very close

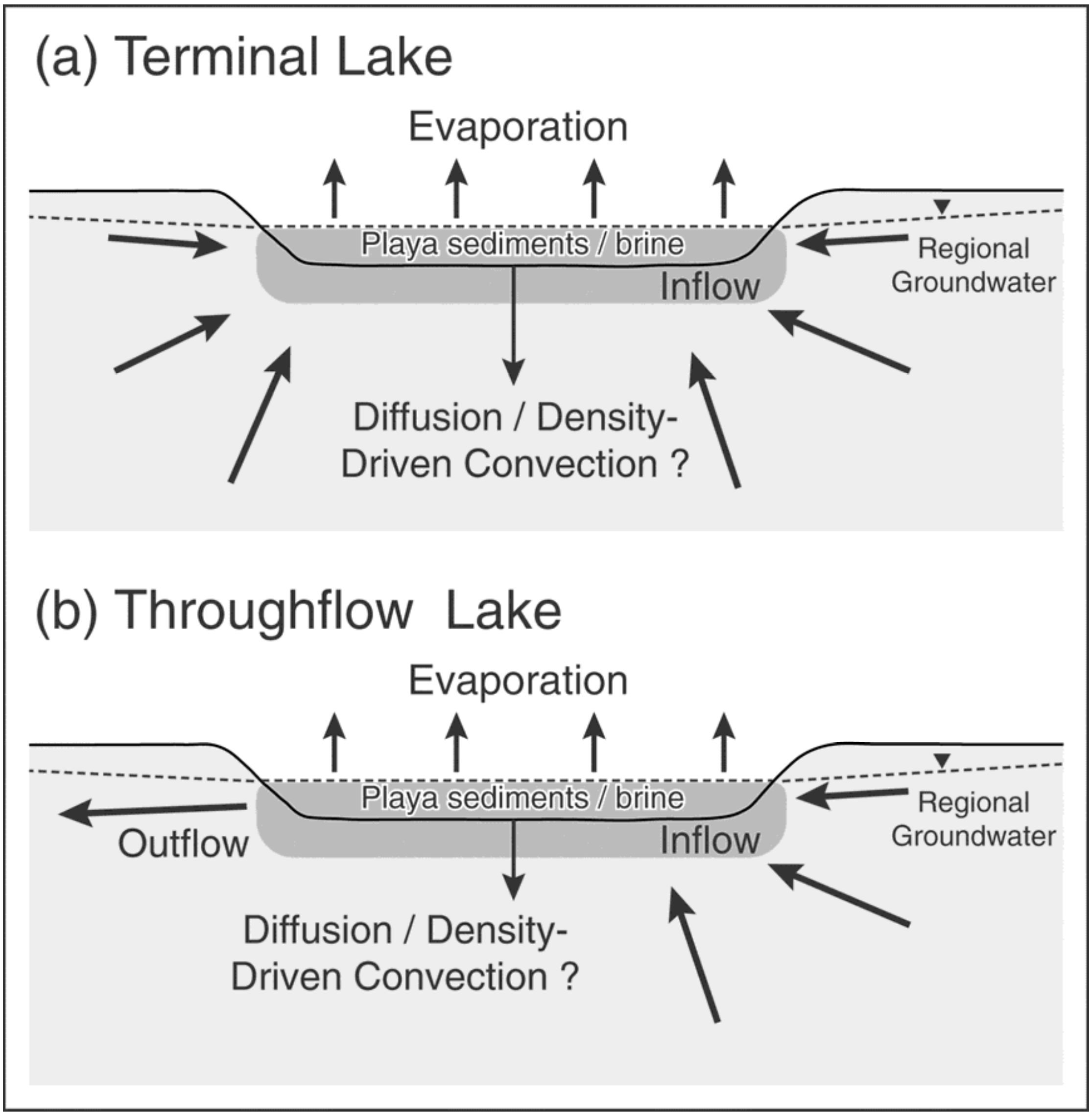

Figure 1.1. Conceptual models of the interactions between groundwater-fed playa lakes (groundwater discharge zones) and the regional groundwater system that feeds them for (a) a terminal lake and (b) a throughflow lake. In both cases, inflowing groundwater is evaporated from a shallow water table under arid and semi-arid conditions. The remaining solutes form a hypersaline subsurface brine that can either remain in the sediments below the playa or leak back into the regional groundwater system via mechanisms such as diffusion, advection (in the case of throughflow lakes) or density-driven convection.

to the surface, typically within about 500 mm, due to either geological constraints or topographic low-points in the landscape. High potential evaporation rates cause groundwater to be evaporated through the thin unsaturated zone, forming the highly saline brines beneath the surface (Fig. 1.1) (Jones et al., 1969). The high salinities of these brines (up to 350 g/L) prohibit the growth of even the most halophytic vegetation, resulting in a bare depression, or "playa".

Current and fossil salt and playa lakes have been studied for decades because of the roles they play in regional salt and water balances of semi-arid and arid areas, as well as the palaeohydrologic information recorded in their evaporite deposits and shoreline features (e.g. Bowler, 1986; Dutkiewicz et al., 2000; Yechiechi and Wood, 2002). They are also important sources of commercially valuable evaporite minerals, leading to extensive interest in the geochemistry and evolution of their brines. The wide ranges in brine salinity and chemistry observed in salt lake environments are strongly related to the hydraulic processes occurring there and, hence, an understanding of these processes is required to understand their hydrochemistry and evaporite mineralogy (Macumber, 1992).

Much of the current understanding of salt lakes is based on studies of large (>100 $km^2$), single-lake systems, including examples such as Lake Frome in the southeast of South Australia (Bowler, 1986) and Mono Lake in the USA (Rogers and Dreiss, 1995 (a&b); Phillips et al., 1995). However, complex systems of small (<100 $km^2$), groundwater-fed playa lakes (groundwater discharge complexes) are also common throughout the world. The degree to which knowledge gained from studies of large salt lakes is applicable to these systems is unclear (Fig. 1.2). In groundwater discharge complexes, the sizes of individual playas, their relative locations, and the presence of recharge (i.e. non-discharge) zones between them may govern their interactions with the underlying groundwater system, as well as influencing the geochemical evolution of their brines. For example, if their chemical compositions are sufficiently different, the relative contributions of regional and locally recharged groundwater sources may determine the chemical evolution of the brines. The magnitudes of these contributions at a particular location in a playa lake may be influenced by the size of the playa, i.e. the proximity of the point to a recharge zone (Fig. 1.3). The location of a playa lake may be important in large groundwater discharge complexes due to variations in the depth to the water table and the resulting differences in the degree of evapo-concentration undergone by the groundwater brine (Fig. 1.3). The presence or absence of an aquitard between the playa lakes and the regional aquifer is also known to be important, controlling brine leakage and inflow from regional groundwater (Chambers et al., 1995) (Fig. 1.3).

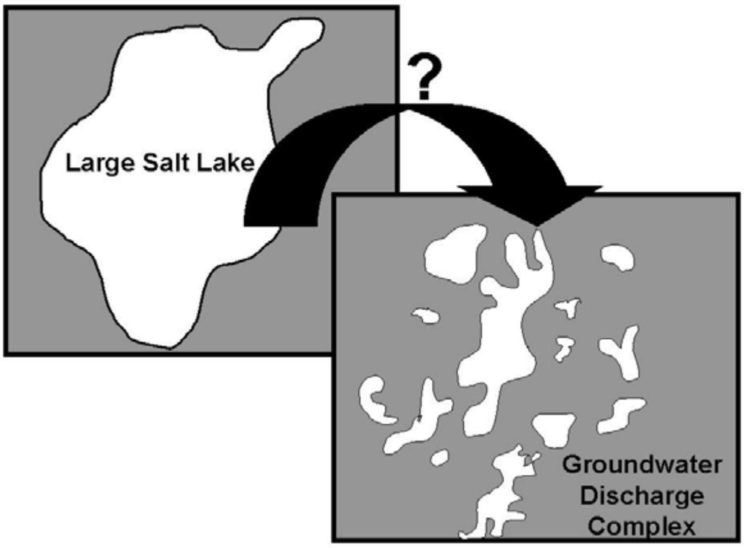

Figure 1.2. Can our understanding of large salt lakes be applied to systems of many small groundwater-fed playa lakes?

In addition to focusing on single large lakes, the majority of studies of salt lake brine hydrochemistry have focused on salt lakes with well-defined surface-water inputs, where the input composition is quite different from that of the resulting brine. Only a few studies, for example of Lake Tyrrell in the central Murray Basin of south-

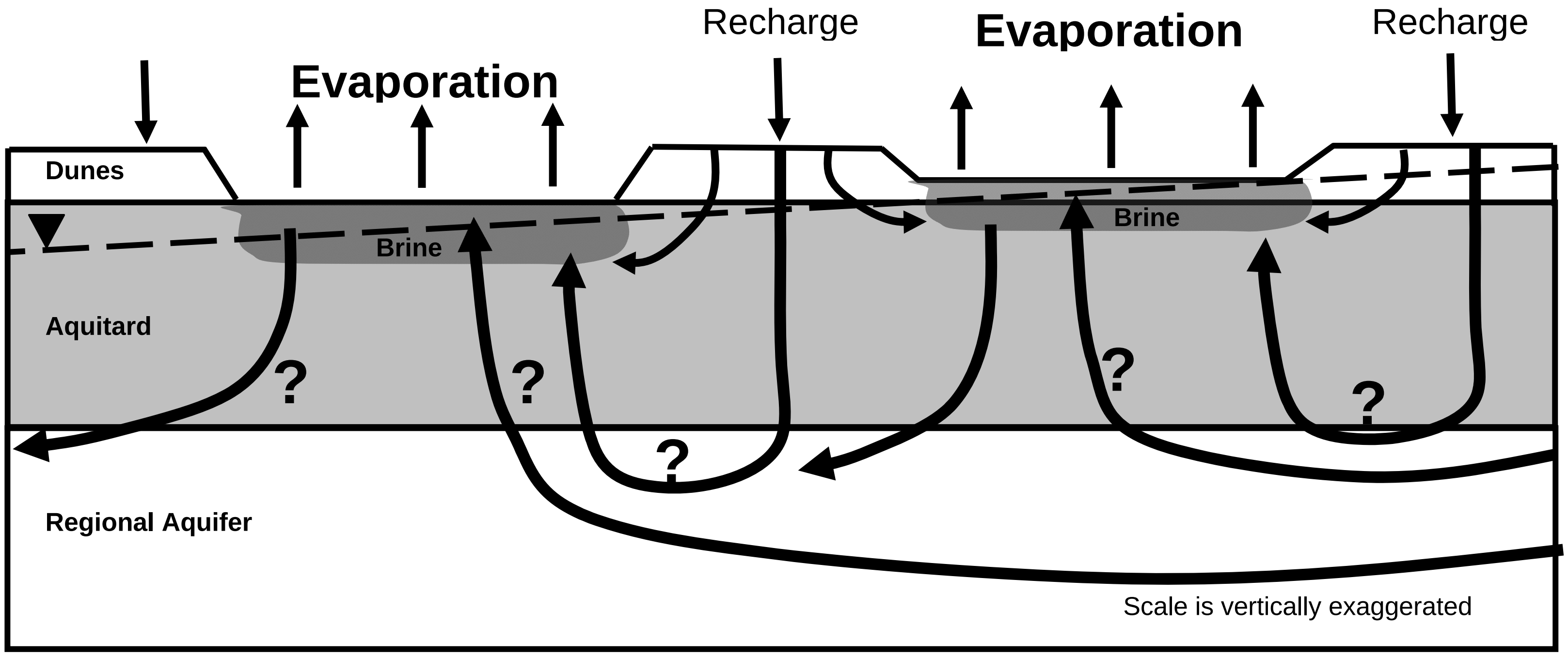

Figure 1.3. Conceptual model of potential groundwater flow patterns below a system of multiple playa lakes separated by areas of net recharge, and underlain by a clay aquitard. The potentiometric surface shown (dashed line) is that of the regional aquifer. Net evaporation of groundwater from the shallow water table forms a hypersaline subsurface brine body below the playa lakes. However, this evaporation rate may vary between playas in large groundwater discharge complexes due to a gradient in the regional potentiometric surface and resulting variations in the depth to groundwater. The water that evaporates may be regional groundwater, locally recharged groundwater, or a mixture of both sources, with the contribution from regional groundwater influenced by the properties of the aquitard (if present) separating the playa lakes from the regional aquifer. The properties of such an aquitard will also control leakage of brine back into the regional aquifer. In large playa lakes, the influence of locally recharged groundwater may vary from the edge to the centre of the playa.

eastern Australia (Herczeg and Lyons, 1991; Macumber, 1992; Herczeg et al., 1992; Hines et al., 1992), the Amadeus Basin in central Australia (Jacobson and Janowski, 1989), Lake Frome in the southeast of South Australia (Draper and Jensen, 1976) and Mono Lake in the USA (Connell and Dreiss, 1995), exist in the literature of brine evolution in predominantly groundwater-fed lakes. These, once again, have focused on single large playas or, at most, the interaction between two playas in a chain of lakes.

Naturally occurring salt lakes can be indicators of the potential long-term effects of salinized land and artificial evaporation basins (Herczeg et al., 1992). In addition to this, they themselves are delicately balanced systems and the imposition of operations, such as salt disposal and salt harvesting, that cause even small changes to their hydrologic balances, may de-stabilize the brine bodies and increase brine leakage (Barnes et al., 1990). These practices, which involve ponding of groundwater at the surface, a step increase in lake level, are becoming increasingly common. In some cases, a substantial aquitard is present, providing the perception that the hypersaline brines are prevented from re-entering the regional aquifer system. However, little observational data are available to confirm this and, in particular, the presence of preferred flow-paths in these aquitards may allow brine migration over greater distances than expected. The long-term impacts of human intervention are difficult to predict when the interactions between playa lakes in their natural states and regional groundwater systems are still not well understood.

The objectives of this thesis are therefore to:

1) Determine the factors influencing the late-stage chemical evolution of the subsurface brines and the resulting evaporite mineral suites in a groundwater

discharge complex. These factors may include (i) the chemical composition (and hence source) of inflow (Hardie and Eugster, 1970), (ii) the properties of the underlying sediments (e.g. the presence / absence of an aquitard) (Chambers et al., 1995; Wood and Sanford, 1990), (iii) playa lake size, (iv) depth to the water table and (v) mineral-solution reactions (Eugster and Hardie, 1978; Eugster and Jones, 1979).

2) Develop a conceptual model for groundwater flow and solute transport below a natural groundwater discharge complex, where a large number of small playa lakes are separated from each other by areas of net recharge and from the regional aquifer by a thick aquitard;

3) Develop a methodology for delineating groundwater flow patterns and identifying brine leakage below groundwater discharge complexes.

4) Determine the impact of increased lake levels (e.g. due to salt disposal or salt harvesting) on brine leakage below natural playa lakes underlain by a clay aquitard.

## 1.2 Methodology

The Raak Plain groundwater discharge complex, located in the central Murray Basin of south-eastern Australia, was selected as the study site for this investigation, due to the fact that it contains a large number (> 50) of small (< 100 km$^2$) playa lakes. Being located at the centre of a large regional groundwater basin, it is also believed to discharge saline (Total Dissolved Solids > 30 g/L) regional groundwater through a 30 m thick clay aquitard. This study adopts a combined approach, using present hydraulic data (water levels and aquifer properties) that give a snapshot of the hydraulic processes currently operating below the discharge complex, and environmental tracers that integrate processes over long time scales. Data collection and interpretation at both the individual playa and discharge complex scales allows assessment of the spatial variability in processes at both these scales. A suite of chemical and isotopic tracers, including major ion chemistry, $^{2}H/^{1}H$ and $^{18}O/^{16}O$, $^{13}C/^{12}C$ and $^{14}C$, and $^{36}Cl$, is utilized to better constrain the large range of hydrochemical and physical processes potentially occurring in the groundwater discharge complex. One particular issue in evaporitic environments is de-coupling between the solute and water systems during the evaporation process, which removes water and leaves solutes behind. In this situation, ionic species can be used as tracers of the solutes, whereas the stable isotopes of water, $^{18}O/^{16}O$ and $^{2}H/^{1}H$, are ideal tracers of the water molecule. The radioactive tracers, $^{36}Cl$ and $^{14}C$ are used to determine the time scales of solute transport below the discharge complex.

## 1.3 Site Description

### 1.3.1 The Murray Basin, South-Eastern Australia

The hydrological balance of the Murray Basin of south-eastern Australia (Fig. 1.4) has been modulated over the last several hundred thousand years by alternating periods of wet (high groundwater levels) and semi-arid to arid (low groundwater levels) climatic conditions (Bowler and Wasson, 1984). At present, the climate in the Basin is semi-arid (rainfall ~ 300 mm/y and potential evapotranspiration ~ 2000 mm/y), and the shallow aquifer system in many parts is saline. The most saline groundwaters occur at the centre of the Basin, where they are discharged either via the River Murray or by evaporation from shallow water tables in groundwater discharge complexes (Brown, 1989; Evans and Kellett, 1989). In the latter case, the residual salts form hypersaline groundwater brines (> 250 g/L). Today, there are many active and "fossil" (currently inactive) groundwater discharge complexes, with associated brine bodies, scattered throughout the centre of the Murray Basin.

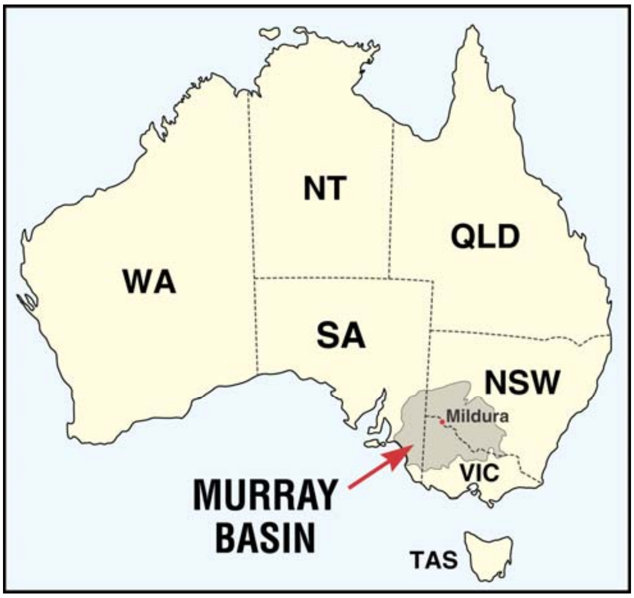

Figure 1.4. Locality map of the Murray Basin in south-eastern Australia.

Rising water tables, caused by clearance of native vegetation, are now bringing saline groundwater to the surface, degrading agricultural land and increasing the rate of discharge of saline groundwater to the River Murray. To alleviate the problem, a number of groundwater interception schemes currently divert saline groundwater to natural playa lakes or man-made basins. These are used as evaporation basins for the storage of saline brines, or for removal of water for salt harvesting. Many of the natural playa lakes are underlain by clay aquitards, making them attractive sites for such operations.

### 1.3.2 The Raak Plain Groundwater Discharge Complex

The Raak Plain groundwater discharge complex is located in the central Murray Basin, in the Mallee region of western Victoria (Figs. 1.5 and 1.6). It is the largest

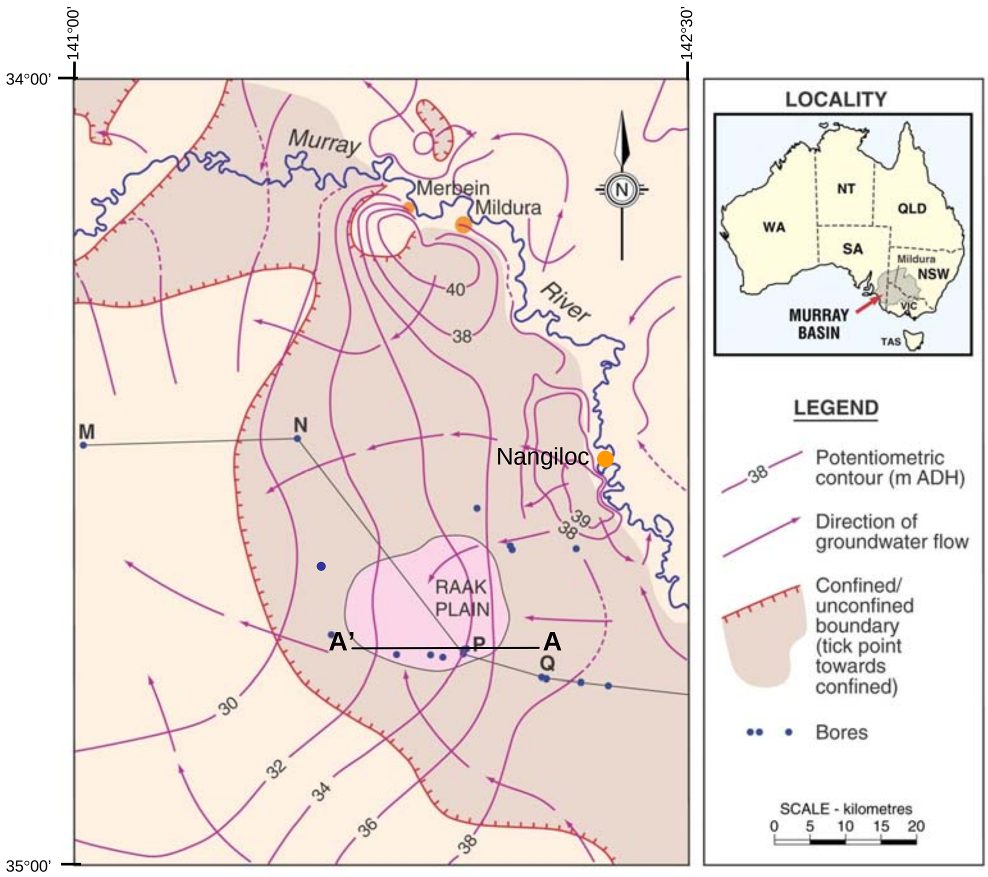

Figure 1.5. Hydrogeological map of Raak Plain and surrounds, showing the extent of the confining Blanchetown Clay aquitard, potentiometric contours for and locations of bores in the Parilla Sand aquifer (after Rural Water Commission, 1991). Cross section MNPQ is discussed in Section 1.2.3 in terms of the regional geology and hydrogeology. Transect AA' is the cross-section along which this study is focused.

groundwater discharge complex in the Murray Basin, covering an area of approximately 400 km$^2$, and containing more than 50 small playa lakes (Fig. 1.6). Varying physical characteristics of the playa lakes (size, shape, presence/absence of surface water) were expected to cause differences in brine evolution, and in turn evaporite mineralogy, supported by the fact that some playas contain a surface salt crust whilst others do not. The playa lakes are also separated from the regional aquifer by the 30 m thick Blanchetown Clay aquitard. It was anticipated that this would greatly affect groundwater and solute movement below the discharge complex, and allow extension of previous work on playa lakes and man-made

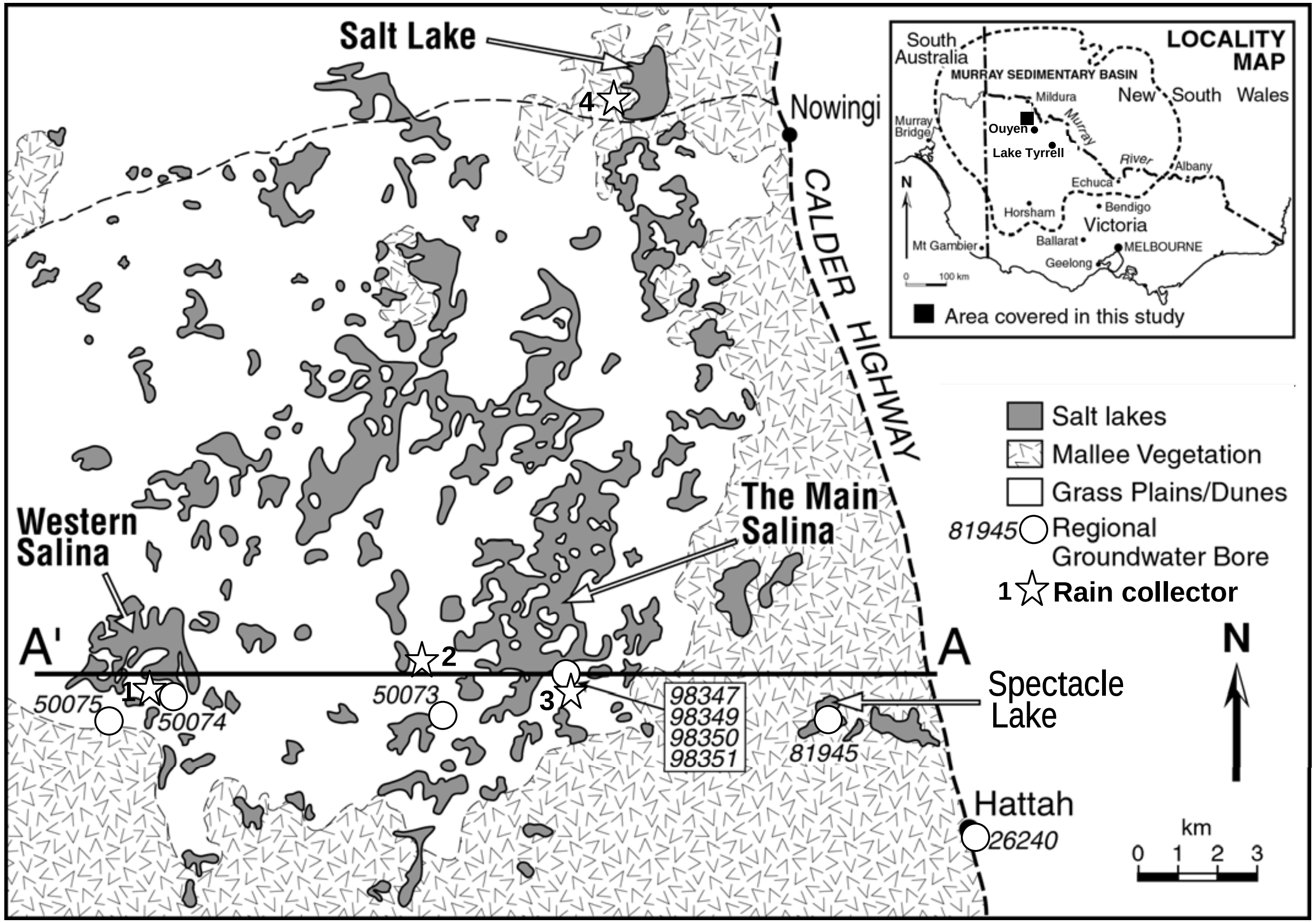

Figure 1.6. Site map of the Raak Plain groundwater discharge complex, showing locations of the playa lakes that are the focus of this study, the bores screened in the Parilla Sand aquifer and transect AA' along which the study is also focused. The regional groundwater flow direction is approximately from east to west. Bulk rainfall / dry deposition collector sites are also shown as stars with site numbers (i.e. 1 = Rain1).

evaporation basins that are in direct connection with the regional aquifer (e.g. Jacobson and Jankowski, 1989; Macumber, 1992; Herczeg et al., 1992; Connell and Dreiss, 1995; Simmons and Narayan, 1998).

The Victorian Mallee region, in which Raak Plain is located, is characterised by a predominantly flat landscape, overlain by systems of transverse dunes. These dunes, which separate the playa lakes at Raak Plain, are usually densely vegetated with mallee, a collective term for the shrubby trees and low-lying scrub or heath that exists mainly in low rainfall areas (250 – 450 mm/y) (Walker et al., 1992). Mallee trees have slender trunks stemming from a single lignotuber just below the surface and are well known for their efficient use of water leading to low recharge rates (Cook et al., 1996; Walker et al., 1992). The landscape of the groundwater discharge complex, consisting of playas intermingled with sand plains, samphire-vegetated gypsum flats and bordering dunes, was described by Macumber (1983, 1991) as a single landform, the “boinka”.

The boundary of the Raak Boinka, with its sparsely vegetated floor approximately 15 to 20 m below the surrounding Mallee dunefields, can be easily identified from aerial photos. The lake-bed elevations are approximately 32 to 34 m AHD, with the surrounding plains and dunes ranging between 35 and 55 m AHD (Sheet 7328 (Edition 1), 1977, National Topographic Map Series). A network of interconnected salinas forms the Main Raak salina in the eastern half of Raak Plain, as described by Macumber (1991) and referred to as the Main Salina in this study (Fig. 1.6). One of the smaller salinas (Spectacle Lake), at the eastern boundary of the boinka, supports a commercial salt harvesting operation. The salinas are active groundwater discharge zones, with brines just beneath the surface reaching chloride concentrations of up to 200 g/L (Howes, 1998). There are no surface water inflows to the playa lakes, although the water table is near or above the playa surfaces. The only input of water is from groundwater in-flow, direct rainfall and some minor runoff from their immediate surroundings (Macumber, 1991). A slight east-west gradient in water table elevation reflects the regional groundwater hydraulic gradient of approximately $1{:}10^4$ in the underlying Parilla Sand aquifer.

Land use in the eastern three quarters of Raak Plain consists mainly of dryland agriculture and light grazing, with the western quarter forming part of the Murray Sunset National Park. Although anecdotal evidence suggests that Raak Plain was never cleared of native vegetation, there is evidence of rising water tables from land clearing and increased irrigation in surrounding areas. Salinized land, identified by changing vegetation from grasses to salt-tolerant samphire vegetation, can be seen encroaching on roads and fencelines.

The climate in the central Murray Basin is semi-arid (Macumber, 1991), with potential evaporation exceeding rainfall by roughly an order of magnitude (the mean annual precipitation is 250 - 350 mm/y compared with a mean annual potential evaporation of around 2000 mm/y (Allison et al., 1988)). Long-term average rainfall data for stations at Ouyen (approximately 30 km south of Raak Plain) and Mildura (approximately 60 km north) is available from the Bureau of Meteorology website, (Bureau of Meteorology, Australia, 2002). Rainfall in the Mallee is scattered throughout the year, but is mostly concentrated in the period between May and September (winter). Graphs of average monthly rainfall and number of raindays are included as Appendix A (Bureau of Meteorology, Australia, 2002). The mean annual rainfall is 290 mm at Mildura and 335 mm at Ouyen. Raak Plain lies between these two stations and the mean at this location is therefore expected to be approximately 300 mm/y. Rainfall is fairly evenly distributed throughout the year, with most monthly averages being greater than 20 mm (Appendix A). The driest months are March and April and the wettest month is October.

### 1.3.3 Geology and Hydrogeology

The 3 x $10^5$ $km^2$ Murray Basin, part of the larger Murray-Darling Basin, is a low-lying, saucer-shaped basin with a surface drainage system consisting solely of the River Murray and its tributaries. Groundwater flows from up-basin recharge areas to zones of groundwater discharge (playa lakes) in the semi-arid centre, and ultimately to the River Murray. The basin consists of up to 600 m of unconsolidated Cainozoic sedimentary rocks that are the result of successive marine transgressions in the Oligocene – Early Miocene and Late Miocene – Early Pliocene times. These form at least four major regional aquifer systems – the Renmark Group, Murray Group and Pliocene Sands aquifer systems and the Shepparton Formation partial aquifer system (Brown and Radke, 1989; Lawrence, 1975) (Fig. 1.7). In the western half of the Murray Basin, in the vicinity of Raak Plain, the Renmark Group is overlain by the Murray Group, which includes the Duddo or Murray Group Limestone. This is up to 130 m thick and is overlain by the Bookpurnong Beds, a clay layer up to 100 m thick deposited during a marine transgression (Macumber, 1991, 1992).

The Parilla Sands Aquifer (also known as the Loxton or Pliocene Sands Aquifer in South Australia) is the main unconfined to semi-confined aquifer over the western part of the Murray Basin. It is a 60-70 m thick layer of unconsolidated to partially consolidated sands and is semi-confined when overlain by thicker deposits of the Plio-Pleistocene Blanchetown Clay, a sequence of gypsiferous clays, silts and minor fine sands (Macumber, 1992; Allison et al., 1985; Rogers, 1995). Aeolian reworking of the Parilla Sands and Blanchetown Clay has caused the linear dunefields (Woorinen Formation) that cover much of the Mallee (Macumber, 1992). At the top of the profile are the playa deposits (Yamba Formation), consisting of lacustrine gypsiferous clay and gypsum-quartz sand mixtures, associated with gypsiferous dunes, in the bed of the former Lake Bungunnia, the inland lake that once covered the central mallee region (Rogers, 1995).

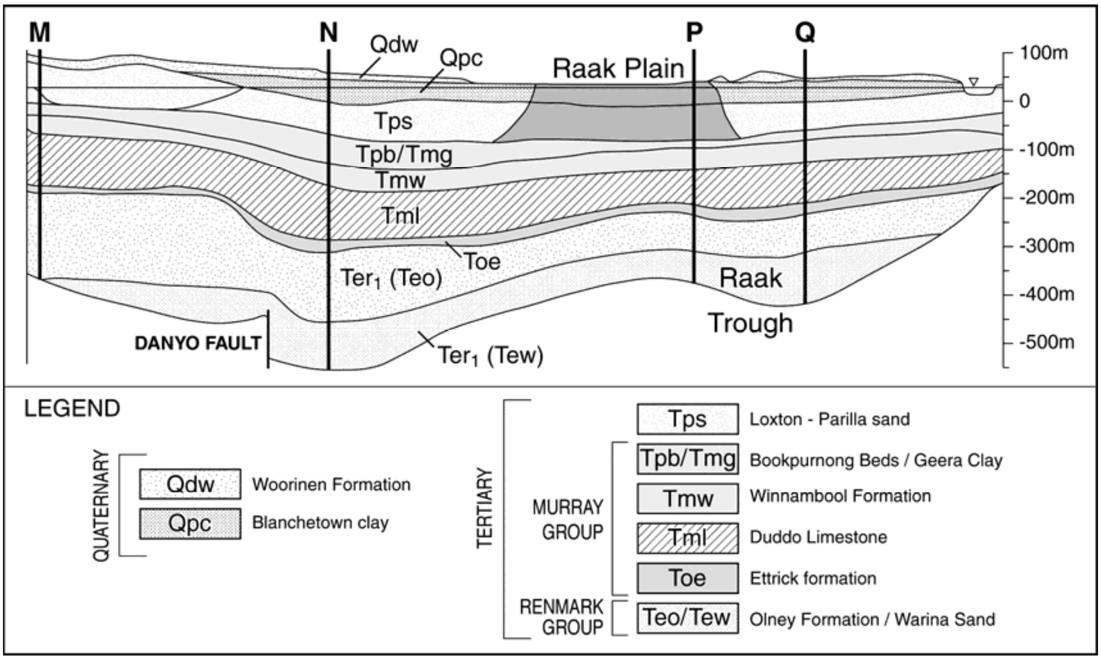

Figure 1.7. Cross section showing the three main aquifer systems in the vicinity of Raak Plain, the Renmark Group, Murray Group and Parilla Sand aquifer systems (after Rural Water Commission, 1991). The location of transect MNPQ is shown on Figure 1.5.

The groundwaters of the central Murray Basin contain dissolved solutes that are of predominantly oceanic origin. Marine aerosols deposited at the land surface on a basin-wide scale are recharged predominantly by winter rains (Jones et al., 1994; Herczeg et al., 2001). Hence, groundwater compositions are remarkably similar to that of seawater, with only slightly higher calcium, bicarbonate, sulphate and silica concentrations, and slightly lower potassium due to mineral-solution reactions during its evolution (Macumber, 1991). The hydrochemically well-evolved nature of these groundwaters (Herczeg et al., 2001) provides the opportunity to study the late-stage hydrochemical evolution of brines as they become evapo-concentrated in playa lakes.

Groundwater flow in the Parilla Sand, as well as the underlying units, in the vicinity of Raak Plain is from east to west. However, as the discharge complex is a groundwater sink, the local flow system in the Parilla Sands aquifer may be directed radially inward towards it (see Fig. 1.5). Very little potentiometric data is available in this region to confirm this. Values for hydraulic conductivity (2 m/day), hydraulic gradient (0.2 m/km to 0.3 m/km) and groundwater flow velocity (0.001 m/day to 0.005 m/day) in the Parillla Sand aquifer below the Mallee region are given by Macumber (1991). The groundwater discharge status of Raak Plain can be seen in the standing water levels of the bores screened in the Parilla Sand aquifer, which are up to 2 m above the playa floors. Hence, the Parilla Sand aquifer is believed to be a major source of salt and water to the playa lakes of Raak Plain.

### 1.3.4 Previous Investigations at Raak Plain

Macumber (1991, 1992) conducted a study of surface water/groundwater interactions in northern Victoria, and included Raak Plain as a study site. He observed that the salinas are occasionally covered by a shallow sheet of water in winter, but dry out in the warmer months, and follow a seasonal cycle of halite dissolution and re-precipitation. He also proposed that each salina may be categorized as either halite producers, with a high Cl/Br ratios when wet, or as through-flushing systems, with lower Cl/Br ratios. By comparing the hydrochemistries of some of the lakes of the Raak boinka he also suggested that the lake waters are simply concentrated versions of the regional groundwater, and that the groundwater brines and their parent lake waters have compositions pre-determined by the composition of this source. He noted that, although the shallow groundwaters beneath the salina floor are close to halite saturation, very few salinas are halite producers, indicating that just the presence of the shallow brine is not sufficient to produce a halite evaporite body at the surface.

### 1.3.5 Characteristics of the Playa Lakes Selected for This Study

Locations of the playas included in this study are represented in Table 1.1 by their distances from the eastern margin of the discharge complex (designated here as the Calder Highway), approximately along the regional groundwater flow path (transect AA'; Fig. 1.6). They cover a range of sizes ($10^4$ $m^2$ to $10^7$ $m^2$) and locations, and include some that contain a surface water body and salt crust, as well as dry salt pans (Table 1.1). Spectacle Lake was chosen because it now acts as a series of evaporation ponds for a salt harvesting operation, and is an example where the hydraulic balance of the lake has been altered by the ponding of groundwater pumped onto the playa surface from the Parilla Sand aquifer.

The shallow (< 3 m deep) sedimentary sequences in the lakes at Raak Plain generally comprise a 20 to 50 cm layer of chocolate-brown silty fine sand (the Yamba Formation playa sediments) (Appendix B). This may be covered by a surface salt crust or thin algal mat, depending on the conditions in the lake. Algae can grow on the playa floors in winter, when long periods of rain maintain temporary pools of comparatively fresh water in the lower-lying parts of the lakes. The compositions of the playa sediments vary slightly between playas, but are generally dominated by fine quartz sand, with some kaolinite, muscovite and potassium- and sodium-feldspar (see Appendix B).

Table 1.1 Summary of general lake characteristics. Water table information is from piezometers installed in playa sediments. Maximum chloride concentration of the brine is from pore water extracted from shallow playa sediments.

| | WESTERN SALINA | | MAIN SALINA | | SALT LAKE | SPECTACLE LAKE (HARVESTED) | |
|---|---|---|---|---|---|---|---|
| Approximate Area (km$^2$) | 4 | | 15 | | 1.1 | 0.4 | |
| Shape | Irregular | | Irregular | | Sub-rounded | Sub-rounded | |
| Distance From Eastern Margin (km) | 17 | | 8.5 | | 2.5 (located in the north of the discharge zone) | 2.2 | |
| Surface Water Catchment | Lake surface. Some sand dunes on western margin. Poorly vegetated. | | Lake surface. Some sand dunes scattered around margin. Poorly vegetated. | | 50-100 m beyond lake margin. Well-vegetated (mallee & sheoak) sand dunes on all sides. | 50-100 m beyond lake margin. Well-vegetated (mallee) sand dunes on all sides. | |
| Salt Crust? | No | | No | | Yes – dissolves in winter | Yes, controlled. | |
| Surface Water? | Rare - only after heavy rain | | Rare - only after heavy rain | | Yes - up to 15 cm deep | Controlled application. Pumped from Parilla Sand aquifer. | |
| Site Name | West1 | West2 | Main1 | Main2 | Salt1 | SM5 | SM1 |
| Approximate Distance From Shore (m) | 100 | 20 | 100 | 20 | 50 | 50 | 5 |
| Sample Depth (m below ground) | 1.2 | 1.25 | 1.95 | 0.5 | 0.5 | | 1.7 |
| Lake Floor Elevation (m AHD) | 32.1 | 32.2 | 32.5 | 32.5 | na | na | na |
| Hydraulic Head (m AHD) | 31.6 to 32.3 | 31.9 to 32.5 | 32.6 to 32.9 | 32.2 to 32.5 | na | na | na |
| Hydraulic Head (m above ground) | -0.5 to 0.2 | -0.3 to 0.3 | 0.1 to 0.4 | -0.3 to 0.0 | 0.5 | na | 0.95 to 1.1 |
| Max. Pore Water salinity (mg/kg TDS) | 242 500 | 234 000 | 243 800 | 260 700 | 259 200 | 250 200 | 251 800 |

The playa sediments are underlain by a tight grey silty, clayey fine sand, consisting mainly of quartz with kaolinite and Fe-oxyhydroxides (Appendix B). The clays fill the space between the quartz grains and the Fe-oxyhydroxides form coatings on the grains, in some cases forming a weak cement (Appendix B). Iron oxyhydroxides occur heterogeneously in the sediment profiles, ranging from small (<0.5 cm) red and yellow zones and pebbles, up to large chunks of ironstone and entire depth intervals of red or yellow colour. The increased clay content and dramatic colour change from brown to grey, red and yellow indicates the transition from playa sediments to the top of the Blanchetown Clay (Fig. 1.8). Mottling occurs in well-defined zones corresponding to past water table levels. Variations between playas in evaporite mineralogy and the degree of iron mineralization are described in Chapter 3.

Figure 1.8. Trench cut into playa surface at Western Salina, showing ferruginization in the Blanchetown Clay. The brown sediments in the top 20 cm are the playa sediments (Yamba Formation).

### 1.3.5.1 Western Salina

Western Salina is located near the western margin of Raak Plain (Figure 1.6), and is a large (≅ 4 $km^2$), irregularly shaped salina (Table 1.1). The playa is normally dry, although a small ponded surface water body, less than 10 cm deep, occasionally forms after heavy rainfall (see Appendic C). This water blows across the surface of the playa with the prevailing wind and is eventually re-evaporated or infiltrates to the shallow water table.

Western Salina is surrounded by flat grassy plains, approximately 2 m above the playa surface, except along the western boundary of the playa, where sand dunes, up to 20 m high and sparsely vegetated with mallee, are present (see Appendix C). Recharge through these dunes is expected to contribute, along with direct rainfall onto the playa surface, to the salt and water balance of the lake, particularly during high rainfall events. The lack of a significant surface water body in this playa, however, is reflected in its irregular shape, as discussed in Section 1.3.5.5. The hydraulic head in a piezometer screened 1.2 m below the playa surface fluctuates between 50 cm below and 20 cm above ground. There is no surface salt crust, however a temporary efflorescence of tiny white crystals can often be observed on the playa floor after rain, usually within 20 m to 50 m of the playa edge.

### 1.3.5.2 The Main Salina

The Main Salina is the large salina stretching north-south along the eastern side of Raak Plain, with an area of approximately 15 $km^2$ (Fig. 1.6; Table 1.1). Surface characteristics are very similar to those of Western Salina (Appendix C). Surface water occurs periodically after heavy rain, only as a thin film that blows across the lake surface and eventually evaporates or infiltrates to the shallow water table (Appendix C). The surroundings of the lake are similar to those of Western Salina, with extensive grassy plains and low sand dunes sparsely vegetated with mallee and sheoak trees (Appendix C). The piezometric surface, reflected by the playa surface elevation, is approximately 40 cm higher than at Western Salina, which is expected due to the westerly trending hydraulic gradient across the entire discharge complex. Hydraulic heads in a piezometer at the centre of the lake fluctuate seasonally between 0.1 and 0.4 m above the playa surface (Table 1.1). Surface efflorescences were occasionally observed on the playa surface at the Main Salina after periods of rain, despite no substantial salt crust. These are normally most prevalent within 20 to 50 m of the edges of the playa, as at Western Salina.

#### 1.3.5.3 Salt Lake

Salt Lake is the only playa lake included in this study that does not lie along the east-west transect AA’ (Fig. 1.6). It is the smallest of the three natural lakes selected for this study, with an area of 1.1 km$^2$, and lies on the north-eastern border of Raak Plain, where surrounding land is now being cropped for dryland agriculture (Fig. 1.6, Table 1.1). It is 2.5 km from the eastern boundary of the discharge complex and is buffered from the surrounding cropped areas by a 50 m wide strip of mallee and sheoak trees (Table 1.1, Appendix C). The natural physical setting of Salt Lake would have been different from those in the interior of Raak Plain prior to land clearance. It is at the margin of the discharge complex, where the landscape is undulating, with east-west trending sand dunes that are densely vegetated with mallee trees (see Section 1.3.2). This is in contrast to the centre of the discharge complex, which is comparatively flat and bare of vegetation, due to the high salinity of and shallow depth to groundwater (see Section 1.3.2).

The lake edge at Salt Lake has a steeper slope than at Western Salina and the Main Salina and surface water, either from groundwater discharge or direct rainfall, can be up to 15 cm deep, particularly around the edges of the lake (Table 1.1, Appendix C). This surface water body diminishes in summer due to evaporation, and the centre of the lake becomes dry whilst the remaining water is blown around the lake.

During each trip to the site, there was a surface salt crust up to 5 cm thick covering much of the lake surface (Appendix C), but this almost completely dissolves in the height of winter. Large cracks were occasionally observed in the salt crust, forming large polygons, approximately 2-3 m wide (Appendix C). At the single piezometer site at the centre of the lake, the hydraulic head 2.6 m below the lake surface has been constantly 0.5 m above ground level, and did not fluctuate as much as in the other lakes (Table 1.1). Ground and hydraulic head elevations at Salt Lake could not be determined relative to the AHD, as there was no known reference point in the vicinity.

#### 1.3.5.4 Spectacle Lake

Spectacle Lake is located 2.2 km from the eastern boundary of Raak Plain and is the smallest of the lakes included in this study (0.4 km$^2$) (Table 1.1, Fig. 1.6). Regional groundwater, pumped from the Parilla Sand aquifer, is currently ponded on the surface of the lake and evaporated to enhance the precipitation of evaporite minerals (Appendix C). Anecdotal evidence indicates that, before human intervention, the lake was similar to Salt Lake in that it always supported a surface water body and salt crust (Duncan Thompson, Hattah Salt, pers. comm., 2001). The natural physical setting of Spectacle Lake is also similar to that of Salt Lake, as it is surrounded by mallee-vegetated sand dunes (Fig. 1.6; Appendix C).

Spectacle Lake has been harvested for its naturally produced evaporite minerals from as early as 1900. The first production bore was installed in 1980 to pump water from the Parilla Sand aquifer onto the surface of the lake to enhance the production of salt by solar evapo-concentration. The base of the lake was not lined to contain the brine due to the presence of more than 30 m of Blanchetown Clay directly underlying the lake. Groundwater is now pumped from bores around the edges of the lake into a series of three evaporation basins. Water is first pumped into Pond 1 for volume reduction in late autumn and spring, and iron oxyhydroxides and $CaCO_3$ are removed from solution as precipitates. This water is then allowed to flow into Pond 2 for further evapo-concentration and gypsum ($CaSO_4{\cdot}2H_2O$) precipitates. When the specific gravity of the water reaches 1.216, the water is pumped into the smaller Pond 3 where halite (NaCl) is crystallized (Appendix C). This halite is contaminated with iron, causing it to be granular in shape and brownish in colour. Finally, the remaining bittern is pumped into the low volume crystallizers, where the high value minerals such as epsomite ($MgSO_4{\cdot}7H_2O$), bischofite ($MgCl_2{\cdot}6H_2O$) and sylvite (KCl) are extracted (Appendix C). The mineral extraction rate at Spectacle Lake was 2 000 to 3 000 tonnes per year between 1982 and 1996, and 4 000 to 6 000 tonnes per year from 1996 to present. The ponded surface water in Ponds 2 and 3 can be up to approximately 50 cm deep, although both are allowed periodically to dry out for harvesting (Appendix C).

#### 1.3.5.5 Surface Water vs Dry Lakes

Bowler (1986) classified Australian lakes in terms of their current hydrologic stage of evolution, with each type distinguished by its surface morphology. The types range from Type A, with a permanent, relatively deep surface water body of low salinity, to Type E basins, with little surface-water influence that are dominated by groundwater processes such as groundwater bevelling and salt-weathering. The types are distinctive in their morphology, particularly their plan outlines, due to different relative influences of surface- and groundwater processes such as wave action and salt weathering respectively. Irregular plan outlines are caused by playa migration into inter-dunal corridors via salt weathering, the destabilization of sediments by surface salt efflorescences that make them prone to aeolian deflation (Bowler, 1986). Lakes that support even a shallow surface water body for much of the year tend to have smoother outlines as a result of wave action. Based simply on their surface physical characteristics and the classification scheme of Bowler (1986), the lakes at Raak Plain can be divided into two categories:

Salt Lake and Spectacle Lake fall into the category of Type D basins, ephemeral and high salinity, with comparatively regular plan outlines (Fig. 1.6). Some other examples of Australian Type D lakes are Lakes Eyre and Tyrrell. According to the description of Bowler (1986), under prolonged dry conditions in basins of this type, the surfaces may dry sufficiently to permit salts to effloresce. Salt Lake (and probably Spectacle Lake in its natural state) has a thin layer of surface water for most of the year, which dries up only in the driest summer conditions, and a surface salt crust that is partially re-dissolved in the winter rains.

Western Salina and Main Salina can be categorised as Type E basins, with little surface-water influence, and hence irregular plan outlines. They rarely contain ponded surface water and never a surface salt crust, with the exception of minor surface efflorescences. These playas expand laterally via salt weathering as described above, and are modified by episodic aeolian deflation, which forms “islands” within the dry lakes (Bowler, 1986). Some other examples of Type E basins in Australia are Lakes Amadeus, Gairdner and Torrens.

## 1.4 Preliminary Conceptual Models of the Playa Lakes at Raak Plain

A series of preliminary conceptual models can be constructed for the water and solute balances of the playa lakes at Raak Plain, based on a general understanding of the hydrogeology (Fig. 1.9 (a-d)). The geology consists of the regional Parilla Sand aquifer, the confining Blanchetown Clay unit, the thin layer of playa sediments in the lake bed and the dune / plain Woorinen Formation at the margins of the lake. For the purpose of this study, no interaction between the Parilla Sand and the underlying Geera clay is considered. In the conceptual model, the Blanchetown Clay is divided into the Upper and Lower Blanchetown Clay, with the Upper Blanchetown Clay being that depth interval containing the brine body.

The potential sources of water and salt that undergo evaporation in the lakes and ultimately form brines are groundwater discharged from the Parilla Sand aquifer, recharge through the adjacent sand dunes, and direct rainfall onto the lakes. The two scenarios for the fate of the brine body that is formed below the lake are a) confinement within the Blanchetown Clay by the low conductivity of the aquitard and the upward pressure exerted by the Parilla Sand aquifer, or b) transport of solutes by some mechanism back into the Parilla Sand aquifer.

Possible conceptual models can therefore be characterized by two end-members, the Isolated Systems Model (Fig. 1.9a) and the Connected Systems Model (Fig. 1.9(b-d)). In the Isolated Systems Model, there is no interaction between the playa lake and the regional groundwater system. The main sources of solute and water are direct rainfall onto the lake or recharge through the adjacent sand dunes, and the brine body is confined within the Blanchetown Clay. In the Connected Systems Model, there is some exchange of solutes between the regional groundwater system and the playa lake and inputs from direct precipitation or local recharge are negligible. In one possible scenario, the dominant source of solute and water is upward discharge from the Parilla Sand aquifer, but salt is accumulated in the subsurface brine body and does not re-enter the aquifer (Fig. 1.9b). The second possible Connected Systems scenario is similar, but with solutes re-entering the aquifer by either advection (Fig. 1.9c) or diffusion (Fig. 1.9d). Real playa lake systems represent a continuum between these conceptual models.

A water and solute balance can be defined for each of the above conceptual models. For the water balance, the assumption is made that the hydraulic systems of the natural lakes are at steady state, based on the fact that water levels in the lakes are maintained approximately at the lake floor by evaporation and do not fluctuate significantly over large time scales. Under these conditions, the sum of inputs, i.e. direct rainfall onto the playa surface ($R_p$), inflow from peripheral dunes ($I_d$) and upward leakage from the Parilla Sand ($I_{PS}$) equals the sum of outflows, i.e. evaporation (E) and advective leakage to the Parilla Sand (L):

$$R_p + I_d + I_{PS} = E + L \qquad (1.1)$$

For solutes, the brine body may be either at steady state (sum of solute inputs equal to the sum of outputs), in a state of net accumulation (inputs > outputs) or in a state of net loss (inputs < outputs). In the case of the Isolated Systems model (Fig. 1.9a), net accumulation is inferred unless there is loss of efflorescent salts from the lake surfaces by deflation (Bowler and Wasson, 1984; Bowler, 1986; Wood and Sanford, 1995). This is also the case for the first Connected Systems Model. However, for the two Connected Systems Models where solute is lost to the Parilla Sands aquifer

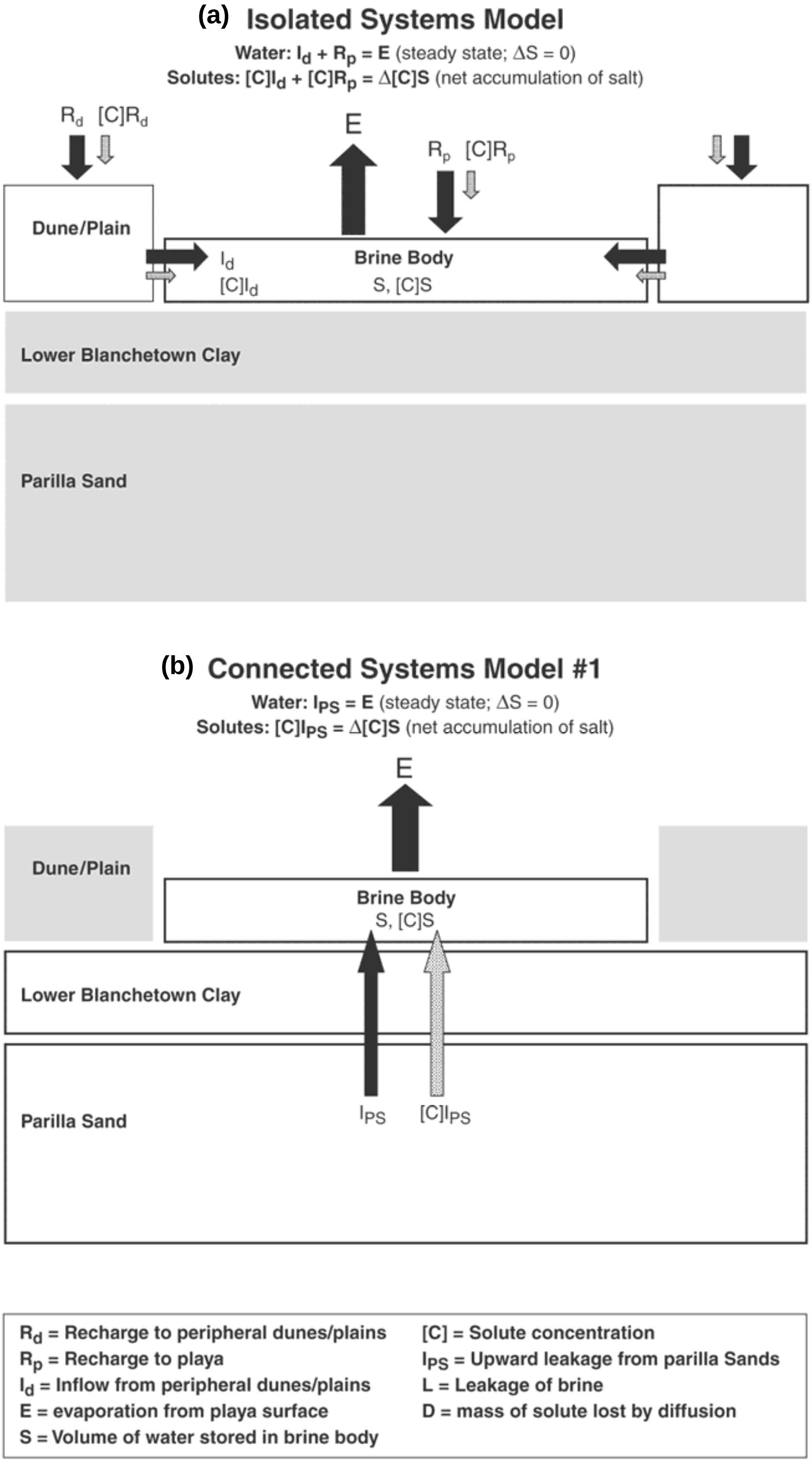

Figure 1.9. Preliminary conceptual models of the water and solute balances of the playa lakes at Raak Plain: (a) An Isolated Systems model, assuming negligible interaction between the playas and the regional Parilla Sand aquifer. In this model, the major sources of water and solutes to the brines are local recharge through adjacent dunes and plains and direct rainfall deposition and there is no brine leakage into the Parilla Sand. (b) A connected systems model assuming that regional Parilla Sand groundwater is the major source of solutes and water to the playas, but that leakage of the brine does not occur.

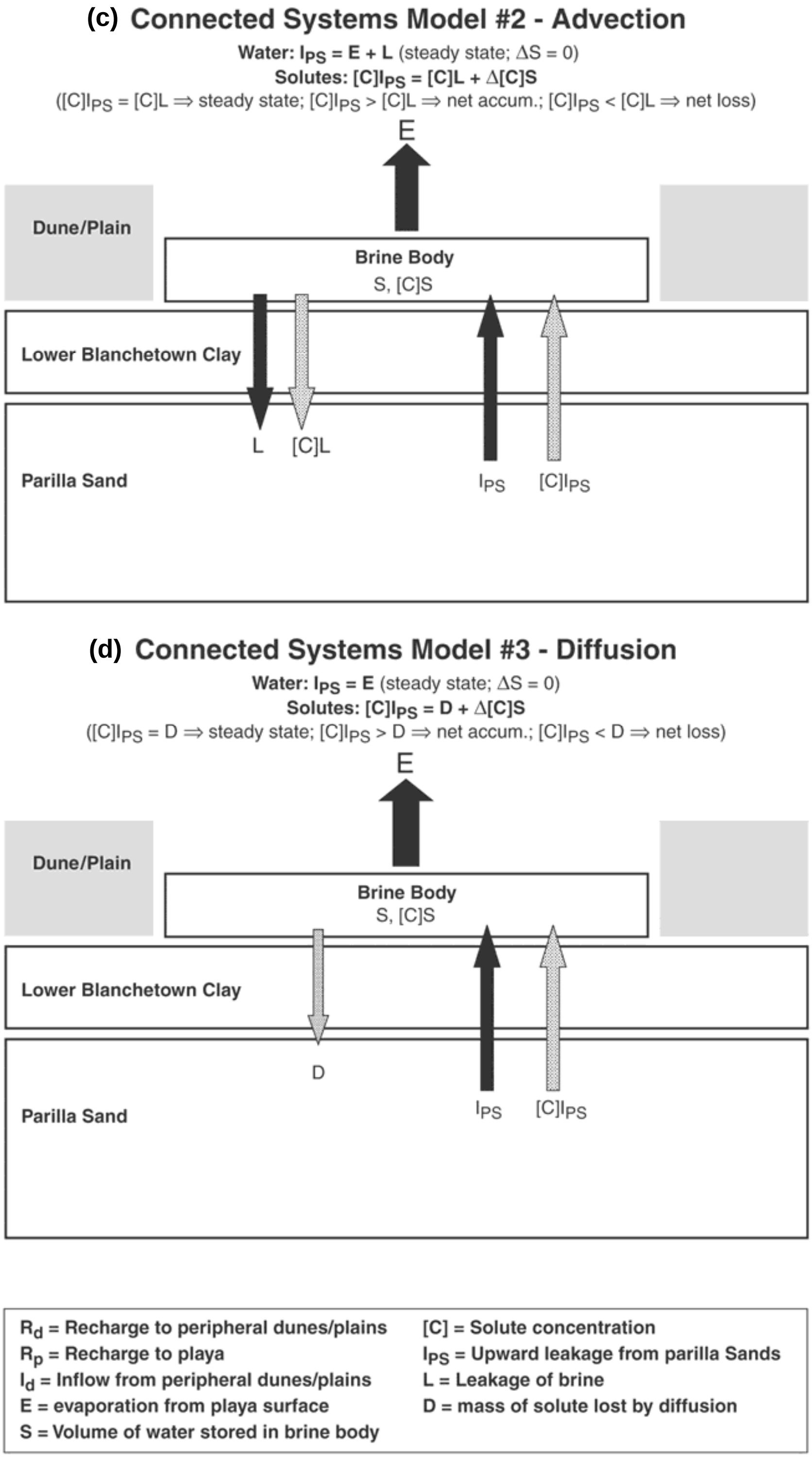

Figure 1.9 (continued). Preliminary conceptual models of the water and solute balances of the playa lakes at Raak Plain: (c) A connected systems model incorporating advective leakage of brine. (d) A connected systems model incorporating leakage of solutes from the brine body by diffusion only.

via either advection or diffusion, the brine body may be at steady state, or experiencing a net loss or accumulation, depending on the magnitudes of the fluxes.

These conceptual models will be used as a basis for interpreting the results of the environmental tracer and hydraulic studies of the playa lakes at Raak Plain, which are described in the following chapters. Chapter 3 investigates the physical and mineralogical controls on the chemical evolution of the subsurface brines at Raak Plain, and what this can tell us about groundwater flow and solute transport below the discharge complex. Hydraulic data are used in Chapter 4 to develop a conceptual model of groundwater flow below the groundwater discharge complex and a numerical model is used in Chapter 5 to test the validity of this model and its sensitivity to various parameters. Chapter 6 compares conclusions drawn from the isotopic tracer signatures of the brines and groundwaters at Raak Plain with the conceptual model derived in Chapter 4 in order to improve confidence in and refine this model. Chapter 7 focuses specifically on processes occurring below Spectacle Lake, and how they relate to the change in the hydraulic balance of the playa by the imposition of a salt harvesting operation.

## 1.5 Overview of Previous Work on the Hydrology and Hydrochemistry of Salt Lakes and Groundwater Discharge Zones (Playa Lakes)

Previous investigations of salt lakes and groundwater discharge zones have focused mainly on their roles in regional water budgets (evaporation rate estimations), the leakage of brines back into regional groundwater systems and the geochemical evolution of their surface and subsurface brines. This section provides an overview of this work, and various aspects will be subsequently discussed in more detail in the relevant chapters.

### 1.5.1 Evaporation Rate Estimations

The fact that playa lakes accumulate large quantities of salt and are often points of regional groundwater discharge led to an early interest in quantifying both their hydrologic and solute budgets. Estimation of groundwater evaporation rates using physical methods was problematic in salt lake environments due to the harsh conditions and low evaporation rates (Tyler et al., 1997). Methods using open-water evaporation pans (Lee, 1912) have now been replaced by lysimeters (Lopes, 1986; Cochran et al.; 1988), mass and energy balance techniques (e.g. Malek and Bingham, 1993) and pore water chloride and $\delta^2$H vs depth profiles (Ullman, 1985; Allison and Barnes, 1985). The latter method, employing environmental tracers, has been applied at Raak Plain (Howes, 1998).

The use of $\delta^2$H vs depth profiles to estimate groundwater evaporation rates originated from a study by Zimmerman et al. (1967), who showed that pore water isotope vs depth profiles formed by evaporation in a saturated medium have a predictable shape resulting from a balance between upward evaporative downward diffusive fluxes. Barnes and Allison (1983) and Allison and Barnes (1985) extended this work to chloride and $\delta^2$H depth profiles in non-vegetated unsaturated soils, where water contents change with depth, estimating an evaporation rate of 63 mm/y from the "normally dry" surface of Lake Frome, Australia. Ullman (1985) also used chloride and bromide profiles to estimate evaporation rates of between 9 and 28 mm/y from the salt-crusted surface of Lake Eyre, South Australia.

### 1.5.2 Brine Leakage

Early physical and chemical studies of salt lakes (e.g. Langbein, 1961; Hahl et al., 1965; Eugster and Jones, 1979) assumed closed systems where there were no surface or subsurface water and solute outflows. However, more recent studies have emphasized the role of pore fluids in the storage of solutes, preservation of evaporites and leakage of brine back into regional groundwater systems (e.g. Jones and Van Denburgh, 1966; Lerman, 1979; Berner, 1980; Spencer et al., 1985 (a&b); Bowler, 1986). Bowler (1986) suggested that vertical transfer of large volumes of brine from a subsurface brine pool to the regional groundwater system occurs at Lake Frome, Australia, despite the presence of a relatively impermeable clay / sand layer. The subsurface brine pool at Lake Frome partially penetrates the aquifer, as do those at Owens Lake, California (Rogers, 1993) and the Smith Creek Valley playa, Nevada (Thomas et al., 1989).

In other cases, for example the Tyrrell Basin, Australia (Teller et al., 1982; Macumber, 1991, 1992), and Mono Lake, California (Rogers, 1993; Rogers et al., 1992), the brine body has completely filled the aquifer below the playa. The Tyrrell Basin will be discussed separately in Section 3.3, as it is the closest well-studied system of playa lakes in hydrogeological setting and brine chemistry to Raak Plain. At Mono Basin, snowmelt and rainfall, originating in the adjacent Sierra Nevada, enter Mono Lake (approx. 200 km$^2$) via streams and groundwater seepage and are evaporated. The resulting saline (> 18,000 ppm) groundwater plume extends 2 km below the lake to the bottom of the basin fill and accounts for 80% of the dissolved solutes in the basin (Rogers, 1991). However, Rogers (1993) used a $^{36}$Cl/Cl mass balance model at Mono Basin to show that the current inventory of chloride, including the subsurface brine , does not account for inflows over the past 3 to 4 million years, indicating leakage of solutes out of the basin by some undetermined mechanism.

### 1.5.3 Salt Lake Geochemistry and Brine Evolution

The hydrochemical evolution of salt lake brines has also been the subject of rigorous study over the past 3 to 4 decades, and has developed in parallel with the understanding of salt lake hydraulics. As described above, the earliest studies of brine hydrochemistry assumed evapo-concentration of inflow in basins that were closed to both surface outflow and groundwater leakage (e.g. Garrels and Mackenzie, 1967; Hardie and Eugster, 1970). The resulting model for brine evolution was based on the fundamental principle of the chemical divide, discussed in more detail in Section 3.2. However, this was an over-simplification of real world systems and further work considered other mechanisms that can influence the final compositions of brines, including magnesium ion removal by dolomitization, sulfate reduction, ion exchange and adsorption and successive wetting and drying cycles (Drever and Smith, 1978; Eugster and Hardie, 1978; Eugster and Jones, 1979).

The Eugster-Jones-Hardie model (Eugster, 1970; Eugster and Hardie, 1978; Eugster and Jones, 1979) was based on the saline Na-$CO_3$-$SO_4$-Cl brines of the Lake Magadi Basin, in the East African Rift Valley, Kenya. Also studied extensively have been the Na-(Mg)-Cl and Na-(Mg)-Cl-($SO_4$) brines of Great Salt Lake, Utah, a surface water lake fed by mountain runoff (Hahl and Langford, 1964; Hahl and Handy, 1969; Whelan, 1973; Spencer et al., 1985 (a&b)), Mono Basin, California, described above and the Tyrrell Basin, Australia (Herczeg and Lyons, 1991; Macumber, 1991, 1992; Long et al., 1992). These will be discussed in more detail in Sections 3.2 and 3.3.

### 1.5.4 The Influence of Leakage on the Chemical Evolution of Brines

The process of brine leakage described in Section 1.5.2 above has often been used to explain deficits in the solute budgets for terminal basins, the presence of non-equilibrium evaporite mineral assemblages, and the transport of brine plumes over large distances (e.g. Wood and Sanford, 1990; Barnes et al., 1990). Both Wood and Sanford (1990) and Chambers et al. (1995) used geochemical models to show that observed mineral assemblages in playa lakes are strongly dependent on the ratio of brine leakage to inflow.

# Chapter 2 Field and Analytical Techniques

## 2.1 Field Methods

### 2.1.1 Piezometer Installation and Sediment Sampling

This thesis is based on data obtained from 26 piezometers, 17 of which had been previously installed to shallow (< 3 m) depths in the three natural playa lakes (Western Salina, the Main Salina and Salt Lake) and at “recharge” sites, on dunes or inter-dunal areas adjacent the playas (Howes, 1998) (Fig. 2.1). A series of 8 deeper (> 6 m) piezometers were additionally installed, using an Investigator Mark 4 rotary drill rig mounted on a Mercedes Benz 4x4 truck, in and at the edges of the playas to sample the deeper brines. These deeper piezometers included 5 at Spectacle Lake (the harvested lake) (Fig. 2.2). One shallow piezometer (SM2) was also installed at Spectacle Lake to monitor changes in the chemical composition of the shallow brine at this location (Fig. 2.2).

Although the surfaces of the natural playa lakes appear to be dry for most of the year, the close proximity of the water tables to the ground surface at the natural lakes causes the sediments to be extremely boggy and inaccessible to vehicles. For this reason, drilling at the natural playa lakes was restricted to as close as practical to the edge. An attempt to install piezometers in the lakes using a portable soft-sediment piston core sampler and rig (Peter et al, 2000) was abandoned as this method could not penetrate the playa sediments (Yamba Formation) beyond about 2 m, due to their high sand content. The deeper piezometers were located close to nests of pre-existing shallow piezometers and bores screened in the Parilla Sand aquifer.

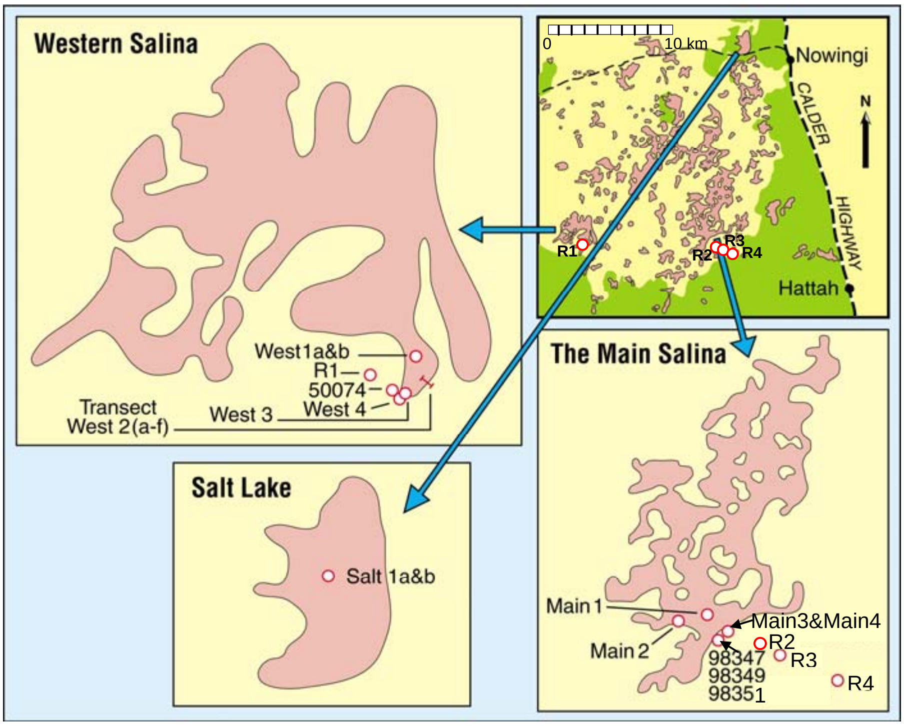

Figure 2.1.  Locations of Parilla Sand bores (50074, 98347, 98349, 98351) and piezometers at the three natural playa lakes included in this study.  Parilla Sand bores were pre-existing, whilst the piezometers were installed as part of this study or the previous reconnaissance study (Howes,1998).

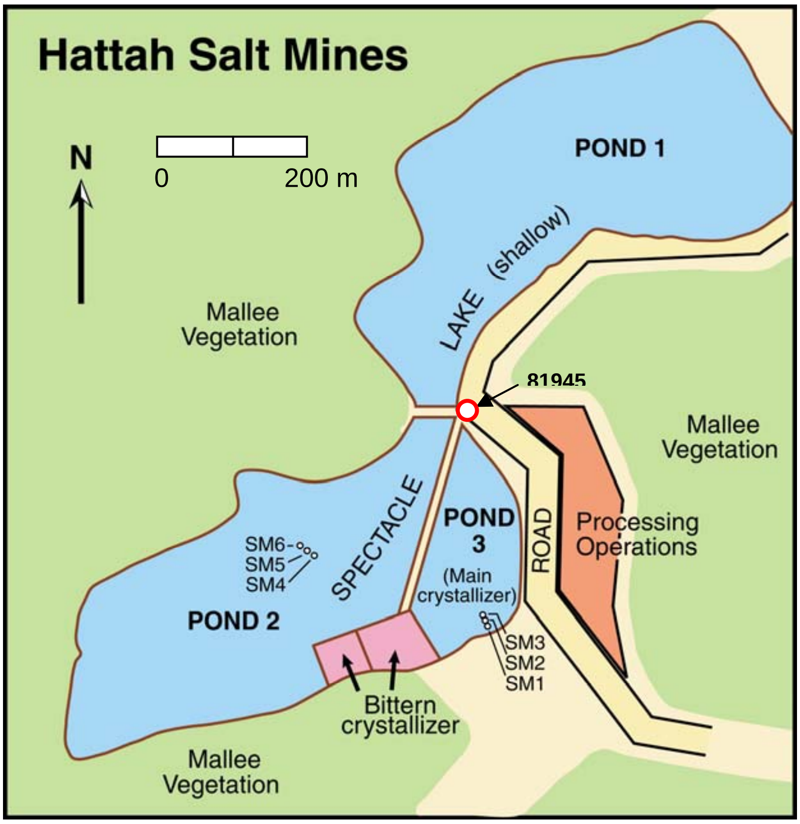

Figure 2.2.  Map of the harvesting operation at Spectacle Lake, including the locations of piezometers installed as part of this study and the regional Parilla Sand bore (81945) located at this site.

Installation of deeper piezometers was possible at the centre of Spectacle Lake because of the greater thickness and compaction of the surface evaporite deposits there.

All piezometers were constructed from 50 mm diameter PVC pipe with slotted screens and filter sock covering the slotted area. The holes were back-filled with coarse sand / gravel around the screens of the piezometers, topped by a layer of bentonite to prevent preferential downward leakage. The locations, screen depths and other details of the piezometers are included as Appendix D.

A solid auger was used in March 1999 to drill the two deep holes to 33 m and 18 m at West4 and Main3/Main4 respectively. Sediment samples were collected from drill spoil at West4 and sealed in 500 ml glass jars, which were then stored upside down to prevent escape of water vapour. Drilling ceased at 33 m at site West4 where the distinctively coarse-grained Parilla Sand was encountered. One piezometer was installed at West4 and two at site Main3 (Main3 and Main4; Fig. 2.1, Appendix D). The geological log of the drill spoil recovered from West4 is included in Appendix E. The dominant lithology, below the sands and silts of the Woorinen and Yamba Formations was the Blanchetown Clay, distinctive by the extremely stiff clays interlayered with sandier layers. The sandier layers, particularly a thick one between approximately 8 m and 10 m, presented problems in drilling and were also encountered at the other drill sites. Large upward hydraulic gradients across these layers caused sand to collapse into the drilled hole when the auger was removed, and the piezometers could not be installed to the full depth of the original hole. A wire-line core recovery device, in conjunction with a hollow-stemmed auger, was used to sample a continuous sediment core to a depth of 8.5 m at Spectacle Lake, site SM5 (see Fig. 2.2). Samples from each depth interval were mixed and stored upside down in 500 ml glass jars. The geological log from this site is also included in Appendix E. The same sand layer to that at West4 was encountered at this site at approximately 8.5 m, with the added problem that the sand was forced into the hollow stem of the auger by the strong upward hydraulic gradient, requiring complete recovery of the drill flights to unblock them. A piezometer was installed at this site at a depth of 6 m, and another was installed using a solid auger at a depth of 18.8 m (see Appendix D).

A second drilling program was carried out in June 2000, during which a second complete core was collected at Spectacle Lake, at the edge of Pond 3 to a depth of 22.5 m (site SM1, see Fig. 2.2). Similar problems with the sandy layers were encountered at this site, and sediment samples could not be collected from within these layers. The geological log of SM1 is presented in Appendix E. Sediment samples were collected as described above for site SM5. A piezometer (SM1) was installed in the hole and two others, SM2 and SM3 were installed at depths of 2.7 and 8.6 m respectively, using a solid auger. Piezometer SM4 was also installed to a depth of 7.5 m near the previously installed SM5 and SM6 at the centre of Pond 2 (see Fig. 2.2 and Appendix D).

Piezometer levels were corrected relative to the Australian Height Datum (AHD) for Western Salina and the Main Salina, where nearby government bores of known elevation were available for surveying reference points (i.e. bore 50074 for Western Salina and bore 98349 for the Main Salina; see Figure 1.6 for locations). At Salt Lake, levels are expressed relative to the playa surface, and at Spectacle Lake, they are relative to the top of the salt crust at site SM5 in Pond 2.

### 2.1.2 Groundwater Sampling

Groundwater from all pre-existing and newly installed piezometers was sampled on four occasions during the period June 1999 to July 2001, to add to data from shallow piezometer network in the natural playas collected by Howes (1998). Sampling was scheduled to obtain data at the end of the summer and winter seasons, and to ensure that even those piezometers installed towards the end of the study were sampled at least once in summer and winter.

Piezometers were purged of standing water (either 3-4 bore volumes or until they were dry), using either a 675 mL plastic bailer or a 12V battery-operated submersible pump. The piezometers were allowed to recover at least overnight before sampling. Samples were collected using a plastic bailer, which was rinsed with groundwater prior to each sample. Analyses of the groundwater samples for electrical conductivity (EC), pH, temperature, dissolved oxygen content and redox potential were carried out in the field using a portable TPS 90FLMV Temperature-pH-Salinity meter (T.P.S. Pty. Ltd.). Field measurements of alkalinity were made using a Hach® field titration kit, using 0.16M $H_2SO_4$ to a pH 4.3 fixed end-point and reported as a $HCO_3^-$ equivalent in mg/L. 125 ml aliquots of water for major cation and anion analyses were filtered through a 0.45 μm membrane and pre-filter and those for cation analysis were acidified with $HNO_3$ before being stored in 50 or 100 mL polyethylene bottles. Separate, un-filtered samples were taken for $\delta^2H$ and $\delta^{18}O$ analysis and stored upside-down in 30 mL glass McCartney bottles with rubber sealed caps. Samples for $^{14}C$, $\delta^{13}C$ and $^{36}Cl$ analysis were collected in 2L polyethylene bottles. Samples of surface salt crusts and efflorescences were also collected at various times and stored in plastic bags or polyethylene jars.

Regional groundwater samples from existing bores installed in the Parilla Sand aquifer were collected in November 1999, using a submersible Grundfos pump. Completion details of these bores are included in Appendix D, however, geological logs were not available. Measurements of temperature, pH and EC were made using a portable TPS 90FLMV Temperature-pH-Salinity meter (T.P.S. Pty. Ltd.) meter during pumping, and samples were not collected until at least 4 times the volume of the bore casing had been purged and these parameters had become stable. Samples were collected for major ion, $\delta^2H$, $\delta^{18}O$, carbon isotope and $^{36}Cl$ analyses, as described above. In addition, samples for $^{14}C$ analysis were collected in multiple 20L polyethylene drums (the volume required to obtain a minimum of 2 g of carbon was calculated from the field alkalinity measurements). 600 mL of 1.7M $BaCl_2$ solution was added for every 20L collected, along with approximately 50 mL of 10M NaOH solution (or enough to raise the pH to >9) and 5-10 mL of an anionic flocculating agent (MAGNAFLOC-156), to form a heavy, white $BaCO_3/BaSO_4$ precipitate. As this settled, the precipitate was transferred to 2L or 5L polyethylene bottles. Unfortunately, the concentration of sulphur in the samples was underestimated and most of the Ba precipitated as $BaSO_4$. Not enough carbon was retained for $^{14}C$ analysis by liquid scintillation counting and water samples were then sent to the Australian Nuclear Science and Technology Organisation (ANSTO) laboratory in Sydney for analysis by Accelerator Mass Spectrometry.

### 2.1.3 Shallow Sediment Profile Sampling

Profile samples of the lake floor sediments at two sites at Western Salina were taken in July 2001 for comparison with those taken during a summer season by Howes (1998). Samples were collected by digging a trench into the unsaturated zone and taking sediment samples using a flat knife and spade from the wall of the trench.

Samples were taken at two centimetre intervals for approximately the first 20 cm, followed by 5 and 10 cm intervals with increasing depth until the profile appeared to be saturated. Sediment samples were mixed well, sealed in 500 mL glass jars and stored upside down.

### 2.1.4 Aquifer Testing

Slug tests were carried out at Spectacle Lake in September, 2000 using three piezometers installed during the previous drilling programs. Approximately 1.5 L of water was removed from each piezometer, with a depth logger installed at a fixed depth inside the piezometer. The recovery of the water level towards its original standing water level was recorded by the logger and downloaded to a laptop computer after approximately 1-2 hours. Data was interpreted using the Hvorslev (1951) method (see results, Appendix F).

## 2.2 Laboratory Methods

### 2.2.1 Particle Size Distributions

Particle size analyses were carried out, following the method of Lewis (1983), on selected sediment samples to estimate the storage properties of the Yamba Formation and discrete units of the Blanchetown Clay, as well as to allow better estimates of hydraulic conductivity. Specific yields were estimated by plotting on the textural classification triangle of Johnson (1967). Hydraulic conductivities were estimated from the graph of Shepherd (1989) for sediment textures between those of consolidated sediments and channel deposits, with average particle sizes estimated assuming that clay = 0.001 mm, silt = 0.01 mm and fine sand = 0.02 mm.

### 2.2.2 Extraction of Pore Water from Sediment Samples

Pore waters for major ion and $\delta^{2}H$ and $\delta^{18}O$ analyses were extracted by centrifuging the samples for one hour at 4000 rpm, using the heavy liquid, trichloroethylene to displace the water. The supernatant water was then pipetted off and stored in 30 mL glass McCartney bottles for $\delta^{2}H$ and $\delta^{18}O$ analyses or VACUTAINER® blood collection tubes for major ion analyses. The pore water samples for major ion analyses were not filtered, as it was considered that centrifuging separates most suspended particles from the water and this is sufficient for major ion analyses of such hypersaline waters. Samples for $\delta^{2}H$ and $\delta^{18}O$ analyses were then stored upside down at approximately 20°C prior to distillation.

### 2.2.3 Major Ions

Major ion analyses of groundwater and extracted pore water samples were carried out at the CSIRO Land and Water, Adelaide Laboratory. Salt crusts from Salt Lake and Spectacle Lake were dissolved in deionised water and analysed for Na, K, Cl, and Br, also at the CSIRO Land and Water, Adelaide Laboratory. Here, Na, K, Mg, Ca and total Fe were analysed by Inductively Coupled Plasma Optical Emission Spectroscopy (ICPOES), on a Spectroflame Modula model instrument (supplied by Spectro Analytical Instruments, Germany), with a precision of ± 5%. This instrument uses simultaneous lines for all reported elements, with a forward power of 1200 watts and an observation height of 14 mm. Dilutions (up to 100x) were required to get [Na] below 1000 mg/L.

Because Cl concentrations were so much higher than those of the other elements, Cl was analysed colorimetrically using the automated ferricyanide method (method

4500-Cl E in Greenberg et al., 1999) on an Alpkem (Alpkem is a Division of O.I Analytical, USA) Flow Solution IV segmented flow analyser. Dilutions were required to get [Cl] below 150 mg/L. The precision of this method was ± 4%.

Br and $SO_4$ were analysed by ion chromatography using a Dionex 4000i ion chromatograph (Dionex Corp., USA) using 50 µL sample injection to 4 mm AG9-HC/AS9-HC guard and separator columns with 9 mM $Na_2CO_3$ eluent and conductivity detection. An appropriate dilution, usually 10x, was required to get the total salt load down below seawater concentrations for these analyses. The precision of the method was ± 4%.

Si was analysed for molybdate reactive silica using a method similar to method 4500-Si F (Greenberg et al., 1999), with the exception that ascorbic acid was used as the reducing agent and the colour was determined at 815 nm rather than 660 nm using a Perstorp Analytical Environmental part number 000293. Sr was analysed by flame atomic absorption spectrometry (method 3500-Sr B in Greenberg et al., 1999), using a GBC 906 spectrometer (GBC Scientific Equipment Ltd, Victoria Australia) with a Sr hollow cathode lamp at 10 mA and wavelength of 460.7 nm with a nitrous oxide-acetylene flame. Strontium standards were matrix matched to the sodium concentration of the samples to avoid ionization effects.

All dilutions described above were carried out using a Gilson model 401 dilutor (Gilson Medical Electronics, France) and sequential dilutions were used if the final dilution required was more than 25 x.

Chloride analyses of the sediment pore water samples were carried out on solutions of 10g of sediment (a sub-sample of each sediment sample) in 50g of deionised water. These were analysed by a first-derivative potentiometric endpoint titration with $AgNO_3$ using an ORION Model 960 Autotitrator. The $AgNO_3$ titrant was standardised with a 1000 ppm chloride standard solution and the sample volume used was 1 ml. Uncertainty for this method determined by replicating standards is ± 3%. Chloride measurements were then corrected for the dilution factor, water content and mass of dissolved salts contained in the sample. The water contents of the samples were obtained gravimetrically by oven drying the sample and measuring the wet and dry weights. A correction was applied to account for the mass of retained salts on drying.

### 2.2.4 Stable Isotopes: Oxygen-18 and Deuterium

Pore water samples for stable isotope analyses were distilled by the azeotropic method described by Revesz and Woods (1990) to avoid a build up of salts in the mass spectrometer. A Europa Scientific Ltd. GEO 20-20 dual inlet gas ratio mass spectrometer was then used for analyses of both oxygen-18 and deuterium.

#### 2.2.4.1 Oxygen-18

Water samples for oxygen-18 analyses were equilibrated with $CO_2$ of known isotopic composition (Socki et al., 1992) and $\delta^{18}O$‰ was determined by mass spectrometry of the equilibrated $CO_2$ gas. 1 ml of sample is required for $CO_2$ equilibration and the precision of this method is ± 0.1‰. Results are expressed as $\delta^{18}O$ ($^{18}O/^{16}O$) in 'per mil' (‰) as a deviation from the standard, Vienna Standard Mean Ocean Water (V-SMOW), where:

$$\delta^{18}O‰ = \frac{(^{18}O/^{16}O)_{sample} - (^{18}O/^{16}O)_{V\text{-}SMOW}}{(^{18}O/^{16}O)_{V\text{-}SMOW}} \times 1000 \quad (2.1)$$

### 2.2.4.2 Deuterium

For analysis of $\delta^2H$, 20 µl of sample was reduced to hydrogen gas by circulating it as vapour across hot uranium at 810°C. This was then introduced into the mass spectrometer. A precision of ± 1‰ is achieved by this method and results are expressed as $\delta^2H$ ($^2H/^1H$) in 'per mil' (‰) relative to V-SMOW, where:

$$\delta^2H ‰ = \frac{(^2H/H)_{sample} - (^2H/H)_{V\text{-}SMOW}}{(^2H/H)_{V\text{-}SMOW}} \times 1000 \quad (2.2)$$

Including errors induced by the azeotropic distillation, the overall precision of the oxygen-18 and deuterium analyses are ± 0.1 ‰ and ± 1 ‰ respectively.

### 2.2.4.3 Isotope Activity Corrections in Concentrated Brines

The extremely high ionic strength brines associated with salt lakes present problems in the interpretation of isotopic data. In such high salinities, the isotope activity ratios of water ($^1H^2HO/H_2O$ and $H_2{}^{18}O/H_2{}^{16}O$) on the activity scale are different from the ratios on the concentration scale due to the presence of salts or "the salt effect" (Taube, 1954; Horita, 1989). Sofer and Gat (1972) were able to experimentally quantify the effect of different salts on the fractionation factor between the solution and the $CO_2$ gas it is equilibrated with during the analysis procedure. Sofer and Gat (1975) also showed that deviations from a straight evaporation line for saline solutions on a conventional $\delta^2H$ vs $\delta^{18}O$ diagram could be explained by fact that $\delta^2H$ is measured as an isotopic concentration and $\delta^{18}O$ as an activity. The application of an appropriate correction factor eliminated this problem and led them to re-evaluate previously published data on the origin of Dead Sea waters, an issue that was taken up again by Horita and Gat (1989).

In addition, because of the high salinities, presently accepted methods of $\delta^2H$ and $\delta^{18}O$ analyses of brines involve azeotropic distillation of the water sample, which, in the presence of alkaline earth ions, causes isotopic fractionation by hydration, dehydration and hydrolysis reactions (Horita and Gat, 1989). There is substantial fractionation between free water molecules and those in the hydration sphere of cations (up to 10 ‰ for $\delta^2H$ observed by Horita and Gat, 1989). Distillation with NaF recovers both free water and the water molecules associated with the hydration sphere of cations (Horita and Gat, 1989; Revesz and Woods, 1990), yielding an isotope concentration. It is usually the isotopic activities of the free water that is of interest in studies of evaporation and atmospheric exchange (Gat, 1995). Hence, Dutkiewicz et al. (2000) applied the following corrections to the Na-Cl-Mg-$SO_4$ brines of the Lake Malata-Greenly playa lake complex in South Australia, to convert from isotope concentrations to activities for both $\delta^2H$ and $\delta^{18}O$ (after experimental data of Horita (1989)):

$$\Delta\delta^2H = mNaCl.(-2.4) + mMgCl_2.(-5.1) + mCaCl_2.(-6.1) + mKCl.(-2.4) \qquad (2.3)$$

$$\Delta\delta^{18}O = mMgCl_2.(0.8) + mCaCl_2.(0.5) + mKCl.(-0.1) \qquad (2.4)$$

where $\Delta\delta^2H$ and $\Delta\delta^{18}O$ are the difference between the delta values on the concentration and activity scales ($\Delta\delta = \delta_c - \delta_a$). These corrections were applied to all $\delta^2H$ and $\delta^{18}O$ from Raak Plain.

### 2.2.5 Carbon Isotopes

Radiocarbon contents were determined by Accelerator Mass Spectrometry at the ANSTO ANTARES facility, following the method of Lawson et al. (2000) and reported following the method of Stuiver and Polack (1977). Stable carbon compositions were determined by continuous-flow mass spectrometry on a Micromass PRISM III stable-isotope mass spectrometer in the School of Geosciences at the University of Woolongong, NSW. Both the radiocarbon and the stable carbon isotope analyses were carried out under the Australian Institute of Nuclear Science and Engineering (AINSE) Grants 01/192 and 98/092.

### 2.2.6 Chlorine-36

Water samples for $^{36}Cl$ analysis were precipitated as AgCl following the method of Conard et al. (1986), and then sent to the Australian National University for analysis by AMS. The precision for this analysis is 1 atom in $10^{15}$, however, at the low $^{36}Cl/Cl$ ratios observed in the groundwater samples from Raak Plain, an uncertainty of approximately 10% should be assumed.

# Chapter 3 Chemical Evolution of the Brines and Groundwaters at Raak Plain

## 3.1 Introduction

Chemical evolution of brines in salt lakes and groundwater discharge zones occurs via evapo-concentration and the successive precipitation of evaporite minerals, according to the principle of the chemical divide (Hardie and Eugster, 1970) (See Section 3.2.1 below). Most field studies of salt lake brine evolution to date have been of large lakes, many having well-defined low-salinity surface water inputs, where most of the chemical evolution of the brines occurs in the lakes themselves. Examples include Lake Magadi, Kenya (Eugster and Jones, 1979) and Mono Lake, California (Connell and Dreiss, 1995). However, many salt lakes throughout the world are fed by groundwater that is already chemically well-evolved and brine evolution and the resulting evaporite mineral suites in these systems can be expected to be quite different from their surface-water fed counterparts.

As the brines at Raak Plain are believed to be essentially evapo-concentrated versions of a high TDS groundwater inflow to the playa lakes there (Macumber, 1991), the discharge complex provides an opportunity to expand on earlier work by studying late-stage salt lake brine evolution processes in detail. It presents an opportunity to investigate the subtle differences in brine evolution and evaporite mineralization that occur across large systems of numerous small playa lakes. Most existing knowledge of salt lake geochemistry is from studies of single large salt lakes or, at most, chains of two to three lakes in which one has been the main focus (e.g. Eugster and Jones, 1979; Jacobson and Janowski, 1989; Macumber, 1992; Long et al., 1992; Connell and Dreiss, 1995; Chambers et al., 1995). However, as described in Chapter 1, brine evolution in playas of large groundwater discharge complexes may vary due to differences in size, location relative to other playas, regional water table elevation, and the presence of recharge zones between them.

As well as being of economic importance to industries such as salt harvesting, and of academic interest to geochemists, an understanding of the hydrochemical evolution of brines in evaporating salt lakes can provide information on sources of salt and water, and the physical processes that transport salt through these systems. The record provided is a cumulative one, of processes that have occurred over geologic time scales, rather than a "snapshot" of the present system, as provided by in-situ measurements of water levels and fluxes. This can be extremely useful in salt lakes, which are usually very slowly evolving systems, often located in regions with flat topography and low rainfall, and hence low hydraulic fluxes.

The main objectives of this chapter are therefore to:

- Determine the major factors influencing brine composition in a complex system of evaporating playa lakes with a chemically well-evolved, seawater-like inflow composition.
- Examine in more detail whether hydrochemistry can be used to determine the major source of solutes to the brines, where the potential sources have similar origins (i.e. rainfall), but vastly different residence times and flow paths. If this is possible, estimate the relative contributions of local recharge (direct rainfall and recharge through adjacent dunes) and regional groundwater to the solute balances of the playas at Raak Plain.

- Determine the importance of any carbonate mineral reactions that will influence the interpretation of $^{14}C$ data in Chapters 6 and 7.

## 3.2 Previous Investigations of the Hydrochemical Evolution of Evaporating Brines

### 3.2.1 Model Development

The chemical models of brine evolution in salt lakes were briefly introduced in Chapter 1, and will be discussed in more detail here. Such models have been developing since the 1960s (e.g. Garrels and Mackenzie, 1967), and have become more and more complex as the complexities of the systems themselves have been realised. Garrels and Mackenzie (1967) calculated what should happen to the chemical composition of water from the Sierra Nevada springs if it was progressively evaporated under a series of specific conditions. This calculation was then generalized to cover a wide range of starting compositions (Hardie and Eugster; 1970), and the resulting model for brine evolution was based on the fundamental principle of the chemical divide (Figure 3.1a). By this principle, if two ions involved in the precipitation of a salt during evaporation are not present in stochiometric concentrations, the species that is originally present in the highest concentration will build up in solution, whilst the other will diminish relative to the other ions. The Hardie-Eugster model (Hardie and Eugster, 1970) determines the chemistry of waters undergoing evaporation based on a series of chemical divides. The implications of the model are that the resulting brines should be chemically simple, containing only a few ions as major species, and that the composition of the final brine is pre-

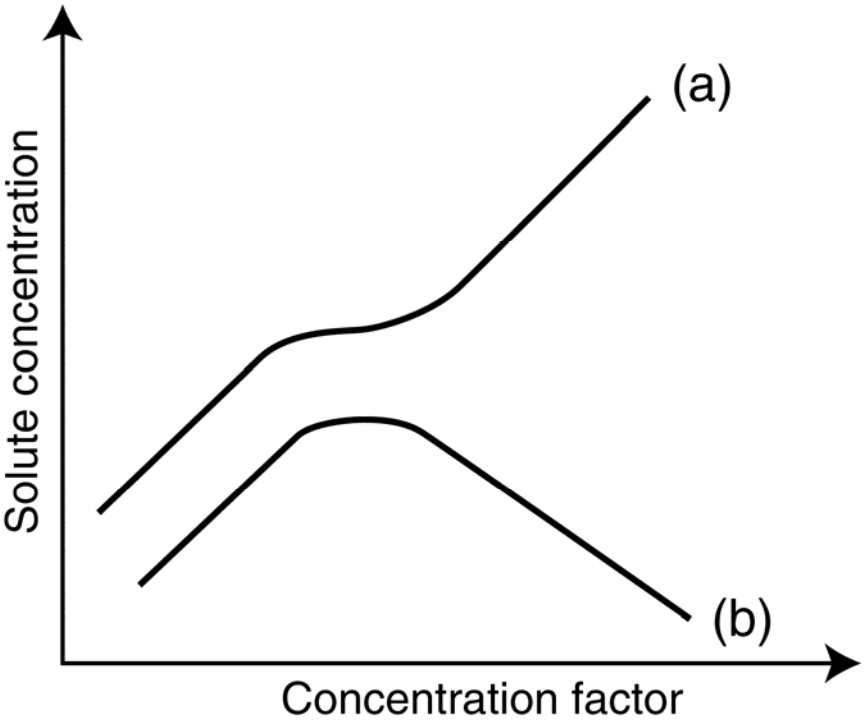

Figure 3.1a. Schematic plot of the concentrations of two solutes, a cation and an anion, during evapo-concentration, illustrating the principle of the chemical divide. By this principle, if two ions involved in the precipitation of a salt during evaporation are not present in stochiometric concentrations, the species that is originally present in the highest concentration (a) will build up in solution, whilst the concentration of the other (b) will diminish (after Eugster and Jones, 1979).

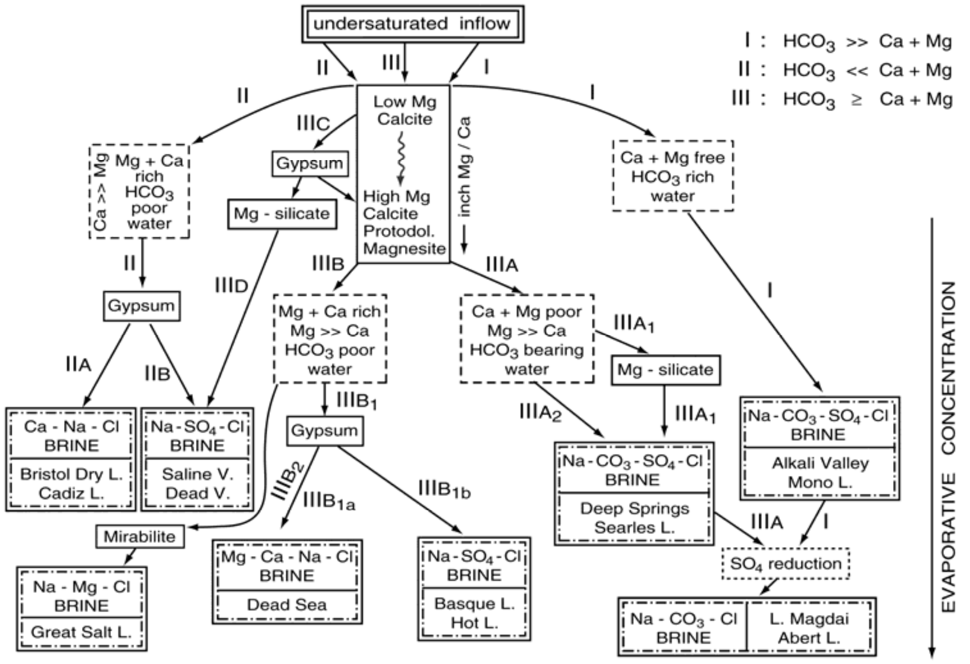

Figure 3.1b. Flow diagram for the geochemical evolution of closed basin brines (the Eugster-Jones-Hardie Model), from Eugster and Hardie (1978).

determined by the composition of the dilute inflow water that is subsequently evaporated.

This original model of Hardie and Eugster (1970) was an over-simplification of real world systems. Further work by Drever and Smith (1978), Eugster and Hardie (1978) and Eugster and Jones (1979) considered other mechanisms that can influence final brine compositions, including magnesium ion removal by dolomitization, sulfate reduction, ion exchange and adsorption and successive wetting and drying cycles. The resulting model is shown in Figure 3.1b (Eugster and Hardie, 1978).

### 3.2.2 Brine Evolution in Surface Water Lakes

Establishment of the models of brine evolution by evapo-concentration of certain inflow water compositions led to numerous investigations of real systems. Many of these have been of alkaline surface water lakes. For example, the Eugster-Jones-Hardie model (Fig. 3.1b) (Eugster, 1970; Eugster and Hardie, 1978;Eugster and Jones, 1979) was based on the saline Na-$CO_3$-$SO_4$-Cl brines of the Lake Magadi Basin, in the East African Rift Valley, Kenya. Inflow to the playa lake at the centre of the basin has a similar composition to that of the Sierra Nevada springs, originally investigated by Garrels and Mackenzie (1967), due to the presence of volcanic bedrock in both of the recharge areas. Recharge in the Magadi Basin occurs in the highlands and flows as perennial streams, before disappearing underground and emerging as springs at the edge of the playa lake. The water evaporates in the arid climate at the centre of the basin and the surface of Lake Magadi is solid trona ($Na_2CO_3 \cdot NaHCO_3 \cdot 2H_2O$), with carbonate species precipitating over the entire concentration range, from the recharge area, to springs at the edge of the lake and to the lake itself. The highly evaporated interstitial brines provided an example of the alkaline (pH up to 10.5) Na-$CO_3$-$SO_4$-Cl end-member in the Eugster-Jones-Hardie model (Fig. 3.1b). The only exception is that sulfate is removed continuously in the Magadi Basin by sulfate reduction and other unknown processes.

Like Lake Magadi, the surface and subsurface brines at Mono Lake, California, are Na-$CO_3$-$SO_4$-Cl dominated, with similar inflow compositions due to the presence of volcanic bedrock in the highlands surrounding both lakes (Rogers et al., 1992; Connell and Dreiss, 1995). Mono Basin is a hydrologically closed basin, with Mono Lake (approx. 200 $km^2$) being the regional groundwater sink. The main source of inflow is snowmelt and rainfall in the adjacent Sierra Nevada, which enters the lake via streams and groundwater seepage. Evaporation from the lake and near-surface groundwater is the main mechanism for water loss. The saline (> 18,000 ppm) groundwater plume associated with the lake extends 2 km to the bottom of the basin fill, and accounts for 80% of the dissolved solutes in the basin. Rogers et al. (1992) attempted to quantify the processes responsible for the distribution of solutes between shoreline sediments, lake and groundwater using a solute transport model, but did not evaluate the behaviour of individual solutes. Connell and Dreiss (1995) furthered this, attempting to quantitatively discriminate between hypothesised sources of the shallow brine beneath Mono Lake. They used saturation state calculations and geochemical modelling of the evapo-concentration of inflow, mixing of lake water with inflow and the precipitation of minerals to derive the important factors influencing the shallow groundwater geochemistry: a) the degree of mixing with historical lake water, b) the evaporative concentration and redissolution cycles and c) a variety of chemical fractionation mechanisms (e.g. Ca-, Mg- and Na-carbonate precipitation, sulphate reduction, ion exchange and Mg-silicate formation).

The brines at Great Salt Lake, Utah, which is also a surface water lake (8.5 m max. depth), fed by runoff from the Uinta and Wasatch Mountains, are examples of Na-(Mg)-Cl and Na-(Mg)-Cl-($SO_4$) types (Eugster and Hardie, 1978), closer to those that occur in the Murray Basin. The hydrochemistry of the Great Salt Lake brines and inflow waters have been studied extensively (e.g. Hahl and Mitchell, 1963; Hahl and Langford, 1964; Hahl and Handy, 1969; Mundorff, 1971; Whelan, 1973). A seasonal crust of mirabilite ($Na_2SO_4 \cdot 10H_2O$) forms around the lake edge. The hydrology of the lake was modified by the construction of a causeway in 1959, causing the development of two distinct brine bodies, one of which is now chemically stratified.

An early study by Hardie and Eugster (1970), found that the chemical composition of the Great Salt Lake brines could be obtained by the evaporation of the dilute inflow, coupled with precipitation of calcite ($CaCO_3$), sepiolite and gypsum ($CaSO_4 \cdot 2H2O$), but that actual sediment compositions suggested that more complicated processes were occurring. Spencer et al. (1985 (a&b)) investigated brine evolution, both as a result of short-term (last 150 years) and long-term (Pleistocene-Holocene) processes. The present system was shown to be dynamic, with the major sources of water being river discharge and direct rainfall onto the lake, and a major source of solute being hydrothermal springs. Precipitation and re-dissolution of salts, mainly halite (NaCl) and mirabilite ($Na_2SO_4 \cdot 10H_2O$) occur in response to fluctuations in lake level, causing fluctuations in concentrations of the associated solutes and stratification of the brines (the present stratification is also partly due to the construction of the causeway). Major removal of solutes from the lake was also found to occur through transport into the underlying pore fluids. Long-term trends in lake composition were calculated by combining the principles of closed basin brine evolution of Hardie and

Eugster (1970) and the aqueous solution model of Harvie and Weare (1980), with models of the hydrologic evolution of the lake. By additionally considering interactions with pore fluids, Spencer et al. (1985 (a&b)) were able to obtain a satisfactory solute budget for the system.

### 3.2.3 Brine Evolution in Dry Playas

Most of the above salt lakes are surface water lakes, fed mainly by surface water inflows. Here, the brines undergo much of their evolution in the lakes themselves. In comparison, if it is regional groundwater that evaporates from the playa surfaces to form the brines at Raak Plain, it has already undergone long-term mineral-solution reactions as it has flowed 300 km from the margins of the Murray Basin towards the discharge complex at the centre. Even groundwater recharged locally through the dunes adjacent the playas may have undergone high degrees of evapotranspiration in the semi-arid conditions, and may be well-equilibrated with aquifer materials due to low hydraulic gradients and consequently long residence times. It is therefore expected that the hydrochemical data from Raak Plain will reveal late stage evolution processes, i.e. little influence from processes such as cation exchange, adsorption and low solubility (e.g. carbonate) mineral interactions.

There have been few other studies of normally dry playa lakes with a predominantly groundwater inflow. Owens Lake, part of the same chain of lakes as Mono Lake, is one example of a study site that is now an almost entirely dry playa (Levy et al., 1999). This has occurred recently due to diversions of inflow from the Owens River, and the exposure of the playa surface has caused the deflation of salts, contributing an estimated 6% of the breathable dust in continental USA (Blum, 1993). This has resulted in extensive investigation of hydrochemical processes leading to the formation of the Na-$CO_3$-$SO_4$-Cl brine, particularly those controlling the dissolved concentrations of arsenic and fluoride, which have been identified in potentially hazardous concentrations in the dust. The Australian examples of Lake Frome (Draper and Jensen, 1976; Allison and Barnes, 1985; Ullman and McLeod, 1986; Ullman and Collerson, 1994) and Lake Eyre (Ullman, 1985), in Australia have been mainly concerned with the chemistry in the top few metres of a brine body, and with estimating evaporation from the playa surface.

### 3.2.4 The Influence of Leakage on Brine Compositions

Wood and Sanford (1990) recognized the potential for brine leakage or reflux in the lakes of the Southern High Plains of Texas and New Mexico and proposed a conceptual model for the water and solute budget of an evaporative lake basin, which included groundwater seepage of brines. They suggested that this could be used to explain a) the simple suites of evaporite deposits that occur in many real basins, and b) the lack of solute mass balance that usually occurs when applying closed basin models. Using a geochemical model to evaluate the effects of various flux ratios (ratio of groundwater inflow to outflow), they found that, when a steady-state ratio is reached, large thicknesses of two or three minerals can form rather than the thin veneers of many minerals predicted by closed basin models. They proposed mechanisms such as diffusion, advection and density-driven flow for brine leakage to the regional groundwater system.

Chambers et al. (1995) used chemical modelling to predict the equilibrium evolutionary paths of evaporating brines from two operating disposal basins and two natural salt lake complexes in the Murray Basin. They found that the predicted evaporite suites for the two disposal basins differed because their inlet waters were derived from different sedimentary regions of the basin. However, they also concluded that, in the natural salt lake complexes, brine evolution is a complex process of evaporation and re-solution of salts, and that it is strongly influenced by the presence or absence of thick clayey sediments below the lakes, and hence the occurrence of brine leakage.

## 3.3 The Tyrrell Groundwater Discharge Complex, Murray Basin, Australia

The Tyrrell groundwater discharge complex, located in the western Murray Basin, Australia, is the closest well-studied playa lake system to Raak Plain, in both its physical setting and the geochemistry of its inflow waters (Macumber, 1992; Long et al., 1992; Herczeg et al., 1992). Because of the highly evolved nature of the groundwater throughout the centre of the Murray Basin, regional groundwater flowing into the Tyrrell groundwater discharge complex also has a similar composition to that at Raak Plain (Macumber, 1991). In contrast to Raak Plain, however, the Tyrrell Basin contains only three main playa lakes, which are in direct connection with the Parilla Sand aquifer. Lake Tyrrell, the largest single groundwater discharge lake in the Murray Basin with an area of 160 km$^2$, much larger than any of the playas at Raak Plain, has been the main focus of geochemical studies there.

Inflow to Lake Tyrrell includes brine that has been recycled from the up-gradient Lakes Wahpool and Timboram via density-driven convection. This process of brine reflux and throughflow can occur because Lakes Tyrrell, Timboram and Wahpool sit directly on top of the high permeability Parilla Sand aquifer. A similar process of throughflow of brine between the many small playas at Raak Plain may also be possible, although the presence of the 30 m thick Blanchetown Clay aquitard may inhibit this. Therefore, despite similarities in setting, the sizes and number of playas and the underlying hydrogeology may result in the hydrochemical evolution of the brines at Raak Plain being quite different from those in the Tyrrell Basin.

The Tyrrell Basin is an example of an acid-hypersaline lake system with complex geochemical interactions occurring between the lake brines and the regional groundwater (Macumber, 1991, 1992). Acid-hypersaline groundwater and lakes occur extensively throughout southern Australia. In the Murray Basin, this is thought to be due to the oxidation of pyrite in the regional Parilla Sands aquifer, and the low buffering capacity of the aquifer material (Long et al., 1992). The acidity is then further enhanced by evaporation and the precipitation of Fe-oxides and alunite and jarosite in the groundwater discharge areas (Long et al., 1992). The hydrogeology, geochemistry and evolutionary paths of the brines, and the mineralogy at Lake Tyrrell have been described by Macumber (1983, 1991, 1992), Herczeg et al. (1992), Long et al. (1992), Jones et al. (1994) and Lyons et al. (1995).

The Timboram-Wahpool reflux brine is neutral, with a salinity of approximately 110,000 mg/L, while the Tyrrell lake waters (250 g/L to 330 g/L) are a concentrated version of the acidic regional groundwater (40 g/L) that also flows into the lake at springs around the margin (Macumber, 1991, 1992). The composition has been further influenced by halite dissolution and precipitation cycles and variations in inputs from surface inflows and the Timboram-Wahpool reflux brine. Geochemical interactions occur between these components at the surface, producing an interesting array of evaporites, redbeds and metal sulphide minerals (Long et al., 1992).

An additional branch to the Eugster-Jones-Hardie model (Hardie and Eugster, 1970; Eugster and Hardie, 1978; Eugster and Jones, 1979) was suggested by Long et al. (1992) to describe the evolutionary pathways leading to the production of the acid-hypersaline brines at Lake Tyrrell. The original model (Fig. 3.1b) describes the evolution of lacustrine systems. The additional branch proposed by Long et al. (1992) describes the closed-basin evapo-concentration of marine-derived recharge waters and is applicable to extensively weathered continents (low buffering capacity) in arid climates. Acid conditions result in high Fe and Al concentrations so that the precipitation of alunite ($KAl_3(SO_4)_2(OH)_6$), jarosite ($KFe_3(SO_4)_2(OH)_6$) and Fe-oxides may be important. Herczeg and Lyons (1991) also developed a chemical model to calculate the chemical compositions of such waters.

## 3.4 Results

### 3.4.1 General Overview

The chemical compositions of all water samples collected at Raak Plain are shown in Table 3.1, including:

- Groundwater brines sampled from all piezometers in and adjacent the four playa lakes.
- Near-surface pore water brines extracted from shallow playa sediments.
- Locally recharged groundwater from below the dunes and plains between the playas (piezometers R2, R3 and R4; see Fig. 2.1 for locations).
- Regional groundwater from the set of regional bores screened in the Parilla Sand aquifer along transect AA’ (see Fig. 1.6 for locations).
- Surface water from Salt Lake and Spectacle Lake (Pond 2 and Pond 3; See Fig. 2.2 for locations).
- Rainfall + dry fallout samples collected over a 12 month period from various locations across Raak Plain.

Table 3.1. Chemical compositions of groundwater and pore water ("Profile") samples from the Raak Plain groundwater discharge complex, as sampled in April 2001 (unless otherwise stated). Data from other sampling dates are included as Appendix H. The regional Parilla Sand bores were sampled in November 1999. Alk is alkalinity as $HCO_3^-$. Sample locations are shown on Figures 1.6, 2.1 and 2.2.

| PIEZOMETER/ SITE NAME | SAMPLE DEPTH m below ground | TDS g/kg | $Na^+$ | $Mg^{2+}$ | $K^+$ | $Ca^{2+}$ | $Cl^-$ | $SO_4^{2-}$ | Alk | $Br^-$ | $Fe^{2+}$ | $Sr^{2+}$ | pH | Eh | D O | T |
|---|---|---|---|---|---|---|---|---|---|---|---|---|---|---|---|---|
| | | | moles/kg | | | | | | mmoles/kg | | | | | mV | % Sat | °C |
| Parilla Sand Groundwater Bores | | | | | | | | | | | | | | | | |
| 26240 | 50 | 41.4 | 0.542 | 0.058 | 0.006 | 0.008 | 0.652 | 0.039 | 0.88 | 0.78 | 0.48 | 0.36 | 5.92 | - | - | 22.8 |
| 81945 | 37-43 | 53.1 | 0.684 | 0.074 | 0.006 | 0.008 | 0.857 | 0.047 | - | 1.13 | 1.33 | 0.25 | 5.53 | 109 | - | 20.2 |
| 98347 | 38-42 | 51.0 | 0.702 | 0.078 | 0.006 | 0.009 | 0.763 | 0.054 | 0.82 | 0.71 | 2.70 | 0.18 | 6.07 | -293 | 8.9 | 19.1 |
| 98349 | 68-74 | 49.0 | 0.662 | 0.082 | 0.006 | 0.011 | 0.729 | 0.054 | 0.91 | 0.60 | 1.45 | 0.21 | 6.21 | -205 | 8.8 | 20.7 |
| 98351 | 37-48 | 51.2 | 0.702 | 0.078 | 0.006 | 0.008 | 0.768 | 0.054 | 0.89 | 0.71 | 2.65 | 0.17 | 5.95 | -325 | 6.0 | 20.9 |
| 50073 | 36 | 65.3 | 0.915 | 0.083 | 0.008 | 0.011 | 0.999 | 0.062 | 0.90 | 1.28 | 0.34 | 0.37 | 6.28 | - | - | 22.3 |
| 50074 | 54-57 | 82.1 | 1.122 | 0.099 | 0.009 | 0.019 | 1.297 | 0.069 | 0.19 | 1.64 | 0.06 | 0.50 | - | - | - | - |
| 50075 | 55-60.5 | 66.5 | 0.881 | 0.093 | 0.007 | 0.017 | 1.016 | 0.072 | 0.19 | 1.23 | 0 | 0.48 | 6.59 | - | - | 22.2 |
| Dune/Plain Groundwater | | | | | | | | | | | | | | | | |
| R1 | 13.0-14.0 | 76.4 | 1.065 | 0.103 | 0.008 | 0.015 | 1.123 | 0.065 | 2.36 | 1.27 | 0 | 0.31 | 6.87 | 82 | 32 | 20.7 |
| R2 | 1.5-2.0 | 45.2 | 0.642 | 0.063 | 0.006 | 0.018 | 0.613 | 0.064 | 0.60 | 0.72 | 0 | 0.30 | 6.68 | 137 | 59 | 22.6 |
| R3 | 5.3-5.8 | 24.3 | 0.331 | 0.032 | 0.004 | 0.015 | 0.322 | 0.038 | 1.15 | 0.34 | 0 | 0.28 | 7.37 | 125 | 54 | 22.3 |
| R4 | 4.8-5.3 | 54.4 | 0.804 | 0.074 | 0.006 | 0.007 | 0.769 | 0.064 | 0.86 | 0.95 | 0 | 0.26 | 6.72 | 55 | 36 | 20.6 |
| Western Salina | | | | | | | | | | | | | | | | |
| West1 Profile | 2-4 cm | 242.5 | 3.13 | 0.364 | 0.015 | 0.006 | 3.793 | 0.201 | 3.15 | 4.07 | - | 0.26 | 7.42 | - | - | - |
| (Jan 1998) | 8-10 cm | 216.7 | 2.823 | 0.284 | 0.014 | 0.01 | 3.442 | 0.169 | - | 3.53 | - | 0.33 | 7.09 | - | - | - |
| | 20-25 cm | 199.1 | 2.602 | 0.262 | 0.012 | 0.012 | 3.136 | 0.159 | - | 3.71 | - | 0.38 | 7.05 | - | - | - |
| | 60-70 cm | 193.7 | 2.518 | 0.251 | 0.011 | 0.012 | 3.070 | 0.153 | - | 2.93 | - | 0.37 | 6.81 | - | - | - |
| | 80-90 cm | 194.7 | 2.548 | 0.253 | 0.011 | 0.013 | 3.073 | 0.155 | - | 3.02 | - | 0.35 | 7.12 | - | - | - |
| | 153-160 cm | 192.8 | 2.465 | 0.252 | 0.011 | 0.013 | 3.081 | 0.152 | - | 3.13 | - | 0.34 | 6.51 | - | - | - |
| | 166-177 cm | 193.1 | 2.508 | 0.256 | 0.012 | 0.013 | 3.05 | 0.155 | - | 3.13 | - | 0.34 | 6.99 | - | - | - |
| | 274-292 cm | 193.1 | 2.462 | 0.256 | 0.012 | 0.013 | 3.079 | 0.156 | - | 2.83 | - | 0.35 | 6.95 | - | - | - |
| West1a | 2.5-3.0 | 180.5 | 2.595 | 0.236 | 0.012 | 0.013 | 2.654 | 0.154 | 0.11 | 2.05 | - | 0.12 | 5.75 | 284 | 35 | 19.4 |
| West1b | 0.7-1.2 | 186.7 | 2.650 | 0.248 | 0.012 | 0.012 | 2.758 | 0.161 | 0.08 | 2.34 | - | 0.11 | 6.41 | 202 | 48 | 20.1 |

Table 3.1 (continued)

| PIEZOMETER/ SITE NAME | SAMPLE DEPTH | TDS | $Na^+$ | $Mg^{2+}$ | $K^+$ | $Ca^{2+}$ | $Cl^-$ | $SO_4^{2-}$ | Alk | $Br^-$ | $Fe^{2+}$ | $Sr^{2+}$ | pH | Eh | D O | T |
|---|---|---|---|---|---|---|---|---|---|---|---|---|---|---|---|---|
|  | m below ground | g/kg | moles/kg |  |  |  |  |  | mmoles/kg |  |  |  |  | mV | % Sat | °C |
| West5 Profile | 0-2 cm | 264.2 | 3.224 | 0.552 | 0.015 | 0.005 | 3.507 | 0.400 | - | 4.62 | - | 0.77 | - | - | - | - |
| (Apr 1998) | 2-4 cm | 234.5 | 2.960 | 0.481 | 0.014 | 0.007 | 3.218 | 0.308 | - | 5.15 | - | 0.75 | - | - | - | - |
|  | 4-6 cm | 231.0 | 3.022 | 0.441 | 0.014 | 0.008 | 3.266 | 0.263 | - | 4.59 | - | 0.78 | - | - | - | - |
|  | 6-8 cm | 212.6 | 2.861 | 0.371 | 0.014 | 0.010 | 3.091 | 0.210 | - | 4.45 | - | 0.91 | - | - | - | - |
| West2a | 1.7-2.2 | 90.2 | 1.302 | 0.116 | 0.005 | 0.016 | 1.296 | 0.080 | 1.89 | 1.25 | - | 0.27 | 7.4 | -39 | 42 | 21.7 |
| West2b | 1.1-1.6 | 92.7 | 1.322 | 0.116 | 0.006 | 0.016 | 1.357 | 0.080 | 1.65 | 1.25 | - | 0.27 | 7.28 | 62 | 42 | 21.8 |
| West2c | 1.4-1.9 | 110.3 | 1.591 | 0.139 | 0.007 | 0.019 | 1.584 | 0.102 | 1.44 | 1.56 | - | 0.25 | 7.11 | -47 | 20 | 21.6 |
| West2d | 1.3-1.8 | 104.4 | 1.519 | 0.126 | 0.007 | 0.015 | 1.539 | 0.084 | 1.45 | 1.68 | - | 0.27 | 6.95 | 140 | 28 | 21.7 |
| West2e | 0.4-0.9 | 152.5 | 2.238 | 0.189 | 0.009 | 0.016 | 2.266 | 0.115 | 0.68 | 2.33 | - | 0.21 | 7.05 | 131 | 30 | 22.1 |
| West2f | 1.7-2.2 | 131.5 | 1.915 | 0.168 | 0.010 | 0.017 | 1.854 | 0.127 | 0.43 | 1.63 | - | 0.18 | 6.95 | 128 | 33 | 22.3 |
| West3 | 3.3-3.8 | 153.1 | 2.236 | 0.209 | 0.001 | 0.016 | 2.243 | 0.124 | 0.24 | 2.65 | - | 0.24 | 6.43 | 125 | 41 | 22.5 |
| West4 | 11.0-12.0 | 85.9 | 1.237 | 0.109 | 0.007 | 0.017 | 1.238 | 0.075 | 0.18 | 1.37 | - | 0.33 | 6.67 | -14 | 33 | 21.9 |
| Main Salina |  |  |  |  |  |  |  |  |  |  |  |  |  |  |  |  |
| Main1 Profile | 0-2 cm | 232.4 | 3.178 | 0.405 | 0.017 | 0.005 | 3.221 | 0.356 | - | 3.00 | 0 | 0.54 | - | - | - | - |
| (Jan 1998) | 2-4 cm | 243.8 | 3.363 | 0.444 | 0.018 | 0.005 | 3.640 | 0.265 | - | 2.86 | 0.15 | 0.59 | - | - | - | - |
|  | 13-16 cm | 212.4 | 2.984 | 0.340 | 0.016 | 0.007 | 3.169 | 0.229 | - | 3.11 | 0.18 | 0.67 | - | - | - | - |
|  | 30-35 cm | 206.1 | 2.93 | 0.323 | 0.015 | 0.008 | 3.060 | 0.221 | - | 3.02 | 0.30 | 0.75 | - | - | - | - |
| Main1 | 1.5-2.0 | 187.1 | 2.730 | 0.276 | 0.015 | 0.010 | 2.762 | 0.193 | 0.26 | 2.63 | - | 0.13 | 4.57 | 201 | 29 | 21.4 |
| Main2 | 0.4-0.5 | 190.9 | 2.848 | 0.277 | 0.011 | 0.009 | 2.708 | 0.226 | 0.28 | 3.01 | - | 0.09 | 6.87 | 140 | 26 | 19.2 |
| Main3 | 14.0-15.0 | 50.7 | 0.734 | 0.074 | 0.007 | 0.008 | 0.743 | 0.050 | 0.92 | 0.83 | 2.55 | 0.15 | 6.07 | -5 | 49 | 19.7 |
| Main4 | 6.5-7.0 | 50.9 | 0.725 | 0.074 | 0.007 | 0.008 | 0.748 | 0.054 | 0.45 | 0.83 | 2.21 | 0.15 | 5.77 | 9 | 23 | 21.6 |
| 98348 | 0.5-3.5 | 51.3 | 0.702 | 0.078 | 0.006 | 0.011 | 0.779 | 0.051 | 0.04 | 0.71 | 1.57 | 0.20 | 4.35 | -26 | 18.9 | 19.6 |

Table 3.1 (continued)

| PIEZOMETER/ SITE NAME | SAMPLE DEPTH | TDS | $Na^+$ | $Mg^{2+}$ | $K^+$ | $Ca^{2+}$ | $Cl^-$ | $SO_4^{2-}$ | Alk | $Br^-$ | $Fe^{2+}$ | $Sr^{2+}$ | pH | Eh | D O | T |
|---|---|---|---|---|---|---|---|---|---|---|---|---|---|---|---|---|
|  | m below ground | g/kg | moles/kg |  |  |  |  |  | mmoles/kg |  |  |  |  | mV | % Sat | °C |
| Salt Lake |  |  |  |  |  |  |  |  |  |  |  |  |  |  |  |  |
| Salt1 Profile | 0-2 cm | 259.2 | 2.649 | 0.870 | 0.025 | 0.002 | 3.873 | 0.396 | 3.36 | 5.74 | - | 0.01 | 6.14 | - | - | - |
| (Jan 1998) | 2-4 cm | 258.0 | 2.784 | 0.746 | 0.024 | 0.003 | 3.893 | 0.370 | 1.82 | 5.65 | - | 0.18 | 7.09 | - | - | - |
|  | 4-6 cm | 255.9 | 2.948 | 0.587 | 0.020 | 0.003 | 3.974 | 0.307 | 0.65 | 5.19 | - | 0.23 | 6.56 | - | - | - |
|  | 50-55 cm | 235.3 | 2.881 | 0.379 | 0.013 | 0.006 | 3.651 | 0.211 | 0.04 | 3.10 | - | 0.20 | 6.03 | - | - | - |
|  | 100-110 cm | 235.9 | 2.974 | 0.320 | 0.012 | 0.006 | 3.725 | 0.183 | 0.13 | 2.64 | - | 0.25 | 6.02 | - | - | - |
|  | 255-263 cm | 203.9 | 2.474 | 0.277 | 0.010 | 0.009 | 3.034 | 0.164 | - | 2.37 | - | 0.29 | 5.88 | - | - | - |
| Salt1a | 2.1-2.6 | 199.5 | 2.698 | 0.276 | 0.010 | 0.009 | 2.701 | 0.182 | 0.07 | 1.91 | 0 | 0.01 | 5.2 | 193 | 52 | 16.4 |
| Salt1b | 0.2-0.5 | 236.5 | 3.145 | 0.417 | 0.015 | 0.005 | 3.454 | 0.228 | - | 2.83 | 0 | 0.09 | 5.2 | 142 | 28 | 14.8 |
| Lake Water | - | 242.2 | 3.874 | 0.159 | 0.007 | 0.011 | 3.703 | 0.091 | 0 | 1.19 | 0 | 0.09 | 4.96 | 173 | 30 | 10.6 |
| Spectacle Lake |  |  |  |  |  |  |  |  |  |  |  |  |  |  |  |  |
| SM1 Profile | 0.5-1.0 | 249.9 | 1.997 | 1.374 | 0.086 | 0.003 | 3.406 | 0.468 | - | 17.46 | - | 0.37 | - | - | - | - |
| (Jul 2001) | 1.0-1.1 | 251.8 | 1.989 | 1.346 | 0.082 | 0.003 | 3.482 | 0.47 | - | 17.51 | - | 0.28 | - | - | - | - |
|  | 1.1-1.2 | 234.1 | 1.646 | 1.299 | 0.069 | 0.003 | 3.327 | 0.443 | - | 17.35 | - | 0.22 | - | - | - | - |
|  | 2.2-2.3 | 238.1 | 3.062 | 0.577 | 0.037 | 0.005 | 3.396 | 0.324 | - | 6.74 | 0 | 0.22 | - | - | - | - |
|  | 2.5-2.6 | 200.8 | 2.685 | 0.317 | 0.018 | 0.006 | 3.062 | 0.223 | - | 5.75 | 0 | 0.06 | - | - | - | - |
|  | 3.9-4.0 | 191.6 | 2.679 | 0.293 | 0.017 | 0.006 | 2.801 | 0.234 | - | 3.01 | 0 | 0.08 | - | - | - | - |
|  | 7.4-7.5 | 107.3 | 1.553 | 0.163 | 0.018 | 0.015 | 1.493 | 0.138 | - | 2.12 | 0 | 0.35 | - | - | - | - |
|  | 8.1-8.2 | 85.6 | 1.233 | 0.124 | 0.014 | 0.016 | 1.210 | 0.105 | - | 1.31 | 0 | 0.38 | - | - | - | - |
|  | 19.7-19.9 | 83.5 | 1.176 | 0.109 | 0.013 | 0.015 | 1.250 | 0.086 | - | 1.60 | 0 | 0.18 | - | - | - | - |
|  | 19.9-20.0 | 81.8 | 1.159 | 0.106 | 0.014 | 0.013 | 1.227 | 0.082 | - | 1.72 | 0 | 0.16 | - | - | - | - |
|  | 20.2-20.3 | 82.1 | 1.143 | 0.113 | 0.012 | 0.012 | 1.247 | 0.081 | - | 1.60 | 0 | 0.16 | - | - | - | - |
|  | 21.2-21.3 | 83.0 | 1.197 | 0.122 | 0.012 | 0.016 | 1.182 | 0.098 | - | 1.54 | 0 | 0.39 | - | - | - | - |
| SM1 | 16.1-18.1 | 99.5 | 1.439 | 0.152 | 0.013 | 0.014 | 1.503 | 0.094 | 1.71 | 1.57 | 0 | 0.19 | 6.61 | -11 | 25 | 20.7 |
| SM2 | 0.7-2.7 | 226.6 | 3.214 | 0.381 | 0.025 | 0.006 | 3.330 | 0.247 | 0.44 | 4.60 | 0 | 0.07 | 6.17 | 60 | 22 | 19.7 |
| SM3 | 6.6-8.6 | 85.2 | 1.206 | 0.135 | 0.012 | 0.015 | 1.232 | 0.095 | 1.49 | 1.60 | 0 | 0.19 | 6.96 | -68 | 24 | 19.1 |
| SM4 | 5.5-7.5 | 99.0 | 1.422 | 0.167 | 0.023 | 0.009 | 1.469 | 0.091 | 0.92 | 2.14 | 0 | 0.18 | 6.15 | 42 | 36 | 20.1 |

Table 3.1 (continued)

| PIEZOMETER/ SITE NAME | SAMPLE DEPTH | TDS | $Na^+$ | $Mg^{2+}$ | $K^+$ | $Ca^{2+}$ | $Cl^-$ | $SO_4^{2-}$ | Alk | $Br^-$ | $Fe^{2+}$ | $Sr^{2+}$ | pH | Eh | D O | T |
|---|---|---|---|---|---|---|---|---|---|---|---|---|---|---|---|---|
| | m below ground | g/kg | moles/kg | | | | | | mmoles/kg | | | | | mV | % Sat | °C |
| SM5 Profile | 0.0-0.1 | 56.2 | 0.960 | 0.010 | 0.001 | 0.002 | 0.929 | 0.009 | - | <0.5 | 0 | 0.03 | - | - | - | - |
| (Mar 1999) | 0.1-0.2 | 122.6 | 2.055 | 0.058 | 0.004 | 0.010 | 1.975 | 0.034 | - | <0.5 | 0 | 0.21 | - | - | - | - |
| | 2.0-2.1 | 250.2 | 3.085 | 0.068 | 0.055 | 0.004 | 3.624 | 0.346 | - | 4.22 | - | 0.15 | - | - | - | - |
| | 3.0-3.1 | 236.6 | 2.947 | 0.558 | 0.048 | 0.005 | 3.417 | 0.329 | - | 5.14 | 0 | 0.17 | - | - | - | - |
| | 3.7-3.8 | 209.5 | 2.616 | 0.482 | 0.042 | 0.005 | 3.025 | 0.293 | - | 4.44 | - | 0.19 | - | - | - | - |
| | 4.0-4.1 | 209.7 | 2.616 | 0.482 | 0.042 | 0.005 | 3.031 | 0.292 | - | 4.57 | - | 0.20 | - | - | - | - |
| | 4.4-4.5 | 180.7 | 2.258 | 0.401 | 0.044 | 0.006 | 2.599 | 0.253 | - | 6.23 | - | 0.25 | - | - | - | - |
| | 5.1-5.2 | 148.5 | 1.950 | 0.293 | 0.041 | 0.008 | 2.183 | 0.172 | - | 8.10 | - | 0.34 | - | - | - | - |
| | 6.0-6.1 | 126.5 | 1.701 | 0.218 | 0.044 | 0.009 | 1.870 | 0.138 | - | 3.38 | - | 0.42 | - | - | - | - |
| | 6.5-6.6 | 110.3 | 1.504 | 0.172 | 0.029 | 0.011 | 1.706 | 0.094 | - | 4.68 | - | 0.46 | - | - | - | - |
| | 6.7-6.8 | 103.2 | 1.439 | 0.158 | 0.030 | 0.009 | 1.584 | 0.087 | - | 2.24 | - | 0.43 | - | - | - | - |
| | 7.2-7.3 | 105.7 | 1.473 | 0.154 | 0.032 | 0.010 | 1.617 | 0.092 | - | 2.15 | - | 0.47 | - | - | - | - |
| | 8.4-8.5 | 106.2 | 1.472 | 0.151 | 0.032 | 0.01 | 1.635 | 0.092 | - | 2.78 | - | 0.44 | - | - | - | - |
| SM5 | 5.5-6.0 | 106.2 | 1.483 | 0.194 | 0.024 | 0.01 | 1.552 | 0.111 | 1.05 | 2.34 | 414 | 0.18 | 6.18 | 14 | 33 | 20.0 |
| SM6 | 18.0-18.8 | 72.0 | 1.035 | 0.111 | 0.011 | 0.01 | 1.076 | 0.066 | 0.74 | 1.39 | 1989 | 0.18 | 6.07 | 4 | 36 | 20.4 |
| Pond 1 Lake Water | | | | Not sampled in April 2001. See Appendix G for other sampling dates. | | | | | | | | | | | | |
| Pond 2 Lake Water | - | 247.1 | 3.406 | 0.478 | 0.036 | 0.005 | 3.720 | 0.241 | 0 | 5.22 | 4003 | 0.20 | 2.69 | 374 | 33 | 16.2 |
| Pond 3 Lake Water | - | 252.7 | 2.953 | 0.793 | 0.066 | 0.003 | 3.550 | 0.375 | 0 | 9.30 | 5531 | 0.20 | 2.34 | 375 | 27 | 13.5 |
| <u>Rainfall + Dry Depos<sup>n</sup> Samples</u> | | | | | | | mg/L | | | | | | | | | |
| Rain1 | - | 44.9 | 16 | 3.1 | 0.9 | 1.6 | 16.4 | 10.8 | <0.1 | - | - | - | - | - | - | - |
| Rain2 | - | 37.4 | 9.6 | 1.3 | 3.4 | 2.7 | 18.5 | 5.4 | 0.1 | - | - | - | - | - | - | - |
| Rain3 | - | 10.1 | <0.1 | <0.1 | 0.5 | 1.1 | 7.8 | 1.5 | 0.2 | - | - | - | - | - | - | - |
| Rain4 | - | 76.6 | 25 | 2.6 | 0.4 | 2.4 | 43 | 9.6 | <0.1 | - | - | - | - | - | - | - |

The groundwaters sampled at Raak Plain have a large range of salinities (TDS), from 24.3 g/kg, for shallow groundwater on top of a sand dune (site R3), up to 259 g/kg for shallow brines 0-2 cm below the playa surface at Salt Lake. However, despite this large range, their relative major ion compositions are remarkably similar to each other, and to that of seawater, as indicated by the similar shapes of their graphs in Figure 3.2. All of the groundwaters are dominated by $Na^+$, $Cl^-$, $Mg^{2+}$ and $SO_4^{2-}$, reflecting the meteoric and ultimately oceanic origins of their dissolved solutes (Jones et al., 1994; Herczeg et al., 2001). The largest variations occur in the relative concentrations of the minor ions, $Ca^{2+}$ and alkalinity (expressed as $HCO_3^-$) (Fig. 3.2).

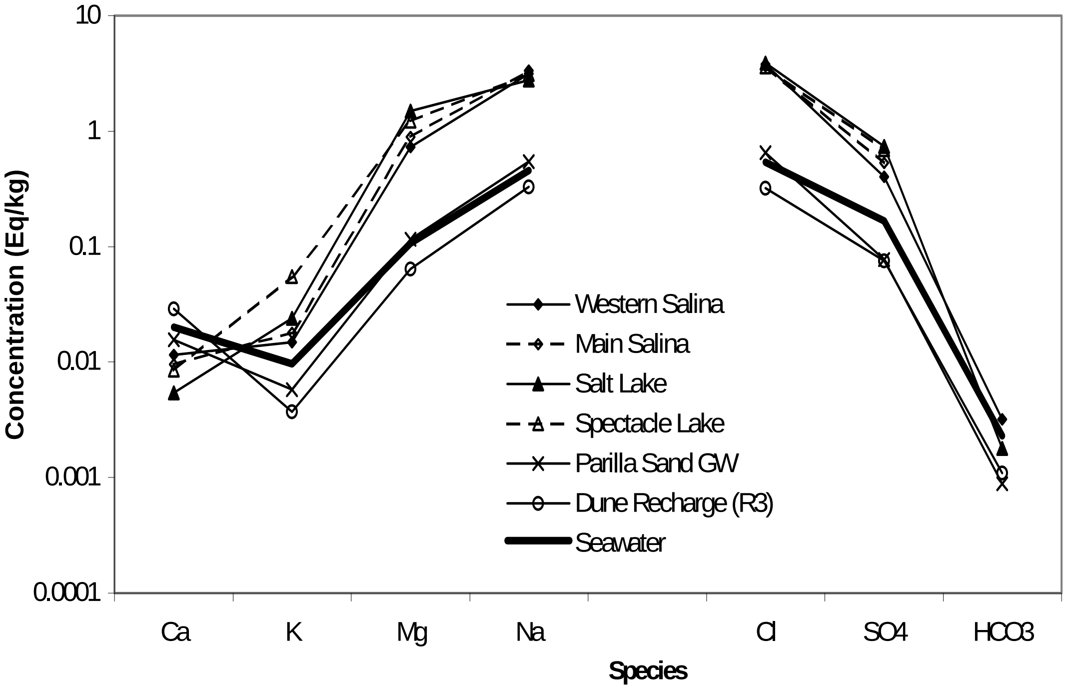

Figure 3.2. Schoeller diagram showing the chemical compositions of the highest TDS brines below the centre of each playa at Raak Plain (see Table 3.1), regional Parilla Sand groundwater flowing into the discharge complex at the eastern margin (bore 26240) and shallow groundwater below a sand dune, representing locally recharged groundwater (R3). Seawater composition is also shown for reference. $HCO_3$ refers to total alkalinity expressed as $HCO_3$.

### 3.4.2 Brine Chemistry

The highest TDS brines (up to approximately 250 g/kg) generally occur in the top 2 to 4 cm of playa sediment (Table 3.1; see Appendix G). TDS concentrations below this may decrease to between approximately 190 g/kg and 210 g/kg within the top 20 cm of sediment pore water, but remain constant at this value to at least 2 m depth (see TDS vs depth profiles in Appendix G). pH of the brines generally ranges between 6.5 and 7.5, although values as low as 4.3 were consistently measured at site Main1 at the centre of the Main Salina, where excess amounts of Fe-oxyhydroxide minerals were also observed. The oxidation of $Fe^{2+}$ and precipitation as Fe-oxide was identified by Macumber (1991) as a potential mechanism causing low pH brines at Lake Tyrrell (see Section 3.3). Groundwater $Fe^{2+}$ concentrations were generally negligible across Raak Plain, with the exception of below the Main Salina, where concentrations up to 150 mg/kg were measured in the Blanchetown Clay and underlying Parilla Sand aquifer.

### 3.4.3 Parilla Sand Groundwater

As described in Section 1.3.3, groundwater in the Parilla Sand aquifer, believed to be a major source of salt to the playas of Raak Plain, has a seawater-like salinity and chemical composition, dominated by $Na^+$, $Cl^-$, $Mg^{2+}$ and $SO_4^{2-}$ (Macumber, 1991). It can also be very acidic ($pH < 5$) at some locations, due to pyrite oxidation in the aquifer and the low buffering capacity of the aquifer material (Macumber, 1991; Long et al., 1992). The seawater-like characteristics, caused by the accession of aerially deposited sea salts with recharge, develop early in the evolution of the groundwater, near the margins of the Murray Basin, becoming more apparent as the groundwater flows towards the centre of the Basin, near Raak Plain (Maddocks, 1967; Herczeg, 1977; Jones et al., 1994; Herczeg et al., 2001). By the time it reaches the centre of the Murray Basin, the major ion composition of the Parilla Sand groundwater is remarkably constant, and is in equilibrium with aquifer minerals (Herczeg, 1977; Macumber, 1991).

As regional groundwater flow in the vicinity of Raak Plain is approximately from east to west (Fig. 1.5) (Rural Water Commission; 1991), groundwater sampled from bore 26240 at the south-eastern margin of Raak Plain (Fig. 1.6) should therefore represent the initial composition of groundwater flowing into the discharge complex. There is an apparent general increase in dissolved solute concentrations as the groundwater in the Parilla Sand aquifer flows from east to west below Raak Plain (Fig. 3.3). Groundwater in bore 26240 (east) has a TDS concentration of 41.4 g/kg, whilst groundwater in bore 50074, below Western Salina has a TDS concentration of 82.1 g/kg. Although there is a slight TDS increase in the vicinity of Spectacle Lake, the majority of this increase occurs to the west of the Main Salina, i.e. below the main part of the discharge complex (Fig. 3.3). At the eastern margin of the Main Salina, where bores 98347, 98349 and 98351 are screened at different depths in the Parilla Sand aquifer (see Fig. 3.3), dissolved ion concentrations are fairly constant with depth (Table 3.1).

### 3.4.4 Locally Recharged Groundwater

The shallow groundwater between the playas at Raak Plain, represented by piezometers R1, R2, R3 and R4, has a range of salinities. The highest were observed below groves of mallee and sheoak trees adjacent Western Salina (site R1, 75.2 g/kg TDS), and the Main Salina (site R4, 53.6 g/kg TDS) respectively, probably due to higher degrees of evapotranspiration of soil water by the trees. The lowest salinity

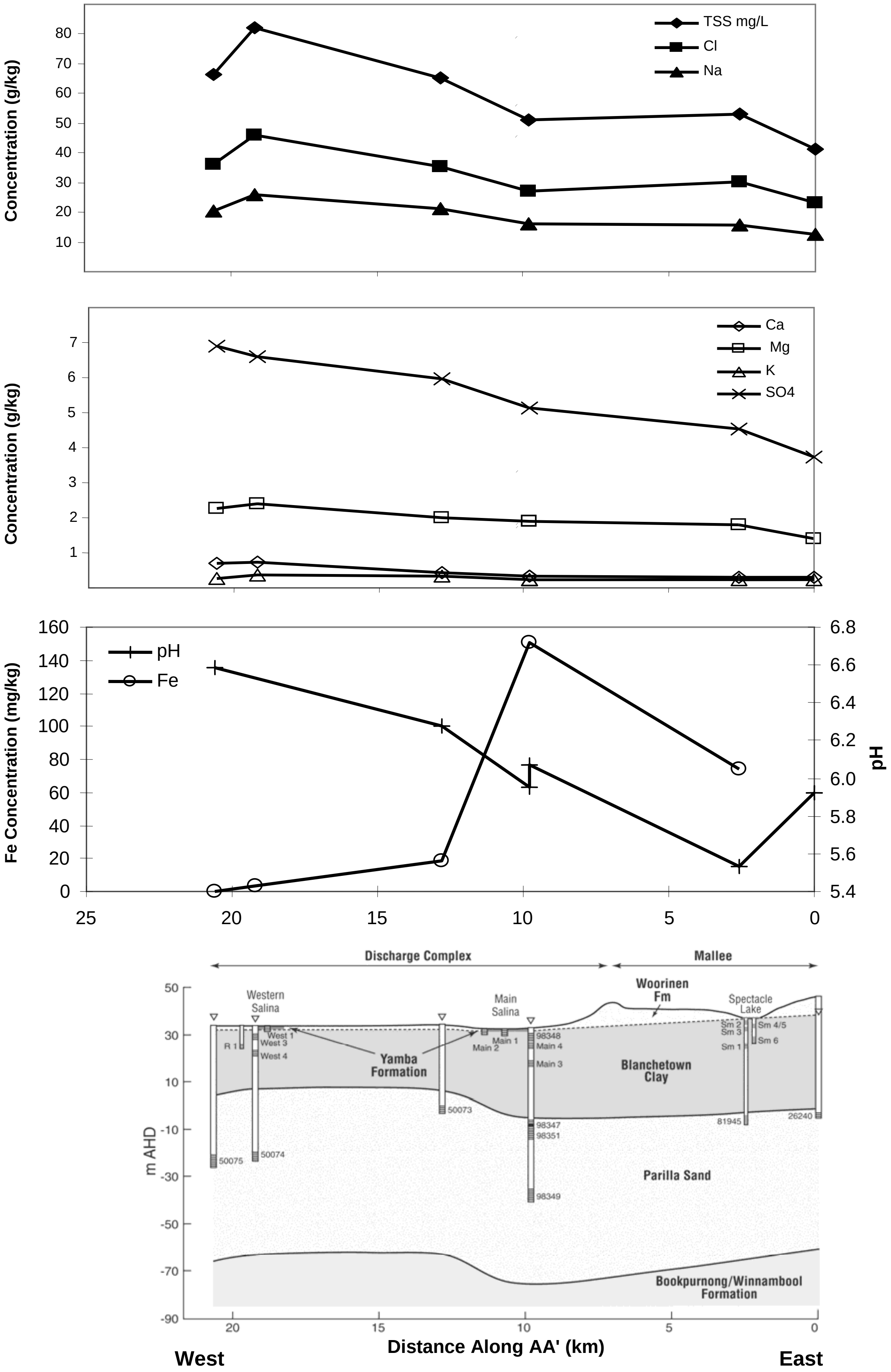

Figure 3.3. Ion concentrations and pH versus distance along transect AA’ in the regional Parilla Sand aquifer below Raak Plain. See Figure 1.6 for location of transect AA’.

occurs below a dune up-gradient of the Main Salina (site R3, 23.5 g/kg TDS), and is probably due to rapid infiltration of recharge through the sandy sediments at this site and a consequently low degree of evapotranspiration. The chemical compositions of the groundwater sampled from these piezometers between April 1998 and July 2001 remained relatively constant with time. All chemistry data is included in Appendix H, and the July 2001 data for R1, R2, R3 and R4 are shown in Table 3.1. Photos of sites R1, R2, R3 and R4 are included in Appendix C.

### 3.4.5 Rainfall and Dry Deposition

Another source of salt to the groundwaters of the Murray Basin, and ultimately the playa brines at Raak Plain, is atmospheric deposition, in the form of wind-borne sea salt that falls with rain, and terrestrial dust. This salt may infiltrate with recharge, to eventually enter the groundwater discharge complex via groundwater inflow. It may also be directly deposited on the playa surfaces and infiltrate the shallow brines with rainfall. The longest available record of bulk deposition of salt (in rainfall and dry deposition) in the Murray Basin is that of Blackburn and McLeod (1983), which was collected for 28 day intervals over a 3 year period ending in 1977. Average TDS for the two stations nearest to Raak Plain, Merbein (60 km north of Raak Plain) and Walpeup (40 km south of Raak Plain), from that study were 25.5 mg/L and 20.1 mg/L respectively.

During the course of the present study, bulk samples of both rainfall and dry fallout were also collected over a one year period from four sites within Raak Plain (see Fig. 1.6 for sampling locations). Their chemical compositions are shown in Table 3.1. With the exception of Rain3, collected on top of a sand dune to the east of the Main Salina, all of the samples from Raak Plain have higher TDS than those from Merbein and Walpeup reported by Blackburn and McLeod (1993). The prevailing wind direction at Raak Plain is from the east (Bureau of Meteorology, Australia, 2002), and hence Rain3 is up-wind of the majority of the Raak Plain playas. TDS of the rainfall + dry deposition samples increase from east to west (i.e. Rain3 → Rain2 → Rain1), consistent with deposition of airborne salt deflated from the playa surfaces. The highest TDS concentration occurs in sample Rain4, adjacent the down-wind margin of Salt Lake, which has a surface salt crust for most of the year. This result is consistent with deflation of salt from the surface of the playa and deposition in the local environment down-wind.

A large charge balance error of 37 % identified for sample Rain3 may be due to contamination of one of the sub-samples collected for analysis, or cross-contamination during the analysis itself by brine samples analysed within the same batch. In such dilute samples, a small amount of contamination can cause extremely large charge balance errors. In recognition of these potential inaccuracies, TDS concentrations only and not ionic ratios of rainfall + dry deposition samples across Raak Plain are compared in this chapter.

### 3.4.6 Mineralogy

As described in Section 1.3.5, analysis of shallow sediment cores collected from each of the sites within the playa lakes at Raak Plain indicated that the brown silty fine sands of the Yamba Formation (playa sediments) generally extend to depths of 20 cm to 50 cm below the playa surface. Below this, the silty Blanchetown Clay is mottled with red and yellow zones, caused by Fe-oxyhydroxide coatings on quartz grains. The extent of this mottling is by far the greatest at the Main Salina, where hard red and yellow nodules were also observed below 40 cm in the centre of the playa

(Main1) (Appendix B). Scanning Electron Microscope (SEM) analyses indicated that hard, low permeability and hence dry-textured layers in the profiles are caused by clay and small amounts of Fe-oxyhydroxide that form a cement between quartz grains.

Seed-like gypsum crystals were observed between 2 cm and 30 cm depths at the centre of the Main Salina (Main1) and between 35 cm and 40 cm at the edge (Main2). Gypsum was not obvious in the profiles at the other playas, nor was it picked up by mineralogical analyses of selected sediment samples. SEM analyses of selected samples indicated the presence of some zircon ($ZrSiO_4$) and a Ti-bearing mineral, possibly rutile ($TiO_2$) or ilmenite ($FeTiO_3$) in the profiles at Western Salina and Salt Lake (Appendix B). Distinctive crystals of celestite ($SrSO_4$) were identified using SEM at a depth of 10 cm at the edge of Western Salina (West2) and trace amounts were also identified in the profile at the edge of the Main Salina (Main2).

The surface salt efflorescences occasionally observed at Western Salina were not analysed. However, some tiny white crystals with a similar appearance observed at site Main2 in July 2001 were identified via XRD to consist of co-dominant proportions of halite and bloedite ($Na_2SO_4MgSO_4 \cdot 5H_2O$) with minor gypsum. Two centimetre thick deposits of halite (NaCl) were also observed in “strand-line” formations on the salina floor at the Main Salina in April 2001. In contrast to Western Salina and the Main Salina, a 1 cm thick layer of salt occurs across the surface of Salt Lake, and samples of this collected in January 1998, April 2001 and July 2001 were identified by XRD as being predominantly halite, with minor or trace amounts (< 20%) of gypsum. The sample collected in January 1998 also contained trace amounts of bischofite ($MgCl_2 \cdot 6H_2O$). The thickness of this salt crust varies seasonally. See Appendix C for photos of salt crusts and efflorescences.

The mineralogy at Spectacle Lake is more complex than at the natural playas, probably due to the influence of the salt harvesting operation. Here, the 20 cm thick surface salt crust consists predominantly of halite, with traces of gypsum and bischofite ($MgCl_2·6H_2O$) (Appendix B). At the edge of Pond 3 (site SM1; see Fig. 2.2), trace concentrations of calcite ($CaCO_3$), gypsum ($CaSO_4·2H_2O$) and hexahydrite ($MgSO_4·6H_2O$) occur in the predominantly quartz sand fill that occurs below the salt crust at this site (Appendix B). Below the sand, the profile returns to that observed at the natural playas. A saturated, sandy black organic layer occurs below the halite crust at the centre of Pond 2 (site SM5; Fig. 2.2), between 20 cm and 70 cm depth, with large quantities of cubic halite crystals and a strong $H_2S$ smell. The XRD analysis of a sample from this layer indicated dominant halite, with traces of quartz, gypsum, glauberite ($Na_2SO_4CaSO_4$), rozenite ($FeSO_4·4H_2O$) and bischofite ($MgCl_2·6H_2O$).

### 3.4.7 Ion vs Depth Profiles at Spectacle Lake

Figure 3.4 shows ion concentrations plotted against depth at the edge of Pond 3 (site SM1) and the centre of Pond 2 (site SM5). A hypersaline brine body can be seen above approximately 8 m depth at both sites. Concentrations below this, at the edge of Pond 3, are relatively constant with depth down to 22 m. Sediment sampling was not carried out below 8.5 m depth at the centre of Pond 3, however concentrations generally decrease between this depth and the piezometer screened approximately 18.5 m below ground level.

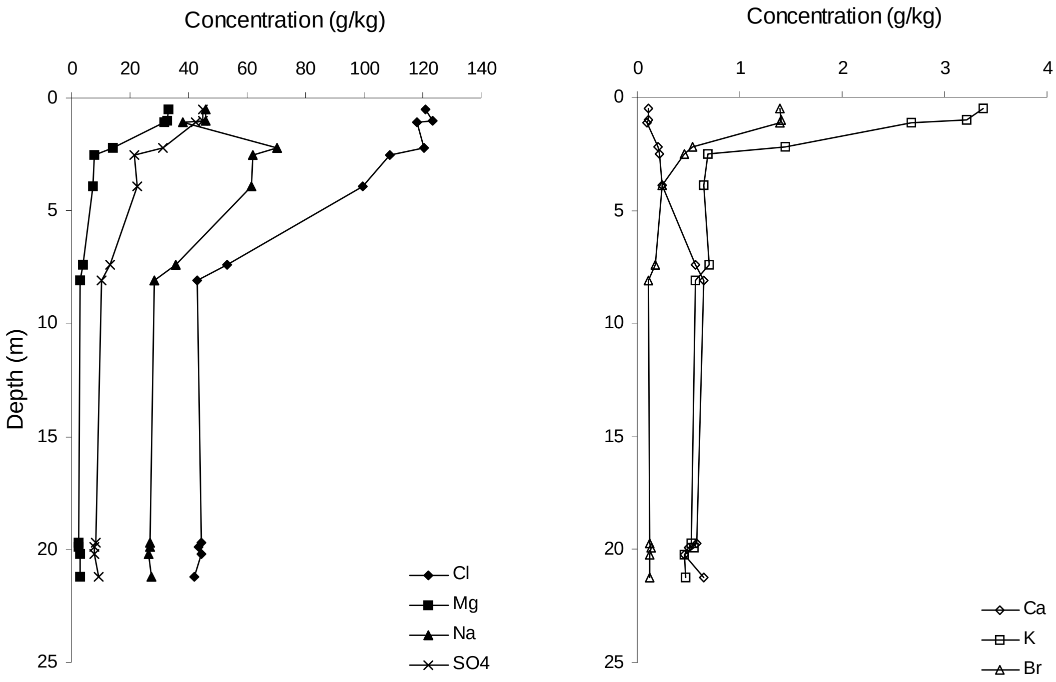

(a) Edge of Pond 3 (SM1)

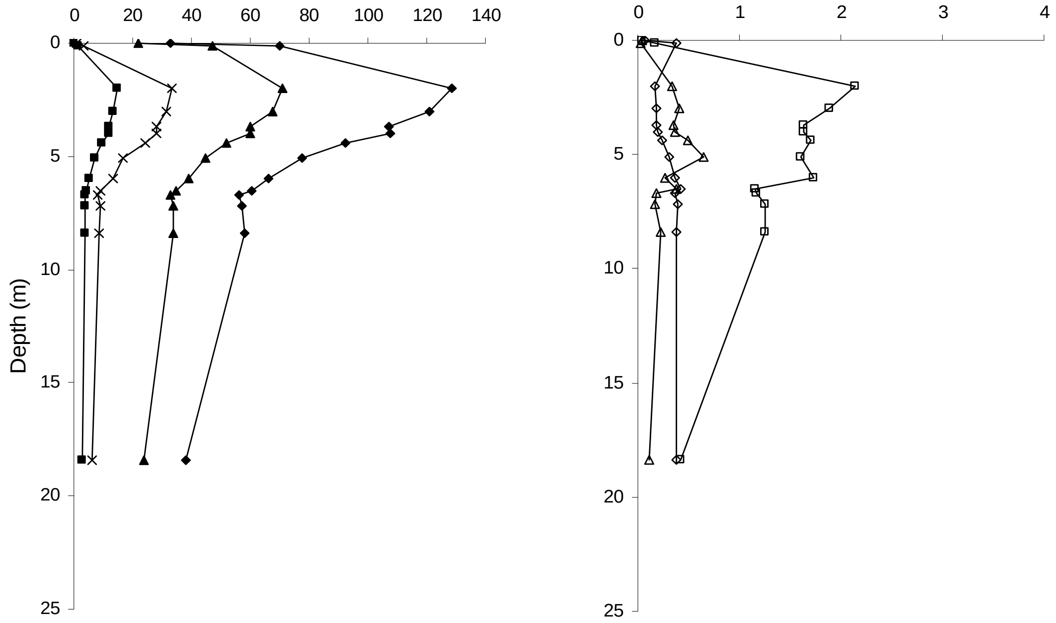

(b) Centre of Pond 2 (SM5)

Figure 3.4. Ion concentration versus depth profiles for (a) the edge of Pond 3 and (b) the centre of Pond 2 at Spectacle Lake. Analyses were of pore water extracted from sediments, however, the values at 18.4 m depth at the centre of Pond 2 were of groundwater obtained from piezometer SM6.

### 3.4.8 Major Ions Versus Brine Concentration Factor ([$Br^-$])

One way of identifying relationships between different water types and the processes influencing their chemical compositions is by examining changes in major ion concentrations with increasing concentration factor. Conservative evapo-concentration and two end-member mixing processes produce linear trends on plots of ion concentration vs the concentration factor of the water sample. Deviations from these straight evaporation/mixing lines indicate addition or removal of solutes as a result of chemical reactions, such as mineral dissolution or precipitation, or mixing with a third end-member. Chloride concentrations ([$Cl^-$]) are often used to represent the concentration factor of a water sample due to the normally conservative nature of the $Cl^-$ ion. However, halite (NaCl) is present as surface salt crusts and efflorescences in many of the lakes at Raak Plain (Section 3.4.6), and $Cl^-$ cannot be expected to behave conservatively where the ion activity product of NaCl is above halite saturation. Bromide, like chloride, is not involved in most mineral-solution reactions, and it also tends to be excluded from evaporite minerals, making it a more conservative chemical tracer than $Cl^-$ in hyper-saline environments. As Raak Plain is an evaporative environment, linear trends would be expected on ion concentration vs [$Br^-$] plots (Figs. 3.5 – 3.10), with dilute inflow waters as low concentration end-members and the hyper-saline brines as the high concentration end-members. Different degrees of evapo-concentration and mixing between these end-members will cause a linear distribution of points.

Plots of ion concentrations vs [$Br^-$], (Figs. 3.5 - 3.10) show that shallow groundwaters below the dunes between the playas (R2 and R4) have similar compositions to Parilla Sand groundwater in the eastern half of the discharge

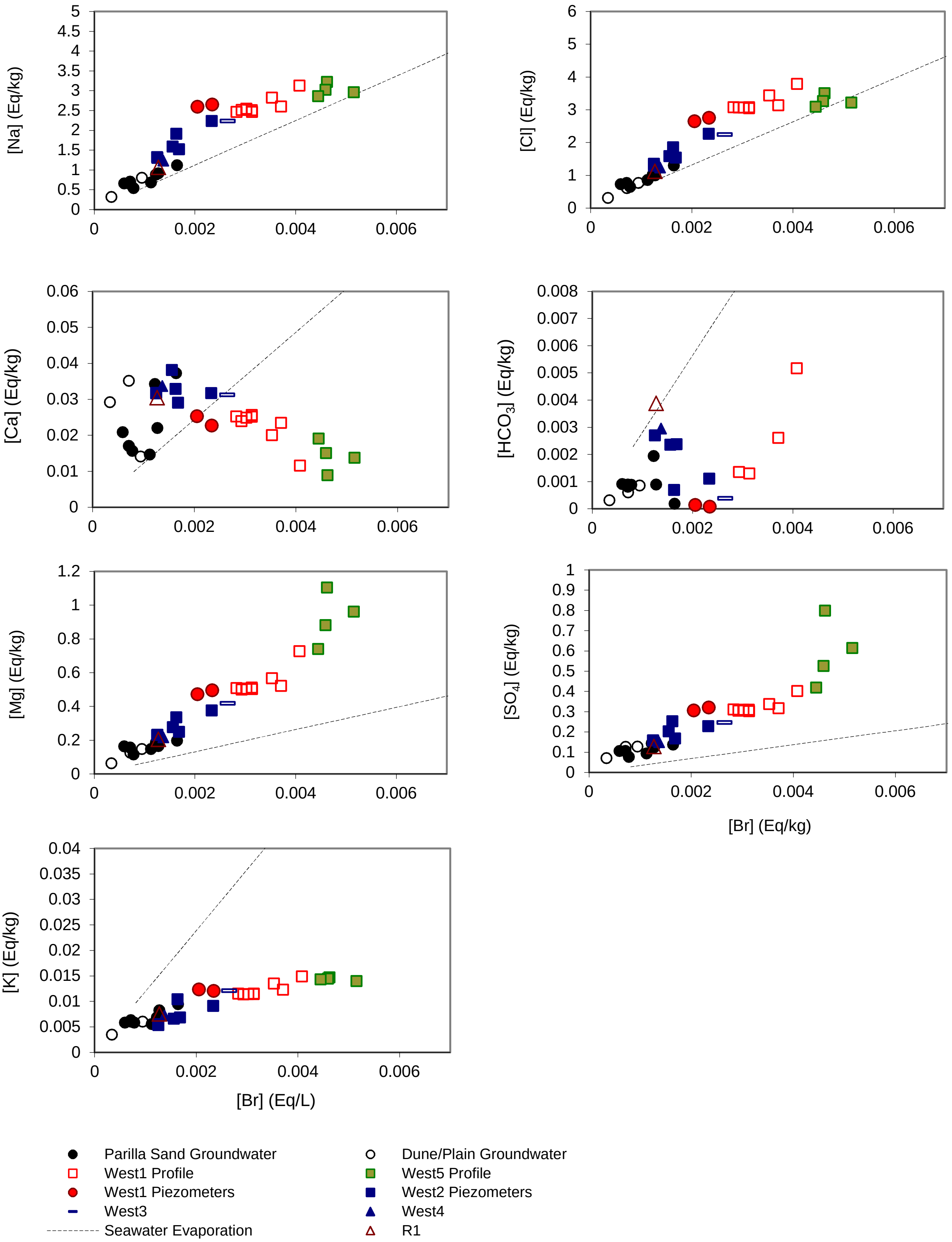

Figure 3.5. Major ion versus bromide plots for pore waters and groundwaters from Western Salina. Sample locations are shown on Figure 3.11. Regional Parilla Sand groundwater and shallow groundwater from below dunes and plains between the playas are shown for reference. The seawater evaporation line represents the evapo-concentration of seawater, in the absence of mineral precipitation.

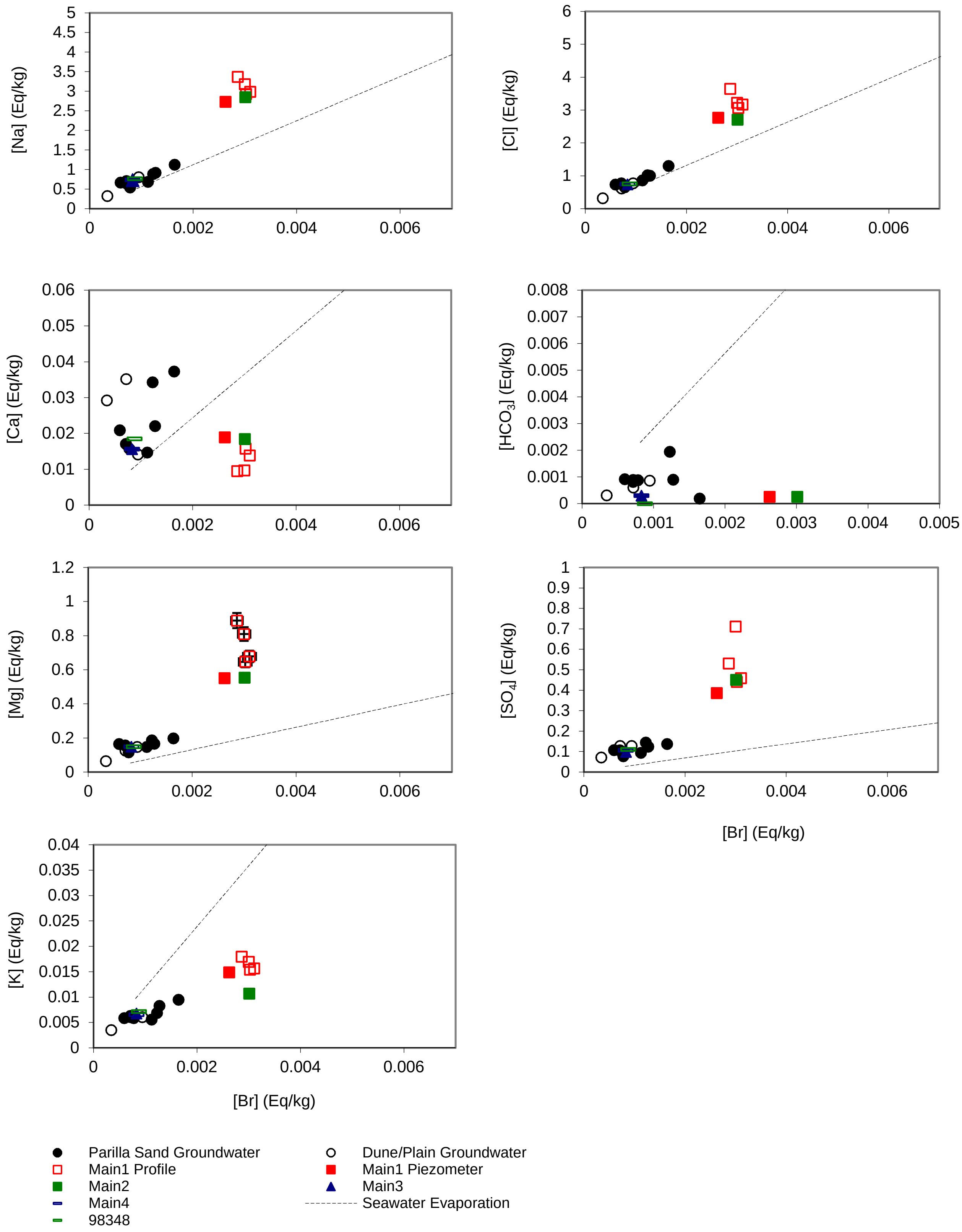

Figure 3.6. Major ion versus bromide plots for pore waters and groundwaters from the Main Salina. Sample locations are shown on Figure 3.12. Regional Parilla Sand groundwater and shallow groundwater from below dunes and plains between the playas are shown for reference. The seawater evaporation line represents the evapo-concentration of seawater, in the absence of mineral precipitation.

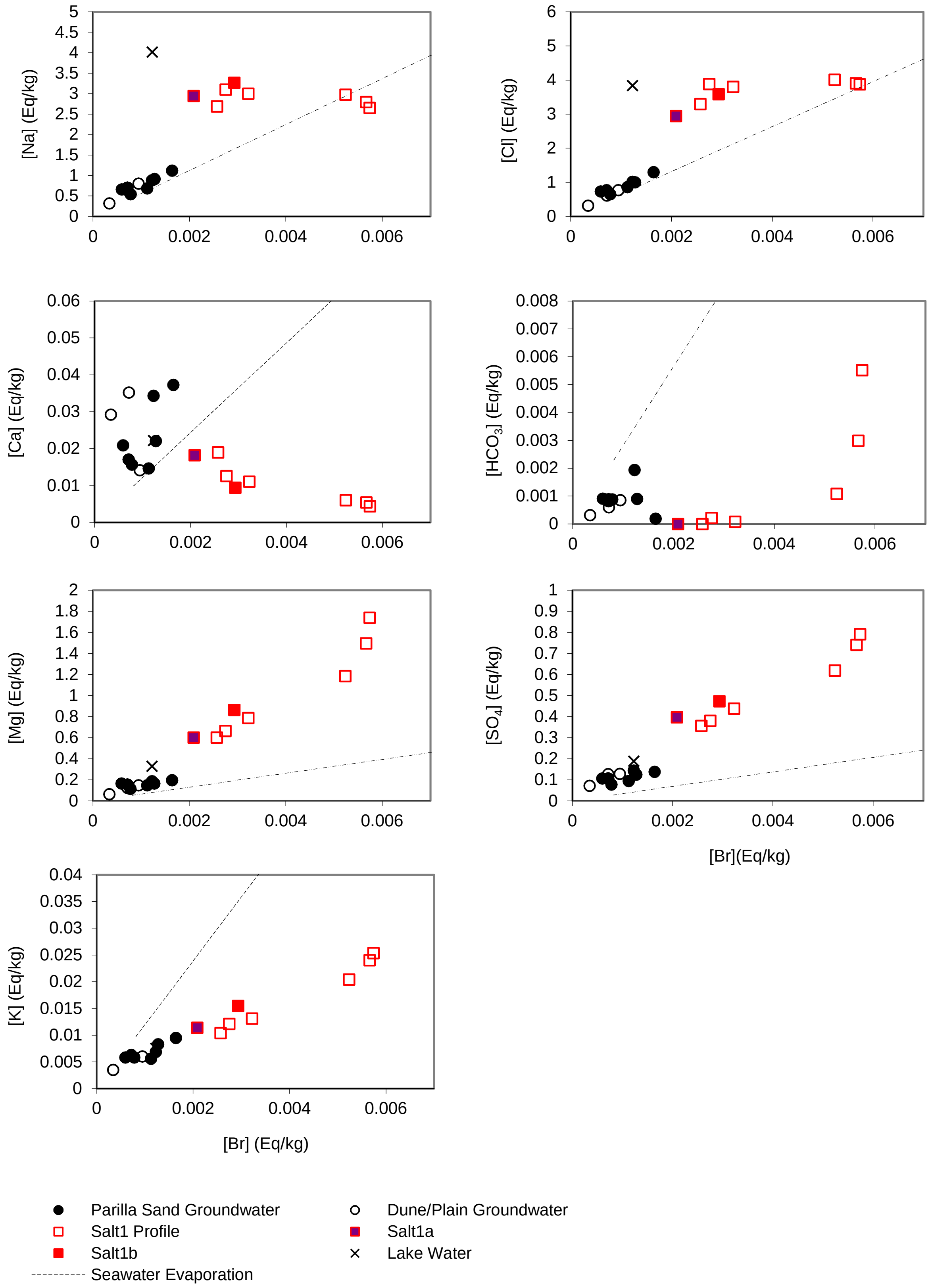

Figure 3.7. Major ion versus bromide plots for pore waters and groundwaters from Salt Lake. Samples were collected from one site at the centre of the playa, with a maximum depth of 2.6 m. Regional Parilla Sand groundwater and shallow groundwater from below dunes and plains between the playas are shown for reference. The seawater evaporation line represents the evapo-concentration of seawater, in the absence of mineral precipitation.

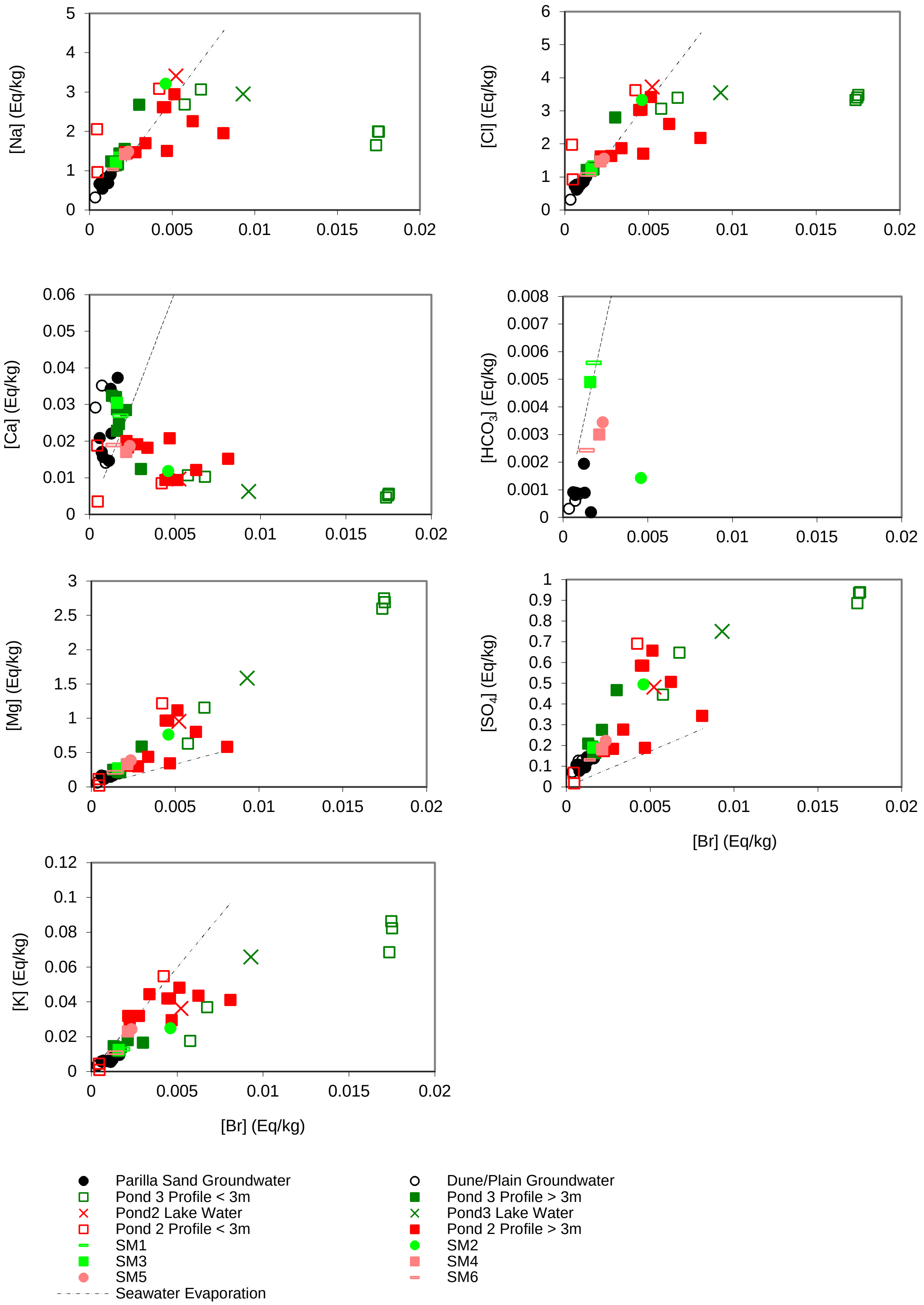

Figure 3.8. Major ion versus bromide plots for pore waters and groundwaters from Spectacle Lake, including data from both the centre of Pond 2 and the edge of pond 3. Sample locations are shown on Figure 3.13. Regional Parilla Sand groundwater and shallow groundwater from below dunes and plains between the playas are shown for reference. The seawater evaporation line represents the evapo-concentration of seawater, in the absence of mineral precipitation.

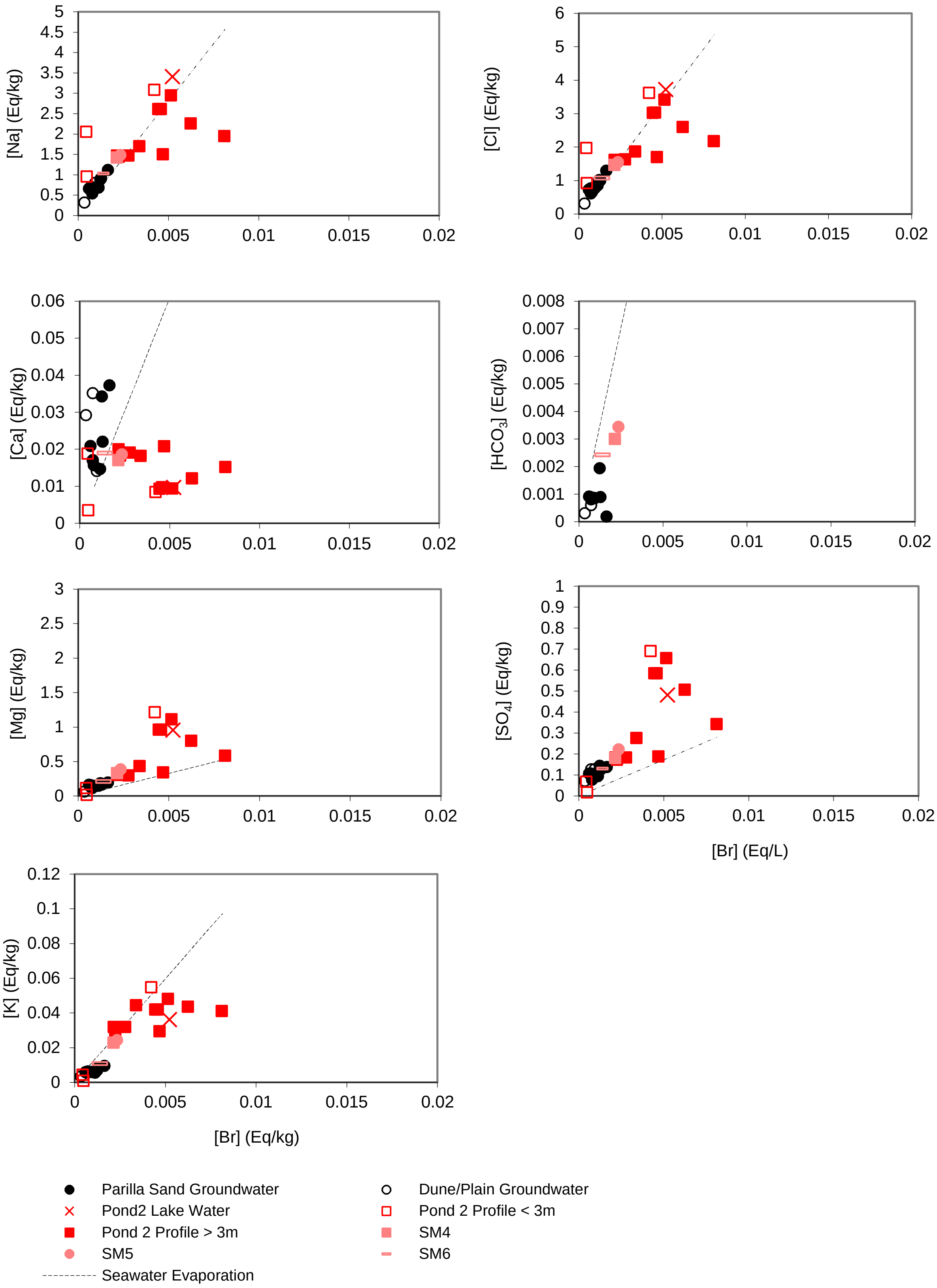

Figure 3.9. Major ion versus bromide plots for pore waters and groundwaters from Spectacle Lake (centre of Pond 2 only). Sample locations are shown on Figure 3.13. Regional Parilla Sand groundwater and shallow groundwater from below dunes and plains between the playas are shown for reference. The seawater evaporation line represents the evapo-concentration of seawater, in the absence of mineral precipitation.

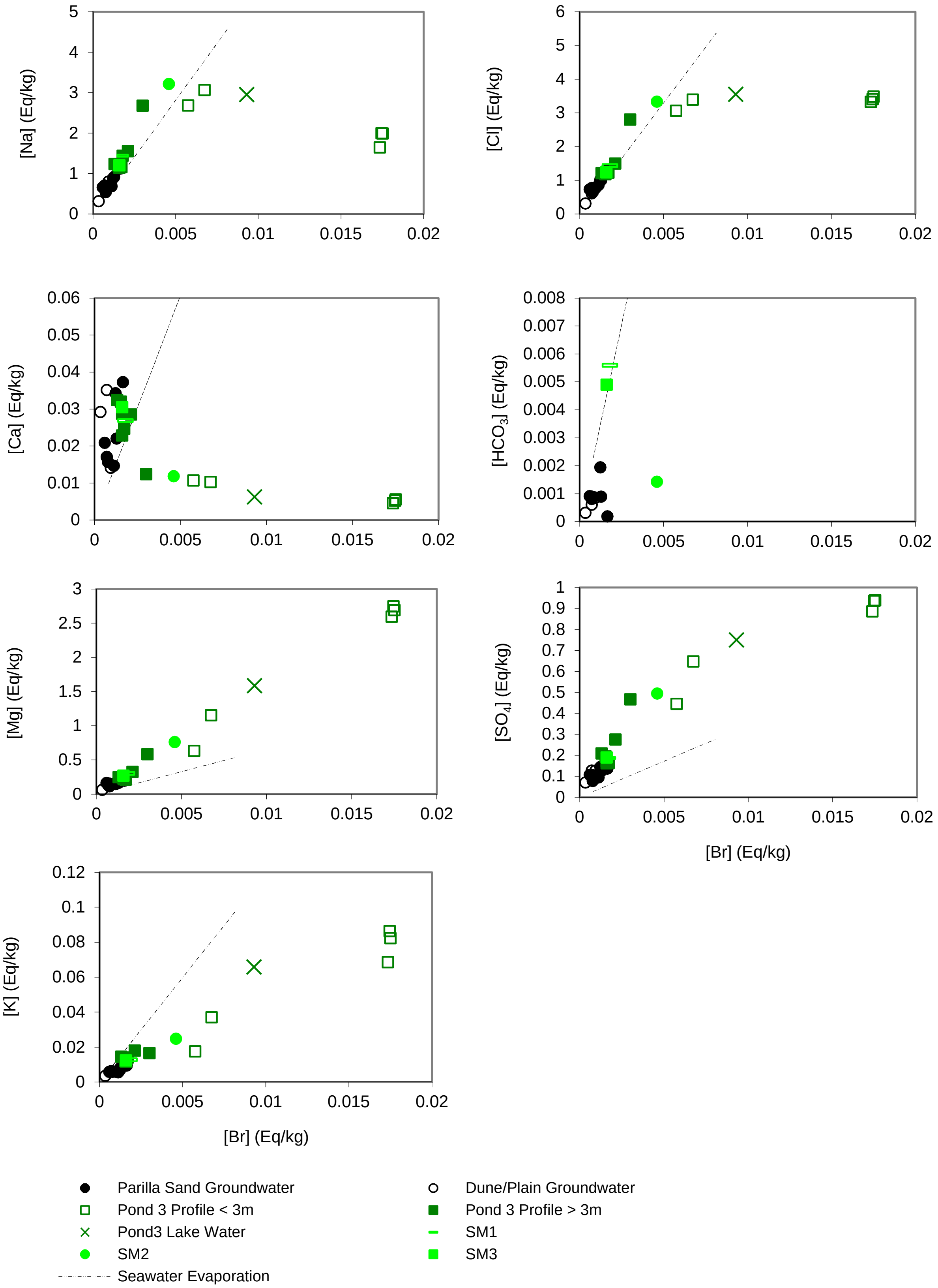

Figure 3.10. Major ion versus bromide plots for pore waters and groundwaters from Spectacle Lake (edge of Pond 3 only. Sample locations are shown on Figure 3.11. Regional Parilla Sand groundwater and shallow groundwater from below dunes and plains between the playas are shown for reference. The seawater evaporation line represents the evapo-concentration of seawater, in the absence of mineral precipitation.

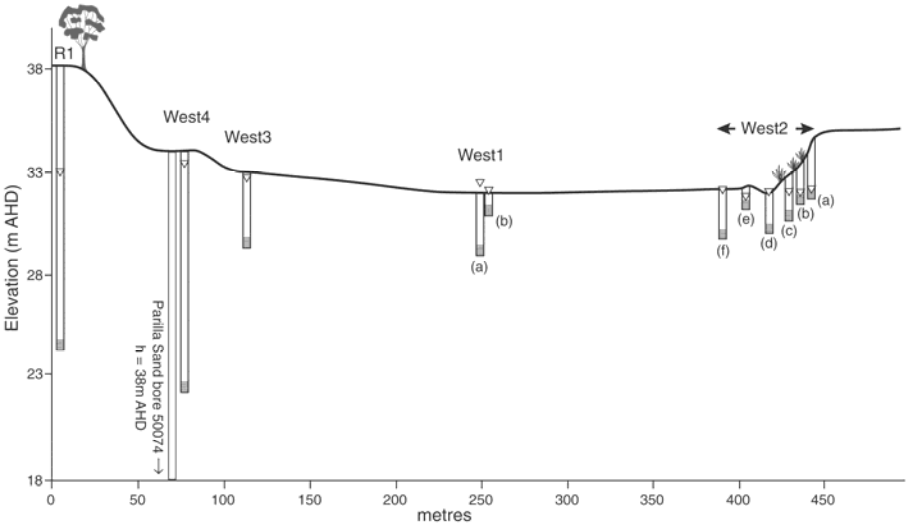

Figure 3.11. Cross sectional view of sampling locations at Western Salina. See Figure 2.1 for piezometer locations in plan view.

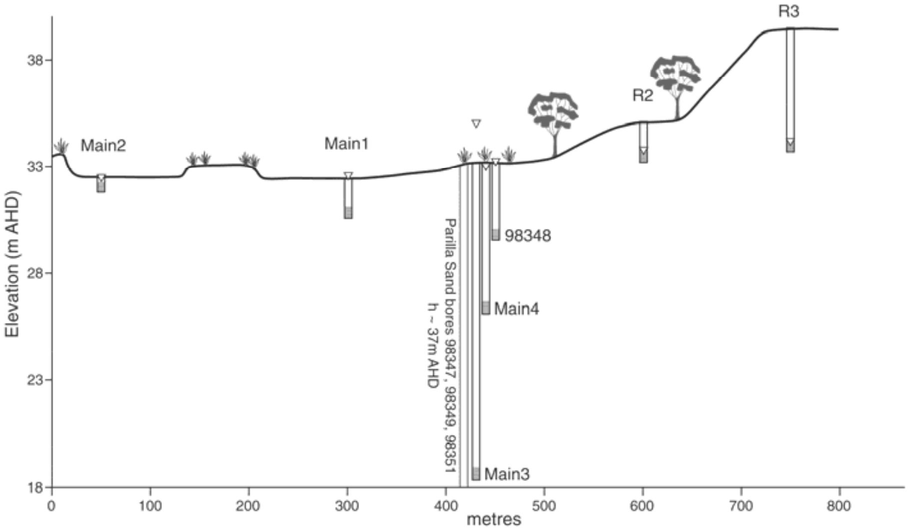

Figure 3.12. Cross sectional view of sampling locations at the Main Salina. See Figure 2.1 for piezometer locations in plan view.

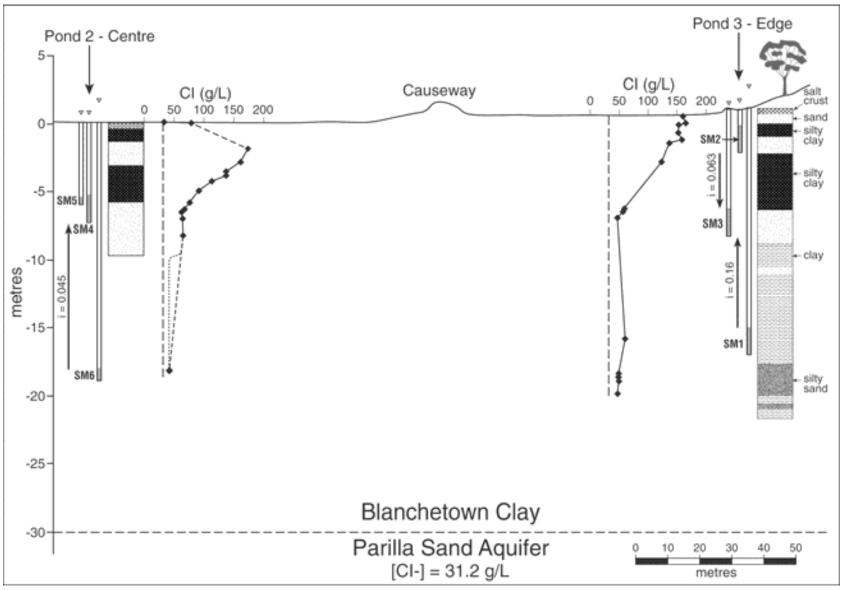

Figure 3.13. Cross sectional view of sampling locations at Spectacle Lake,also showing pore water [$Cl^{-]}$ vs depth from Figure 3.4. See Figure 2.2 for piezometer locations in plan view.

complex (bores 26240, 98347, 98349, 98351), whereas shallow groundwater from on top of a sand dune (R3) generally has a lower [$Br^-$]. As discussed in Section 3.4.4, although R2, R3 and R4 are all probably locally recharged groundwaters, R2 and R4 have probably undergone greater degrees of evapotranspiration leading to their higher concentration factors. The overall salinity of the Parilla Sand groundwater increases along an east-west transect across Raak Plain (see Fig.3.3), resulting in a spread of data in Figures 3.5 to 3.10. This may be due to addition of salt from the subsurface brines associated with the overlying discharge complex, something that willbeinvestigated in subsequent sections of this thesis. One exception is that the salinity in bore 50075, located at the western margin of Raak Plain, is lower than in bore 50074 (below Western Salina), which is up-gradient of it. However, bore 50075 is located slightly to the south of transect AA', near the southern margin of the discharge complex, and is hence probably less affected by mixing with the brines.

[$Na^+$], [$Cl^-$], [$Mg^{2+}$], [$SO_4^{2-}$] and [$K^+$] are approximately linearly correlated with [$Br^-$] for all of the playa lakes, suggesting the occurrence of evaporation and / or mixing processes with regional and locally recharged groundwater as the low salinity end-member and the most saline brines as the high salinity end-members. However, some significant deviations from the linear trends suggest mineral precipitation / dissolution processes. In addition, alkalinities (as [$HCO_3^-$]) are generally very low compared with the other ions and do not correlate well with [$Br^-$], and decreasing [$Ca^{2+}$] with increasing [$Br^-$] in all of the lakes suggests precipitation of a $Ca^{2+}$ evaporite mineral, possibly gypsum.

### 3.4.9 Mineral Saturation Indices

To assist with the interpretation of the major ion versus [$Br^-$] diagrams in terms of mineral precipitation and dissolution reactions, saturation states of the brines were calculated using the computer code, PHRQPITZ (Plummer et al., 1988). Table 3.2 shows saturation indices (SI) of various minerals calculated for a range of water samples from each of the playa lakes at Raak Plain. Commonly used methods for calculating activity coefficients, such as the Davies equation, are not applicable in solutions with ionic strengths (I) greater than about 0.5. PHRQPITZ uses the virial coefficient approach of Pitzer (1973) and Harvie and Weare (1980) to calculate ion activities for solutions with high ionic strengths, and the database of Plummer et al. (1988) to calculate saturation indices and the distributions of major aqueous species.

There are a number of uncertainties in the analytical and thermodynamic data used in these calculations, as well as in the field measurement of pH in such saline brines (Plummer et al., 1988). Therefore, the saturation indices calculated can be used only as an approximate guide to those minerals that are most likely to precipitate or be dissolved. Furthermore, actual mineral precipitation and dissolution is controlled by the kinetics of the reaction and those processes that are implied thermodynamically may not actually occur if they are very slow kinetically. With this in mind, equilibrium between the mineral solid phase and the solution is assumed for SI's between –0.5 and 0.5, and supersaturation is assumed for values greater than 0.5. Values between –1.0 and –0.5 are interpreted as being potentially in equilibrium (i.e. borderline). In these cases, mineral precipitation / dissolution reactions are implied as controls over the concentrations of the relevant constituents in solution. The minerals shown in Table 3.2 were selected based on those identified to be important

Table 3.2. Mineral saturation indices calculated for various pore water and groundwater samples at Raak Plain using PHRQPITZ. Values considered to be at or near saturation with respect to a mineral (SI > -0.5) are shown in bold. Values between –1.0 and –0.5 are also considered to be borderline.

| **(a) Western Salina** | | **R1** | **West4** | **West3** | **West1a** | **West1b** | **West1 Profile** | | **West5 Profile** | |
|---|---|---|---|---|---|---|---|---|---|---|
| Depth (m) | | 13.3-13.8 | 11-12 | 3.3-3.8 | 2.5-3.0 | 0.7-1.2 | 2.3-2.7 | 2-4 cm | 6-8 cm | 2-4 cm |
| **Anhydrite** | $CaSO_4$ | -0.6 | **-0.5** | **-0.3** | **-0.3** | **0.5** | **-0.2** | **-0.3** | **-0.2** | **-0.1** |
| **Aragonite** | $CaCO_3$ | -0.7 | -1.0 | -2.0 | -2.9 | -1.6 | -0.9 | **-0.1** | -1.4 | -0.7 |
| **Calcite** | $CaCO_3$ | **-0.5** | -0.8 | -1.8 | -2.7 | -1.4 | -0.7 | **-0.1** | -1.2 | **-0.5** |
| **Dolomite** | $CaMg(CO_3)_2$ | **0.0** | **-0.5** | -2.1 | -3.8 | -0.9 | **0.4** | **2.5** | **-0.5** | **1.2** |
| **Epsomite** | $MgSO_4 \cdot 7H_2O$ | -2.2 | -2.2 | -1.8 | -1.6 | -1.0 | | -1.3 | -1.3 | -1.0 |
| **Glauberite** | $Na_2Ca(SO_4)_2$ | -2.3 | -2.1 | -1.3 | -1.0 | **0.2** | -0.8 | **-0.5** | -0.6 | **-0.3** |
| **Gypsum** | $CaSO_4 \cdot 2H_2O$ | **-0.4** | **-0.3** | **-0.2** | **-0.2** | **0.6** | **-0.1** | **-0.2** | **-0.1** | **-0.0** |
| **Halite** | $NaCl$ | -1.8 | -1.7 | -1.0 | -0.8 | **-0.2** | -0.6 | **-0.3** | -0.6 | **-0.4** |
| **Magnesite** | $MgCO_3$ | **-0.3** | **-0.5** | -1.1 | -1.9 | **-0.3** | **0.2** | **1.5** | **1.6** | **1.0** |
| **Mirabilite** | $Na_2SO_4 \cdot 10H_2O$ | -1.5 | -1.4 | -1.0 | -0.7 | -1.0 | -0.8 | -0.7 | -0.7 | -0.6 |
| **$PCO_2$** | | -1.9 | -1.9 | -2.5 | -2.0 | -3.0 | -2.5 | -2.5 | -3.9 | -2.3 |

| **(b) Main Salina** | | **Main4** | **Main2** | **Main1** | **Main1 Profile** | | |
|---|---|---|---|---|---|---|---|
| Depth (m) | | 6.5-7.0 | 0.4-0.5 | 1.5-2.0 | 0.3-0.35 | 2-4 cm | 0-2 cm |
| **Anhydrite** | $CaSO_4$ | -0.9 | **-0.2** | **-0.3** | **-0.3** | **-0.2** | **-0.2** |
| **Aragonite** | $CaCO_3$ | -2.8 | -1.6 | -5.2 | -5.3 | -5.3 | -5.4 |
| **Bischofite** | $MgCl_2 \cdot 6H_2O$ | -6.8 | -4.6 | -4.6 | -4.5 | -3.8 | -4.1 |
| **Bloedite** | $Na_2Mg(SO_4)\ 5H_2O$ | -4.8 | -2.2 | -2.3 | -2.2 | -1.4 | -1.4 |
| **Calcite** | $CaCO_3$ | -2.6 | -1.4 | -5.0 | -5.1 | -5.1 | -5.2 |
| **Dolomite** | $CaMg(CO_3)_2$ | -4.0 | -0.9 | -8.0 | -8.1 | -7.7 | -8.0 |
| **Epsomite** | $MgSO_4 \cdot 7H_2O$ | -2.3 | -1.4 | -1.5 | -1.4 | -1.1 | -1.0 |
| **Glauberite** | $Na_2Ca(SO_4)_2$ | -2.9 | -0.7 | -0.8 | -0.8 | **-0.3** | **-0.3** |
| **Gypsum** | $CaSO_4 \cdot 2H_2O$ | -0.6 | **-0.1** | **-0.2** | **-0.2** | **-0.2** | **-0.2** |
| **Halite** | $NaCl$ | -2.1 | -0.7 | -0.7 | -0.6 | **-0.3** | **-0.4** |
| **Magnesite** | $MgCO_3$ | -2.2 | **-0.3** | -11.7 | -3.9 | -3.5 | -3.6 |
| **Mirabilite** | $Na_2SO_4 \cdot 10H_2O$ | -1.7 | -0.7 | -2.1 | -0.7 | -0.6 | **-0.5** |
| **$PCO_2$** | | -1.6 | -2.9 | -3.3 | -1.9 | -1.9 | -1.9 |

| **(c) Salt Lake** | | **Salt1a** | **Salt1b** | **Salt1 Profile** | | | | **Lake Water** |
|---|---|---|---|---|---|---|---|---|
| Depth (m) | | 2.1-2.6 | 0.2-0.5 | 2.55-2.63 | 0.5-0.55 | 4-6 cm | 0-2 cm | |
| **Anhydrite** | $CaSO_4$ | **-0.2** | **-0.3** | **-0.2** | **-0.2** | **-0.3** | **-0.3** | **-0.1** |
| **Aragonite** | $CaCO_3$ | -3.8 | -3.9 | -3.8 | -3.2 | -1.7 | -1.6 | -4.3 |
| **Bischofite** | $MgCl_2{\cdot}6H_2O$ | -4.4 | -3.8 | -4.3 | -3.9 | -3.5 | -3.2 | -4.1 |
| **Bloedite** | $Na_2Mg(SO_4)\ 5H_2O$ | -2.2 | -1.5 | -2.2 | -1.6 | -1.0 | -0.7 | -2.4 |
| **Calcite** | $CaCO_3$ | -3.6 | -3.7 | -3.6 | -3.0 | -1.6 | -1.5 | -4.1 |
| **Dolomite** | $CaMg(CO_3)_2$ | -5.3 | -5.1 | -5.2 | -3.6 | **-0.3** | **0.2** | -6.6 |
| **Epsomite** | $MgSO_4{\cdot}7H_2O$ | -1.4 | -1.1 | -1.5 | -1.2 | -0.9 | -0.6 | -1.9 |
| **Glauberite** | $Na_2Ca(SO_4)_2$ | -0.7 | **-0.5** | -0.7 | **-0.4** | **-0.2** | **-0.3** | **-0.5** |
| **Gypsum** | $CaSO_4{\cdot}2H_2O$ | **-0.1** | **-0.2** | **-0.1** | **-0.2** | **-0.2** | **-0.3** | **-0.1** |
| **Halite** | NaCl | -0.6 | **-0.3** | **-0.5** | **-0.3** | **-0.1** | **-0.2** | **-0.1** |
| **Magnesite** | $MgCO_3$ | -2.5 | -2.2 | -2.5 | -1.5 | **0.4** | **0.9** | -3.3 |
| **Mirabilite** | $Na_2SO_4{\cdot}10H_2O$ | **-0.5** | **-0.4** | -0.8 | -0.7 | -0.6 | -0.7 | -1.0 |
| **$PCO_2$** | | -1.8 | -1.8 | -3.2 | -2.8 | -2.2 | -1.0 | -2.3 |

| **(d) Spectacle Lake – Pond 2** | | **SM6** | **SM5** | **SM5 Profile** | | | |
|---|---|---|---|---|---|---|---|
| Depth (m) | | 18.0-18.8 | 5.5-6.0 | 5.1-5.2 | 2.0-2.1 | 0.1-0.2 | 0-0.1 |
| **Anhydrite** | $CaSO_4$ | -0.8 | -0.7 | **-0.5** | **-0.2** | -1.1 | -2.2 |
| **Aragonite** | $CaCO_3$ | -2.3 | -2.0 | -2.0 | -2.0 | -1.9 | -2.6 |
| **Bischofite** | $MgCl_2{\cdot}6H_2O$ | -6.4 | -5.8 | -5.1 | -3.6 | -6.0 | -7.6 |
| **Bloedite** | $Na_2Mg(SO_4)\ {\cdot}5H_2O$ | -4.4 | -3.6 | -2.8 | -1.1 | -4.8 | -7.0 |
| **Calcite** | $CaCO_3$ | -2.1 | -1.8 | -1.8 | -1.8 | -1.7 | -2.4 |
| **Dolomite** | $CaMg(CO_3)_2$ | -2.8 | -2.0 | -1.6 | -0.9 | -2.2 | -3.9 |
| **Epsomite** | $MgSO_4{\cdot}7H_2O$ | -2.2 | -1.8 | -1.5 | -0.9 | -2.8 | -3.9 |
| **Glauberite** | $Na_2Ca(SO_4)_2$ | -2.6 | -2.0 | -1.5 | **-0.2** | -2.6 | -4.8 |
| **Gypsum** | $CaSO_4{\cdot}2H_2O$ | -0.6 | **-0.5** | **-0.4** | **-0.1** | -0.9 | -2.0 |
| **Halite** | NaCl | -1.8 | -1.5 | -1.1 | **-0.3** | -1.2 | -1.9 |
| **Magnesite** | $MgCO_3$ | -1.6 | -1.0 | -0.7 | **0.1** | -1.4 | -2.3 |
| **Mirabilite** | $Na_2SO_4{\cdot}10H_2O$ | -1.4 | -1.1 | -0.9 | -0.6 | -1.4 | -2.2 |
| **$PCO_2$** | | -1.6 | -1.6 | -1.6 | -1.7 | -1.6 | -1.6 |

| **(e) Spectacle Lake – Pond 3** | | **SM1** | **SM3** | **SM2** | **SM1 Profile** | | |
|---|---|---|---|---|---|---|---|
| Depth (m) | | 16.1-18.1 | 6.6-8.6 | 0.7-2.7 | 3.9-4.0 | 2.2-2.3 | 0.5-1.0 |
| **Anhydrite** | $CaSO_4$ | -0.6 | **-0.5** | **-0.3** | **-0.4** | **-0.2** | **-0.3** |
| **Aragonite** | $CaCO_3$ | -1.2 | -0.9 | -2.2 | -2.3 | -2.3 | -2.7 |
| **Bischofite** | $MgCl_2\cdot 6H_2O$ | -6.0 | -6.2 | -4.1 | -4.6 | -3.8 | -3.1 |
| **Bloedite** | $Na_2Mg(SO_4)\ 5H_2O$ | -6.2 | -4.0 | -1.7 | -2.2 | -1.3 | -0.8 |
| **Calcite** | $CaCO_3$ | -9.4 | -0.7 | -2.0 | -2.1 | -2.1 | -2.5 |
| **Dolomite** | $CaMg(CO_3)_2$ | -17.6 | **-0.2** | -1.7 | -2.1 | -1.6 | -1.7 |
| **Epsomite** | $MgSO_4\cdot 7H_2O$ | -3.9 | -2.0 | -1.2 | -1.4 | -0.9 | **-0.4** |
| **Glauberite** | $Na_2Ca(SO_4)_2$ | -7.2 | -2.0 | **-0.5** | -0.9 | **-0.3** | **-0.5** |
| **Gypsum** | $CaSO_4\cdot 2H_2O$ | -4.9 | **-0.3** | **-0.2** | **-0.3** | **-0.1** | **-0.3** |
| **Halite** | NaCl | **0.0** | -1.7 | **-0.4** | -0.7 | **-0.4** | **-0.3** |
| **Magnesite** | $MgCO_3$ | -8.2 | **-0.3** | -0.6 | -0.8 | **-0.4** | **-0.1** |
| **Mirabilite** | $Na_2SO_4\cdot 10H_2O$ | -2.6 | -1.2 | -0.6 | -0.6 | **-0.5** | -0.8 |
| **PCO$_2$** | | -1.8 | -2.2 | -2.0 | -2.0 | -2.0 | -1.9 |

by the PHRQPITZ calculations, mineralogy results (Section 3.4.6) or inferred mineral controls based on interpretation of Figures 3.5 to 3.10. For waters with very low pH, and with zero alkalinity, calculations could not be carried out using PHRQPITZ. Based on the saturation index calculations, all of the solutions are in equilibrium with gypsum ($CaSO_4 \cdot 2H_2O$) and anhydrite ($CaSO_4$), with the exception of two shallow (but comparatively fresh) brine samples in Pond 2 at Spectacle Lake and the deep piezometer, SM1, at the edge of Pond 3. Some of the waters are saturated with respect to various carbonate minerals, particularly dolomite ($CaMg(CO_3)_2$) and magnesite ($MgCO_3$) in the near-surface (top 10 cm) brines at Western Salina and Salt Lake. The shallow (< 3 m deep) brines are also at equilibrium with respect to halite (NaCl), mirabilite ($Na_2SO_4 \cdot 10H_2O$) and glauberite ($Na_2Ca(SO_4)_2$), with the exception of the top 20 cm of the profile at the centre of Pond 2 at Spectacle Lake.

## 3.5 Discussion

### 3.5.1 Origins of the Brines and Intermediate TDS Groundwaters

One factor known to be a major control on brine evolution in salt lakes is the hydrochemistry of the inflow water (Garrels and Mackenzie, 1967; Hardie and Eugster, 1970; Herczeg and Lyons, 1991). Unlike large salt lake systems such as the Tyrrell Basin (Macumber, 1991), also in western Victoria (Section 3.3), and Great Salt Lake, Utah, USA (Spencer et al., 1985 (a&b); Section 3.2.2), there are no surface inflows to the lakes at Raak Plain. Topographic relief is extremely low, and the surface water catchments of the lakes are limited to the lakes themselves and surrounding dunes. Being a regional groundwater discharge complex, however, the groundwater catchment for the playas is a large portion of the Murray Basin.

Potential sources of salt and water to the playas are therefore discharge from the regional Parilla Sand aquifer, and local recharge through the playa surfaces and sand dunes around their margins. Despite their vastly different catchment sizes, however, the chemical compositions of these two sources are extremely similar to each other, as well as to seawater (Fig. 3.2).

The Raak Plain data have a generally linear distribution on Figures 3.5 to 3.10, which can be explained as being the result of (a) different degrees of evapo-concentration of a low TDS source water, (b) linear mixing between a low salinity end-member and a high salinity end-member, or (c) a combination of both (a) and (b). The regional and locally recharged groundwaters plot as low-concentration (low [$Br^-$]) end-members on these evaporation / mixing trends whilst the shallow playa lake brines plot as the high [$Br^-$] end-members. Hence, different degrees of evapo-concentration of regional and / or locally recharged groundwaters may have formed the hypersaline brines at Raak Plain as well as the groundwaters with intermediate TDS concentrations. Because of their similar compositions, with the exception of [$Ca^{2+}$], it is difficult to distinguish between the Parilla Sand groundwater and locally recharged groundwater on these diagrams and hence determine which could be the true low-salinity end-member for the formation of the brines.

Despite the similarities in their major ion compositions, there are subtle variations in the chemical compositions of the brines, Parilla Sand groundwater and locally recharged groundwater at Raak Plain, as shown in their ion ratios (Table 3.3). The groundwaters have molar Br/Cl ratios ranging from $0.8 \times 10^{-3}$ to $1.5 \times 10^{-3}$. All of these are less than or equal to the seawater value of $1.5 \times 10^{-3}$ and, given the predominantly oceanic origin of the dissolved salts, this suggests a net addition of chloride via dissolution of chloride minerals during the evolution of these groundwaters. Similarly, the low $Ca/SO_4$ ratios of the shallow playa lake brines compared with the two potential sources indicate gypsum precipitation, as was identified from the ion vs [Br] graphs (3.5.3.2). Despite the large ranges in ionic ratios, it is still difficult to distinguish the Parilla Sand groundwater from the locally recharged groundwater and hence identify the source of the shallow brines, particularly as mineral-solution reactions appear to have overprinted the ionic ratios.

Table 3.3. Ion ratios of Parilla Sand groundwaters, locally recharged groundwaters and shallow playa lake brines. Shallow brine data is for the summer composition of pore water brines just below the lake floors (2-4 cm unless otherwise specified) at the center of each lake. Ratios are as molar ratios.

| | Br/Cl ($x10^{-3}$) | Na/Cl | $SO_4$/Cl | Ca/$SO_4$ | (Na+K) / (Ca+Mg) |
|---|---|---|---|---|---|
| Seawater | 1.5 | 0.9 | 0.04 | 0.4 | 3.7 |
| Parilla Sand | | | | | |
| 26240 | 1.2 | 0.8 | 0.06 | 0.2 | 8.3 |
| 81945 | 1.3 | 0.8 | 0.05 | 0.2 | 8.5 |
| 98347 | 1.5 | 0.9 | 0.07 | 0.2 | 8.1 |
| 98349 | 0.8 | 0.9 | 0.07 | 0.2 | 7.2 |
| 98351 | 0.9 | 0.9 | 0.07 | 0.15 | 8.2 |
| 50073 | 1.3 | 0.9 | 0.06 | 0.2 | 9.8 |
| 50074 | 1.3 | 0.9 | 0.05 | 0.3 | 9.6 |
| 50075 | 1.2 | 0.9 | 0.07 | 0.2 | 8.1 |
| Local Recharge | | | | | |
| R1 | 1.1 | 1.0 | 0.06 | 0.2 | 9.4 |
| R2 | 1.2 | 1.0 | 0.10 | 0.3 | 7.6 |
| R3 | 1.1 | 1.0 | 0.12 | 0.4 | 6.9 |
| R4 | 1.2 | 1.0 | 0.08 | 0.1 | 9.9 |
| Shallow Brines | | | | | |
| Western Salina | 1.1 | 0.8 | 0.05 | 0.03 | 8.5 |
| Main Salina | 0.8 | 0.9 | 0.07 | 0.02 | 7.5 |
| Salt Lake | 1.5 | 0.7 | 0.10 | 0.01 | 3.8 |
| Spectacle Lake* | 1.2 | 0.85 | 0.10 | 0.01 | 5.1 |

*Data from 200 cm depth (maximum concentration below salt crust).

Alternatively to being formed by different degrees of evapo-concentration, the intermediate TDS groundwaters may have formed via back-mixing between the highly evapo-concentrated brines and their low-salinity sources, also resulting in the observed linear distributions in the data. The intermediate TDS groundwaters that occur in the Blanchetown Clay below the Western Salina (e.g. piezometers West2 (a-f), West3 and West4) have similar compositions to some of the Parilla Sand groundwaters, which occur to the south-east (up-gradient) and west of Western Salina respectively (bores 50073 and 50075, Figure 3.5; see Fig. 1.6 for locations). Hence, an entirely regional groundwater origin for these groundwaters is possible. However, the Parilla Sand groundwater directly below Western Salina (bore 50074) has much higher dissolved ion concentrations than the other regional groundwater samples. This suggests that salt accessions from the discharge complex may have impacted the Parilla Sand aquifer below the western half of Raak Plain and hence mixing with a lower salinity groundwater, for example local recharge would be required for this to be a source of the intermediate TDS groundwaters.

Similarly, deep (> 6 m) groundwater in the Blanchetown Clay at the eastern edge of the Main Salina (piezometers Main3 and Main4), and the 4m deep bore 98348 (see Fig. 3.11 for locations) have identical compositions to the Parilla Sand groundwater directly below, suggesting this to be their source (Fig. 3.6). However, with the exceptions of [$Ca^{2+}$] and alkalinity (Fig. 3.5 (c&d)), they also plot with shallow locally recharged groundwaters below the plains adjacent the Main Salina (R2 and R4), suggesting this as a possible source. Groundwaters approximately 17 m and 19 m below the water table at Spectacle Lake (SM1 and SM6), at the edge and centre of the playa respectively, plot with the higher [$Br^-$] regional groundwaters (Figs. 3.7-3.9). Although these deeper groundwaters in the Blanchetown Clay below the playa plot close to the regional groundwater, mixing between regional groundwater or locally recharged groundwater and the brines cannot be eliminated as possibilities for their chemical origins.

### 3.5.2 Back-Diffusion of the Brines

Data from Western Salina generally follow the seawater evaporation line on $[Na^+]$ and $[Cl^-]$ vs $[Br^-]$ diagrams, consistent with no net addition or removal of these solutes from solution at the lake scale (Figs. 3.5 (a&b)). However, deviations from this line occur in the middle salinity ranges, returning to the line at the higher salinities. At first glance, this may appear to be due to evaporite mineral dissolution in these middle salinity ($[Br^-]$) ranges. However, such an addition of solute by mineral dissolution where significant mineral precipitation is not observed introduces a mass balance problem.

The deviations from the linear trends in the ion vs $[Br^-]$ diagrams can be better understood by considering the effects of diffusion in the top 2 m of the sediment profiles. Large concentration gradients occur between the most saline near-surface brines (top 10 cm) and the brines below approximately 1 m below ground level (for example see the salinity vs depth profiles in Appendix G). The concentration gradients are much greater for the most dominant ions, $Na^+$ and $Cl^-$, than for a minor ion such as $Br^-$. Hence, a greater degree of back-diffusion across the top 3 m of the profile may cause higher concentrations of $Na^+$ and $Cl^-$ relative to $Br^-$ in the intermediate brines, i.e. in the West1 piezometers and pore waters below 1 m depth. This hypothesis is supported by calculations of $Cl^-$ and $Br^-$ diffusion from the top 2-4 cm of the profile at West1 ($[Cl^-]$ = 3.793 Eq/kg, $[Br^-]$ = 0.004 Eq/kg) to the screen depth of piezometer West1b (0.75 m below ground level; $[Cl^-]$ = 2.758 Eq/kg, $[Br^-]$ = 0.0023 Eq/kg), using the diffusion only term of the advection-dispersion equation (Fetter, 1994):

$$C(x,t) = C_0 \mathrm{erfc}(x/2\sqrt{D_s t}) \qquad (3.1)$$

Where C(x,t) is the concentration of the ion (above background) at depth, x and time, t, erfc is the complimentary error function and $D_s$ is the bulk sedimentary diffusion coefficient of the ion of interest. $D_s$ accounts for the effect of tortuosity on diffusion rates in sediments and for sediment porosities ($\phi$) ≤ 0.7, $Ds = D_0 \cdot \phi$, where $D_0$ is the free solution diffusion coefficient of the ion of interest (Ullman and Aller, 1982). At 25ºC and 4M NaCl, $D_0^{Cl}$ is 503 $cm^2/y$ (Robinson and Stokes, 1959). In a similarly concentrated solution, $D_0^{Br}$ is 317$cm^2/y$ (Ullman, 1995). For the average porosity of the sediments at West1 of 0.33, $D_s^{Cl}$ and $D_s^{Br}$ are 166 $cm^2/y$ and 105 $cm^2/y$ respectively.

The results of the calculations suggest a time scale of approximately 150 yrs for both $Cl^-$ and $Br^-$ to reach their measured concentrations in piezometer West1b, assuming background concentrations equal to those in the Parilla Sand groundwater (bore 26240; $[Cl^-]$ = 0.651 Eq/kg, $[Br^-]$ = 0.00078 Eq/kg). An uncertainty of approximately 20% has been shown to exist in the estimation of $D_s$ using the method described above (Ullman and Aller, 1982). Hence, this should be kept in mind when evaluating the estimated time scales. However, the calculations show that the differential diffusion rates of $Cl^-$ and $Br^-$ may explain the deviation from the seawater evaporation line in Figure 3.5b. Although the calculations were not carried out for these ions individually, this may also be the case for $Na^+$, $Mg^{2+}$ and $SO_4^{2-}$, which, like $Cl^-$ are charge determining ions and should hence diffuse at the same rate to maintain charge balance. Similar deviations observed in the data from the top 3 m of the playa sediments at Salt Lake and Pond 3 of Spectacle Lake may also be explained by differential diffusion of ions across this depth interval (Figs. 3.7 and 3.10).

### 3.5.3 Mineral Controls on Brine Compositions

#### 3.5.3.1 Controls on Alkalinity

Removal and / or addition of $HCO_3^-$ (and $CO_3^{2-}$) at all of the playas at Raak Plain by carbonate mineral – solution reactions is suggested in some cases by the non-linearity of the alkalinity vs [$Br^-$] graphs in Figures 3.5 to 3.10. For example, the groundwaters around the edges of Western Salina (West4, R1 and some of the West2 transect) have higher alkalinities, as well as a higher [$Ca^{2+}$] than the potential sources due to evapo-concentration (Fig. 3.5 (c&d)). Both West4 and R1, at the edge, and some of the shallow brines at the centre of the playa (West1), are approximately at saturation with respect to calcite and dolomite, supporting the hypothesis that precipitation of these minerals may control the alkalinity in the higher salinity (more evapo-concentrated) groundwaters (Table 3.2).

Some of the near-surface (top 10 cm) brines at Western Salina and Salt Lake are saturated with respect to various carbonate minerals, particularly dolomite ($CaMg(CO_3)_2$) and magnesite ($MgCO_3$) (Table 3.2). These profiles display increases in alkalinity towards the surface, which are probably due to evapo-concentration, but may also be due to small amounts of calcite or Mg-carbonate mineral dissolution. Dissolution of these minerals would cause an increase in [$Ca^{2+}$] with no increasing concentration factor ([$Br^-$]) (Figs. 3.5 and 3.7). However, as alkalinity is low compared with [$Ca^{2+}$], the effect on the latter is minimal. The amount of solid mineral dissolved by this reaction would also only be small. Hence, the precipitation / dissolution of carbonate minerals in the playa lakes at Raak Plain has a minimal effect on the overall chemical compositions of the brines, but is likely to be significant in terms of the interpretation of carbon isotope signatures of the groundwaters and brines (Chapter 6).

In contrast, groundwaters at depths ranging from 4 m to 15 m at the eastern (up-gradient) edge of the Main Salina (Main3, Main4 and 98348; see Fig. 2.1 for locations) have lower alkalinities and [$Ca^{2+}$] than both of the potential sources (Fig. 3.6). These groundwaters are undersaturated with respect to calcite and dolomite, suggesting that something else, for example acid-producing reactions (e.g. $Fe^{2+}$ and $HS^-$oxidation), is controlling alkalinity in these groundwaters (Table 3.2). Similarly, alkalinity decreases at Western Salina, between the potential sources (regional and locally recharged groundwater) and the shallow brines (West1 piezometers and West3; see Fig. 3.10 for locations). These brines are also unsaturated with respect to carbonate and dolomite (Table 3.2), suggesting that carbonate mineral precipitation may not be the reason for this decrease. Large amounts of iron staining in the playa sediments throughout Raak Plain suggest that $Fe^{2+}$ oxidation and the resulting increase in acidity may be one mechanism for the observed decreases in alkalinity.

#### 3.5.3.2 Gypsum Precipitation

[$Ca^{2+}$] is above the seawater evaporation line for all local and regional groundwaters due to the influence of weathering reactions in the terrestrial environment (Figs. 3.5-3.10). There is an initial increase in [$Ca^{2+}$] at all of the playas, between these potential sources and the intermediate-salinity groundwaters due to evapo-concentration (Fig. 3.5-3.10). However, above a [$Br^-$] of approximately 0.002 Eq/kg, [$Ca^{2+}$] decreases. Although some precipitation of carbonate minerals is suggested by a decrease in alkalinity between here and the more saline brines at [$Br^-$] > 0.003 Eq/kg, this is unlikely to affect [$Ca^{2+}$], as it is in excess of [$HCO_3^-$] + [$CO_3^{2-}$] (Hardie and Eugster, 1970; see Section 3.2.1). The decrease in [$Ca^{2+}$] at all of the playas is therefore probably due to the precipitation of some other $Ca^{2+}$ evaporite mineral. The saturation indices calculated using PHRQPITZ indicate that most of the waters are approximately in equilibrium with gypsum ($CaSO_4 \cdot 2H_2O$), and large quantities of gypsum crystals were observed in the sediment profiles of the playa lakes, around the zone of water table fluctuation (Table 3.2; Section 3.4.6). Increasing [$SO_4^{2-}$] above the seawater evaporation line at all of the playas is also in agreement with this hypothesis. As described in Section 3.2.1, the precipitation of gypsum will cause an increase in [$SO_4^{2-}$] and a decrease in [$Ca^{2+}$] in solution if the starting concentration of the former was higher than of the latter (Hardie and Eugster, 1970). Some of the low TDS waters at Spectacle Lake shown in Table 3.2 are below saturation with respect to gypsum. However these samples do not participate in the [$Ca^{2+}$] decrease described above. Therefore, precipitation of these minerals is a viable explanation for the decreases in [$Ca^{2+}$].

### 3.5.3.3 Precipitation / Dissolution Cycles Near the Playa Surface

Steep increases in the slopes of the [$Na^+$], [$Cl^-$], [$Mg^{2+}$] and [$SO_4^{2-}$] vs [$Br^-$] graphs in the top 30 cm of the profile at the centre of the Main Salina suggest dissolution of evaporite minerals near the surface of this playa (Gig. 3.6). This is also the case in the [$Mg^{2+}$] and [$SO_4^{2-}$] vs [$Br^-$] graphs in the top 10 cm of the profiles at Western Salina and Salt Lake (Figs. 3.5 and 3.7). As corresponding trends occur in [$Na^+$] and [$Cl^-$], and [$Mg^{2+}$] and [$SO_4^{2-}$], mineral – solution reactions involving 1:1 ratios of these ions are suggested, for example, precipitation / dissolution of halite (NaCl) and epsomite ($MgSO_4 \cdot 7H_2O$). All of the shallow brines are approximately in equilibrium with halite (NaCl), suggesting that this is the possible control over the $Na^+$ and $Cl^-$ concentrations at all of the playas (Table 3.2). They are also all undersaturated with respect to epsomite, suggesting that dissolution of small amounts of this mineral is possible.

Apparent dissolution of epsomite ($MgSO_4 \cdot 7H_2O$) is most prevalent in a shallow (< 10 cm deep) profile taken at the edge of Western Salina, (West5), where the most dramatic increases in [$Mg^{2+}$] and [$SO_4^{2-}$] are observed. Also, dilution of the brines at the very surface of West5 and at the centre of the Main Salina (Main1), probably by infiltrating rainwater, is implied by slightly lower [$Br^-$] in these samples compared with those a few centimetres below. The infiltration of fresher water has probably led to the dissolution of the minerals described above, as these samples still have the highest [$Na^+$], [$Cl^-$], [$Mg^{2+}$] and [$SO_4^{2-}$]. Some increase in [$SO_4^{2-}$] was attributed to gypsum precipitation in the previous section. However, this reaction is limited by the availability of $Ca^{2+}$, the concentrations of which are an order of magnitude lower than [$SO_4^{2-}$]. Hence, gypsum precipitation could only account for a small proportion of the observed increases in [$SO_4^{2-}$].

Although mineral – solution reactions with halite and epsomite have been suggested by trends in the ion vs [$Br^-$] graphs, equilibrium of the brines with other minerals such as glauberite ($Na_2Ca(SO_4)_2$) and mirabilite ($Na_2SO_410H_2O$) are suggested by the saturation index calculations (Table 3.2). Also, surface efflorescence collected at the Main Salina were found to consist predominantly of halite and bloedite ($Na_2SO_4MgSO_4 \cdot 5H_2O$) (Section 3.4.6). Hence cyclic precipitation and dissolution of some surface efflorescences, generally containing $Na^+$, $Cl^-$, $Mg^{2+}$ and $SO_4^{2-}$ can be concluded.

### 3.5.4 Evolution of Surface Water in the "Type D" (Surface Water) Lakes

Salt Lake is the only natural lake included in this study to contain surface water for most of the year (Section 1.3.5), being a "Type D" basin according to Bowler (1986), rather than "Type E", which predominates at Raak Plain. Spectacle Lake is also believed to have been a Type D basin prior to establishment of the salt harvesting operation there (Section 1.3.5). During their lifetimes, salt lakes can alternate between lake-full and drying conditions, depending on the global and regional climates at the time, and this in turn influences the evolution of the subsurface brine (Bowler, 1986). Subsurface (groundwater) brines form only during the drying stages of salt lakes, when a concentration gradient causes the transfer of salts from the evaporating surface water to the interstitial waters, or when the groundwater is evaporated directly through a shallow unsaturated zone (Talsma, 1963; Bowler, 1986; Allison and Barnes, 1983). Therefore, if the ponded surface water at Salt Lake (and Spectacle Lake) is locally recharged groundwater or direct rainfall, concentration of the subsurface brine can only occur when this water becomes hypersaline, transferring solutes to the subsurface by diffusion, or dries up completely, allowing evaporation from the shallow water table. In contrast, concentration of the subsurface brines in the Type E basins (Western Salina and the Main Salina) can occur continuously by evaporation from the shallow water table. This can explain the larger concentration gradient in the top 10 cm of pore water at the Western Salina compared with Salt Lake (Appendix G).

Chemical analysis of surface water, collected from Salt Lake after rain in April 2001, revealed a composition that clusters with the Parilla Sand groundwater and dune/plain groundwater samples, and is hence not outcropping brine (Fig. 3.7). It may therefore be regional Parilla Sand groundwater that has discharged into the lake via springs at the playa margins or direct rainfall / locally recharged groundwater. The surface water has high [$Na^+$], [$Cl^-$], [$Ca^{2+}$], [$Mg^{2+}$] and [$SO_4^{2-}$] due to the partial dissolution of the pre-existing surface salt crust, which consists predominantly of halite and gypsum, occasionally with trace amounts of bischofite ($MgCl_2.6H_2O$) (Section 3.4.6). Diffusion of solutes from the hypersaline subsurface brine into this comparatively fresher water also has the potential to occur due to the large concentration gradient that occurs between these two water types. As the time scale of this process for chloride, based on Fick's Law, a bulk sediment diffusion coefficient of 154 $cm^2/y$ and a distance scale of 0.1 m, is estimated to be less than 1 year, it has the potential to affect solute concentrations between rainfall events and sampling.

Precipitation of a surface salt crust from the surface water body in the Type D lakes only occurs when the interstitial waters reach saturation with respect to evaporite minerals, i.e. after long periods of drying (Bowler, 1986), and the surface waters can then also reach saturation to precipitate the minerals. The distinction between the Type D and Type E lakes is also seen in the ionic ratios of the brines, due to the precipitation of the surface salt crusts in the Type D basins (Table 3.3). Salt Lake and Spectacle Lake have the highest Br/Cl, lowest (identical) $Ca/SO_4$, and lowest (Na+K)/(Mg+Ca), all consistent with higher degrees of halite and gypsum precipitation.

### 3.5.5 Trends in the Chemical Composition of the Parilla Sand Groundwater

The dissolved solute concentrations of the Parilla Sand groundwater increase along the east-west flow line below Raak Plain (Transect AA', Fig. 3.3). A small increase occurs between the eastern margin (bore 26240) and Spectacle Lake (bore 81945), and greatest increase occurs to the west of the Main Salina, below the main part of the discharge complex. The compositions of the Parilla Sand bores along this east-west flow path generally move along the evaporation / mixing lines between the least saline bore (bore 26240) and the most saline brines, suggesting mixing between the two and confirming brine leakage to the regional groundwater (shown on Figs. 3.5-3.10). The most saline groundwater in the Parilla Sand occurs below Western Salina, as it has travelled the furthest below the discharge complex and has therefore had the most opportunity to be affected by brine leakage (Fig. 3.3). The composition of this groundwater is extremely similar to that of the deeper groundwater brines in the Blanchetown Clay below Spectacle Lake (SM1 and SM6). This may suggest that the more saline groundwater in the Parilla Sand aquifer is derived from past or present leakage of groundwater from the Blanchetown Clay below the playas.

### 3.5.6 Spectacle Lake (Harvested Lake)

Prior to establishment of the salt harvesting operation there in the 1980s, Spectacle Lake was a natural playa lake, probably similar in its morphology to Salt Lake (Section 1.3.5.4). Hence, it is expected that the effects of the salt harvesting operation may not be evident in the chemistry of the deeper brines that occur there and data from Spectacle Lake has been included in the previous discussions of natural salt lake processes. However, some unique chemical features of the brines, which may be the result of the salt harvesting operation, can be observed in the data from Ponds 2 and 3 and will be discussed below. There is much more scatter in the major ion vs [$Br^-$] diagrams for Spectacle Lake than the natural lakes, and trends are difficult to identify, with the exception of the fact that there is a general increase ion concentrations with increasing concentration factor [$Br^-$] (Fig. 3.8). As with the natural playa lakes, [$Ca^{2+}$] also decreases with increasing concentration factor at

Spectacle Lake, consistent with gypsum precipitation where $SO_4^{2-}$ is in excess of $Ca^{2+}$. To better identify trends that are specific to the two sites, at the edge of Pond 3 and at the centre of Pond 2, these data have been presented separately in Figures 3.9 and 3.10 respectively. The pore water ion vs depth profiles for the two sites are shown in Figure 3.4.

The shapes of the ion vs [$Br^-$] plots for groundwaters and pore waters from the edge of Pond 3 are similar to those of the three natural playa lakes at Raak Plain (Figs. 3.5 – 3.7). However, the maximum [$Br^-$]s (between 0.5 and 1.2 m below the surface) are more than double those observed at the natural lakes. The approximately exponential shape of the [$Br^-$] vs depth profile is also consistent with advection / diffusion (Fig. 3.4), as has been found for the natural playa lakes (Howes, 1998). However, higher rates of diffusional transport for the charge determining ions (e.g. $Cl^-$, $Na^+$, $SO_4^{2-}$) than for $Br^-$, result in more linear trends in concentration with depth between 2 m and 8 m (Fig. 3.4a). As described in Section 3.5.2, the higher diffusion rates of these ions compared with $Br^-$ are probably the reason for deviations away from the seawater evaporation line in the middle [$Br^-$] ranges of Figure 3.10. Groundwater compositions below approximately 7.4 m are similar to each other and plot approximately on the seawater evaporation line for all ions except $SO_4^{2-}$.

The effects of halite precipitation at the top of the profile can be seen in a decrease in [$Na^+$] and a flattening out in the [$Cl^-$] vs depth trend in the top 2 m of the profile (Fig. 3.4a, Fig. 3.10). All of these samples are at saturation with respect to halite (Table 3.2), which also suggests that precipitation of this mineral controls [$Na^+$] and [$Cl^-$] in the brines near the surface this playa. An alternative explanation for the near-surface trends in [$Na^+$] and [$Cl^-$] is the periodic imposition of a downward advective flux in this depth interval, caused by periodically increasing the amount of water ponded at the surface of the lake (Bill Ullman, pers. comm., 2001). This has the effect of smearing out the ambient diffusional profile. The implications of this for solute transport are that, while diffusion may be the most import process over long time scales, reversible advective fluxes are important over short time scales (months to years).

The lake water sample from Pond 3, collected in April 2001 has a lower concentration factor ([$Br^-$]) than the pore water samples between 0.5 m and 1.2 m depths (Fig. 3.10). However, for most of the major ions, the lake water sample plots on a mixing line between the shallow (0.5 m to 1.2 m) pore water samples, and the deeper ones at 2.3 to 2.6 m. Unlike at Salt Lake, it is known that the ponded surface water in Spectacle Lake is predominantly regional Parilla Sand groundwater that has been pumped onto the playa surface as part of the salt harvesting procedure. Figure 3.10 shows that this water has then undergone evapo-concentration at the playa surface, although not to the concentration factor of the subsurface brines, and precipitated halite.

There is a distinct difference in brine chemical composition at the centre of Pond 2, from those of the natural playas and the site at the edge of Pond 3. There is no single trend in the ion vs [$Br^-$] data, but a distinct break in trend around [$Br^-$] = 0.006 Eq/kg (Fig. 3.9). Below 5 m depth, the trend is similar to those of the natural playa lakes (Figs. 3.5-3.7), including the maximum concentration factor of the brine ([$Br^-$] < 0.01 Eq/kg). The shapes of the ion vs depth profiles below 5 m are also typical of advection / diffusion processes normally observed in the pore water profiles of natural playa lakes (Fig. 3.4b). However, between 2 m and 5 m below ground level, [$Br^-$] decreases towards the surface whilst [$Na^+$], [$Cl^-$], [$Mg^{2+}$] and [$SO_4^{2-}$] increase. The differences in trends in pore water chemical compositions between the two parts of the solute vs depth profiles can be explained in terms of the changed conditions in the lake by the salt harvesting operation, and will be discussed in more detail in Chapter 7.

Low concentration factor (low [$Br^-$]) pore waters occur in the top 20 cm of the sediment profile at Pond 2, within the surface salt crust (Fig. 3.9; Fig. 3.4b). The 0-10 cm sample is similar in its overall chemical composition to the regional groundwater that is pumped onto the surface of the lake. Although this was sampled as pore water, extracted from within the salt crust, it displays only slightly elevated [$Na^+$] and [$Cl^-$] and is undersaturated with respect to all evaporite minerals, including halite (Fig. 3.9, Table 3.2). This may be the result of mixing of ponded surface water with the sample during collection, although it is unknown why the water did not dissolve a sufficient amount of salt crust during transport and storage to reach saturation with respect to those minerals contained within the salt crust. At 10-20 cm, the pore water sample has a similar concentration factor to that at 0-10 cm, but relatively higher [$Na^+$], [$Cl^-$], [$Ca^{2+}$], [$Mg^{2+}$] and [$SO_4^{2-}$], probably due to dissolution of evaporites within the salt crust, although it is still undersaturated with respect to all evaporite minerals except gypsum (Fig. 3.9, Table 3.2). At the time of sampling of the sediment core at Pond 2, there was no surface water in that part of the pond, although some ponded rainwater was observed in other lower-lying parts. The fairly unevaporated waters in the salt crust are probably just rainwater that had infiltrated recently. At other times, when Parilla Sand groundwater was ponded in Pond 2 (e.g. April 2001), samples of this water had a chemical composition similar to those of the subsurface brines below the salt crust (see Appendix G).

### 3.5.7 Conservation of Solutes

The similar chemical compositions of the shallow brines at Raak Plain, and the similarity between these and the chemical compositions of the potential sources suggests that (a) solutes are largely conserved in solution within the playa lake systems. The only exception is the net losses in $Ca^{2+}$ and $SO_4^{2-}$ due to gypsum precipitation observed in Figures 3.5 – 3.10. Only small amounts of salt efflorescences were observed at the surfaces of the Main Salina and Western Salina, and these correspond to minor variations in ionic ratios of the brines closest to the playa surfaces. Variability in TDS of bulk deposition samples from various locations across the discharge complex may be due to aeolian deflation of these salt efflorescences from the playa surfaces, and deposition in the dunes and plains between the playas. In most cases, however, these solutes will then re-enter the groundwater systems of the playa lakes via recharge and ultimately be conserved. Furthermore, the observed increases in TDS of these samples represent minor losses from the playa surfaces via aeolian deflation compared with the mass of salt contained within the playa systems themselves.

### 3.5.8 Geochemical Mass Balances

A conceptual model of the dominant geochemical processes affecting the brines at the natural playa lakes at Raak Plain can be formed from the results of the major ion versus [$Br^-$] plots and the saturation index calculations (Section 3.4.9). The inflow that evaporates to form the brines is assumed to have a composition similar to Parilla Sand groundwater and / or locally recharged groundwater that was sampled from below dunes and plains between the playa lakes at Raak Plain. The following processes have been identified as being the most important affecting the chemistry of the brines across the discharge zone, and are therefore included in the geochemical mass balance model (Table 3.4):

1) Evapo-concentration. Evapo-concentration of a starting composition was calculated based on $[Br^-]$, using the formula:

$$[I]_t = [I]_1 \times [Br^-]_2/[Br^-]_1 \qquad (3.2)$$

where $[I]_t$ is the theoretical concentration of ion, I (moles/L), calculated for evapo-concentration of the starting water composition. $[I]_1$ is the concentration of ion, I in the starting water composition and $[Br^-]_1$ and $[Br^-]_2$ are the measured $Br^-$ concentrations of the assumed source and brine. Theoretical ion concentrations, based on evapo-concentration alone were calculated for each brine sample. Residuals between the measured and theoretical concentrations are calculated using the formula (Table 3.4):

$$\text{Residual} = [I]_{observed} - [I]_t \qquad (3.3)$$

A positive residual indicates that there has been addition of ion, I, to the real water sample above the increase in concentration caused by evapo-concentration (Table3.4). A negative value implies removal of that ion by some other process. The mineral-solution reactions proposed to account for these additions / removals are dissolution / precipitation of gypsum ($CaSO_4 \cdot 2H_2O$), epsomite ($MgSO_4 \cdot 7H_2O$) and halite ($NaCl$), and are assumed to be limited by the respective cation residuals calculated above.

Table 3.4. Mass balance calculations for evapoconcentration and mineral precipitation from a given starting composition. All solution concentrations used in calculations were in moles/kg.

| **Description of Calculation** | | **Calculated Residuals* (Evapo-concentration Only) +ve = addition -ve = removal** | | | | | | **Modelled Moles of Solid Dissolved (+ve) / Precipitated (-ve)** | | | **Final Residual Error*** | |
|---|---|---|---|---|---|---|---|---|---|---|---|---|
| **Starting Composition** | **Product** | **Na** | **Mg** | **K** | **Ca** | **Cl** | **$SO_4$** | **Gypsum $CaSO_4 \cdot 2H_2O$** | **Epsomite $MgSO_4 \cdot 7H_2O$** | **Halite NaCl** | **Cl** | **$SO_4$** |
| Western Salina | | | | | | | | | | | | |
| West4 | West2e | 0.206 | 0.010 | -0.003 | -0.012 | 0.232 | -0.008 | -0.012 | 0.010 | 0.206 | 0.026 | -0.006 |
| | West1a | 0.740 | 0.073 | 0.002 | -0.013 | 0.797 | 0.042 | -0.013 | 0.073 | 0.740 | 0.058 | **-0.018** |
| | West1 80-90 cm | -0.103 | 0.019 | -0.004 | -0.024 | 0.420 | -0.006 | -0.024 | 0.019 | -0.103 | **0.523** | -0.001 |
| West1 274-292 cm | 60-70 cm | -0.032 | -0.014 | -0.001 | -0.001 | -0.119 | -0.008 | -0.001 | -0.014 | -0.032 | -0.087 | 0.007 |
| | 8-10 cm | -0.255 | -0.034 | -0.001 | -0.006 | -0.407 | -0.026 | -0.006 | -0.034 | -0.255 | -0.152 | 0.015 |
| | 2-4 cm | -0.475 | -0.009 | -0.002 | -0.013 | -0.716 | -0.027 | -0.013 | -0.009 | -0.475 | **-0.240** | -0.005 |
| West5 6-8 cm | 4-6 cm | 0.632 | 0.132 | 0.003 | -0.001 | 0.088 | 0.684 | -0.001 | 0.132 | 0.632 | 0.052 | **-0.044** |
| | 0-2 cm | 0.834 | 0.243 | 0.003 | -0.004 | 0.225 | 0.925 | -0.004 | 0.243 | 0.834 | 0.09 | -0.015 |
| Main Salina | | | | | | | | | | | | |
| Main4 | Main1 | 0.459 | 0.044 | -0.006 | -0.015 | 0.419 | 0.027 | -0.015 | 0.044 | 0.459 | -0.040 | -0.002 |
| | Main1 30-35 cm | 0.310 | 0.056 | -0.008 | -0.020 | 0.356 | 0.029 | -0.020 | 0.056 | 0.310 | 0.047 | -0.006 |
| 98347 | Main1 | 0.159 | -0.010 | -0.007 | -0.022 | -0.032 | -0.003 | -0.022 | -0.010 | 0.159 | **-0.191** | **0.028** |
| Main1 30-35 cm | 13-16 cm | -0.044 | 0.006 | 0.000 | -0.001 | 0.007 | 0.001 | -0.001 | 0.006 | -0.044 | 0.051 | -0.004 |
| | 0-2 cm | 0.248 | 0.082 | 0.002 | -0.002 | 0.161 | 0.135 | -0.002 | 0.082 | 0.248 | -0.087 | 0.055 |
| Salt Lake | | | | | | | | | | | | |
| Salt1 255-263 cm | 50-55 cm | -0.315 | 0.021 | 0.001 | -0.006 | -0.268 | 3.439 | -0.006 | 0.021 | -0.315 | 0.047 | -0.016 |
| | 4-6 cm | -2.412 | -0.013 | -0.001 | -0.016 | -2.600 | 3.619 | -0.016 | -0.013 | -2.412 | -0.187 | -0.019 |
| | 0-2 cm | -3.227 | 0.212 | 0.002 | -0.018 | -3.333 | 3.484 | -0.018 | 0.212 | -3.227 | -0.106 | **-0.187** |

*Residuals are the difference between observed and calculated ion concentrations.

2) Gypsum precipitation / dissolution:

$$CaSO_4 \cdot 2H_2O_{(s)} \leftrightarrow Ca^{2+}{}_{(aq)} + SO_4{}^{2-}{}_{(aq)} + 2H_2O \qquad (3.4)$$

3) Epsomite precipitation / dissolution.

$$MgSO_4 \cdot 7H_2O_{(s)} \leftrightarrow Mg^{2+}{}_{(aq)} + SO_4{}^{2-}{}_{(aq)} + 7H_2O \qquad (3.5)$$

4) Halite precipitation / dissolution

$$NaCl \leftrightarrow Na^+ + Cl^- \qquad (3.6)$$

If gypsum and epsomite mineral – solution reactions are the only controls over [$SO_4{}^{2-}$], and halite is the control over Cl, the resulting residuals for $SO_4{}^{2-}$ and $Cl^-$ should be zero (right hand columns of Table 3.4). Uncertainties within the margins of the combined analytical uncertainties for each species involved in the calculation are considered to be reasonable. For the $SO_4{}^{2-}$ residual, this is a combination of the uncertainties in $Ca^{2+}$ (±5%), $Mg^{2+}$ (±5%) and $SO_4{}^{2-}$ (±4%), i.e. a total of 14% of the smallest measured concentration of $SO_4$ in the calculation. For the $Cl^-$ residual, this is a combination of the uncertainties in $Na^+$ (±5%) and $Cl^-$ (±4%), i.e. a total of 9% of the smallest measured concentration of Cl. Those uncertainties greater than the acceptable uncertainty for that calculation are highlighted in Table 3.4, and indicate that other mineral reactions or processes contribute to the final brine composition, besides evapo-concentration and precipitation / dissolution of the specified minerals.

The results show that, in most of the calculations, the conceptual model of evapo-concentration and precipitation /dissolution of a simple mineral suite, consisting of gypsum, epsomite and halite, can account for the compositions of most of the saline brines observed at Raak Plain (Table 3.4). $K^+$ concentrations are controlled mainly by evapo-concentration. However, some minor losses between the low TDS samples and the high TDS brines can be attributed to cation exchange on the kaolinitic clays, particularly since pHs are generally above 4.6, the point of zero charge ($pH_{PZC}$) for kaolinite (Appelo and Postma, 1999). This exchange process is minimal because of the age of the system, and the fact that the groundwater is likely to have reached equilibrium with the clays.

## 3.6 Conclusions

Interpretation of the chemical compositions of the brines and groundwaters at Raak Plain has led to the following conclusions about the sources and evolution of the brines that occur there:

- Regional Parilla Sand and locally recharged groundwater have almost identical chemical compositions, and hence either of these may be sources of solutes to the brines below the playas. Intermediate TDS groundwaters at > 3 m depth below the playas or at the playa margins are probably mixtures of brine and the lower-TDS sources.

- Most of the processes affecting the chemical compositions of the brines occur in the top 3 m of the sediment profiles.

- Differential diffusion rates of ions across the top 3 m of the playa sediments may lead to differences in the ionic ratios of the brines at different depths. This occurs to a depth of 8 m at the edge of Pond 3 at Spectacle Lake.

- Mineral controls on the chemical compositions of the brines are:

  - Carbonate mineral-solution reactions, which are small in magnitude, but likely to be significant in the interpretation of carbon isotope data.

  - Gypsum precipitation, which appears to be consistent in the top 3 m of all of the playas although gypsum crystals were not observed in all of the sediment profiles collected during this study (Chapter 3).

  - Cyclic precipitation / dissolution cycles occur at the surface involving Na, Cl, Mg and $SO_4$. This is consistent with observations of surface halite (NaCl) and bloedite ($Na_2SO_4MgSO_4 \cdot 5H_2O$) efflorescences (Chapter 3). However, the small masses of mineral produced and cyclic natures of these processes mean that they probably have little net effect on the overall geochemistry of groundwaters in the Raak Plain system.

- With the exception of gypsum ($CaSO_4 \cdot 2H_2O$) removal in the sediment profile, solutes are generally conserved in solution within the playas, with the relative ion concentrations of the brines remaining similar to those of the potential sources.

- Ponded surface water at Salt Lake is not brine, but is either regional groundwater that has entered the playa via springs or locally recharged groundwater / direct rainfall onto the playa. Dissolved $Na^+$, $Cl^-$, $Ca^{2+}$, $Mg^{2+}$ and $SO_4^{2-}$ have been added to this surface water by partial dissolution of the surface salt crust.

- An increase in TDS of groundwater in the Parilla Sand aquifer as it flows from east to west below Raak Plain is due to mixing with the brines of the discharge complex rather than dissolution of evaporite minerals.

# Chapter 4 Conceptual Model for Groundwater and Solute Fluxes in a Groundwater Discharge Complex

## 4.1 Introduction

### 4.1.1 Scope and Objectives

A good understanding of the hydrogeological framework and hydraulic processes occurring at Raak Plain is required to explain the wide range of salinities and chemical compositions that exist there over relatively short distances ($10^{-1}$ to $10^{2}$ m) (Chapter 3). A series of simple conceptual models for the salt and water balances of single playa lakes at Raak Plain range between the Isolated Systems Model, where the Blanchetown Clay effectively separates the surface playa lakes from the Parilla Sand aquifer, and the Connected Systems Model, with significant exchange of salt between the two (Figs. 1.9(a-d)). However, to properly understand the relationship between the playa lakes and the regional aquifer system in a discharge complex, these conceptual models must be extended to the discharge complex scale ($10^{4}$ m), incorporating both regional and local hydrogeological information.

Raak Plain is a regional groundwater discharge complex where, at many locations, the piezometric surface in the Parilla Sand aquifer intersects the ground surface due to low topography and thinning of the aquifer caused by faulting to the north-west (Fig. 1.7) (Brown, 1989; Macumber, 1992). Hydraulic heads in the regional aquifer at some locations can be more than 0.5 m above ground level. However, an upward hydraulic gradient does not necessarily imply a significant upward flux through the 30 m thick Blanchetown Clay aquitard, and one fundamental question to be addressed by this study is whether the brines below Raak Plain are derived mainly from the evaporation of (a) regional groundwater that has leaked up from the Parilla Sand aquifer or (b) groundwater that has been recharged locally through the dunes and plains around the playas. The proportion of regional groundwater that is discharged to the lakes and lost by evaporation determines the degree to which Raak Plain acts as a regional groundwater sink. Another important issue addressed by this study is whether the brines at Raak Plain are sinks for the accumulated salt, or whether this salt is eventually returned to the regional groundwater system.

The objectives of this chapter are therefore to:

- Consolidate local and regional-scale hydrogeological and TDS information into a conceptual model for groundwater flow and solute transport in a regional groundwater discharge complex.
- Construct water and solute balances for individual playas of the discharge complex.
- Use this information to investigate the validity of conceptual models for water and solute transfers between the playas of a groundwater discharge complex and the underlying regional aquifer system (Figs. 1.9(a-d)).

### 4.1.2 Formation and Leakage of Subsurface Brines Below Salt Lakes

Many salt lake brines are formed by evapo-concentration of surface water inflows (e.g. Mono Lake, California (Connell and Dreiss, 1995), Great Salt Lake, Utah (Spencer et al., 1985 (a&b)) and Lake Magadi, Kenya (Eugster and Jones, 1979). When the TDS (and density) of these surface waters becomes greater than that of the underlying groundwater, salts can be transported into the subsurface by diffusion and/or convection (Bowler, 1986). Based on a solute mass balance, this was demonstrated to occur at Great Salt Lake by Spencer et al. (1985 (a&b)). The formation of subsurface brine bodies by the evapo-concentration of groundwater from shallow water tables in dry playa lakes has also been demonstrated (e.g. Allison and Barnes, 1985).

The vertical extents of subsurface brine bodies, and hence the degree of brine leakage, have been documented for very few salt lakes throughout the world. Brine bodies may only partially extend into the underlying sediments, for example at Lake Frome, Australia (Bowler, 1986), Smith Creek Valley playa, Nevada (Thomas et al., 1989) and Lake Magadi, Kenya (Eugster, 1970). In other cases, such as Lake Tyrrell, Australia (Teller et al., 1982; Macumber, 1992) and Mono Lake, California (Rogers, 1993), the brine body may completely fill the aquifer below the lake. This occurs to depths of 60 m and 2 km at Lake Tyrrell and Mono Lake respectively.

Allison and Barnes (1983, 1985) showed that, in the presence of evaporation, for example below groundwater discharge zones, the practical upper limit for downward migration of salt by diffusion is less than 1 m. Therefore, in many cases, density-driven convection has been used to explain the movement and mixing of brine bodies over large distances (e.g. Teller et al., 1982; Barnes et al., 1990; Simmons and Narayan, 1997; Wooding et al., 1997 (a&b)). The density inversion between a hypersaline brine and an underlying fresher groundwater body can lead to instability, whereby fingers of dense saline water are freely convected downwards from the lake bed. In the meantime, less dense fluid moves upward towards the lake bed to counterbalance this downward flux and a convection cell is established. Such free convection currents cause mixing of the brines over distances several orders of magnitude greater than due to diffusion alone and therefore represent a very effective salt transport mechanism (Simmons and Narayan, 1997).

Indirect evidence for density-driven convection has been found in many saline lake basins. For example, Langbein (1961) observed that the mass of salts contained in many saline lakes is less than the quantity of solutes that have been carried into them during their lifetime. Teller et al. (1982) suggested that this salt deficit may be partly due to the slow downward convection of the dense saline water below the lakes, along with other processes such as aeolian removal of surface salt deposits. At Lake Frome in south-eastern Australia, Allison and Barnes (1985) observed that salt concentrations decreased with depth, reaching the background concentration within 1 m below the ground surface, whilst Bowler (1986) found a zone of brine extending about 60 m below the surface.

Herczeg et al. (1992) found brines at Lake Tyrrell, in the central Murray Basin, Australia (see Section 3.3), that had isotopic signatures consistent with having undergone several cycles of evaporation and mixing with regional groundwater. Density-driven convection was also used to explain the lateral movement of recent (residence time < 50 yrs) disposal water over a distance of at least 100 m at the Mourquong saline groundwater disposal basin, also in the central Murray Basin (Simmons et al., 2002). The onset of convection through a window in the low permeability Blanchetown Clay aquitard below Lake Mourquong was demonstrated to be possible using a numerical model.

The likelihood of the onset of density-driven convection is often assessed using a non-dimensional number that determines the stability of a system, the Rayleigh number (e.g. Wooding et al., 1997a; Simmons and Narayan, 1997; Simmons et al., 1999):

$$Ra_1 = \frac{K(\Delta\rho/\rho_0)H}{\varphi D_0} = \frac{\text{Buoyancy forces}}{\text{Resistance forces}} \qquad (4.1)$$

where: H is the depth of the porous medium [L], K is hydraulic conductivity [L/T], $\Delta\rho$ is the density "excess" of the brine body ($\Delta\rho = \beta\Delta C$, where $\beta$ is the coefficient of density variation with concentration [$M/L^3$] and $\Delta C$ is the concentration difference between the brine body and the ambient groundwater [M/M]), $\rho_0$ is the reference or base density [$M/L^3$], $\varphi$ is porosity [-] and $D_0$ is the molecular diffusivity in aqueous solution [$L^2/T$].

A critical Rayleigh number ($Ra_c$) of $4\pi^2$ ($\cong 40$) for the onset of convection was derived by Lapwood (1948) using an experimental configuration of two parallel plates and fixed upper- and lower- boundary conditions. Equation 4.1 is known as the "macroscopic Rayleigh number" because it considers that the stability of a system depends on the macroscopic length scale, H, the entire saturated thickness of the aquifer. It also contains assumptions of steady-state flow conditions, a linear and uniform concentration profile across the entire thickness of H, and fixed upper and lower boundary conditions. As discussed by Simmons et al. (2002), these conditions rarely occur in real groundwater systems.

Barnes et al. (1990) and Wooding et al. (1997a) showed that, in steadily evaporating systems, with an evaporation rate E, and where a boundary layer of hypersaline brine of thickness $\delta = D/E$ is formed by competing processes of upward advection and downward diffusion, the Rayleigh number is:

$$Ra_\delta = \frac{\Delta\rho}{\rho_0} \times \frac{K}{E} \qquad (4.2)$$

(note: D is an isotropic dispersion coefficient, exceeding $D_0$ only when hydrodynamic dispersion is present)

Barnes et al. (1990) state that the critical Rayleigh number in this case should be somewhere between that derived by Wooding (1960) for a system with unconstrained flow through the upper boundary ($Ra_c \cong 7$) and that of Lapwood (1948) ($Ra_c \cong 40$). However, if the incoming groundwater has a significantly greater density than pure water, the onset of instability depends largely on the ratio K/E, with a critical ratio of:

$$\frac{K}{E} \cong 100 \qquad (4.3)$$

Since E is usually proportional to K, this ratio depends only on the hydraulic gradient, and the system is stable if the hydraulic gradient is sufficiently large (i.e. > 0.01). However, if a surface salt crust develops or the surface becomes unsaturated, impeding E, then K/E and hence stability depends more on the permeability of the sediments. For evaporation rates between 10 mm/y and 100 mm/y, the critical grain-size for the onset of instability corresponds to a very fine sand-silt-clay (Barnes et al., 1990).

The above discussion relates to steadily evaporating systems. Barnes et al. (1990) recognized that seasonal fluctuations in E and periodic inundation of the lakes with even a shallow layer of surface water can affect the stability of the brine boundary layer. They found that, when E is suddenly reduced, the boundary layer initially remains stable, but as the profile relaxes under diffusion, instability can take over. This also causes an increase in thickness of the boundary layer, and possibly a reduction in $Ra_c$. However, only major inundations, over a few months for faster evaporating lakes and years for slower ones, would result in significant redistribution of salt by this process.

Wooding et al. (1997a) extended the work of Barnes et al. (1990), using numerical and laboratory simulations to investigate the effects of perturbations of the brine boundary layer (i.e. non-steady-state conditions). They investigated whether the one-dimensional stability analyses of Wooding (1960) and Homsy and Sherwood (1976) could be applied in two dimensions. They found that a critical zone for instability, with $Ra_c$ (from Eq. 4.2) between approximately 5.6 and 14.3 (similar to that derived by Wooding (1960) and Homsy and Sherwood (1976)), is relevant to the spectrum of lakes commonly found in semi-arid environments, from ponded surface water lakes to dry lakes. Hence, systems with $Ra < 5.6$ should definitely be stable and those with $Ra > 14.3$ should definitely be unstable.

## 4.2 Conceptual Model Development

### 4.2.1 Hydrogeology

Most of the hydrogeologic and chemistry data from Raak Plain has been collected along the east-west transect AA’, approximately along a regional groundwater flow line through the discharge complex (Fig. 1.6). Hence, a 2-dimensional cross-sectional conceptual model can be constructed along this transect (Fig. 4.1). The upper aquifer system is the focus of the conceptual model and comprises four main stratigraphic units: the regional Parilla Sand aquifer, the confining Blanchetown Clay, and the surface playa lake (Yamba Formation) and sand dune (Woorinen Formation) sediments (Fig. 1.7). The deeper Murray Group and Renmark Group aquifer systems are separated from the Parilla Sand aquifer by the 70 m thick

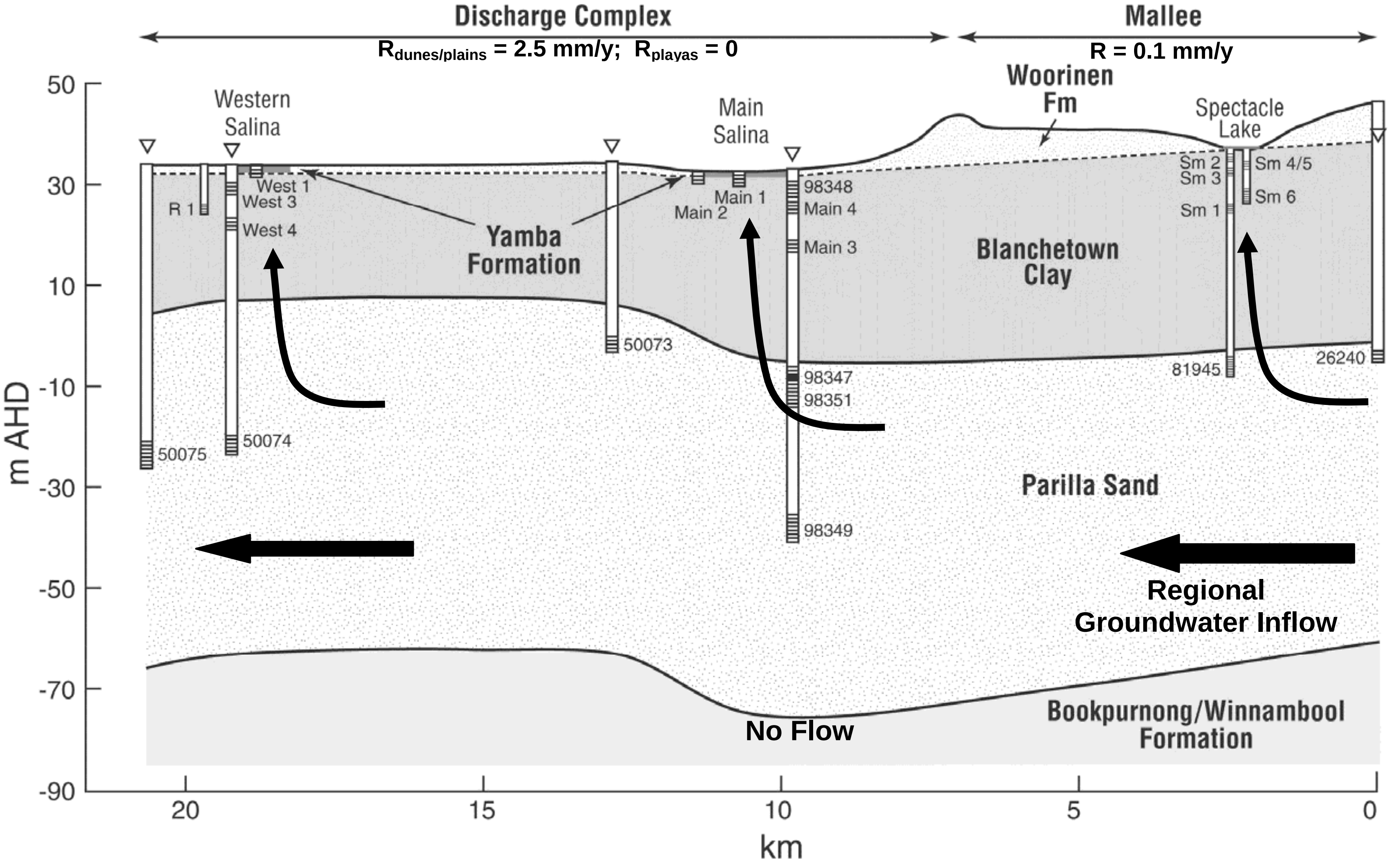

Figure 4.1. Two-dimensional hydrogeological conceptual model of the Raak Plain groundwater discharge complex, showing locations of the playas, bores and piezometers, hypothesized groundwater flow patterns and estimated recharge rates. Triangles indicate the elevations of hydraulic heads in the Parilla Sand bores.

Bookpurnong Beds / Winnambool confining layer (Fig. 1.7). This is considered to be an effective barrier to groundwater flow and hence a no-flow boundary for the purposes of this exercise (Fig. 4.1). The aquifer/aquitard boundaries for the conceptual model of Raak Plain (Fig. 4.1) have been derived from bore logs and aquifer extents recorded in the Victorian state groundwater database (Department of Natural Resources and Environment, 2002). This data is only available where regional bores are located, so minor variations in topography and formation boundaries could not be included. Thin layers of surface sediments (Yamba and Woorinen Formations) are included, although their boundaries are poorly defined. These are not expected to be very important in the regional flow system. The different hydrostratigraphic units are discussed below (from bottom to top).

#### 4.2.1.1 Parilla Sand

Geological logs of bores at Raak Plain suggest that the Parilla Sand aquifer is heterogeneous and comprises a fine clayey sand to a poorly sorted fine/medium/coarse sand (Appendix I; Department of Natural Resources and Environment (NRE), Victoria). Previous estimates of horizontal hydraulic conductivity of the Parilla Sand have ranged between 1 m/day and 3 m/day, and estimates of vertical hydraulic conductivity range between 0.01 m/day and 0.03 m/day (Table 4.1). Regional groundwater flow in the Parilla Sand below Raak Plain is from east to west (Fig. 4.1).

Table 4.1. Hydraulic conductivity values from the literature for the Parilla Sand aquifer, Blanchetown Clay aquitard and Yamba Formation sediments in the Murray Basin.

| HYDROSTRATIGRAPHIC UNIT | HYDRAULIC CONDUCTIVITY | SOURCE OF DATA |
|---|---|---|
| Parilla Sand | $K_H$ = 1-3 m/d | Sinclair Knight Merz (1996) |
| | $K_V$ = 0.01-0.03 m/d | Ferguson et al. (1995) |
| Blanchetown Clay | K = 1.7 x $10^{-4}$ m/d | Ferguson et al. (1995) |
| Yamba Formation | $K_H$ = 3 m/d | Ferguson et al. (1995) |
| | $K_V$ = 0.03 m/d | |

### 4.2.1.2 Blanchetown Clay and Yamba Formation

Heterogeneity in the 30 m thick Blanchetown Clay aquitard, separating the regional Parilla Sand aquifer from the surface playa lake system, was expected to control the exchange of salt between the two and influence local groundwater flow patterns. The Blanchetown Clay is known to be extremely heterogeneous, containing shoestring sandy layers that may be continuous over hundreds of metres (Macumber, 1973; Evans and Kellett, 1989). Although regional groundwater discharge rates should be limited by the lowest hydraulic conductivity unit, high conductivity sandy layers may provide conduits for lateral flow. Two sediment cores obtained from Spectacle Lake (sites SM1 and SM5), and drill spoil obtained from the edge of Western Salina (site West4), showed that the Blanchetown Clay below Raak Plain consists of alternating clay, silt and sand layers, ranging from tight clay to medium-grained sand (see Figs. 2.1 and 2.2 for site locations and Appendix E for geological logs). The clays are grey/green, characteristic of the Blanchetown Clay, with varying degrees of red/yellow mottling occurring in both clay and sandy layers. Several discrete sandy layers were apparently continuous between the two sites at Spectacle Lake, over a distance of at least 200 m (Fig. 4.2).

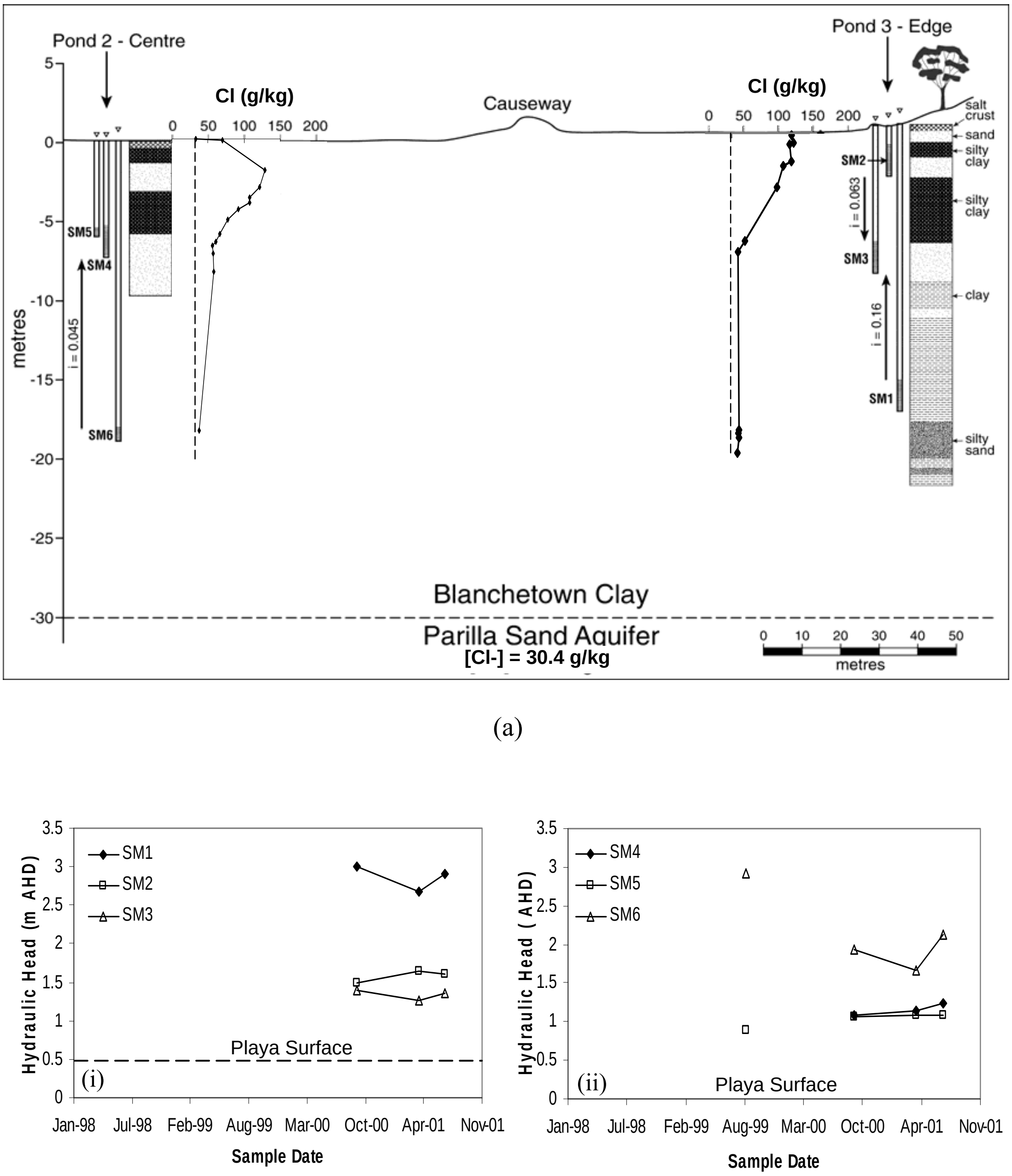

(a)

(b)

Figure 4.2. (a) Cross-sectional diagram of Spectacle Lake, showing piezometer locations and chloride vs depth profiles. Triangles indicate hydraulic heads in the piezometers. Both evaporation ponds contain ponded water (pumped from the Parilla Sand aquifer), of different depths throughout the year. (b) Piezometer hydrographs. Refer to Figure 2.2 for aereal piezometer locations.

A hydraulic conductivity of 1.7 x $10^{-4}$ m/day was reported for the Blanchetown Clay by Ferguson et al. (1995) at Lake Mourquong, which is near Mildura (Table 4.1; see Figure 1.5 for Mildura location). A horizontal hydraulic conductivity of 3 m/day and a vertical hydraulic conductivity of 0.03 m/day have been reported at Lake Mourquong for the thin layer of playa sediments (Yamba Formation) that overlies the Blanchetown Clay in discharge complexes throughout the Murray Basin (Table 4.1).

#### 4.2.1.3 Local Sediment Hydraulic Properties

Local hydraulic conductivities at various depths below Spectacle were estimated by carrying out slug tests on piezometers SM2, SM3 and SM4 (see Fig. 4.2 for locations and Section 2.1.4 for methodology). The water level recovery curves were interpreted using the Hvorslev method (Hvorslev, 1951), which is appropriate for both aquifers and aquitards partially penetrated by a well. Hydraulic conductivity estimates ranged between 0.04 m/day (15 m/y) and 0.17 m/day (62 m/y) (Table 4.2; see Appendix F for calculations and recovery curves). The piezometers were screened across different lithologies, making it difficult to estimate hydraulic conductivities for individual layers. However, the values obtained correspond to fine to silty sand (Freeze and Cherry, 1979), consistent with the geological logs (Appendix F).

Table 4.2. Horizontal hydraulic conductivities estimated from slug tests at Spectacle Lake.

| SITE | SCREENED INTERVAL (m) | CORRESPONDING LITHOLOGY | ESTIMATED HYDRAULIC CONDUCTIVITY (K) | |
|---|---|---|---|---|
| | | | (m/day) | (m/y) |
| SM2 | 0.7-2.7 | Sand and silty clay | 0.04 | 15 |
| SM3 | 6.6-8.6 | Sand and silty clay | 0.08 | 29 |
| SM4 | 5.5-7.5 | Sand and silty clay | 0.17 | 62 |

Specific yields (Sy) and hydraulic conductivities (K) of discrete samples from the Yamba Formation and Blanchetown Clay were also estimated from particle size distributions, following the methods of Johnson (1967) and Shepherd (1989) respectively (see Section 2.2.1). These methods provide only rough estimates of sediment hydraulic properties, which are highly dependent on the detailed structure of the sediment as well as grain size. Estimated specific yield (Sy) ranged between 5-10 % for the clays and 30% for the sand layer between 8.5 m and 10 m depth at Spectacle Lake (Table 4.3). Hydraulic conductivities ranged between 0.03 m/day and 0.18 m/day (Table 4.3), consistent with the results of the slug tests (Table 4.2).

Table 4.3. Results of particle size analyses, showing percentages of clay, silt and sand, sediment classification and estimated specific yield and hydraulic conductivity.

| SITE | SAMPLE DEPTH (m) | %CLAY | %SILT | %SAND | CLASS. | $S_Y$ (%) | K (m/day) |
|---|---|---|---|---|---|---|---|
| SM1 | 2.4-2.5 | 9 | 32 | 58 | Silty sand | 20 | 0.05-0.12 |
| | 6.6-6.7 | 13 | 6 | 81 | Sand | 23 | 0.07-0.18 |
| | 8.2-8.3 | 26 | 14 | 61 | Clay-sand | 5-10 | 0.04-0.11 |
| | 8.4-8.5 | 5 | 2 | 93 | Sand | 30 | 0.08-0.18 |
| | 13.4-13.5 | 23 | 24 | 53 | Clay-sand | 5-10 | 0.04-0.11 |
| | 17.4-17.5 | 11 | 26 | 62 | Silty sand | 20 | 0.05-0.12 |
| West1 | 0.14-0.16 | 7 | 28 | 64 | Silty sand | 25 | 0.05-0.12 |
| | 0.3-0.35 | 49 | 19 | 32 | Sandy clay | 5-10 | 0.03-0.07 |
| | 0.8-0.85 | 46 | 11 | 43 | Sandy clay | 5-10 | 0.03-0.07 |

### 4.2.2 Groundwater Recharge

Based primarily on vegetation and soil type, Raak Plain can be divided into three groundwater recharge zones: (1) the mallee-vegetated areas near the margins of the discharge complex ("Mallee"), (2) the bare dunes and plains between the playa lakes, and (3) the playa lakes themselves (Section 1.3.2; Fig. 4.1). Annual rainfall is approximately 300 mm/y and occurs throughout the year, but is highest between May and September (Section 1.3.2). The native mallee vegetation is found at the eastern, southern and western boundaries of Raak Plain. This vegetation type is extremely efficient at using infiltrating rainwater, resulting in very low recharge rates, ranging between 0.04 and 0.9 mm/y (Allison and Hughes, 1978; Cook et al., 1994; Howes, 1998). Recharge rate estimations of 0.1 mm/y have been made, using a chloride mass balance and a [$Cl^-$] in bulk deposition at Raak Plain of 16.4 mg/L, for two remnant mallee vegetated sites at Raak Plain (Fig. 4.1).

The grassy dunes between the playas in the main part of the Raak Plain discharge complex (western two thirds of transect AA'; Fig. 1.3) are only sparsely vegetated with mallee, comparable to an area that has been cleared of native vegetation and planted with pasture or cereal crops. The recharge rate for similar "cleared" mallee sites in South Australia has been estimated to be between 4 and 28 mm/y (Cook et al., 1994). A recharge rate of 1.3 mm/y was originally estimated at Raak Plain, (Howes, 1998) for a bare sand dune site (R3), but has been revised to 2.3 mm/y based on new $Cl^-$ deposition data (Fig. 4.1). Finally, rain falling directly onto the playa lakes is probably perched above the clayey sediments and subject to evaporation, resulting in negligible recharge to the groundwater system. This hypothesis is verified in Section 6.4.2 by comparing summer and winter $\delta^2H$ vs depth profiles of pore waters in the playa sediments.

### 4.2.3 Hydraulic Heads

The Parilla Sand aquifer is artesian in the low-lying areas of Raak Plain (in and around the playas), with observed hydraulic heads up to 3.5 m above ground level (Table 4.4, Fig. 4.1). Density-corrected hydraulic heads in the shallow sediments of the natural playas are also generally above the ground surface, but decrease towards the surface suggesting upward groundwater fluxes (discharge) (Table 4.5, Fig. 4.3 and Fig. 4.4). This trend was observed consistently throughout the 3 year study, despite seasonal fluctuations in hydraulic head of up to 80 cm in the shallow playa sediments (Figs. 4.3 and 4.4). Note that, although the hydraulic heads in the shallow piezometers can be above the levels of the playa floors, actual water levels are at or below the playa floors, because of the high density of the brines.

Hydraulic heads in the shallow playa sediments generally reflect trends in hydraulic head in the regional Parilla Sand aquifer. The density-corrected hydraulic head at the centre of the Main Salina (Main1) is slightly higher than that at the centre of Western Salina (West1), consistent with the east-west hydraulic gradient in the Parilla Sand aquifer (Tables 4.4 and 4.5). The hydraulic heads in the shallow playa sediments at Salt Lake and Spectacle Lake, which are at the up-gradient margins of Raak Plain, are also generally higher relative to the playa surfaces than at both Western Salina and the Main Salina, in the centre of the discharge complex (Table 4.5, Fig. 4.3 and Fig. 4.4).

Table 4.4. Measured fresh water hydraulic heads in Parilla Sand bores. Survey data was not available for the Spectacle Lake bore (81945), so elevations at this site have been estimated for inclusion in Fig. 4.1.

| BORE # | LOCATION (Fig. 1.3) (km from Calder Highway) | SCREEN ELEV. (m AHD) | SWL (m AHD) | EASTING | NORTHING |
|---|---|---|---|---|---|
| 26240 | Calder Highway (0) | -2.7 | 39.28 | 617100 | 6152200 |
| 81945 | Spectacle Lake (3.1) | 37-43 m bgl* | 1 m agl** | 613196 | 6155084 |
| 98347 | Edge of Main Salina (9.8) | -8.5 to –4.5 | 37.04 | 605500 | 6155750 |
| 98349 | Edge of Main Salina (9.8) | -40.7 to –34.7 | 38.31 | 605500 | 6155750 |
| 98351 | Edge of Main Salina (9.8) | -14.5 to –3.5 | 37.01 | 605500 | 6155730 |
| 50073 | Near Pink Lake (12.8) | -1.6 | 36.51 | 602450 | 6155450 |
| 50074 | Edge Western Salina (19.2) | -23.0 to –20.0 | 38.03 | 596050 | 6155900 |
| 50075 | Western Margin (20.6) | -26.3 to –20.8 | 37.84 | 592950 | 6155200 |

*bgl = below ground level ** agl = above ground level

Table 4.5. Hydraulic heads in the Raak Plain piezometer network (equivalent fresh water heads). Where possible, hydraulic heads are expressed relative to the Australian Height Datum (AHD). Piezometer locations are shown in Figs. 2.1, 2.2, 4.2, 4.3 and 4.4.

| SITE | PIEZOMETER | GROUND ELEV (m AHD) | SCREEN (m AHD) | EQUIVALENT FRESH WATER HEADS (m AHD) | | | | | | | |
|---|---|---|---|---|---|---|---|---|---|---|---|
| | | | | Apr 98 | Oct 98 | Jun 99 | Sep 99 | Nov 99 | Sep 00 | Apr 01 | Jul 01 |
| *Western Salina* | | | | | | | | | | | |
| Centre | West1a | 32.07 | 29.00 to 29.50 | 32.25 | 32.95 | 32.87 | 32.07 | - | 32.46 | 32.51 | 32.36 |
| | West1b | 32.07 | 30.87 to 31.37 | 31.60 | 32.29 | 32.17 | 32.07 | - | 31.99 | 32.09 | 31.93 |
| Edge Transect | Wes2a | 34.14 | 31.97 | - | - | - | - | - | - | 32.05 | 32.12 |
| | West2b | 31.67 | 31.67 | 32.63 | 32.86 | 31.71 | - | - | 32.20 | 32.02 | 32.12 |
| | West2c | 32.76 | 30.9 | 32.49 | 32.71 | 31.98 | - | - | 32.51 | 32.06 | 32.17 |
| | West2d | 32.07 | 30.26 | 31.75 | 32.19 | 32.01 | - | - | 32.27 | 32.04 | 32.41 |
| | West2e | 32.32 | 31.44 | 31.56 | 32.11 | 31.92 | - | - | 32.24 | 31.79 | 32.22 |
| | West2f | 32.19 | 29.97 | - | - | 31.92 | - | - | 32.26 | 32.00 | 32.50 |
| Edge | West3 | 33.04 | 29.24 to 29.74 | 32.78 | 32.88 | 32.77 | - | - | 33.16 | 32.72 | 32.94 |
| | West4 | 33.97 | 21.97 to 22.97 | - | - | 33.44 | 33.49 | - | 33.75 | 33.44 | 33.57 |
| Dune | R1 | 38.18 | 24.38 to 24.88 | - | - | - | - | - | 33.33 | 33.05 | 33.16 |
| *Main Salina* | | | | | | | | | | | |
| Playa - centre | Main1 | 32.53 | 30.58 to 31.08 | 32.64 | 32.96 | 32.90 | - | - | 32.91 | 32.74 | 32.89 |
| Playa – inside edge | Main2 | 32.53 | 32.03 to 32.13 | - | - | 32.52 | - | - | - | 32.24 | 32.21 |
| Edge | Main3 | 33.16 | 18.16 to 19.16 | - | - | - | - | - | - | 35.06 | 29.98 |
| | Main4 | 33.15 | 26.15 to 26.65 | - | - | 32.85 | 33.04 | - | 33.10 | 32.94 | 32.89 |
| | 98348 | 33.12 | 29.62 to 30.12 | - | - | - | - | 33.30 | - | 33.29 | 32.50 |
| *Dune/Plain* | R2 | 35.26 | 33.26 to 33.76 | 33.26 | 33.85 | 33.87 | - | - | - | 33.78 | 33.92 |
| | R3 | 39.53 | 33.78 to 34.28 | 34.80 | 34.17 | 34.16 | - | - | - | 34.21 | 34.19 |
| R4 - relative to ground level | | 0 | -5.25 to –4.75 | -4.19 | -4.06 | -4.10 | - | - | - | -4.26 | -3.84 |
| *Salt Lake – Levels are Relative to the Playa Surface* | | | | | | | | | | | |
| Centre | Salt1a | 0 | -2.63 to –2.13 | 0.55 | 0.56 | - | - | - | - | 0.64 | 0.52 |
| | Salt1b | 0 | -0.5 to –0.2 | - | 0.12 | - | - | - | - | 0.11 | 0.17 |
| *Spectacle Lake – Levels are Relative to Top of Salt Crust at SM5* | | | | | | | | | | | |
| Pond3-Edge | SM1 | 0.9 | -17.2 to –15.2 | - | - | - | - | - | 3.00 | 2.67 | 2.91 |
| | SM2 | 0.547 | -2.15 to –0.15 | - | - | - | - | - | 1.50 | 1.64 | 1.61 |
| | SM3 | 0.28 | -8.32 to –6.32 | - | - | - | - | - | 1.40 | 1.25 | 1.36 |
| Pond2-Centre | SM4 | 0.14 | -7.36 to –5.36 | - | - | - | - | - | 1.08 | 1.15 | 1.25 |
| | SM5 | 0 | -6.00 to –5.50 | - | - | - | 0.9 | - | 1.07 | 1.08 | 1.09 |
| | SM6 | -0.25 | -19.05 to –18.25 | - | - | - | 2.91 | - | 1.92 | 1.66 | 2.12 |

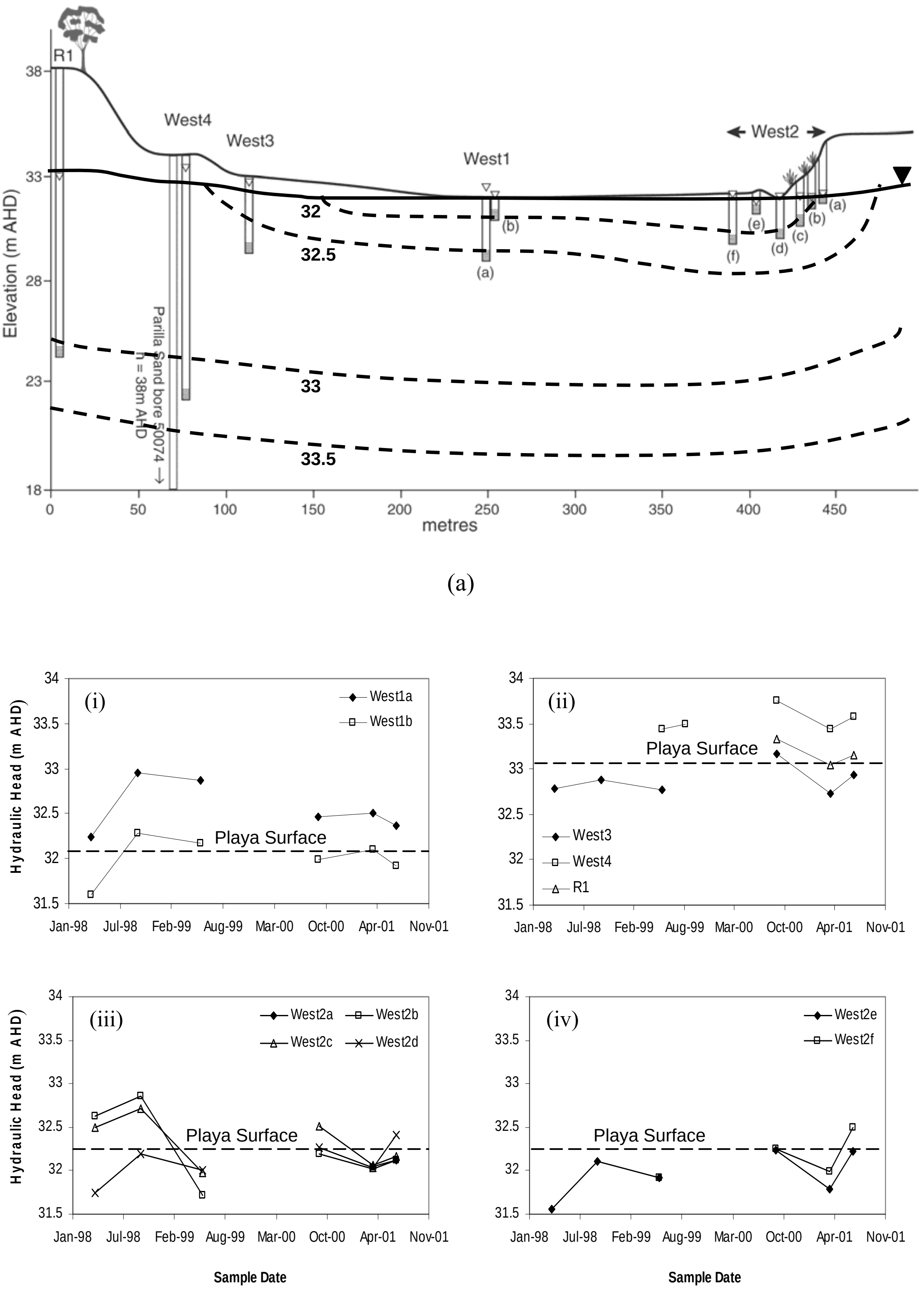

(a)

(b)

Figure 4.3. (a) Cross-section through Western Salina, showing piezometer locations, measured fresh water hydraulic heads (open triangles; April 2001) and inferred equipotential distribution (broken lines). (b) Piezometer hydrographs. Refer to Figure 2.1 for areal piezometer locations.

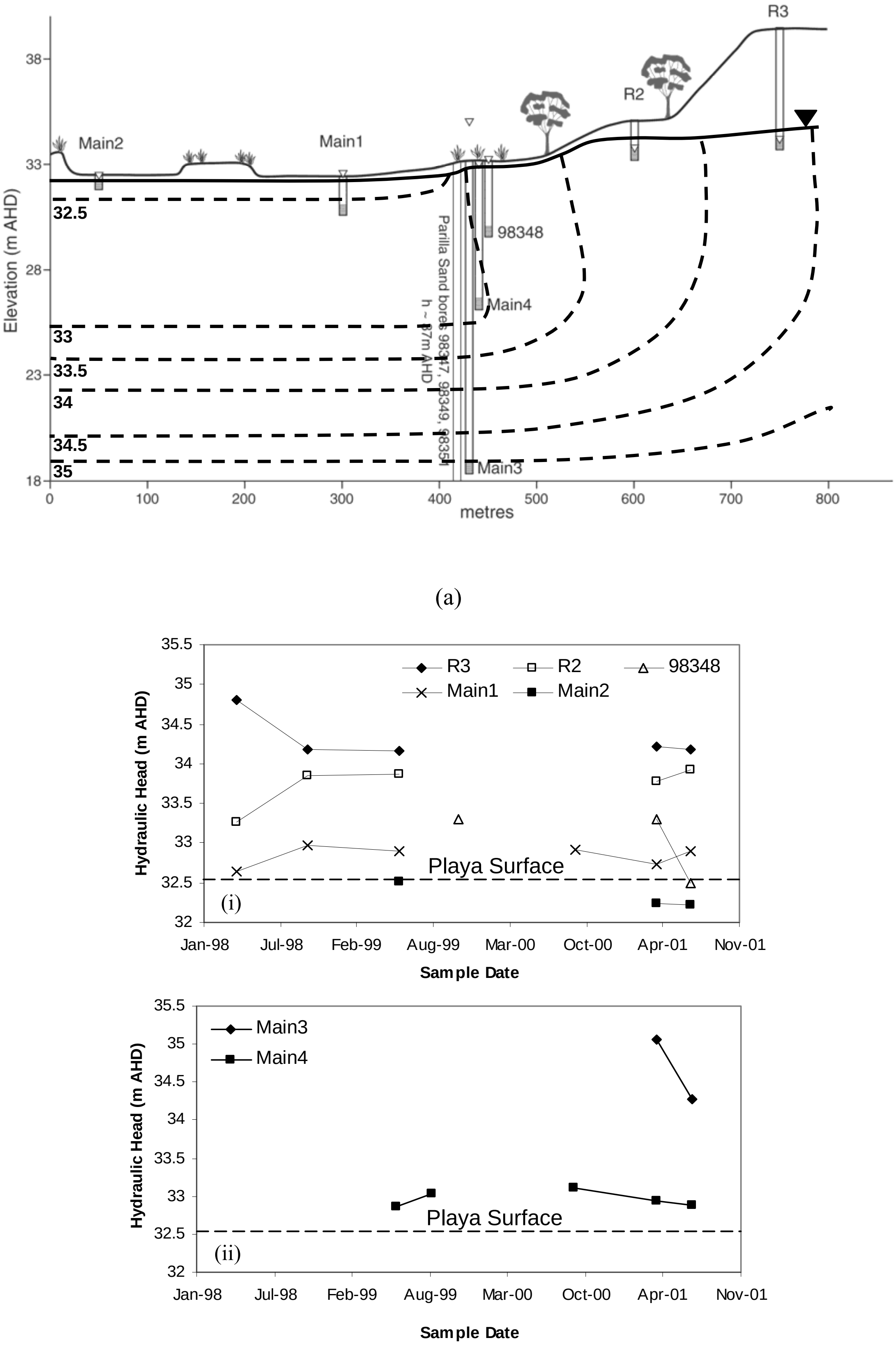

(a)

(b)

Figure 4.4. (a) Cross-section through the Main Salina, showing piezometer locations, measured fresh water hydraulic heads (open triangles; April 2001) and inferred equipotential distribution (broken lines). (b) Piezometer hydrographs. Refer to Figure 2.1 for areal piezometer locations.

Large fluctuations in hydraulic heads in the shallow playa sediments often correspond to hydraulic head fluctuations in the adjacent dunes and deeper in the Blanchetown Clay. For example, at the edge of Western Salina (transect West2), hydraulic heads varied considerably over time (Fig. 4.3b (iii&iv)). Hydraulic head fluctuations in the sandy plain adjacent the playa (Fig. 4.3b(iii)) were mimicked by hydraulic head fluctuations in the playa itself (Fig. 4.3b(iv)). These also corresponded to water level fluctuations in the deeper piezometers (West3, West4 and R1) at another location on the playa margin (Fig. 4.3b(ii)). Hydraulic heads in transect West2 show that a temporary groundwater mound, up to 1 m above water levels in the playa, develops occasionally in the adjacent sandy plain. This is probably in response to larger rainfall events, inducing flow of shallow groundwater into the playa (e.g. April 1998, October, 1998). At other times, the hydraulic gradient between the plain and the playa can be negligible (e.g. April 2001; Fig. 4.3).

An upward hydraulic gradient exists between the Parilla Sand bores and the piezometers in the Blanchetown Clay at the edge of the Main Salina, (Main3 and Main4; Fig. 4.4). However, the hydraulic head in the shallower bore 98348 fluctuates up to 60 cm, and can occasionally be higher than that in the underlying Main4 (Fig. 4.4). Figure 4.4 shows, based on observed hydraulic heads, that bore 98348 intersects a shallow groundwater flow system that is fed by recharge under the adjacent dune. Groundwater in this shallow system flows from the dune at R3, where the hydraulic head is up to 2.2 m above that in the playa (Fig. 4.4a). In contrast, the deeper piezometers, Main3 and Main4, intersect a deeper flow system, with groundwater flowing up from deeper in the Blanchetown Clay or the Parilla Sand aquifer. Piezometer 98348 is therefore hydraulically disconnected from the deeper piezometers. A similar situation probably occurs at Spectacle Lake (the harvested lake), where, the hydraulic head in the shallowest piezometer SM2 (at 1.15 m depth), at the edge of Pond 3, is occasionally above that of piezometer SM3, screened 6 m below it (Fig. 4.2). However, hydraulic head measurements in the adjacent sand dune are not available to construct a detailed equipotential distribution.

Hydraulic head fluctuations in the two deepest piezometers, SM1 and SM6, at Spectacle Lake, are greater than those in the shallower ones (up to 45 cm; Fig. 4.2). The magnitude of this fluctuation decreases towards the surface (piezometers SM3 and SM4), until the water level is static in piezometer SM5 (5.75 m below the playa floor). Inverse fluctuations occur in the shallow SM2 piezometer (Fig. 4.2), suggesting that they may be due to pumping of water from the Parilla Sand, onto the surface of the lake.

### 4.2.4 Chloride Distributions

Chloride concentrations ([$Cl^-$]) have been used to investigate brine distributions instead of TDS because $Cl^-$ (a) is by far the dominant ion in any of the waters at Raak Plain, (b) is simple to measure, and (c) behaves conservatively until NaCl saturation. The most saline brines at Raak Plain (TDS ≅ 240 g/kg to 260 g/kg) occur just below the playa surfaces, but salinities decrease very quickly, by up to 50 g/kg, within the top 30 cm of the sediment profiles (Section 3.4.2; Appendix G). Very little spatial variation in the maximum TDS of the brines is seen both between playas and within individual playas (variations < 20 g/kg) (Table 1.1).

There is a general east-west increase in groundwater [$Cl^-$] from 23.1 g/kg to 46.0 g/kg in the Parilla Sand aquifer below Raak Plain, which is mirrored by the trend in

TDS concentrations. The major increase occurs to the west of the Main Salina, with the highest [Cl$^-$] occurring below Western Salina (Fig. 4.5).

Soft sediments caused inaccessibility of the natural playas to heavy drilling equipment and limited the investigation to the playa edges, where it was expected that the brine body may still occur (see Chapter 2). Pore water [Cl$^-$] vs depth profiles were constructed from drill spoil collected at the edges of Western Salina (site West4; 33 m deep) and the Main Salina (Main3; 19 m deep) (See Fig. 2.1 for locations), and continuous cores collected at the centre of Pond 2 (8.5 m deep) and edge of Pond 3 (22.5 m deep) at Spectacle Lake (the harvested lake) (Fig. 4.6). In general, the profiles show a hypersaline brine body just below the surface that extends to a depth of up to 10 to 14 m. Pore water Cl$^-$ concentrations below this at the natural playas are approximately the same as that of the underlying Parilla Sand groundwater. The situation is different below Spectacle Lake (the harvested lake), where Cl$^-$ concentrations higher than the Parilla Sand groundwater are observed below the main brine body.

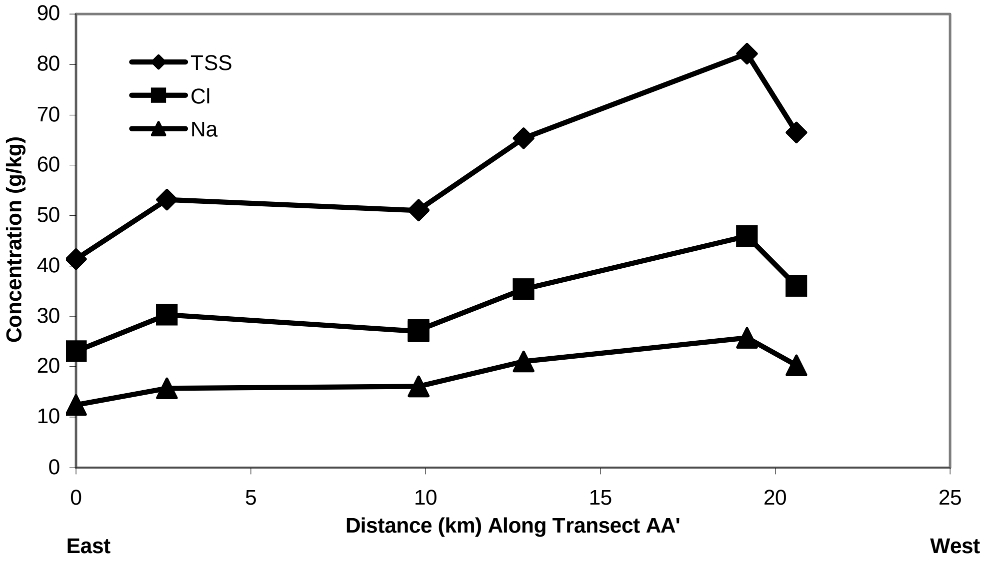

Figure 4.5. Total soluble salts (TSS), Cl$^-$ and Na$^+$ concentrations in Parilla Sand groundwater along the east-west transect AA’ below Raak Plain. See Figure 1.6 for transect location.

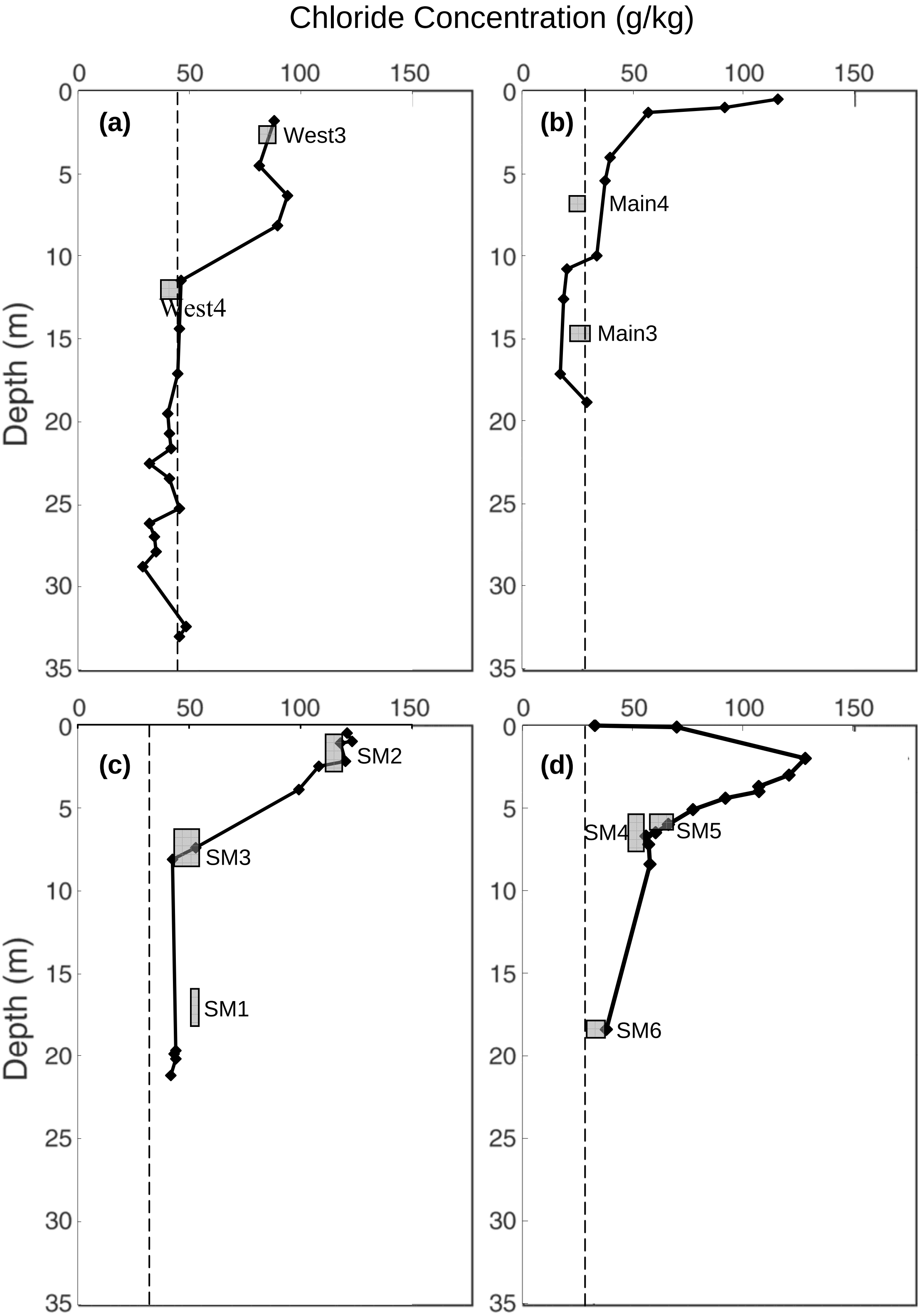

Figure 4.6. [Cl$^-$] of sediment pore waters versus depth at the edges of two natural playa lakes at Raak Plain (a&b), and at the edge and centre of the harvested lake (Spectacle Lake) (c&d). Concentrations measured in adjacent piezometers are also shown, and dashed lines represent [Cl$^-$] of underlying Parilla Sand groundwater. See Figures 2.1 and 2.2 for site locations.

[Cl$^-$]s of up to 94 g/kg occur above 8.5 m depth at the edge of Western Salina (site West4) (Fig. 4.6a). There is a decrease in concentration between 8.5 m and 14 m depths to 46 g/kg, which is equal to that in the underlying Parilla Sand aquifer. The shape of the profile between 8.5 m and 14 m is unknown due to loss of sample in this region. Below 14 m, [Cl$^-$] remains relatively constant, at or below 46 g/kg to 33 m, where sampling stopped. [Cl$^-$] in piezometer West4, screened between 11 m and 12 m depths also ranged between 44 g/kg and 46 g/kg during the sampling period (June 1999 to July 2001), and was similar to that in the pore water profile at these depths. [Cl$^-$] in piezometer West3, screened 3.8 m below the lake surface ranged between 79 g/kg and 83 g/kg, and was also similar to the observed pore water concentrations at that depth. The maximum [Cl$^-$] at a depth of 0.5 m below the edge of the Main Salina (site Main3) is 116 g/kg (Fig. 4.6b). This drops quickly to 40 g/kg and then gradually to approximately the regional groundwater concentration (between 26 g/kg and 27 g/kg) at 5 m depth.

[Cl$^-$] is approximately 121 g/kg at a depth of 0.5 m below the edge of Pond 3 at Spectacle Lake (site SM1), decreasing gradually to approximately 43 g/kg at 8.1 m depth (Fig. 4.6c). Below this, the pore water remains at this concentration to the maximum sample depth of 21.2 m. This [Cl$^-$] is still above that measured in July 1997 in the Parilla Sands bore screened 40 m below Spectacle Lake (30.4 g/kg).

[Cl$^-$] in the top 2 m of the pore water profile below the centre of Pond 2 (site SM5) is between 32.9 g/kg and 128.5 g/kg, with concentrations decreasing towards the surface (Fig. 4.6d). [Cl$^-$] then drops gradually to approximately 56 g/kg at 6.7 m depth, below which it remains constant to the maximum sample depth of 8.4 m. A groundwater sample from a piezometer (SM6) screened between 18 m and 18.8 m depth had a [$Cl^-$] of 38.1 g/kg, which is still well above the concentration of Parilla Sand groundwater (30.4 g/kg).

## 4.3 Discussion

### 4.3.1 Water Fluxes in a Regional Groundwater Discharge Complex

#### 4.3.1.1 Regional Groundwater Discharge

Artesian hydraulic heads in the Parilla Sand aquifer, and upward hydraulic gradients across the Blanchetown Clay and playa sediments below Raak Plain, are consistent with regional groundwater discharge (Fig. 4.1). Upward hydraulic gradients are remarkably constant across each playa, and across the whole of Raak Plain, as shown in Figure 4.7, on which a constant upward flux (hydraulic gradient) should produce a straight line distribution of points. Outliers from the linear trend are the shallow piezometers at the edges of the lake (West2 (d-f) and West3; see Fig. 4.3), which are most likely to be affected by transient local recharge processes. Some of the scatter in Figure 4.7 may also be due to variations in vertical hydraulic conductivity, which alters the hydraulic head at that location in order to maintain a constant flux (conservation of mass).

With the exception of minor variations, an upward hydraulic gradient of 0.1 generally occurs across Raak Plain. For a vertical hydraulic conductivity of the Blanchetown Clay ($K_{VB}$) between $5 \times 10^{-6}$ m/d ($1.8 \times 10^{-3}$ m/y) and $5 \times 10^{-4}$ m/d ($1.8 \times 10^{-1}$ m/y), and a porosity of 0.45, this translates into upward hydraulic fluxes of regional groundwater between 0.4 mm/y and 40 mm/y.

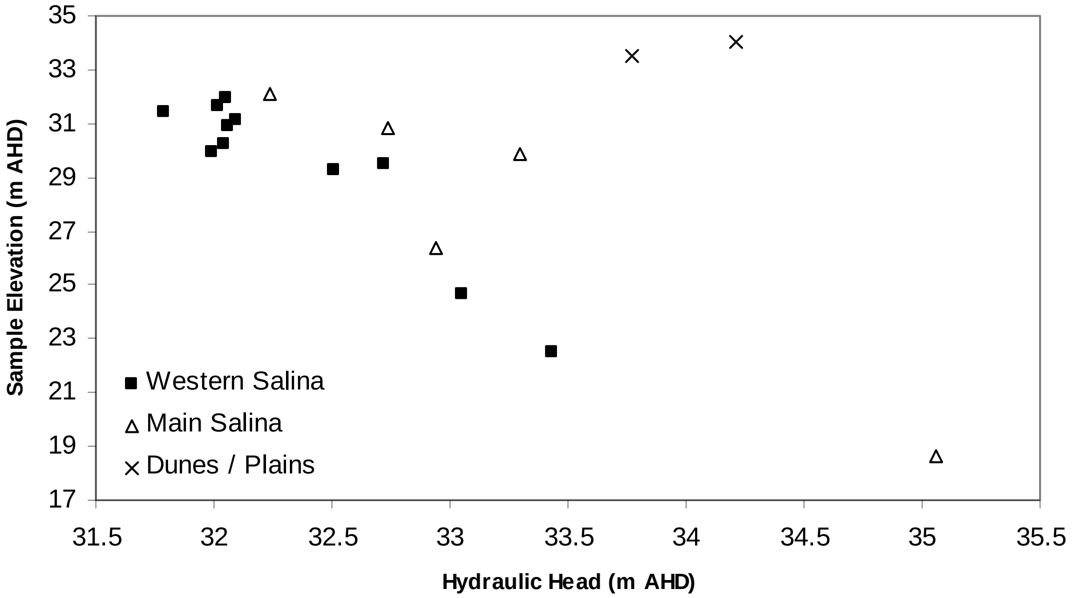

Figure 4.7. Graph showing the relationship between sample elevation and hydraulic head for sites from Western Salina, the Main Salina and dune / plain sites between the playas. A straight line represents a constant hydraulic gradient, and for constant sediment hydraulic properties, this suggests a constant vertical flux.

### 4.3.1.2 Local Groundwater Flow Systems

Groundwater flow patterns are normally controlled by topography or, more specifically, differences in hydraulic head between recharge and discharge areas (Toth, 1963; Freeze and Witherspoon, 1967). Where local topographic relief is negligible, only regional groundwater flow systems develop (Fig. 4.8a). Where there is pronounced topographic relief, local groundwater flow systems dominate (Fig. 4.8b). The hydraulic heads in recharge and discharge areas are a function of recharge rate, which is in turn a function of topography, soil type and vegetation (Fetter, 1994). Below sand dunes, sandy soils (high infiltration rates) and comparatively deep water tables (> 5 m) reduce evaporation of recharge, resulting in high recharge rates and comparatively high hydraulic heads. In comparison, on lower elevation sandy plains, water may directly evaporate from shallower water tables, maintaining the lower hydraulic heads there. At Raak Plain, large variations in topography and the presence of areas of both net recharge and net discharge suggest that local groundwater flow systems should be quite important in the discharge complex, as well as discharge of regional Parilla Sand groundwater (Fig. 4.9).

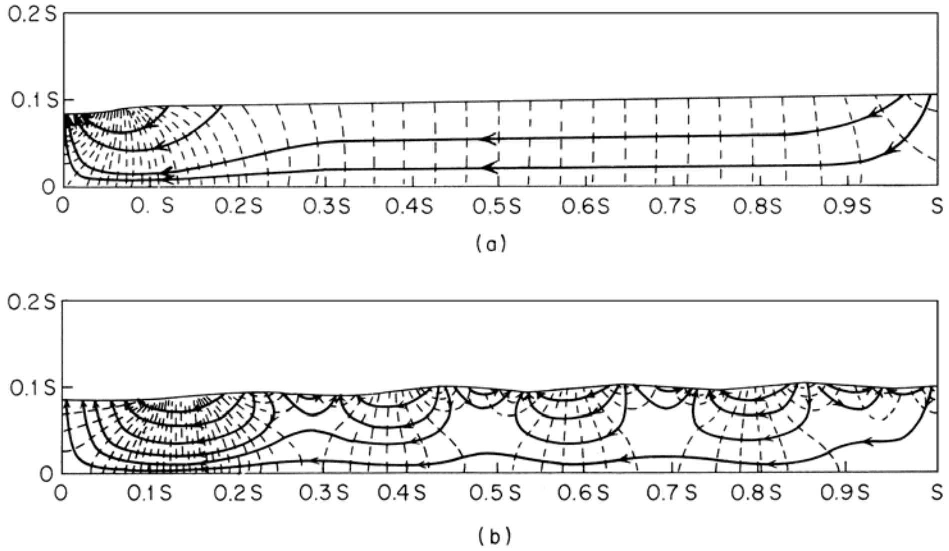

Figure 4.8. Effect of topography on regional groundwater flow patterns (from Freeze and Cherry, 1979; after Freeze and Witherspoon, 1967).

The regional Parilla Sand aquifer discharges groundwater through the playas at Raak Plain via upward leakage through the Blanchetown Clay, whilst local flow systems transport groundwater recharged locally through dunes and sand plains to eventually discharge in adjacent playas. Over large time scales, the regional and local groundwater systems can be assumed to be in hydraulic balance, with water tables in the lakes maintained approximately at the playa surfaces by evaporation and fluctuating very little. However, over short time scales (months), the surface systems are transient, with hydraulic heads fluctuating by up to 1.5 m.

The transient nature of the shallow flow systems can be seen at Western Salina, where hydraulic head fluctuations of up to 1 m in the adjacent recharge area

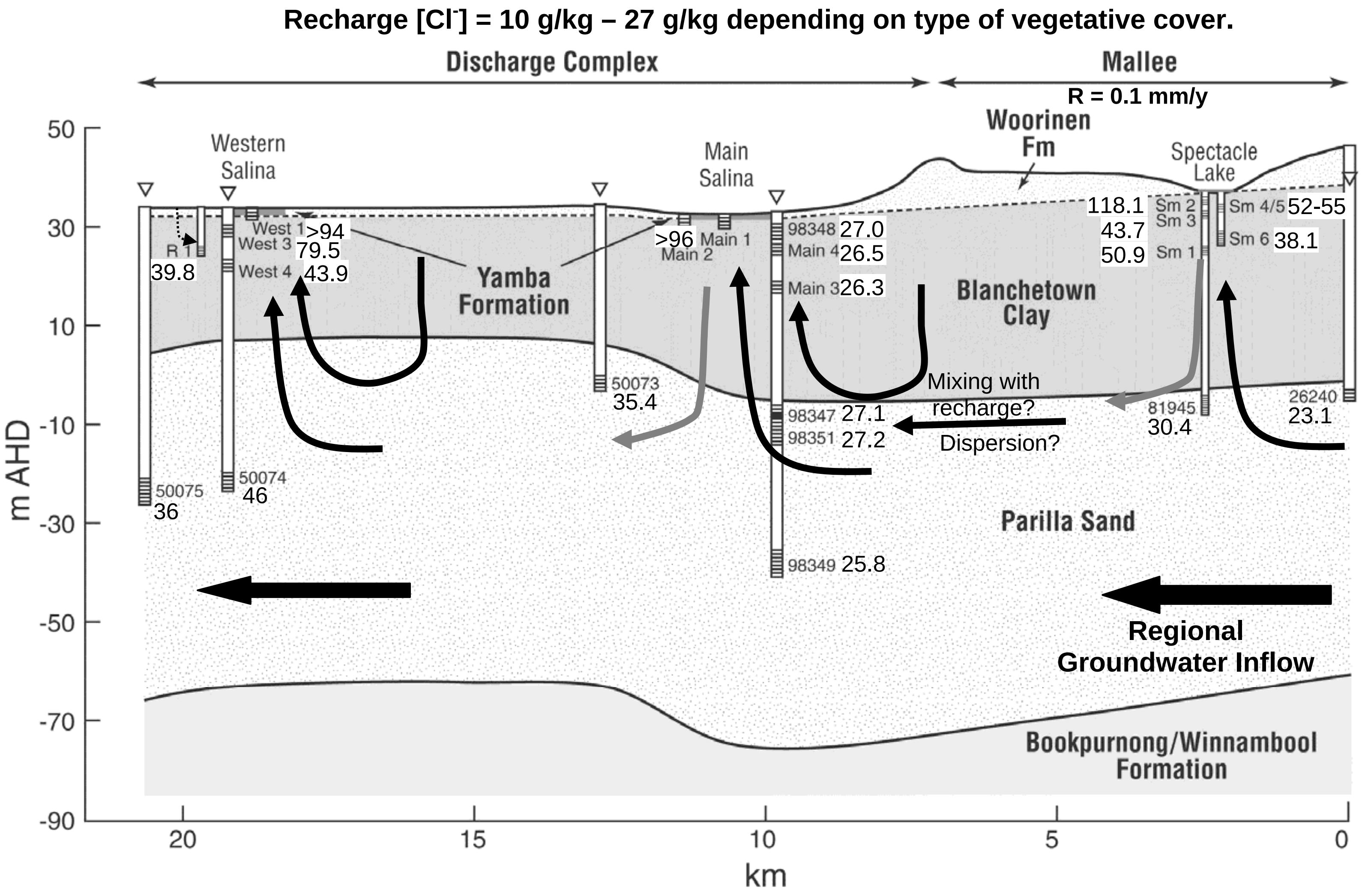

Figure 4.9. Conceptual diagram of groundwater and solute movement below the Raak Plain groundwater discharge complex. Numbers represent [Cl-] (g/kg) in piezometers and bores. Black arrows represent groundwater (and solute) movement and grey arrows represent salt movement.

(West2(a-d)) are mimicked by hydraulic head fluctuations in the discharge zone (West2(e-f)) (Fig. 4.3b (iii&iv)). Similar water level fluctuations are observed further west along the playa margin, in piezometer West3, screened 3.5 m below the playa, and West4 and R1 more than 7 m below the water table at the edge of the playa (Fig. 4.3b(ii)). The shallow piezometers at the centre of the playa (West1 (a&b); Fig. 4.3b(i)) display these large head fluctuations between April 1998 and June 1999, but behave slightly differently between September 2000 and July 2001 (Fig. 4.3b(i)). This may indicate that the hydraulic heads in the centre of the playa are not affected by smaller fluctuations at the edge, or that the response is delayed.

The potential for shallow groundwater flow systems, with the dunes and plains as recharge areas and the adjacent playa lakes as discharge zones can be seen in the fact that hydraulic heads in the dunes and plains adjacent Western Salina and the Main Salina can be up to 1 m and 2.2 m higher respectively than those in the playas, inducing a horizontal hydraulic gradient towards the playas (Figs. 4.3 and 4.4). At other times, the gradients are zero, or reversed, with the potential for groundwater to flow from the playas into the bases of the dunes, perhaps driven by the high density of the brine (Section 4.2.3). Surface runoff from the marginal dunes and sand plains into the playa has also been observed, particularly after rain, either as a result of rainfall in excess of the infiltration capacity of the soil or due to seepage from the face of the dune.

Uniformity in hydraulic head fluctuations in the piezometers at the edges of Western Salina and the Main Salina suggest common processes affecting hydraulic heads down to at least 10 m below the water table. The unsaturated zone is thin (< 1 m) in and around the playas, so rapid responses in hydraulic heads to high recharge events can be expected. Hydraulic head fluctuations in the shallow sediments appear to be transmitted deeper within the Blanchetown Clay, where heads rise simultaneously to maintain the constant upward flux. In this way, short time-scale transient effects in the surface groundwater system are transmitted deeper, at least 10 m into the Blanchetown Clay.

#### 4.3.1.3 Water Balances of the Playa Lakes

Following on from the preliminary generic conceptual models for the water and solute balances of the playa lakes at Raak Plain presented in Section 1.4, quantitative water and solute mass balances have been constructed for the three main playas included in this study (The Main Salina, Western Salina and Spectacle Lake) and are shown in Figures 4.10(a-c). Calculations are based on a 1 m wide transect in the direction of regional groundwater flow (along Transect AA'; Fig. 1.6). The length of the shallow groundwater catchment for each playa along this transect was estimated from a topographic map, along with the length of the groundwater discharge zone that occurs within these catchments (Sheet 7328 (Ed. 1), 1977, National Topographic Map Series). Calculations for Spectacle Lake are for the playa in its natural state, prior to salt harvesting. This was done for comparison with the other two natural playas and is considered reasonable, as salt harvesting over the last 20 years would only have affected the brine in the top few metres of the profile. The following assumptions are also made:

- Recharge rate (R) is 2.5 mm/y in the dunes and plains around the Main Salina and Western Salina, as these areas are fairly bare of mallee vegetation, and 0.1 mm/y in the dunes around Spectacle Lake, which are densely vegetated with mallee (see Section 4.2.2).

- Rainfall onto the playa surface is evaporated immediately and does not contribute to the water balance.
- Upward leakage from the Parilla Sand aquifer ($I_{PS}$) = 0.4 mm/y to 40 mm/y, based on a $K_V$ for the Blanchetown Clay ($K_{VB}$) between 5 x $10^{-6}$ m/d and 5 x $10^{-4}$ m/d and an observed average upward hydraulic gradient of 0.1 (Section 4.3.1.1).
- Volume evaporated (E) = $I_{PS}$ + R
- Rainfall [$Cl^-$] = 4.2 mg/L (Blackburn and McLeod, 1983). Salt from rainfall is deposited over the entire playa catchments to be eventually incorporated into the brines in the discharge zones. Salt inputs to the playas via local recharge are therefore included in the estimate of inputs via rainfall over the entire catchment.
- Loss of $Cl^-$ from individual catchments by aeolian deflation is negligible.
- [$Cl^-$] of evaporated water = 0 mg/L.
- [$Cl^-$] of Parilla Sand groundwater input to each playa is equivalent to [$Cl^-$] measured in regional Parilla Sand bores below that playa.
- Total $Cl^-$ in the brine bodies below the playas ($Cl^-_t$) is calculated assuming an average [$Cl^-$] of 46 g/kg to a depth of 10 m over the entire area of the playa, which is an approximation based on the pore water $Cl^-$ vs depth profiles in Figure 4.6.
- The time scale for development of the brine body (t) is calculated by dividing $Cl^-_t$ by the total annual input of chloride to the playas ($Cl^-_i$), i.e. the inputs from rainfall deposition and upward leakage from the Parilla Sand aquifer.

The results of the water balance calculations for Western Salina and the Main Salina suggest total annual groundwater discharge rates from the playas of between 3 mm/y and 43 mm/y (Fig. 4.10 (a&b)). If an intermediate $K_{VB}$ of 5 x $10^{-5}$ m/d (1.8 x $10^{-2}$

(a) The Main Salina

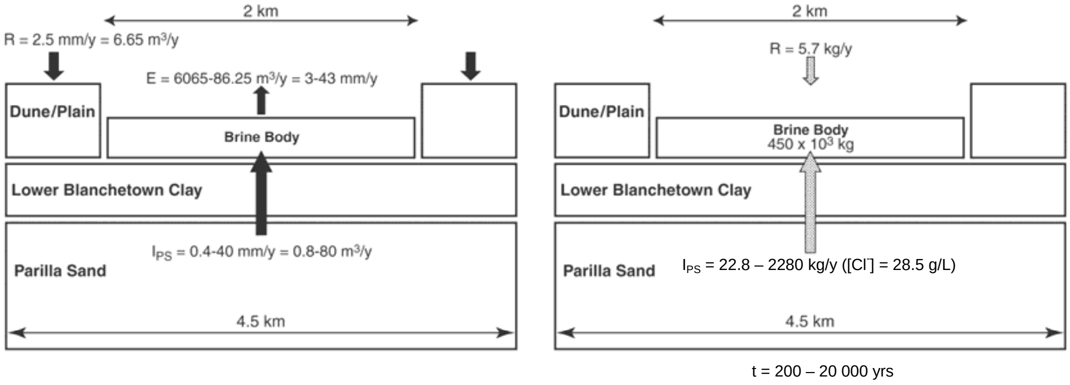

(b) Western Salina

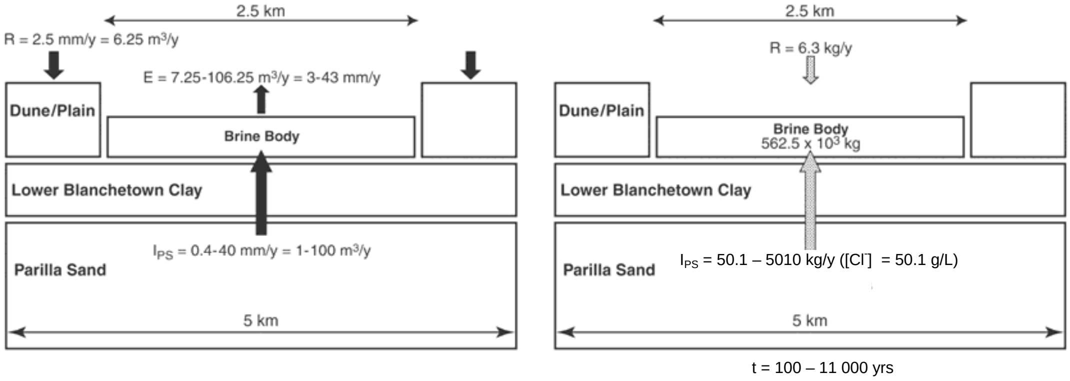

(c) Spectacle Lake

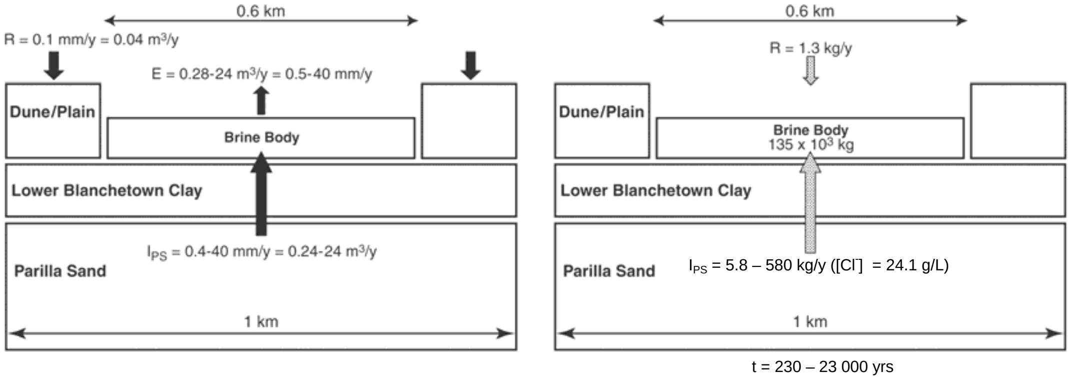

Figure 4.10. Water (left) and solute (right) balances for the three main playa lakes included in this study of Raak Plain.

m/y) is assumed for the Blanchetown Clay, this narrows to between 4 mm/y and 7 mm/y, which is at the lower end of the range of values estimated using pore water [$Cl^-$] and $\delta^2H$ vs depth profiles (Howes, 1998). The estimate is lower for Spectacle Lake (prior to the salt harvesting operation) due to lower recharge rates assumed in the surrounding mallee-vegetated dunes (Fig. 4.10c).

The relative importance of regional groundwater in the water budgets of the playas depends heavily on the vertical hydraulic conductivity of the Blanchetown Clay aquitard. In the lowest conductivity case ($K_{VB} \cong 5 \times 10^{-6}$ m/d), regional groundwater represents approximately 10% of the water evaporated from the Main Salina and Western Salina, whilst this is 85% at Spectacle Lake, largely due to much lower local recharge rates in the surrounding dunes. The importance of locally recharged groundwater in the water balances of the playas is therefore greater in the main part of the discharge complex. The contributions from regional groundwater become greater if the assumed $K_v$ of the Blanchetown Clay is greater.

#### 4.3.1.4 Hydraulic Processes Leading to the Presence of Both "Type D" (Surface Water) and "Type E" (Dry) Basins

The classification scheme used by Bowler (1986) to describe the hydraulic status of lakes was described in Section 1.3.5.5. The presence of both surface water ("Type D") and dry playa ("Type E") lakes at Raak Plain may be due to differences in their physical settings and locations with respect to the regional potentiometric head. Western Salina and the Main Salina (the groundwater dominated Type E lakes) are located in the interior of the discharge complex, where the surrounding landscape is comparatively flat and poorly vegetated and the regional groundwater hydraulic head is slightly lower. In contrast, Salt Lake and Spectacle Lake are located at the eastern margin of the discharge complex, where the surrounding dunes are densely vegetated with native mallee and the regional groundwater hydraulic head is higher (Table 5.4). The coverage of native vegetation at a particular location can be expected to influence recharge rates and hence hydraulic heads directly below the dunes (Section 4.2.4). The balance between the heads in the regional aquifer and in the dunes may determine the importance of surface or shallow groundwater flow to the water and salt balances of the lakes. The importance of shallow subsurface groundwater flow into Spectacle Lake has been suggested by the owner of the salt harvesting operation, who has observed that springs form around the edges of the dunes adjacent the playa after heavy rainfall (Duncan Thomson, Hattah Salt, pers. comm., 2000). Perching of local runoff and shallow groundwater flow at the surfaces of the Type D playas may be enhanced by the presence of an extremely dry, low porosity silty clayey fine sand layer below 20 to 50 cm depth that was observed at all of the playas.

The above discussion suggests that the thin film of surface water occurring in Salt Lake (and probably in Spectacle Lake in its natural state) may be runoff and/or locally recharged groundwater from the dunes surrounding the playas, and direct rainfall onto the playa surfaces. However, as the potentiometric surface in the Parilla Sand aquifer is near or above the playa surfaces, the occurrence of surface water in the eastern playa lakes may also be due to greater upward leakage of regional groundwater through the Blanchetown Clay at the up-gradient margin of the discharge complex. The shallow groundwater tables at Salt Lake and Spectacle Lake are higher relative to the lake floor than those at Western Salina and the Main Salina (Table 3.1). In this case, differences in the hydrologic status of the playa lakes would be determined by the position of the regional water table relative to the ground surface at the lake location. This will be investigated further in the following two sections of this thesis.

### 4.3.2 Movement of Salt in a Regional Groundwater Discharge Complex

#### 4.3.2.1 Solute Balances of the Playa Lakes

Regardless of its importance in the playa water balances, regional groundwater is the dominant source of solutes to the subsurface brines that have formed by evapo-concentration in the playa lakes (Fig. 4.10). The solute mass balance calculations (Fig. 4.10) suggest time scales of the order of 100 yrs to 20 k yrs for development of the brine bodies. For the intermediate $K_V$ of 5 x $10^{-5}$ m/d, this narrows to approximately 2 k yrs at the Main Salina and Spectacle Lake. The estimate for Western Salina is much lower (690 years) because the current higher observed TDS of the Parilla Sand groundwater at that location (bore 50074; [$Cl^-$] = 46 g/kg) was used as input for the calculations. However, as discussed in the following section, this high TDS may be due to brine leakage from the playa lakes up-gradient of Western Salina and hence may not have prevailed over the entire time of brine development. A time scale between 690 yrs and 2 000 yrs could therefore be assumed for this playa, with the latter time scale calculated based on Parilla Sand compositions from up-gradient of Western Salina.

The time scale estimates assume no removal of $Cl^-$ by deflation from the surfaces of the playas although evidence for recycling of $Cl^-$ by this mechanism was seen in elevated TDS of bulk rainfall and dry deposition samples (Section 3.4.5). Wood and Sanford (1995) observed that aeolian deflation of surface salt from saline lakes can cause elevated unsaturated zone pore water salinities up to tens of kilometres down-wind of the lakes. However, the similarity between the brine compositions and those of their potential sources indicates that solutes are generally conserved in solution and hence losses by aeolian deflation are probably negligible in comparison with other solute fluxes and the total solute storages in the brine bodies (Chapter 3).

The estimated brine accumulation times suggest that the brines at Raak Plain have developed since the last glacial maximum, which was 20 k yrs ago (Bowler and Wasson, 1984). Calculations using the higher $K_{VB}$ values ($5 \times 10^{-5}$ m/d to $5 \times 10^{-4}$ m/d) imply accumulation times much lower than this (< 2 k yr). It is highly likely that Raak Plain was an active groundwater discharge complex during the extremely dry and windy glacial maximum, 20 k yr ago, as well as during other dry periods prior to and since this (Bowler and Wasson, 1984). Therefore, an accumulation time of 2 k yrs, for example suggests (a) an underestimate of the vertical extent of the brines and hence the amount of salt stored below the playas, (b) large losses of salt by deflation from the playa surfaces, or (c) losses of salt via leakage into the regional aquifer system.

#### 4.3.2.2 Mixing of Brine With Regional Parilla Sand Groundwater

The two-fold increase in TDS of groundwater in the Parilla Sand aquifer below Raak Plain (Fig. 4.5) is unusual in the central Murray Basin, where groundwater chemistry is extremely uniform over large distances (Macumber, 1991). There has been no evidence of evaporite deposits in the Parilla Sand, and ion vs [$Br^-$] graphs suggest that the TDS increases are due to mixing with brine from the discharge complex (Chapter 3).

The increase in [Cl$^-$] of Parilla Sand groundwater between the eastern margin of Raak Plain (bore 26240) and Spectacle Lake is probably due to diffusive or advective mixing with brine from Spectacle Lake (Fig. 4.9). The saline brines at both the edge of Pond 3 (site SM1) and at the centre of Pond 2 (site SM5) ([Cl$^-$] > 50 g/kg) extend to depths between approximately 7 m and 7.5 m (Fig. 4.6 (c&d)). Although the main brine body appears to be confined above this depth, pore water [Cl$^-$] 10 to 12 m below in the Blanchetown Clay is still approximately 38 g/kg, much higher than that of the underlying Parilla Sand groundwater (30.4 g/kg). This suggests downward movement of salt from the main brine body by some process (Fig. 4.9). Above 7.5 m, the profiles have shapes similar to each other and consistent with diffusion between high TDS brine near the surface and the lower TDS groundwater below 7.5 m (Fig. 4.6 (c&d)). However, the profiles have a convex rather than concave shape, probably due to downward displacement of brine by the downward hydraulic gradient imposed by impoundment of water at the playa surface. The processes occurring at Spectacle Lake are discussed in more detail in Chapter 7.

The [Cl$^-$] of the Parilla Sand groundwater at the eastern margin of the Main Salina is lower than in the up-gradient bore below Spectacle Lake (bore 81945), possibly due to either dispersion along the groundwater flow path between these two points or mixing with infiltrated recharge (Fig. 4.9). [Cl$^-$] in the Parilla Sand then increases again down-gradient of the Main Salina (bore 50073), until reaching a maximum below Western Salina. The boundary between the brine and underlying groundwater at the eastern (up-gradient) edge of the Main Salina occurs at a depth of 5 m, with [Cl$^-$] decreasing exponentially from 116 g/kg at the surface towards the concentration of the regional groundwater at 5 m (Fig. 4.6b). The exponential shape is characteristic of a combined process of upward advection of groundwater and back-diffusion of salt across the concentration gradient resulting from evapo-concentration of this groundwater at the surface (Ullman, 1985). Although the brine body is confined within the top 5 m of the Blanchetown Clay at this location, the increase in TDS of the Parilla Sand groundwater suggests that this may not be the case in other parts of the playa. Downward movement of salt must be occurring, or have occurred in the past, from the centre or down-gradient (western) side of this large playa (Fig. 4.9).

The boundary between the concentrated brine and less concentrated groundwater at the edge of Western Salina (site West4; Fig. 2.1) occurs somewhere between the depths of 8 m and 14 m (Fig. 4.6a). A [$Cl^-$] of approximately 90 g/kg is maintained fairly constantly to 8 m. However, below 14 m, [$Cl^-$] in the Blanchetown Clay pore water is generally below that of the underlying Parilla Sand groundwater (bore 50074; Fig. 4.6a). Again, this suggests that diffusion from the present brine body at this location is not the source of the TDS increase observed in the underlying aquifer. Other scenarios such as (a) local diffusion or advection of brine below other parts of the playa, (b) leakage from other playas in the system or (c) historical brine leakage under a different hydrologic regime are all plausible reasons for the observed salinity increase in the Parilla Sand groundwater that cannot be adequately investigated based on the current data.

Some low [$Cl^-$] values that occur in the profile are probably a result of mixing between the regional groundwater ([$Cl^-$] = 46 g/kg) and locally recharged groundwater ([$Cl^-$] = 10 g/kg to 27 g/kg) (Fig. 4.9). Similarly, a groundwater [$Cl^-$] of 40 g/kg occurring 8 m below the water table 50 m away from the playa margin (R1), is also probably due to mixing between locally recharged and regional groundwater.

#### 4.3.2.3 Potential for Density-Driven Convection of Brine

The likelihood for density-driven convection of brine to occur at Raak Plain can be investigated theoretically based on both the macroscopic Rayleigh number ($Ra_l$: Eq. 4.1) and the boundary-layer Rayleigh number ($Ra_\delta$: Eq. 4.2). Calculations of both Rayleigh numbers have been carried out for brines in the Blanchetown Clay, based on a saturated thickness (for $Ra_l$) of 30 m, a porosity of 0.45 and a diffusivity of $7.1 \times 10^{-10}$ $m^2/s$ (Ullman, 1985). Results are given for evaporation rates of 1 mm/y and 100 mm/y, and vertical hydraulic conductivities of $5 \times 10^{-5}$ m/d and $5 \times 10^{-4}$ m/d to span the ranges expected to occur at Raak Plain (Section 4.2.1) (Table 4.6). The calculated Rayleigh numbers are then compared with the relevant critical Rayleigh numbers to assess the likelihood of the onset of density-driven convection.

Based on the macroscopic Rayleigh number calculations ($Ra_l$), the brines at Raak Plain may be unstable for a $K_v$ at the higher end of the range of those expected for the Blanchetown Clay, irrespective of the evaporation rate (Table 4.6). The boundary layer Rayleigh number calculations ($Ra_\delta$) suggest that the brines will only be unstable under conditions of low evaporation (e.g. $E \leq 1$ mm/y) and high $K_{VB}$. Hence, instability could occur in the higher conductivity sediments observed in the top of the Blanchetown Clay, particularly if evaporation is low, and if a significantly concentrated boundary layer builds up above them. This instability will probably then be damped out by the lower conductivity layers observed at various depths in the Blanchetown Clay, and could hence only be an effective solute transport mechanism over short distances.

Table 4.6. Rayleigh number calculations for brines in the Blanchetown Clay at Raak Plain.

| | $Ra_c$ | $K_{VB} = 5 \times 10^{-5}$ m/d | | $K_{VB} = 5 \times 10^{-4}$ m/d | |
|---|---|---|---|---|---|
| | | E = 1 mm/y | E = 100 mm/y | E = 1 mm/y | E = 100 mm/y |
| $Ra_l$ | $4\pi^2 \cong 40$ | 7.2 | 7.2 | 72.2 | 72.2 |
| $Ra_\delta$ | 5.6 – 14.3 | 2.4 | 0.02 | 24 | 0.24 |

#### 4.3.2.4 Time Scales For Solute Transport

Transport of salt, both vertically and horizontally, can occur by three main processes: advection, diffusion and density-driven convection. By comparing the time scales over which each of these processes occurs over a given distance, we can determine the degree to which each is likely to contribute to the transport of salt from the brines at Raak Plain, into the Parilla Sand aquifer.

*Advection*

Hydraulic gradients (**i**) below the playa lakes suggest that the advective groundwater flux is uniformly upward, with a flux between 0.4 mm/y and 40 mm/y (Section 4.3.1). This translates into a travel time for water and solutes to move upward across the 30 m thick Blanchetown Clay of between 75 yrs and 7 500 yrs (Table 4.7). Downward advection may be possible below the dunes and plains between the playas, particularly in the west where the hydraulic heads in the Parilla Sand aquifer are lower and recharge rates are higher. Head differences there are likely to be of the order of 10 cm to 1 m ($\mathbf{i} = 10^{-3}$ to $10^{-2}$), translating into downward advective travel times across the Blanchetown Clay of the order of several thousand to several million years (Table 4.7).

Table 4.7.  Time scales (years) for solutes to travel via various processes (a) 30 m downward across the Blanchetown Clay (in both the presence and absence of upward advection) and (b) 10 m horizontally in the Parilla Sand and Blanchetown Clay.

| | Vertical (down) (30 m) | | Horizontal (10 m) |
|---|---|---|---|
| | Upward advection (playa) | No upward advection (dune/plain) | |
| Advection | 750 – 7 500 (up) | 1 000 – 1 000 000 | Parilla Sand: 10<br>Blanchetown: 500 |
| Diffusion | - | 10 000 | 1 000 |
| Convection | 2 500 | 2 500 | - |

*Diffusion*

As discussed in Section 4.1.2, diffusion cannot lead to significant vertical re-distribution of brine below playas lakes in the presence of evaporation.  Therefore, diffusion alone could not lead to the observed pore water [$Cl^-$] vs depth profiles, where brine extends more than 5 m into the Blanchetown Clay.  It may only be an important process affecting vertical leakage of salt at Raak Plain in areas where upward advection is negligible.  Under these conditions, the characteristic time scale (t) for solutes to travel a distance L by diffusion would be approximated by:

$$t = L^2/4D \qquad (4.4)$$

where D is the effective diffusion coefficient in porous media ($D = 7.1 \times 10^{-10}$ $m^2/s$ for $Cl^-$).  The time for $Cl^-$ to travel the 30 m through the Blanchetown Clay via diffusion in the absence of significant upward advection is therefore approximately 10 k yrs (Table 4.7).

*Convection*

As described above, convection is only likely to occur in the higher permeability sediments of the Blanchetown Clay (i.e. $K_v \cong 5 \times 10^{-4}$ m/d), and if evaporation rates are low. It may therefore be responsible for the extension of the brine bodies to depths of a few metres, but will be quickly damped out by the extremely low hydraulic conductivity layers observed in the Blanchetown Clay. If conditions of instability exist, the characteristic velocity of the resulting brine fingers is given by (Wooding et al., 1997a):

$$U_c = K(\Delta\rho/\rho_0) \qquad (4.5)$$

However, because convection is a circulation process, the actual velocity of solutes across a given distance is $U_c/2$ (Narayan and Armstrong, 1995). $U_c$ at Raak Plain would be approximately $3 \times 10^{-5}$ m/d, with a travel time of approximately 2 500 yrs for brine to cross the 30 m depth interval to the Parilla Sand aquifer (Table 4.7).

*Horizontal Fluxes*

Equation 4.4 also applies to horizontal movement of solutes by diffusion, so that $Cl^-$ may move 1 m in approximately 10 yrs, or 10 m in approximately 1 000 yrs by diffusion alone, provided that there is not an opposing advective flux (Table 4.7). Assuming a uniform horizontal hydraulic gradient across Raak Plain of $2 \times 10^{-4}$ (i.e. that between bore 26240 and 98347), a horizontal conductivity of 3 m/d and a porosity of 30%, an advective horizontal velocity of approximately 1 m/y is estimated for solutes in the Parilla Sand. Horizontal hydraulic gradients in the Blanchetown Clay around the playa lakes vary both spatially and temporally.

However, under the low regional hydraulic gradient of 2 x $10^{-4}$, and in the higher conductivity sandy layers ($K_H \cong 0.1$ m/d; Table 4.2), an advective velocity of 0.02 m/y is estimated, with solutes taking approximately 500 yrs to travel 10 m (Table 4.7).

Density-driven convection is the only process that could cause significant downward movement of salt below the playa lakes themselves in the presence of evaporation. Even then, this is only likely to occur in fairly high permeability sediments (the sandier layers) in the top of the Blanchetown Clay and will be restricted by the lower permeability layers. In areas between the playas, where vertical hydraulic gradients may be negligible or downwards, advection and diffusion may carry solutes downward, with travel times across the Blanchetown Clay of several to ten thousand years (Table 4.7). For salt to reach the Parilla Sand aquifer in this way, horizontal transport from the playas is required, and this is most likely to occur in the sandy lenses observed in the Blanchetown Clay.

### 4.3.3 Influence of Heterogeneity in the Blanchetown Clay

Lateral continuity of sandy layers at Spectacle Lake was observed over distances of at least a few hundred metres (Fig. 4.2). In particular, a sand layer encountered approximately between 8 m and 10 m depth at the two Spectacle Lake sites, as well as at the Western Salina (site West4), may be continuous across the entire discharge complex. Such sand layers, with possibly 2-3 orders of magnitude higher hydraulic conductivity than other sections of the Blanchetown Clay, may provide pathways for preferential lateral flow. Periodic reversals of the vertical hydraulic gradients by episodic recharge events may be able to push brine into these sandy layers where it can be transported laterally and may have built up over areas larger than the playas themselves.

## 4.4 Conclusions

Construction of the hydrogeological conceptual model for Raak Plain (Fig.4.9), and playa-scale salt and water balances (Fig. 4.10) have led to the following conclusions about groundwater flow and solute transport below this regional groundwater discharge complex underlain by a thick aquitard:

- The upward hydraulic flux across the Blanchetown Clay is spatially constant across the entire discharge complex, between 0.4 mm/y and 40 mm/y, depending on the hydraulic conductivity assumed for the Blanchetown Clay aquitard ($K_{VB}$).

- Regional groundwater is the dominant source of solutes to the subsurface brines. However, its importance in the water balances of the playas depends on the value assumed for $K_{VB}$. For low $K_{VB}$ values, regional groundwater can make up as little as 10% of the water input to the playas.

- As well as regional groundwater discharge, local groundwater flow systems fed by recharge through adjacent sand dunes are important in the water balances of the playas, and the importance of these becomes greater in the main part of the discharge complex (e.g. near the Main Salina and Western Salina). This is due to higher recharge rates through the dunes in the main part of the discharge complex compared with at the native mallee-vegetated rim (e.g. near Spectacle Lake).

- Two types of salt lake exist at Raak Plain, surface water (Type D) and dry playa (Type E) lakes, where the former may receive a greater proportion of surface and shallow groundwater flow. This may be related to the position of the lakes in the discharge complex, where the surface water lakes tend to occur at the eastern margins and the dry playas near the centre of the discharge complex.

- Based on broad assumptions of hydrogeology and vertical extents of the brines, the time scale for accumulation of the brines is estimated to be < 20 k yrs. For an intermediate estimate of $K_{VB}$, this is narrowed to approximately 2 k yrs. Therefore, the amount of salt estimated to be stored in the subsurface brines below Raak Plain is less than what should have accumulated since the beginning of the Last Glacial Maximum (approximately 20 k yrs ago). This may suggest brine leakage back into the regional groundwater system or an underestimation of the extents of the brine bodies. Present or historical leakage of brine is also supported by large increases in TDS of the Parilla Sand groundwater below the main part of the discharge complex.

- Density-driven convection of the brines may occur only in the higher conductivity sandy layers of the Blanchetown Clay, and is more likely under evaporation rates at the lower end of the range estimated for the playas at Raak Plain. This may have led to the observed penetration of the brine bodies to depths of up to 10 m in the Blanchetown Clay, but is eventually damped out by extremely low hydraulic conductivity layers in the aquitard.

- In the absence of upward advection (i.e. below the dunes and plains of the discharge complex where recharge rates are high), downward movement of brine across the Blanchetown Clay may occur by advection, with time scales between $10^3$ and $10^6$ yrs or by diffusion with a time scale of $10^4$ yrs. Lateral movement of brine along sandy lenses in the Blanchetown Clay is one potential mechanism for transporting brine into these areas.

# Chapter 5 A Numerical Model of Groundwater Flow Below a Regional Groundwater Discharge Complex

## 5.1 Introduction

The upward hydraulic flux of regional groundwater through the Blanchetown Clay at Raak Plain is controlled by the hydraulic gradient between the Parilla Sand aquifer and the playa surfaces, and the vertical hydraulic conductivity of the Blanchetown Clay, $K_{VB}$ (Section 4.3.1). Hydraulic head measurements from piezometer nests in the Parilla Sand, Blanchetown Clay and playa sediments have shown that the vertical hydraulic gradient is fairly constant at approximately 0.1 below the discharge complex (Section 4.3.1). In contrast, $K_{VB}$ can only be estimated to within two orders of magnitude, between approximately $5 \times 10^{-6}$ m/d and $5 \times 10^{-4}$ m/d (Section 4.2.1). This large uncertainty is propagated through hydraulic flux calculations, resulting in estimates of discharge from the regional aquifer that range between 0.4 mm/y and 40 mm/y, and a subsequently broad range of outcomes from water and solute balance calculations (Section 4.3.1).

Recharge rates through the bare dunes between the playas of the discharge complex are approximately 25 times those in the mallee vegetated landscape surrounding Raak Plain (2.5 mm/y compared with 0.1 mm/y; Section 4.2.2). The resulting large differences in hydraulic head between the playa lakes and the dunes are likely to increase the importance of local groundwater flow systems in this regional groundwater discharge complex. The effect is similar to an increase in topographic relief, as shown in Figure 4.8. The large area of Raak Plain and the paucity of boreholes have meant that information on hydraulic head, groundwater TDS and aquifer properties at a limited number of locations may yield a biased view of such a potentially complex flow system.

A 2-dimensional steady state numerical groundwater flow model, based on the simple conceptual model developed in Chapter 4 (Fig. 4.9), was therefore used to improve our understanding of the system. The assumption of steady state was based on the fact that hydraulic heads throughout the discharge complex fluctuate very little over long time scales (> 1 year) and the hydraulic heads in the playas themselves are maintained approximately at the playa surface by evaporation (Section 4.2.3). The groundwater flow model was used to investigate the long-term prevailing groundwater flow pattern below Raak Plain, rather than the effects of seasonal changes in the shallow system.

Many previous numerical modelling investigations of salt lakes and evaporation basins have been interested in the effects of density-driven flow of saline subsurface brines (e.g. Narayan and Armstrong, 1995; Simmons and Narayan, 1998; Simmons et al., 2002). Density-driven convection is only possible in the sandier (high K) layers of the Blanchetown Clay at Raak Plain if evaporation (upward advection) is low (< 1 mm/y), and the density difference between the brine and the underlying groundwater is significant (Section 4.3.2.3). If these conditions are satisfied, a time scale of 2.5 k yrs was predicted for brine to travel vertically through the Blanchetown Clay to the Parilla Sand aquifer. However, low conductivity layers in the Blanchetown Clay are likely to limit this process to within the top 10 m of the aquitard, below which advection or diffusion dominate, depending on the prevailing groundwater flow pattern. Rather than attempting to accurately simulate solute transport based on a simplified conceptual model, the objectives of the numerical model were to:

- Provide a better understanding of the prevailing groundwater flow pattern below Raak Plain, allowing identification of the processes likely to cause re-distribution of salt to the regional aquifer system.

- Evaluate the sensitivity of the system to key parameters such as hydraulic conductivity and recharge rates, and to better constrain estimates of these.

The groundwater flow model, MODFLOW (McDonald and Harbaugh, 1988), was used to simulate groundwater flow below Raak Plain. MODFLOW uses a finite difference method to solve the governing equations of groundwater flow. Density effects on groundwater flow patterns are not considered. As described above, this was considered to be negligible at the discharge complex scale. Hence, despite the limitation, MODFLOW was considered adequate to achieve the objectives of the modelling exercise. Pre- and post-processing was facilitated by the Visual MODFLOW package (Waterloo Hydrogeologic Inc., 2000).

## 5.2 Adaptation of the Conceptual Model to the Numerical Model

### 5.2.1 Spatial Discretization

A two-dimensional slice model was constructed to represent the conceptual model by creating a cross-sectional model domain (1 km thick) with the dimensions 42 km in the horizontal direction by 123 m in the vertical direction (Fig. 5.1). This was divided into 276 columns ranging in width from 100 m to 1 km, and 50 layers ranging from 50 cm to 2 m in height (Fig. 5.1). The horizontal boundaries of the active model domain were assigned to be between x = 6 km and x = 30.7 km, represented by Transect AA’ (Fig. 1.6) due to limited computer power available for the simulations (Fig. 5.1). The effect of extending the active domain was

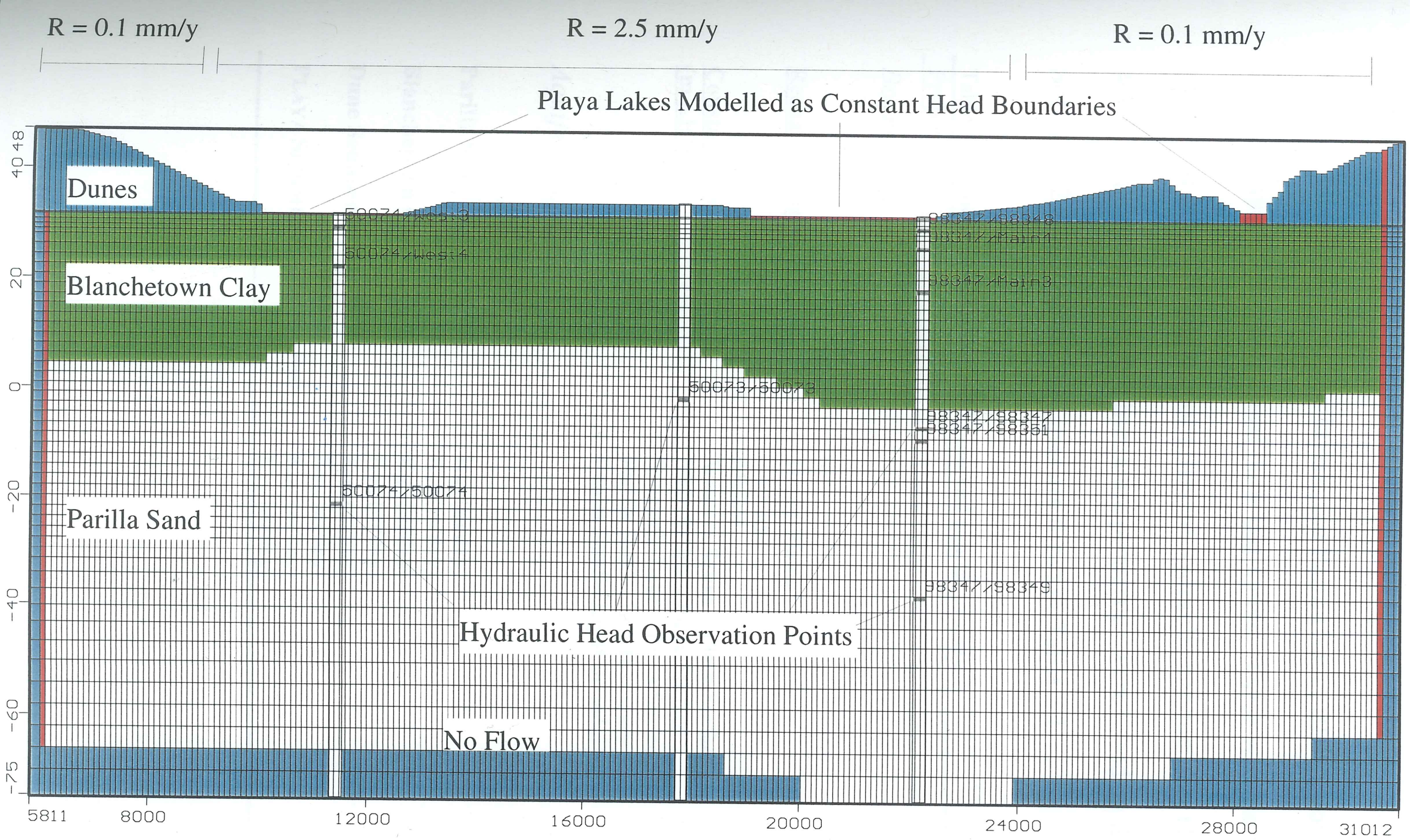

Figure 5.1. Cross-sectional view of the active model domain, showing model grid, regions of different hydraulic properties and boundary conditions for the three-lake scenario. Locations of hydraulic head observation points (observation wells) are also shown. Constant head boundaries are indicated in red. Note that the scale is vertically exaggerated. Recharge (R) is applied to the top layer of the model.

investigated as part of the sensitivity analysis.

### 5.2.2 Hydraulic Properties

The conceptual model of the Raak Plain groundwater discharge complex (Fig. 4.9) includes three hydrogeologic layers: the Parilla Sand, Blanchetown Clay and a thin surficial layer of playa and sand dune sediments. These were defined in the numerical model by regions of different hydraulic conductivity (Fig. 5.1). Modelled aquifer/aquitard extents and hydraulic properties were based on those discussed in Section 4.2.1 above, and the latter are listed in Table 5.1.

Table 5.1 Modelled boundary conditions and aquifer properties.

| **Property** | | **Value** |
|---|---|---|
| *Boundaries* | | |
| **Recharge (mm/y)** | Dunes/Plains | 2.5 |
| | To Playas | 0 |
| | Mallee | 0.1 |
| **Constant Head Boundaries (m AHD)** | Western Salina – Playa Surface | 32.19 |
| | Main Salina – Playa Surface | 32.53 |
| | Spectacle Lake – Playa Surface | 34.0 |
| | Parilla Sand – Left Boundary | 32.00 |
| | Parilla Sand – Right Boundary | 39.28 |
| *Aquifer Properties* | | |
| **Parilla Sand** | $K_{HP}$ (m/day) | 3 |
| | $K_{VP}$ (m/day) | 0.03 |
| **Blanchetown Clay** | $K_{HB}$ (m/day) | $5 \times 10^{-3}$ |
| | $K_{VB}$ (m/day) | $5 \times 10^{-5}$ |
| **Dune Sediments** | $K_{HD}$ (m/day) | 2 |
| | $K_{VD}$ (m/day) | 1 |
| **PLAYA SEDIMENTS (YAMBA FM)** | $K_{HY}$ (m/day) | 0.05 |
| | $K_{VY}$ (m/day) | 0.05 |

### 5.2.3 Boundary Conditions

For the purpose of this exercise, a no-flow boundary was modelled at the base of the Parilla Sand, as the underlying Bookpurnong Beds / Winnambool Formation are a thick, low hydraulic conductivity aquitard, and leakage through this is expected to be minimal (Fig. 5.1). The east and west boundaries of the Parilla Sand aquifer and Blanchetown Clay were modelled as constant head boundaries to simulate interaction with the regional groundwater system. The constant heads were based on hydraulic heads measured in bores 26240 and 50075 (Table 4.4) at the east and west margins of the discharge complex. The dependence of the model results on this choice of boundary conditions was investigated during the sensitivity analysis.

The playa lakes of the discharge complex were modelled as constant head boundaries, as evaporation from their surfaces maintains hydraulic heads in the shallow sediments approximately at the playa floors over long time scales ($> 10^{-1}$ yrs). The extent of the topographic surface to be modelled as playa lake was uncertain. The major discharge zones along transect AA’ are Spectacle Lake, the Main Salina and Western Salina, with predominantly dunes and plains in between (Fig. 1.6). However, a large playa lake occurs to the north of the transect, near the centre of Raak Plain, and smaller ones are scattered in between, which may significantly influence the groundwater flow pattern (Fig. 1.6). Therefore, although the main focus of the modelling exercise is a three-lake model, incorporating Spectacle Lake, the Main Salina and Western Salina, the influence of the number of lakes along the transect has also been investigated, using a two- and four- lake model.

Recharge rates of 0.1 mm/y over the mallee-vegetated section of transect AA’, 2.5 mm/y over the dunes and plains of the discharge complex, and 0 mm/y over the playas were applied to the topographic surface of the model, consistent with the conceptual model developed in Chapter 4 (Fig. 5.1).

## 5.3 Model Calibration

The objectives of this modelling exercise outlined above do not require perfect calibration of the groundwater flow model to observed heads and fluxes. In fact, as the model is based on a simplified conceptual model, and there are large uncertainties in a number of the hydraulic parameters and boundary conditions, this would be an unreasonable expectation. In a system where fluxes and hydraulic gradients are low, it is likely that a number of permutations of hydraulic property values and boundary conditions will lead to reasonable matches with observation data. An approximate calibration was therefore achieved by adjusting the most sensitive parameters to obtain reasonable fits between observed and predicted hydraulic heads, and the root mean square (RMS) deviation of this fit was then used as criteria for assessing model sensitivity to these parameters (Table 5.2). Predicted fluxes from the playa lakes and the predicted groundwater flow pattern were also assessed against our understanding of the processes occurring at Raak Plain (Table 5.2, Figs. 5.2-5.12). The outcome was a range of possible scenarios rather than one accepted representation of the groundwater flow system.

## 5.4 Results

### 5.4.1 Three- Lake Groundwater Flow Model Incorporating Spectacle Lake, the Main Salina and Western Salina (Base Case)

The potentiometric contours produced by the steady-state numerical groundwater flow model, incorporating the three main lakes along transect AA', are shown in Figure 5.2. Also included are flow paths of particles released at different locations in the model domain, calculated using the MODPATH package. These particle flow paths are approximate in cross-section, and hence do not always plot at right angles to the equipotentials. Time scales for advective particle transport, indicated by distances between arrowheads on the flow lines, are accurately represented, however.

The model domain was divided into six zones: (1) the Parilla Sand aquifer, (2) the Blanchetown Clay, (3) the Sand Dunes (Woorinen Formation), (4) Western Salina, (5) the Main Salina and (6) Spectacle Lake. Water fluxes between these zones were calculated using the Zone Budget package (Table 5.2). The RMS deviation between observed and simulated hydraulic heads in the Parilla Sand bores and deeper piezometers in the Blanchetown Clay was 13.2 % for this simulation. Based on the simplicity of the conceptual model and the objectives of the modelling exercise, this degree of discrepancy was considered reasonable.

The base case model predicts that regional groundwater from the Parilla Sand aquifer is discharged through Spectacle Lake and the Main Salina, with travel times of 60 k yrs and 150 k yrs respectively for this groundwater to reach the playas from the eastern margin of the discharge complex (Fig. 5.2). Groundwater from the top half of the Parilla Sand is captured by the playas, whilst the rest flows through and out at

*Table 5.2. Results of Zone Budget calculations and observed vs simulated hydraulic heads for groundwater flow model incorporating Spectacle Lake, the Main Salina and Western Salina.* First column shows results of the base case simulation, with parameters as shown in Table 5.1. Subsequent columns show the results of varying key parameters. Figure No. refers to the figure in this thesis that displays the equipotentials and particle flow paths calculated by the model for the given scenario. $K_{VB}$ and $K_{HP}$ are the vertical hydraulic conductivity of the Blanchetown Clay and the Horizontal hydraulic conductivity of the Parilla Sand respectively.

| | | **Base Case (Table 6.1)** | **$K_{VB}$ (m/day) =** | | **$K_{HP}$ (m/day) =** | | **Recharge (mm/y) =** | | **$K_{VB}$ = 5x10$^{-6}$** | **$K_{VB}$ = 5x10$^{-4}$** |
|---|---|---|---|---|---|---|---|---|---|---|
| | | | **5 x 10$^{-4}$** | **5 x 10$^{-6}$** | **1** | **5** | **0.5** | **20** | **R=1 mm/y** | **R=20 mm/y** |
| **Figure No:** | | **6.2** | **6.5** | **6.6** | **6.8** | **6.7** | **6.9** | **6.1** | **6.11** | **6.12** |
| **Fluxes**[1] | **($m^3$/d)** | | | | | | | | | |
| From | To | | | | | | | | | |
| Regional[2] | Parilla Sand | 68 | 156 | 54 | 28 | 110 | 85 | 0 | 64 | 77 |
| Parilla Sand | Regional[2] | 81 | 36 | 79 | 36 | 123 | 55 | 372 | 64 | 170 |
| Parilla Sand | Blanchetown | 41 | 193 | 3 | 43 | 40 | 38 | 88 | 5 | 492 |
| Blanchetown | Parilla Sand | 53 | 73 | 28 | 52 | 54 | 8 | 460 | 4 | 585 |
| Dunes | Blanchetown | 61 | 77 | 38 | 60 | 61 | 11 | 505 | 7 | 603 |
| Blanchetown | Dunes | 11 | 48 | 1 | 10 | 11 | 13 | 9 | 2 | 58 |
| Blanchetown | Western Salina | 11.1 | 32.5 | 4.6 | 13.7 | 10.5 | 7 | 45.6 | 1.7 | 164.1 |
| Blanchetown | Main Salina | 23.3 | 90.5 | 6.5 | 24.4 | 22.9 | 18.1 | 68.5 | 3.2 | 252.6 |
| Blanchetown | Spectacle Lake | 3.8 | 26.4 | 0.6 | 3.7 | 3.8 | 3.6 | 5.6 | 0.5 | 34.4 |
| Dunes | Western Salina | 2.2 | 0.5 | 7.4 | 2.4 | 2.2 | 0.9 | 13 | 2 | 3.2 |
| Dunes | Main Salina | 3.8 | 1.4 | 9.5 | 4 | 3.8 | 2 | 19.6 | 2.8 | 5.3 |
| Dunes | Spectacle Lake | 40.9 | 63.5 | 38 | 40.5 | 40.9 | 35.4 | 89.7 | 26.7 | 85.4 |
| Total Flux ($m^3$/d) | Western Salina | 13 | 33 | 12 | 16 | 13 | 8 | 59 | 4 | 167 |
| | Main Salina | 27 | 92 | 16 | 28 | 27 | 20 | 88 | 6 | 258 |
| | Spectacle Lake | 45 | 90 | 39 | 44 | 45 | 39 | 95 | 27 | 120 |
| Total Flux (mm/y) | Western Salina | 3 | 8 | 3 | 4 | 3 | 2 | 13 | 1 | 38 |
| | Main Salina | 3 | 10 | 2 | 3 | 3 | 2 | 9 | 1 | 28 |
| | Spectacle Lake | 33 | 66 | 28 | 32 | 33 | 28 | 70 | 20 | 87 |
| **Observation Wells** | **RMS Deviation**[3] | 13.2 | 33.8 | 16 | 13.2 | 13.5 | 18.9 | 71.6 | 14.8 | 18 |

[1] Calculated from Zone Budget.

[2] Regional = from/to regional groundwater system (I.e. as a result of constant head boundaries in Parilla Sand)

[3] RMS Deviation between simulated and observed heads.

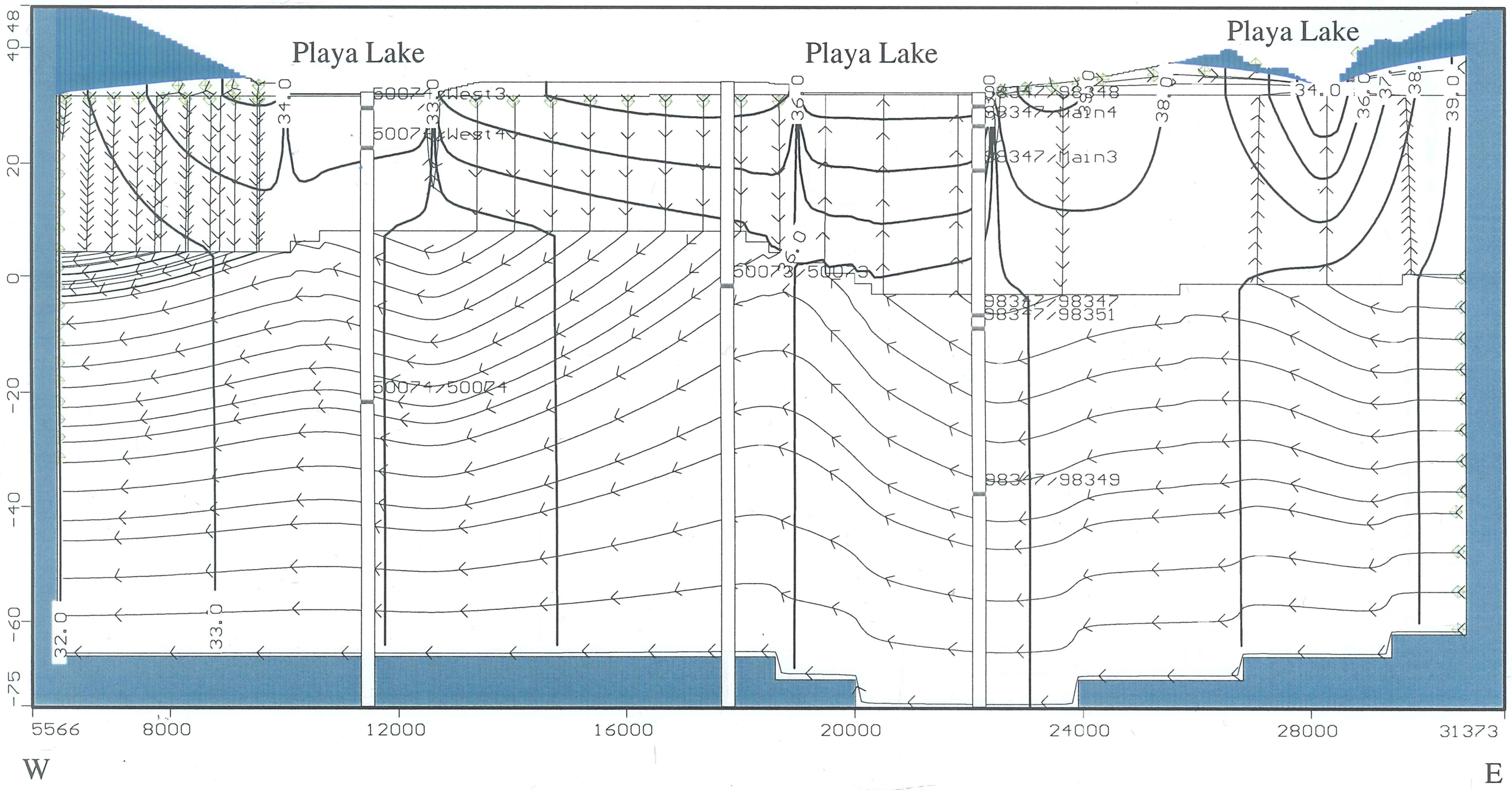

Figure 5.2. Equipotentials (heavy lines) and particle flow paths (arrowed lines) simulated by the numerical model for the base case scenario of three playa lakes along transect AA'. Model parameters are as shown in Table 5.1. Distances between the arrow heads represent travel times of 10 k yr.

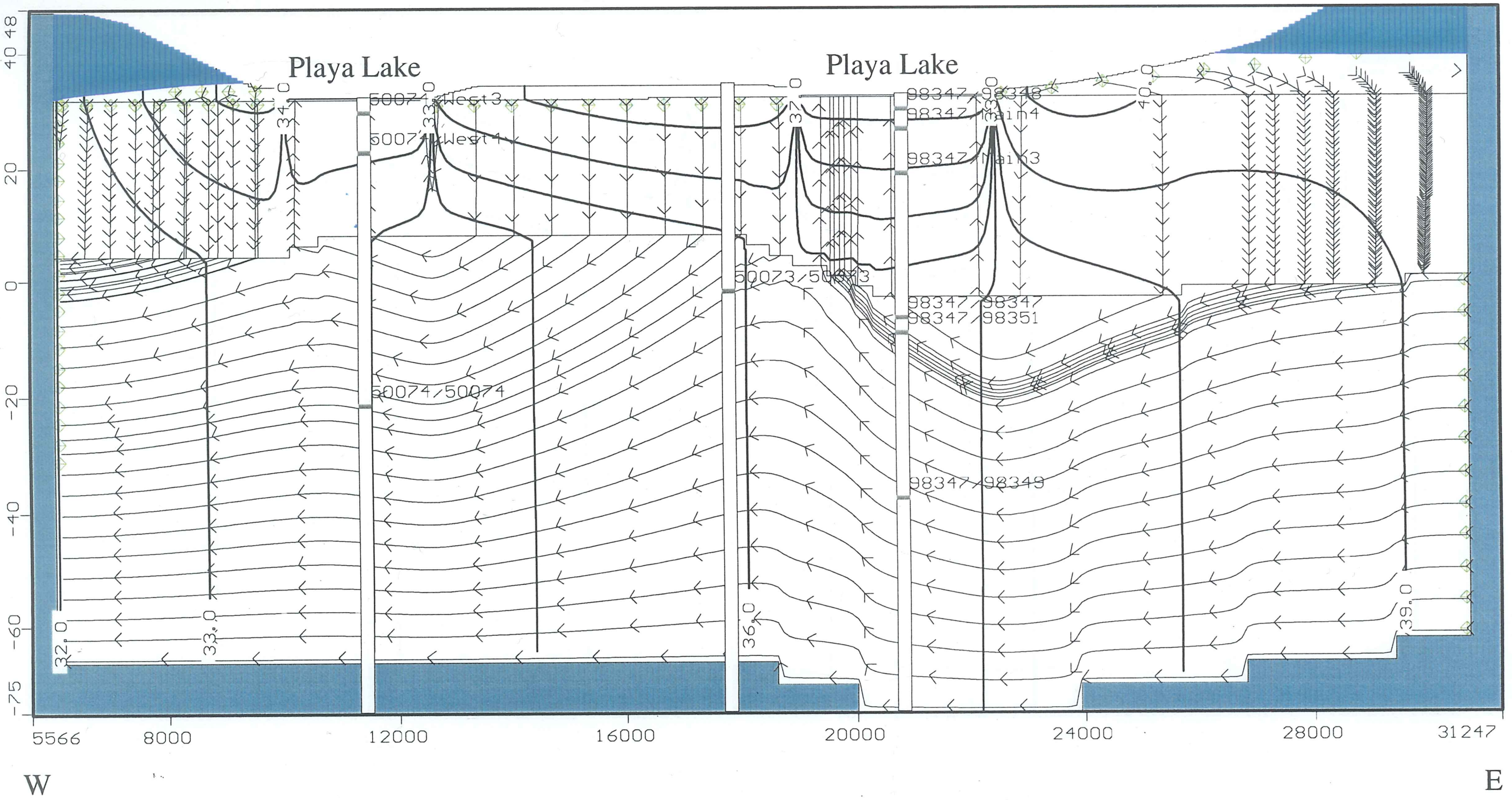

Figure 5.3. Equipotentials (heavy lines) and particle flow paths (arrowed lines) simulated by the numerical model for the two playa lake scenario with model parameters as shown in Table 5.1. Distances between the arrow heads represent travel times of 10 k yr.

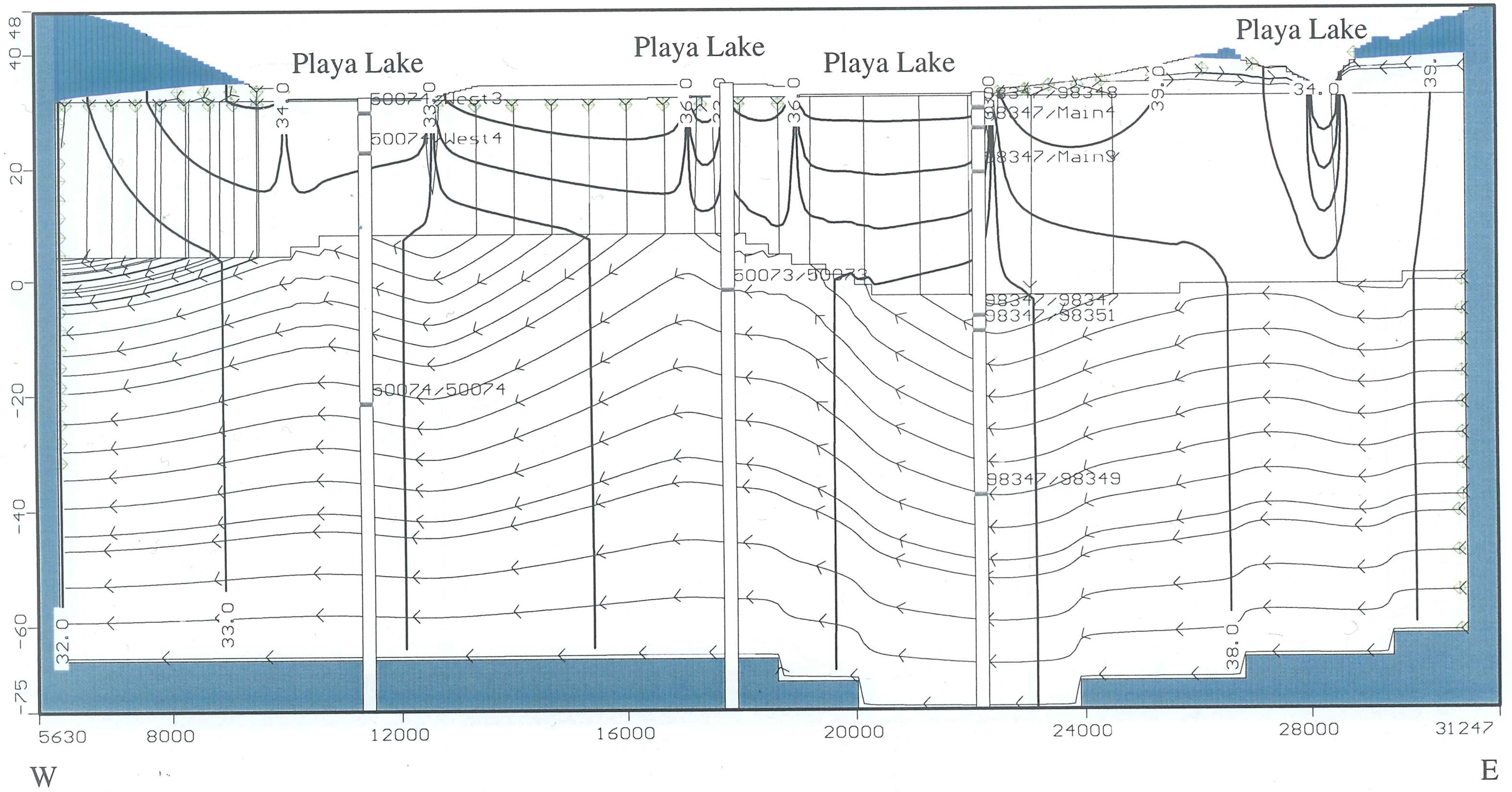

Figure 5.4. Equipotentials (heavy lines) and particle flow paths (arrowed lines) simulated by the numerical model for the four playa lake scenario with model parameters as shown in Table 5.1. Distances between the arrow heads represent travel times of 10 k yr.

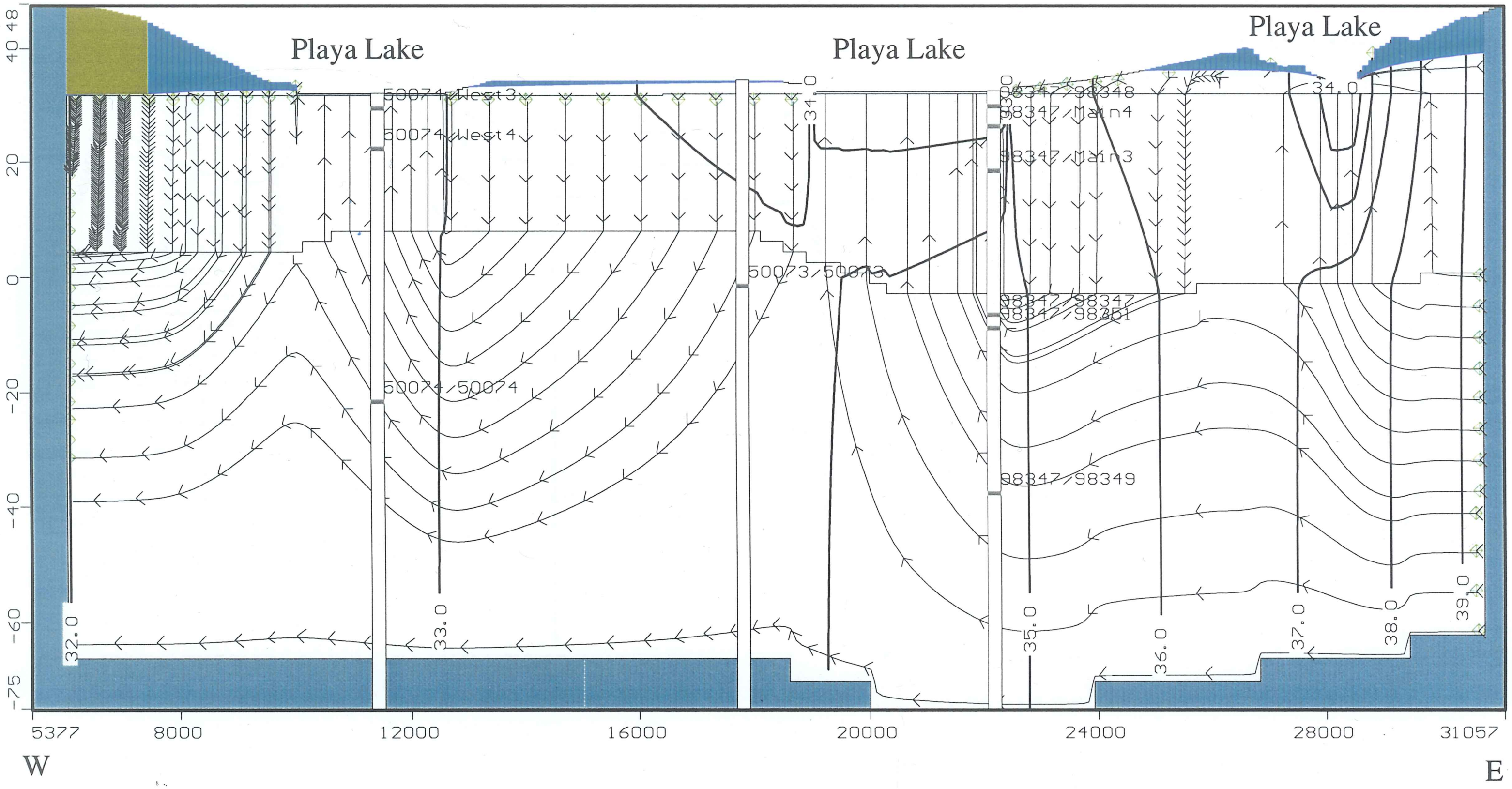

Figure 5.5. Equipotentials (heavy lines) and particle flow paths (arrowed lines) simulated by the numerical model for the three playa lake scenario, increasing K(VB) from 5e-5 m/d to 5e-4 m/d. Distances between the arrow heads represent travel times of 10 k yr.

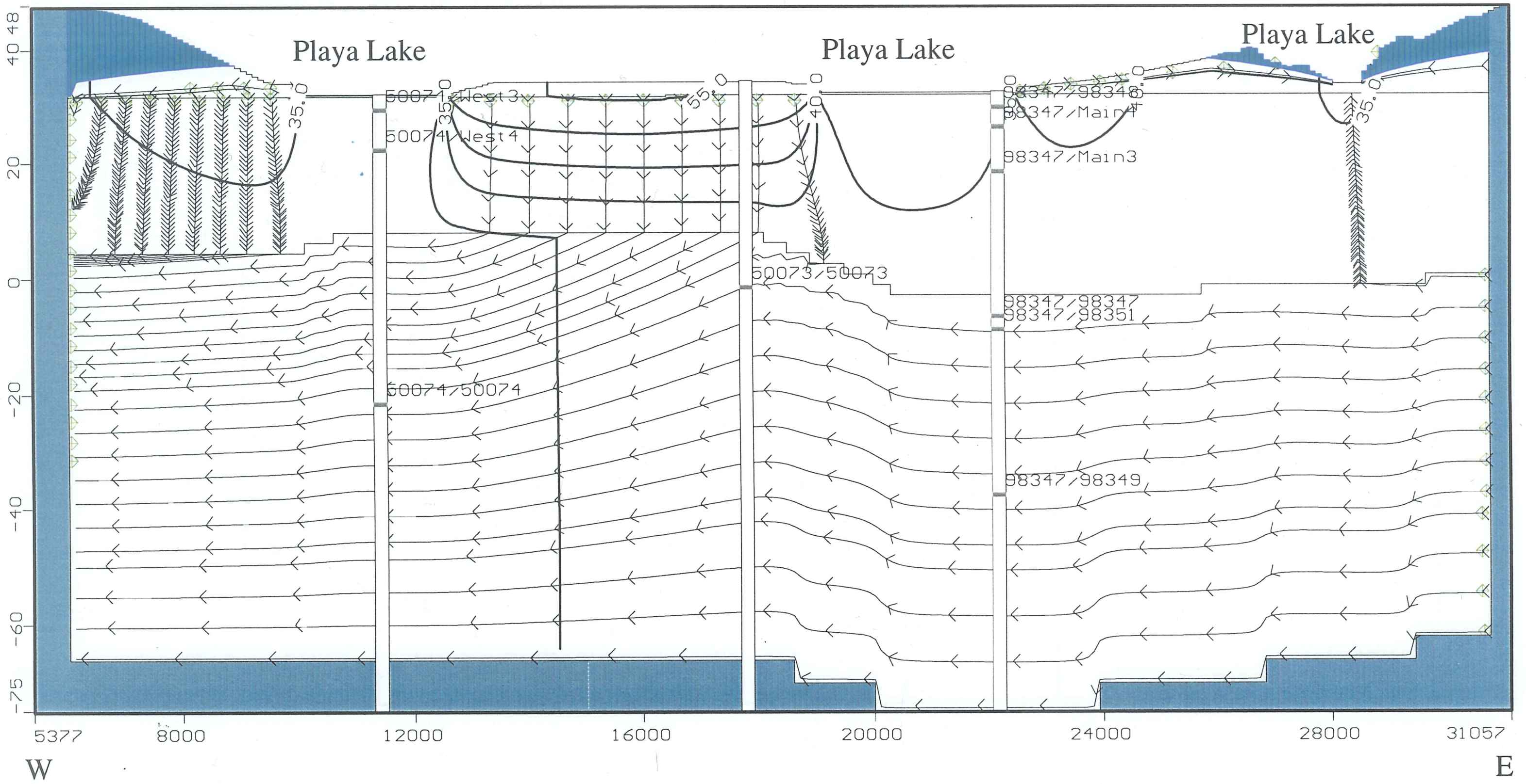

Figure 5.6. Equipotentials (heavy lines) and particle flow paths (arrowed lines) simulated by the numerical model for the three playa lake scenario, with K(VB) reduced from 5e-5 m/d to 5e-6 m/d. Distances between the arrow heads represent travel times of 10 k yr.

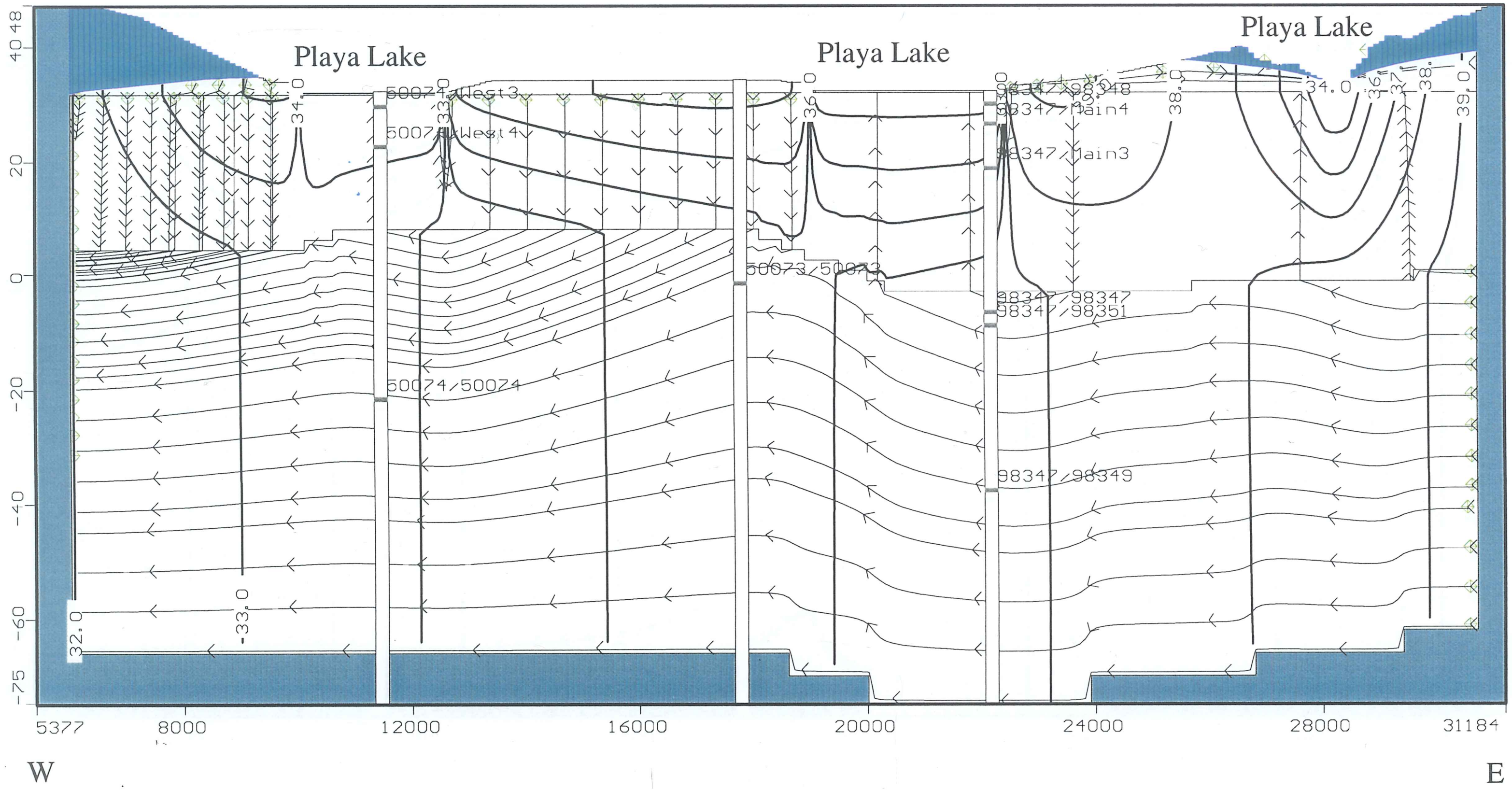

Figure 5.7. Equipotentials (heavy lines) and particle flow paths (arrowed lines) simulated by the numerical model for the three playa lake scenario, with K(HP) increased from 3 m/d to 5 m/d. Distances between the arrow heads represent travel times of 10 k yr.

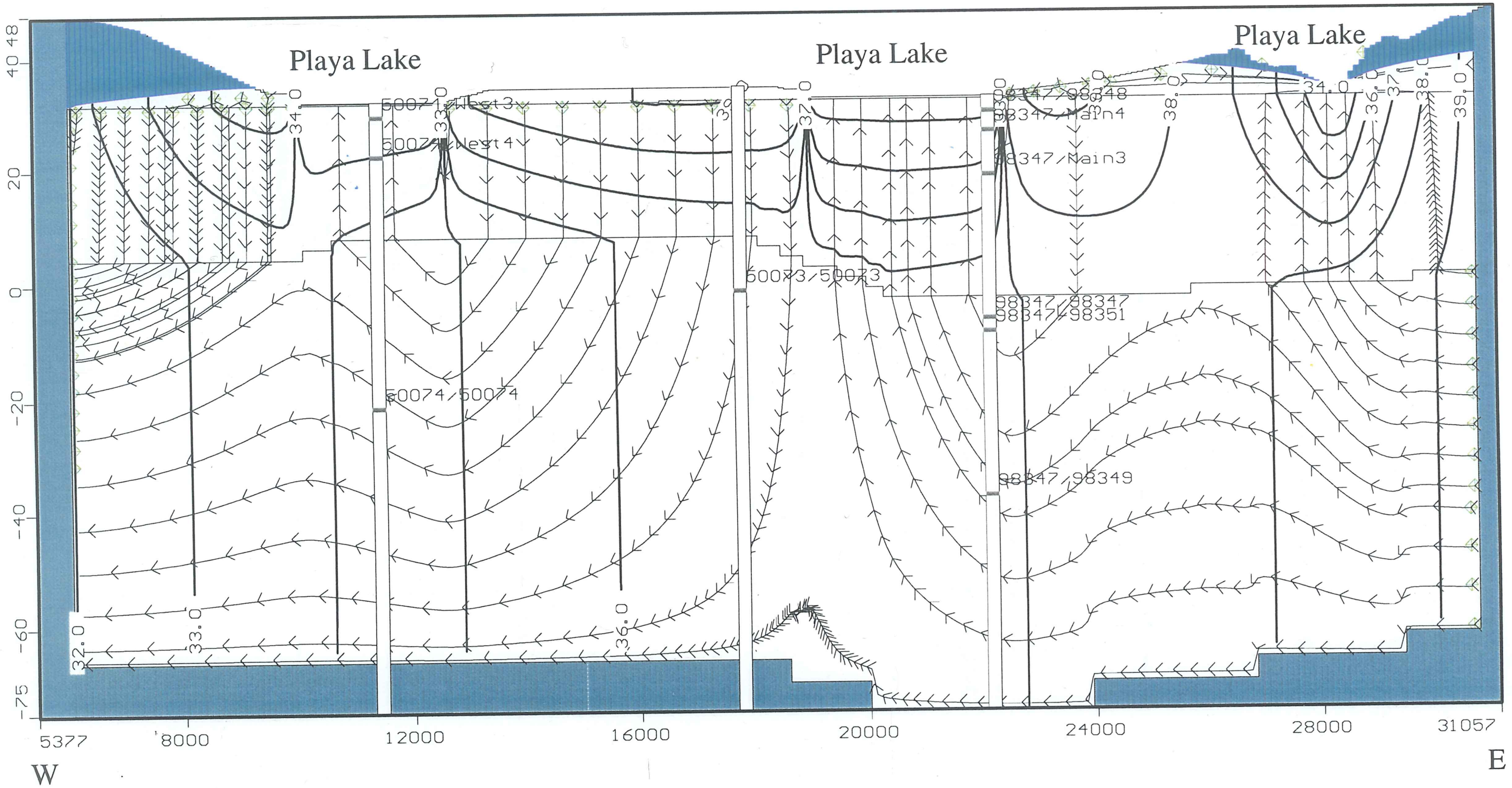

Figure 5.8. Equipotentials (heavy lines) and particle flow paths (arrowed lines) simulated by the numerical model for the three playa lake scenario, with K(HP) reduced from 3 m/d to 1 m/d. Distances between the arrow heads represent travel times of 10 k yr.

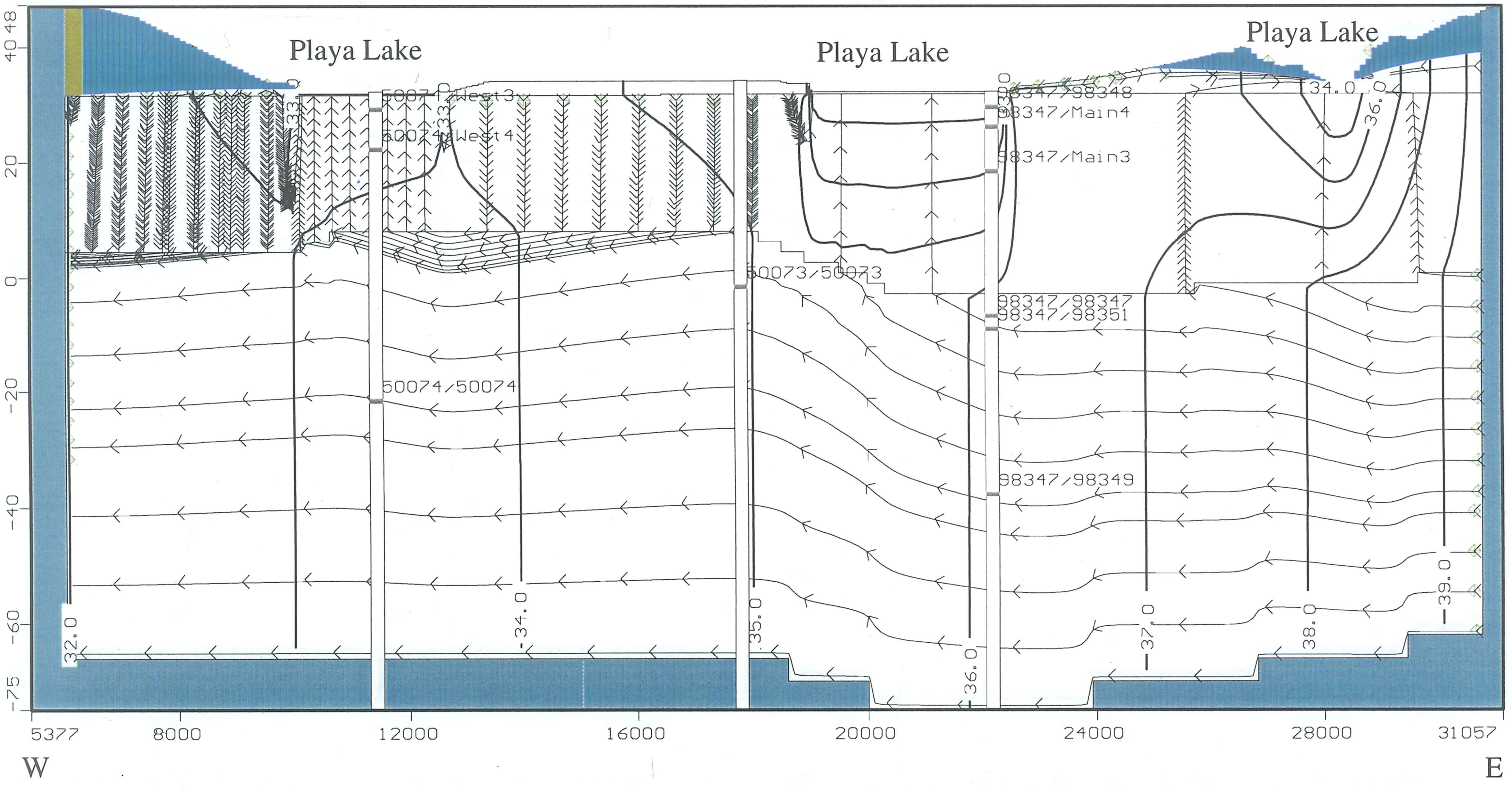

Figure 5.9. Equipotentials (heavy lines) and particle flow paths (arrowed lines) simulated by the numerical model for the three playa lake scenario, with the dune / plain recharge rate across the discharge complex reduced from 2.5 mm/y to 0.5 mm/y. Distances between the arrow heads represent travel times of 10 k yr.

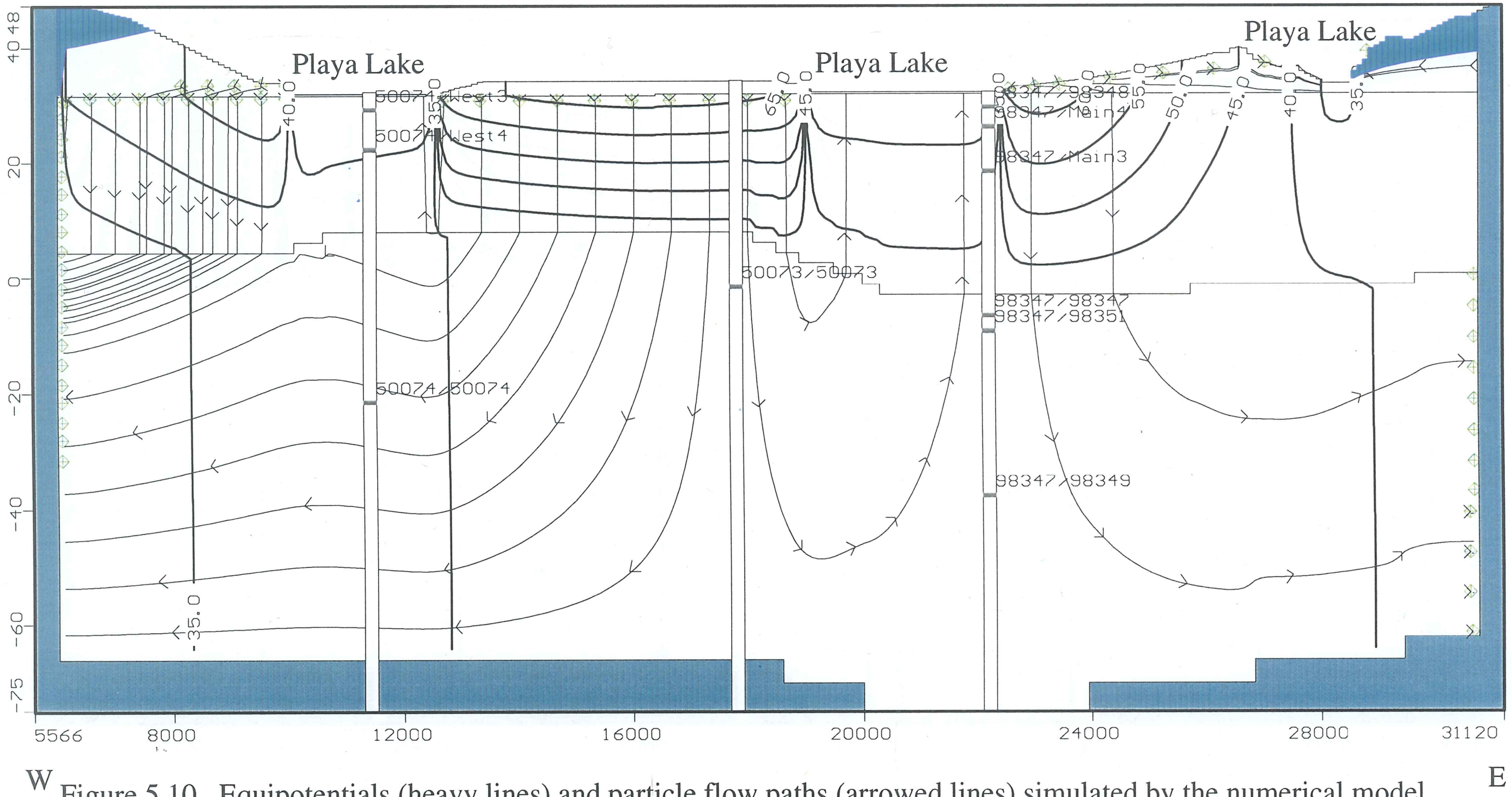

Figure 5.10. Equipotentials (heavy lines) and particle flow paths (arrowed lines) simulated by the numerical model for the three playa lake scenario, with dune / plain recharge across the discharge complex increased from 2.5 mm/y to 20 mm/y. Distances between the arrow heads represent travel times of 10 k yr.

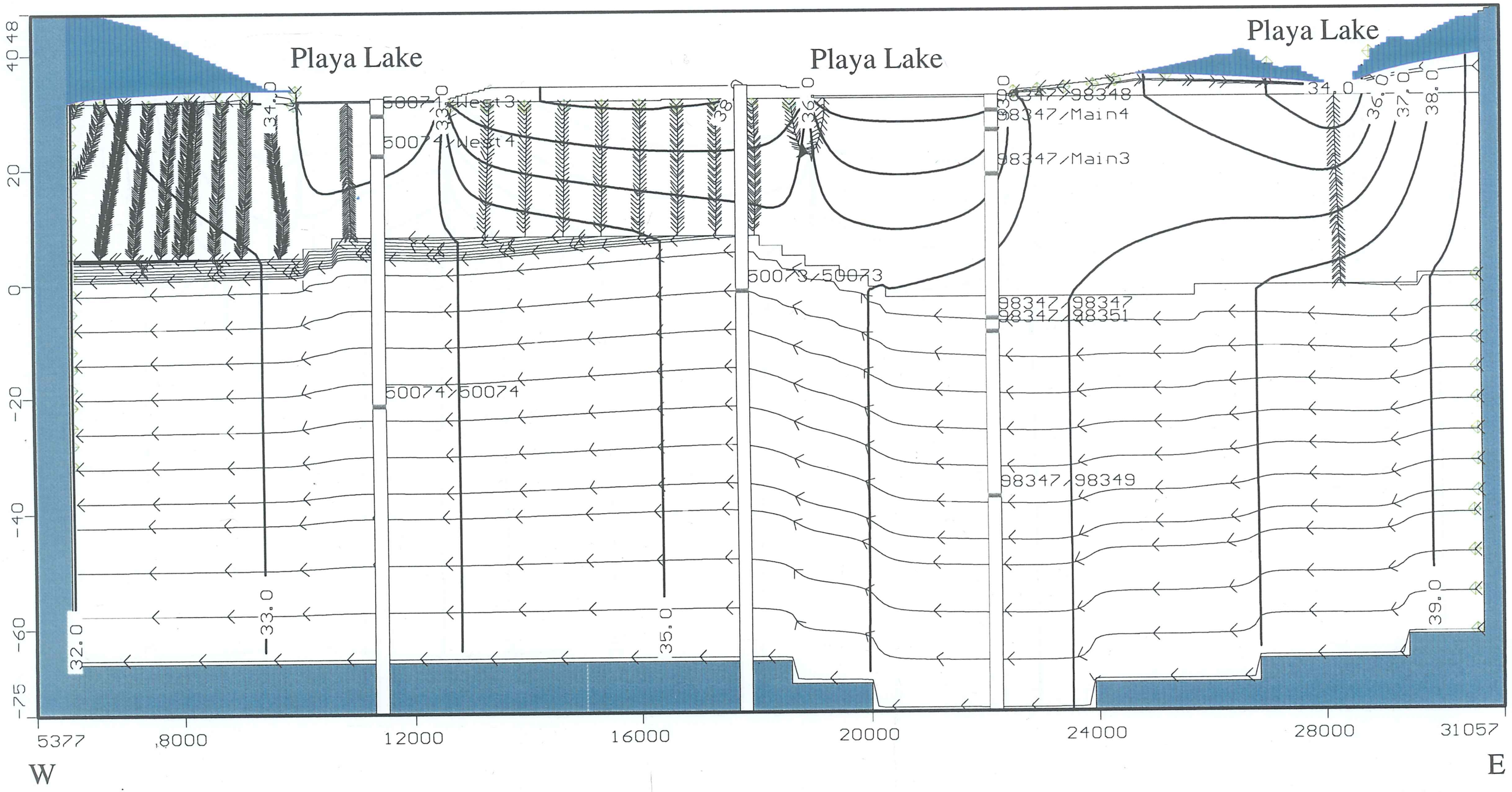

Figure 5.11. Equipotentials (heavy lines) and particle flow paths (arrowed lines) simulated by the numerical model for the three playa lake scenario, with low K(VB) and low R. Distances between the arrow heads represent travel times of 10 k yr.

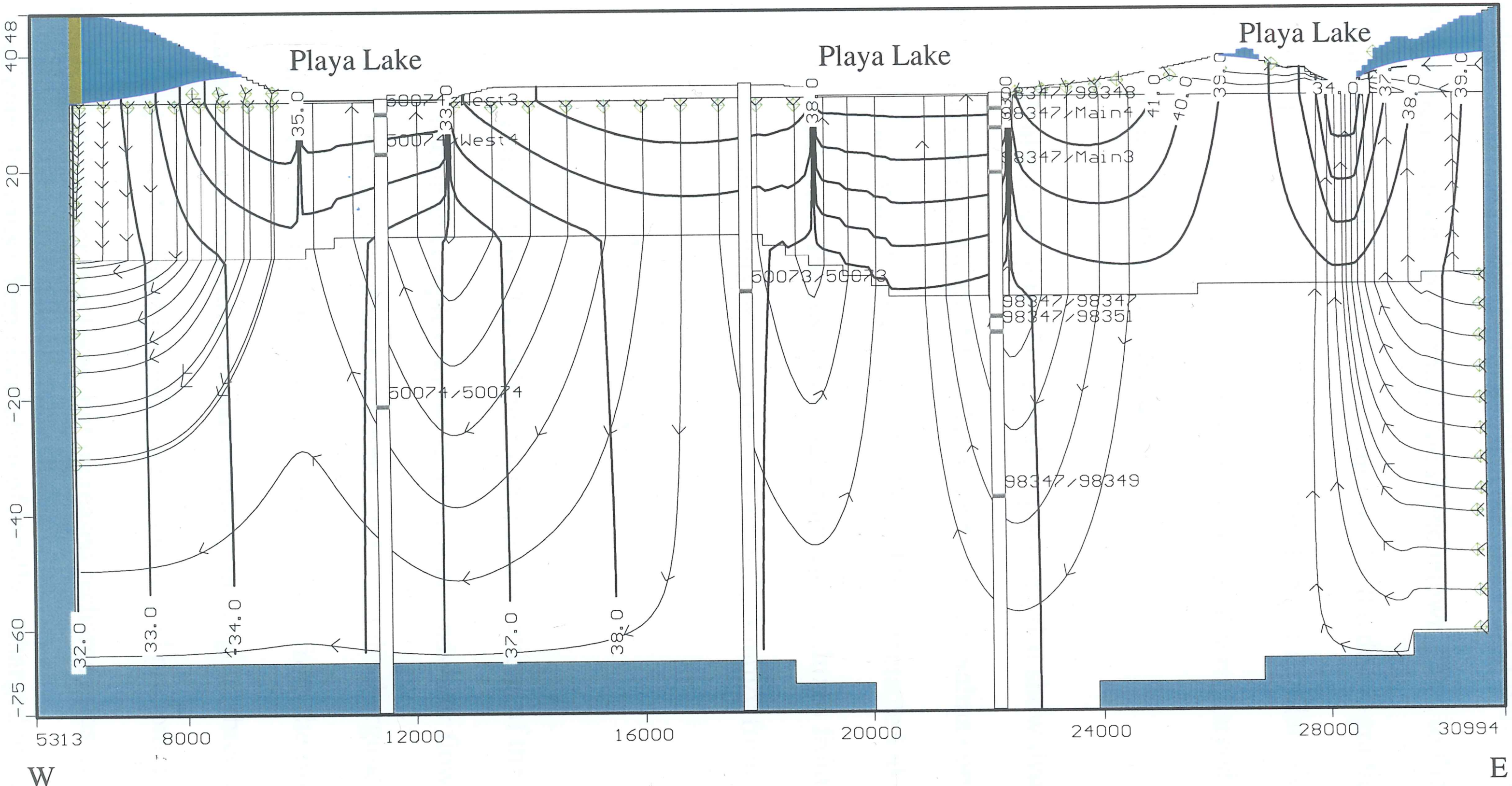

Figure 5.12. Equipotentials (heavy lines) and particle flow paths (arrowed lines) simulated by the numerical model for the three playa lake scenario, with high K(VB) and high R. Distances between the arrow heads represent travel times of 10 k yr.

the western margin. In the east of the discharge complex, where recharge rates are low (0.1 mm/y), locally recharged groundwater flows along the top of the Blanchetown Clay, draining into the nearest playa (e.g. Spectacle Lake). West of the Main Salina, where simulated recharge rates are higher (2.5 mm/y), locally recharged groundwater penetrates deeply through the Blanchetown Clay, to the top of the Parilla Sand aquifer. This is then either captured by the down-gradient playa lakes, or flows out of the discharge complex in the Parilla Sand aquifer. Groundwater discharged by Western Salina is therefore entirely locally recharged groundwater that has circulated through the Parilla Sand.

The fluxes calculated using the Zone Budget package also show that most of the groundwater discharged by the Main Salina and Western Salina comes from the Blanchetown Clay, whilst most of that discharged by Spectacle Lake flows in from the surrounding dunes. The resulting total groundwater fluxes from the playas are 3 mm/y from the Main Salina and Western Salina and 33 mm/y from Spectacle Lake.

### 5.4.2 Two- and Four- Lake Scenarios

In order to investigate the effect of the number and locations of the playa lakes in the groundwater discharge complex on the simulated groundwater flow pattern, two simulations were carried out with different numbers of discharging playa lakes along transect AA’. The groundwater flow patterns resulting from the two-lake and four-lake simulations are essentially similar to that of the original three-lake scenario (Figs. 5.3 and 5.4). Regional groundwater is discharged predominantly from the up-gradient (eastern) one or two lakes, but increased recharge rates in the interior of the discharge complex cause deep circulation of locally recharged groundwater, which is then subsequently discharged from the playa lakes. The absence of Spectacle Lake in the two-lake scenario causes deep (but slow) infiltration of recharge in the east of the discharge complex, and a shorter timescale (~ 70 k yrs) for regional groundwater entering Raak Plain at the eastern margin to be discharged through the Main Salina.

## 5.5 Discussion

### 5.5.1 Sensitivity of the Groundwater Flow Model to Hydraulic Conductivity and Recharge

#### 5.5.1.1 Groundwater Flow Patterns and Fluxes

Preliminary numerical groundwater flow model simulations identified that the patterns of groundwater flow below Raak Plain were most sensitive to the vertical hydraulic conductivity of the Blanchetown Clay ($K_{VB}$), the horizontal hydraulic conductivity of the Parilla Sand aquifer ($K_{HP}$) and the recharge rate over the discharge complex (R). To qualitatively and quantitatively investigate sensitivity of the model to these parameters, simulations were run for the three-lake model with variations of $K_{VB}$ ($5 \times 10^{-4}$ m/d to $5 \times 10^{-6}$ m/d), R (0.5 mm/y to 20 mm/y) and $K_{HP}$ (1 m/d to 5 m/d). These ranges were based on possible values identified in Chapter 4. The resulting flow patterns and particle flow paths for these simulations, as well as for two extreme cases (low $K_{VB}$, low R and high $K_{VB}$, high R) are shown in Figures 5.5 to 5.12. The resulting hydraulic fluxes and RMS deviations are shown in Table 5.2.

An increase in $K_{VB}$ from $5 \times 10^{-5}$ m/d to $5 \times 10^{-4}$ m/d caused all Parilla Sand groundwater entering the discharge complex via the eastern constant head boundary to be discharged via Spectacle Lake and the Main Salina (Fig. 5.5). Local recharge then replenished the regional aquifer in the west of the discharge complex. The increase in $K_{VB}$ increased the discharge rate from all of the playas but significantly reduced the match between observed and predicted hydraulic heads (Table 5.2). A low $K_{VB}$ ($5 \times 10^{-6}$ m/d) caused almost zero discharge from the regional aquifer, and the source of water to the playas became local recharge through those dunes immediately adjacent them (Fig. 5.6). There was little change in the discharge fluxes from the playas, however, and only a slight reduction in the fit between observed and predicted hydraulic heads.

Increasing the horizontal conductivity of the Parilla Sand aquifer ($K_{HP}$) from 3 m/d to 5 m/d caused very little change in the simulated groundwater flow pattern, fluxes and RMS deviation (Fig. 5.7, Table 5.2). However, reducing $K_{HP}$ to 1 m/d had a similar effect to increasing $K_{VB}$. All Parilla Sand groundwater flowing in at the eastern margin of Raak Plain is captured by the first two lakes and, in the main part of the discharge complex, the system is dominated by local recharge (Fig. 5.8). However, the reduction in $K_{HP}$ had little effect on the fluxes from the playas and the RMS deviation.

Lowering the recharge rate across the discharge complex (R) from 2.5 mm/y to 0.5 mm/y reduced the depth of circulation of the local groundwater flow system in the west of the model domain, but only slightly reduced the fluxes from the playas (Fig. 5.9, Table 5.2). Increasing R to 20 mm/y, also a reasonable value for cleared Mallee areas (Cook et al., 1994), caused a dramatic change in the groundwater flow pattern, which became dominated by local flow systems and caused net outflow at the constant head boundary at the eastern margin. This is an unacceptable scenario based on observed hydraulic heads in the Parilla Sand aquifer, which suggest groundwater flow in a westerly direction (Fig. 4.1; Table 4.4). All of the above variations of $K_{VB}$ and R significantly reduced the agreement between simulated and observed hydraulic heads whilst varying $K_{HP}$ had little effect (Table 5.2).

### 5.5.1.2 Quantitative Sensitivity Analysis

The total simulated fluxes to the constant head boundaries at Western Salina, the Main Salina and Spectacle Lake, and the RMS deviation between observed and simulated hydraulic heads were used as quantifiable parameters for measuring model sensitivity to the key variables ($K_{VB}$, $K_{HP}$ and R) (Table 5.2, Fig. 5.13). A dimensionless parameter, S, was used as an indicator of sensitivity of the fluxes/RMS deviation to each variable, where:

$$S= (V_U-V_L)/V_C \tag{5.1}$$

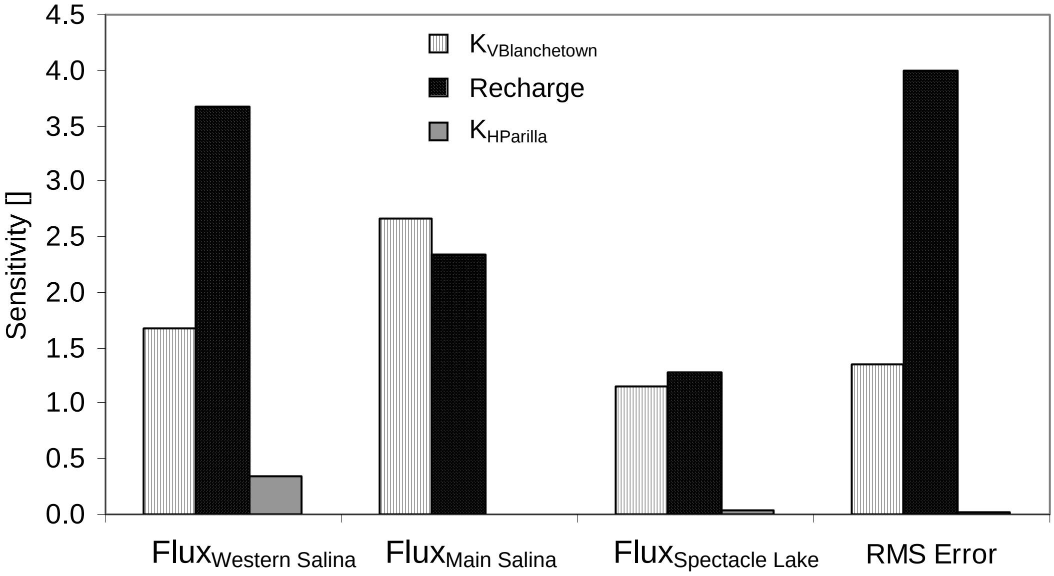

Figure 5.13. Results of the quantitative sensitivity analysis of the groundwater flow model (base case) to the key parameters of $K_{VB}$, $K_{HP}$ and R.

$V_U$ is the flux / RMS deviation simulated for the upper value of the particular variable being investigated (R, $K_{VB}$ or $K_{HP}$). $V_L$ is the flux / RMS deviation resulting from a lower value of that variable, and $V_C$ is the flux / RMS deviation resulting from the original "base case" simulation. The higher the magnitude of S, the greater the sensitivity of that parameter (flux or RMS deviation) to the variable ($K_{VB}$, R, $K_{HP}$) (Fig. 5.13).

In general, the groundwater fluxes from the playa lakes and the RMS deviation between the observed and simulated hydraulic heads in the Parilla Sand aquifer and Blanchetown Clay are most sensitive to the recharge rate applied across the discharge complex (Fig. 5.13). However, the vertical hydraulic conductivity of the Blanchetown Clay is also a key factor affecting simulated hydraulic heads and fluxes (Fig. 5.13), particularly the groundwater flux from the Main Salina. Although reducing $K_{HP}$ dramatically affected the simulated groundwater flow pattern, it had a minimal effect on the fluxes and RMS deviation (Fig. 5.13).

The exercise of extending the model boundaries provided poor calibration with the observed head data due to a lack of available information on the surrounding regional groundwater system (uncertainty in assigning constant head boundaries at the left and right of the Parilla Sand). However, there was not a great impact on the resulting equipotential distribution or particle flow paths by changing these boundaries, and the resulting fluxes were also generally comparable. Therefore, it was concluded that, based on the available information, the applied boundary conditions were sufficient to achieve the objectives of the modelling exercise.

#### 5.5.1.3 Constraint of the Simulated Groundwater Flow Pattern and Key Variables

As described in Section 5.5.1.1, the simulated hydraulic head distribution below Raak Plain depends strongly upon the applied values of three key variables: (a) the vertical hydraulic conductivity of the Blanchetown Clay ($K_{VB}$), (b) the horizontal hydraulic conductivity of the Parilla Sand aquifer ($K_{HP}$) and (c) the recharge rate over the main part of the discharge complex (R) (Figs. 5.5 - Fig. 5.12). By varying these parameters within reasonable limits, groundwater flow patterns ranging between complete discharge of all regional Parilla Sand groundwater inflow (dominance of regional flow systems) and complete throughflow of Parilla Sand groundwater (dominance of shallow local flow systems) can be achieved. In contrast, the simulated fluxes from the playa lakes generally vary within only one order of magnitude, a level of confidence that can be expected from the simple conceptual model (Table 5.2). Therefore, although the simulated discharge fluxes depend very little on the hydraulic properties of the system, the sources of the groundwater that is discharged depend heavily on them, as does the prevailing groundwater flow pattern, which is likely to influence solute transport.

To satisfy the overall objective of the modelling exercise, which is to gain an understanding of the prevailing groundwater flow pattern at the discharge complex scale, these results must be narrowed down, and hence some constraint placed upon the key variables. The model that represents the groundwater flow system as accurately as possible must reproduce the hydraulic heads observed in the regional aquifer and in the aquitard around the playas. Based on minimization of the RMS deviation between the observed and simulated hydraulic heads, the base case, with $K_{VB}$ of the order of $5 \times 10^{-5}$ m/d and R of approximately 2.5 mm/y provides the best representation of the observed hydraulic heads. It is more difficult to constrain $K_{HP}$ because, although reducing the value of this parameter to 1 m/d had no effect on the RMS deviation, it caused a significant change to the simulated groundwater flow pattern and the time scale for groundwater flow in the Parilla Sand aquifer from the eastern margin to the Main Salina. Increasing $K_{HP}$ to 5 m/d had little effect.

Therefore, the closest representation of the actual flow pattern may be somewhere between those shown in Figures 5.7 and 5.8, with $K_{HP}$ ranging between 1 m/day and 5 m/day.

### 5.5.2 Groundwater Flow Patterns Below a Regional Groundwater Discharge Complex

Despite the uncertainty in the conceptual model, the numerical simulations have shown that regional groundwater from the Parilla Sand aquifer is most likely to discharge from the playa lakes in the eastern (up-gradient) part of the discharge complex, i.e. Spectacle Lake and the Main Salina (e.g. Fig. 5.2). Local groundwater flow systems become more important in the western three-quarters of the model domain, where recharge rates are higher, and deep circulation of locally recharged groundwater is possible there. This deeply circulating recharge can infiltrate the Parilla Sand aquifer before either being captured by the next playa lake along the flow line or exiting to the regional flow system at the western margin of the discharge complex (e.g. Fig. 5.2). Hence, although locally recharged groundwater, with a comparatively short residence time, may be the dominant source of water to the playa lakes in the western part of Raak Plain, it may have mixed with regional groundwater in the Parilla Sand aquifer.

It is logical that the groundwater inputs to the playa lakes at Raak Plain should be derived from a combination of both local and regional sources (Bill Ullman, pers. comm., June 2003). If the comparatively low TDS local groundwater flow systems were to dominate, it would take time scales far greater than can be considered here to build up the observed hypersaline brine bodies. In contrast, if regional groundwater dominated the input, salinities would quickly surpass saturation with respect to the various evaporite minerals and extensive salt crusts would be observed. Hence, the currently observed brine bodies and lack of substantial surface salt crusts suggest a mixture of both inputs. Additionally, as the TDS of the regional Parilla Sand groundwater increases from east to west below the discharge complex, an east-west increase in the ratio of local to regional input would cause little difference in the accumulated brine body or presence / absence of a salt crust, as is observed.

Hydraulic heads in the Parilla Sand in the eastern part of the model domain are higher and recharge rates are lower due to the dense cover of mallee vegetation. Here, locally recharged groundwater tends to perch on top of the Blanchetown Clay and follow a shallow flow path into the nearest playa, Spectacle Lake (e.g. Fig. 5.2). In contrast to Western Salina and the Main Salina, the flux of groundwater from the dunes to Spectacle Lake is a much greater component of the total inflow to this playa than discharge from the Blanchetown Clay (Table 5.2). This is in agreement with the hypothesis raised in Section 4.3.1.4, that the presence of surface water, salt crusted lakes predominantly around the margin of the discharge complex is due to locally recharged groundwater following shallow flow paths in these areas and perching on top of the Blanchetown Clay. The number and locations of playa lakes in the discharge complex has only a subtle effect on groundwater flow patterns.

### 5.5.3 Groundwater Discharge Rates From the Playas of a Regional Groundwater Discharge Complex

The simulated average total groundwater discharge from the surfaces of Western Salina and the Main Salina were similar in all of the model scenarios despite their different locations along the groundwater flow path, and potentially different groundwater sources. For the control scenario (Table 5.1, Fig. 5.2), the simulated flux was approximately 3 mm/y, in agreement with the estimate from simple water balance calculations for the intermediate $K_{VB}$ of 5 x $10^{-5}$ m/d (Fig. 4.10). The simulated flux from Spectacle Lake is an order of magnitude higher (33 mm/y). This does not agree with the water balance calculations, which suggested fluxes from Spectacle Lake of the same order of magnitude as those from Western Salina and the Main Salina. However, as discussed in the previous section, most of the flow to Spectacle Lake is via shallow flow paths and is therefore more influenced by topography. Hence, the difference between the high simulated flux and that derived from the water balance may be due to poor control on topography in this area of the model.

### 5.5.4 Implications for Solute Transport

Constraint of the vertical hydraulic conductivity of the Blanchetown Clay ($K_{VB}$) to approximately 5 x $10^{-5}$ m/d provides more confidence in chloride flux estimates and brine accumulation times of approximately 2 k yrs made using this value in Chapter 4. However, the estimate of accumulation time is also based on broad assumptions of vertical extents and chloride concentrations of the brines, and should still be viewed with a confidence limit of an order of magnitude (see Section 4.3.2). Time scales of particle flow paths predicted by the numerical model suggest approximately 150 to 300 k yrs for Parilla Sand groundwater entering Raak Plain at the eastern margin to be discharged from the Main Salina, and approximately 80 k yrs from Spectacle Lake (Fig. 5.2). The time scale for locally recharged groundwater to infiltrate the Parilla Sand aquifer and then discharge from the Main Salina and Western Salina is 180 k yrs and 80 k yrs respectively.

As suggested earlier, downward hydraulic fluxes of recharge to the Parilla Sand aquifer between the Main Salina and Western Salina can provide a pathway for the downward movement of any brine that has moved laterally from the playa lakes (Fig. 5.2). The time scale for this vertical advective flux across the Blanchetown Clay is approximately 40 k yrs (Fig. 5.2), slower than the time scale for diffusive transport across the Blanchetown Clay, which is approximately 10 k yrs (Table 4.7). However, the former process does not require the development of a large concentration gradient between the top of the Blanchetown Clay and the Parilla Sand. Hence, vertical leakage of brine can be expected to occur via either diffusion or advection at time scales of 10 – 40 k yrs. It was concluded, based on theoretical analysis in Chapter 4, that density-driven convection is unlikely to be a major process affecting solute transport in such a thick clay aquitard as the Blanchetown Clay, with extremely low hydraulic conductivity ($K_{VB} < 5 \times 10^{-5}$ m/d) clay layers occurring throughout it. However, if density-driven convection was to occur through some window or preferential flow path, in between or below the playas, the travel time for brine to reach the Parilla Sand could be reduced to approximately 2.5 k yrs (Table 4.7).

## 5.6 Conclusions

Development of a numerical groundwater flow model of the Raak Plain groundwater discharge complex has improved our understanding of the system in the following ways:

- A $K_{VB}$ of the order of $5 \times 10^{-5}$ m/d is reasonable as a first estimate for calculating vertical groundwater fluxes from the Parilla Sand aquifer. This value is between that of $5 \times 10^{-4}$ m/d estimated by Ferguson et al. (1995) for the Blanchetown Clay in the Lake Mourquong region (Table 5.1) and the value of 5 x $10^{-6}$ m/d for a tight marine clay such as that observed in layers at Raak Plain (Freeze and Cherry, 1979). Using this $K_{VB}$ value, total average fluxes of the order of 3 mm/y from playa lakes in the interior of the discharge complex are estimated, with most of this water being regional groundwater or locally recharged groundwater that has circulated deeply through the Parilla Sand aquifer. Brine accumulation times, estimated to be of the order of 2 k yrs in Section 4.3.2 are also suggested.

- Water (and solutes) in the playas at the up-gradient mallee vegetated margin of the discharge complex are derived mainly from dune recharge that follows a shallow flow path along the top of the Blanchetown Clay and perches there, forming “surface-water” lakes. The water (and solute) balances of these lakes are therefore strongly controlled by topography.

- Downward advective fluxes in the high recharge areas between the playas provide potential pathways for the downward movement of brine to the Parilla Sand aquifer by advection, with time scales of 40 k yrs. This is much slower than solute transport via diffusion, although it may allow transport of salt where there is not a large concentration gradient. The only other solute transport process that may lead to faster vertical travel times through the Blanchetown Clay is density-driven convection, with a time scale for salinization of the Parilla Sand of 2.5 k yrs. However, the onset of density-driven convection in the Blanchetown Clay is unlikely unless some preferential flow path is available.

- Advective transport within the discharge complex may occur at time scales ranging from a few thousand years (shallow local flow systems) up to approximately 300 k yrs.

- Although the number and locations of the playa lakes in the groundwater discharge complex has subtle effects on the groundwater flow pattern, the above general conclusions still apply.

# Chapter 6 Isotopic Tracers to Constrain the Conceptual Model of a Groundwater Discharge Complex

## 6.1 Introduction

A numerical groundwater flow model, based on a discharge complex scale conceptual model of Raak Plain, revealed that the groundwater flow pattern linking the playas to the regional sand aquifer is sensitive to the vertical hydraulic conductivity of the aquitard separating them and the local recharge rate (Chapter 5). Because of the size (400 km$^2$) and complexity of the discharge complex (> 50 playa lakes of different shapes and sizes), and difficulties in obtaining water levels and sediment properties at depth, the amount of hydrogeological information required to constrain even a simplified model is not available. Hence, such an approach can yield only broad generalizations about groundwater flow below Raak Plain. The objective of this chapter is to assess the value of applying a suite of naturally occurring isotopic tracers, $^{2}$H / $^{1}$H and $^{18}$O / $^{16}$O, $^{13}$C / $^{12}$C and $^{14}$C, and $^{36}$Cl to constrain the conceptual model of groundwater flow and solute transport below Raak Plain. Each of these tracers has characteristic sources and sinks and is involved in different geochemical processes, and so provides different information on physical and geochemical history of solutes and water as they move through the discharge complex.

The stable isotopic ratios ($^{18}$O / $^{16}$O and $^{2}$H / $^{1}$H) of the water molecule have been used extensively in studies of salt lakes and groundwater discharge zones because they are strongly fractionated by evaporation (e.g. Dincer, 1968; Zuber, 1983; Allison and Barnes, 1985; Thomas et al., 1989; Herczeg et al, 1992; Yadav, 1997;

Dutkiewicz et al., 2000; Simmons et al., 2002). Additionally, in evaporitic environments, water and solutes are de-coupled by evaporation. $\delta^{2}H$ and $\delta^{18}O$ provide cumulative information on the history of the water molecules themselves, rather than inferences derived from solutes dissolved in the water, or point measurements of hydraulic heads and aquifer properties.

$^{14}C$ and $^{36}Cl$ are naturally occurring radioactive tracers that are applicable to estimating groundwater residence times and delineating groundwater flow paths in slowly evolving systems, such as groundwater discharge zones, because of their long half-lives (5730 yrs and 301 000 yrs respectively) (Ingerson and Pearson, 1964; Bentley et al., 1986a; Phillips, 2000). $^{14}C$ is useful for groundwater residence times up to approximately 30 k yrs, and $^{36}Cl$ between about 50 k yrs and 1 Ma. Simple calculations of diffusion and hydraulic fluxes at Raak Plain have suggested processes operating over time scales of thousands to hundreds of thousands of years, meaning that both tracers may be useful in determining solute sources and flow paths. In a study of $^{36}Cl$ in the Murray Basin, Davie et al. (1989) found anomalously low and variable groundwater $^{36}Cl/Cl$ ratios below groundwater discharge zones, including Raak Plain, suggesting recycling of salt and that $^{36}Cl$ may also be a useful tracer in these environments.

The potential for application of two radioactive tracers with such different temporal resolutions can also be seen in the palaeohydrologic history of groundwater discharge in the Murray Basin. Since the end of the “penultimate” glaciation 130 k yrs ago, conditions in the Murray Basin have oscillated between expanded lacustral and dune-building, which, in the context of lakes, translates into variations between high lake level (groundwater recharge) and lake desiccation (groundwater discharge) phases (Bowler and Wasson, 1984). Hence, the signatures of groundwater brines formed under previous groundwater discharge regimes may now be overprinted by processes occurring under the present regime. Tracers of solutes at different time scales may assist with deciphering this. Additionally, $^{14}$C and $^{36}$Cl are involved in very different geochemical systems, meaning that they potentially record information on different processes influencing the evolution of groundwater. $^{36}$Cl is an isotope of $Cl^-$, the most dominant and conservative (besides $Br^-$) anion in the groundwaters and brines at Raak Plain. Hence, $^{36}$Cl should be a good tracer of physical processes affecting solute distributions. In contrast, $^{14}$C is strongly influenced by reactions in the carbonate system, its signature revealing more information about the geochemical evolution of groundwater.

Although dissolved inorganic carbon (DIC) is a minor constituent of groundwaters and brines at Raak Plain compared with other solutes, concentrations vary considerably between sites, and in a much less regular manner than the other, more dominant ions (Chapter 4). This suggests more complex reactions affecting carbon than the other solutes in the discharge complex. The stable isotopic ratio, $^{13}$C/$^{12}$C, generally expressed using delta notation as $\delta^{13}$C, is used to constrain estimates of residence time made based on radioactive decay of $^{14}$C. However, it can also be used to trace the origin and evolution of dissolved inorganic carbon (DIC), from the unsaturated zone, to reactions with carbonate minerals in the groundwater system. Since major ion chemistry has proven fairly inconclusive in distinguishing between groundwaters recharged locally and derived from the regional groundwater system, $\delta^{13}$C may be of great value here.

## 6.2 Review of Isotopic Methods in Salt Lakes

### 6.2.1 $\delta^{2}$H and $\delta^{18}$O: Tracers of the Water Molecule

There are two naturally occurring, stable isotopes of hydrogen and three of oxygen that form a range of heavy and light water molecules. Their approximate abundances in the environment are shown in Table 6.1:

Table 6.1. Natural abundances of the stable isotopes of hydrogen and oxygen in the environment (Coplen et al., 2000).

| Isotope | Abundance (%) |
|---|---|
| $^{1}$H | 99.985 |
| $^{2}$H | 0.015 |
| $^{16}$O | 99.757 |
| $^{17}$O | 0.038 |
| $^{18}$O | 0.205 |

Of the oxygen isotopes, only $^{16}$O and $^{18}$O are commonly used in hydrologic studies due to the low abundance of $^{17}$O. These isotopes form numerous species of the water molecule, the most abundant being $^{1}H^{1}H^{16}O$, $^{1}H^{1}H^{18}O$ and $^{1}H^{2}H^{16}O$. The amount of heavy isotope ($^{18}$O or $^{2}$H) in a water sample is normally expressed as a ratio of the amount of heavy isotope to the light isotope, in delta notation (δ), as a permil (‰) difference from a standard. The accepted international standard is V-SMOW (Vienna – Standard Mean Ocean Water, kept by the I.A.E.A. at Vienna) and has, by definition, delta $^{18}$O and $^{2}$H values of 0.00. The values of the world's oceanic waters are all close to this. Delta values are calculated according to the equation:

$$\delta_i(‰) = \frac{R_{sample} - R_{standard}}{R_{standard}} \times 1000 \qquad (6.1)$$

where i is the isotope of interest and R is the heavy-to-light isotope atom ratio ($^2H/^1H$ or $^{18}O/^{16}O$, corresponding to $^1H^2H^{16}O/H_2{}^{16}O$ and $H_2{}^{18}O/H_2{}^{16}O$ respectively, in natural waters).

The isotopic compositions of natural waters have been studied extensively by many workers, such as Epstein and Mayeda (1953), Craig (1961), Ehalt et al. (1963) and Dansgaard (1964). Fractionation (a change in the ratios) of $^2H$ / $^1H$ and $^{18}O$ / $^{16}O$ of a water body occurs via both equilibrium and kinetic processes during phase changes and chemical reactions. Exchange between liquid water and water vapour can be either an equilibrium or a kinetic process. At equilibrium, a water body is more enriched in $^2H$ and $^{18}O$ than the associated water vapour by an amount that is determined by the equilibrium fractionation factor, $\alpha_{eq}$. This enrichment occurs due to generally lower activation energies in reactions involving the isotopically "light" molecules. Because of the difference in vapour pressures of $H_2{}^{18}O$ and $^2H^1HO$, the enrichment in $^2H$ is approximately 8 times the enrichment in $^{18}O$. Hence, at 25°C and 1 atm., water vapour is less enriched in $\delta^2H$ and $\delta^{18}O$ by about 70‰ and 9‰ respectively than the associated liquid water, and the actual fractionation varies as a function of temperature (Friedman and O'Niel, 1977).

In the terrestrial environment, particularly arid and semi-arid areas, liquid-vapour exchange occurs at humidities << 100%. The lower humidity means that water – vapour exchange is minimized and the evaporation process becomes increasingly non-equilibrium (kinetic). During kinetic evaporation, fractionation occurs due to different diffusivities of the isotopes across the liquid / vapour boundary layer. The effects of this can be observed on a $\delta^2H$ vs $\delta^{18}O$ diagram, on which groundwater $\delta^2H$ and $\delta^{18}O$ data is commonly plotted and compared with rainfall compositions (Fig.

6.1). Rainfall samples generally plot along a single line, the Meteoric Water Line (MWL) and groundwater samples usually plot to the right of the MWL due to evaporation of rainfall under non-equilibrium conditions prior to recharge. The progressive evaporation of a water sample, with decreasing fraction of water remaining (*f*), follows an evaporation curve to the right of the MWL, which approximates a straight line (Fig. 6.1). Deflections from a straight line are only apparent at very low *f* values and the slope of this line is a function of humidity, TDS, temperature and wind speed during evaporation, with humidity being by far the dominant influence (Gat, 1971, 1981; Gonfiantini, 1986). Isotopic effects during non-equilibrium evaporation from surface water bodies have been studied both theoretically and experimentally by Craig and Gordon (1965), Gonfiantini (1965), Merlivat (1970) and Gat (1971) and a good summary is provided by Gonfiantini (1986).

Spatial variations in $\delta^2H$ and $\delta^{18}O$ can be explored more easily using the single parameter, deuterium excess (d):

$$d = \delta^2H - 8\delta^{18}O \qquad (6.2)$$

The concept of deuterium excess was first introduced by Dansgaard (1964) as an indicator of non-equilibrium processes affecting the $\delta^2H$ and $\delta^{18}O$ compositions of seawater and rainfall samples from IAEA and World Meteorological Organization (WMO) monitoring stations around the world. From Equation 6.2, d corresponds to the y-intercept of a line with a slope of 8 on a $\delta^2H$ vs $\delta^{18}O$ diagram (Fig. 6.1). A deuterium excess of 10 corresponds approximately to a point on the Global Meteoric Water Line (GMWL, $\delta^2H = 8\delta^{18}O + 10$). Rainfall from Adelaide, Australia (the closest rainfall isotope monitoring site to Raak Plain) plot on a $\delta^2H$ vs $\delta^{18}O$ diagram as a line with equation $\delta^2H = 7.7\delta^{18}O + 13$ (J. Dighton, CSIRO Land and Water, unpublished data; Fig. 6.1) and hence have a deuterium excess of 13.

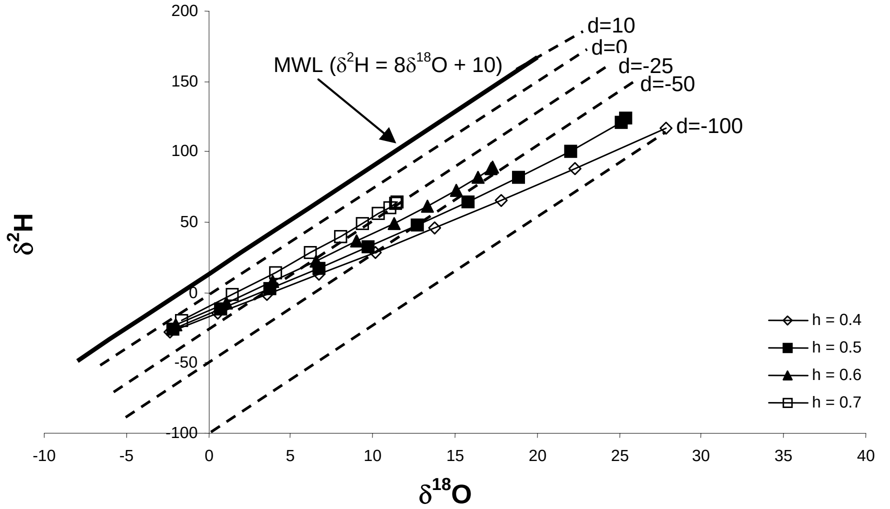

FIGURE 6.1. $\delta^2H$ VS $\delta^{18}O$ DIAGRAM SHOWING THE GLOBAL METEORIC WATER LINE (MWL), WHICH HAS A DEUTERIUM EXCESS OF 10, AND LINES OF EQUAL DEUTERIUM EXCESS (DASHED LINES). GROUNDWATER SAMPLES PLOT TO THE RIGHT OF THE METEORIC WATER LINE DUE TO THE EFFECTS OF EVAPORATION. PROGRESSIVE EVAPORATION CAUSES WATER COMPOSITIONS TO MOVE FURTHER TO THE RIGHT ALONG A LINE WITH A SLOPE DEPENDENT LARGELY ON HUMIDITY (H), AND WITH DEUTERIUM EXCESSES BECOMING MORE NEGATIVE.

Equilibrium simply shifts the isotopic composition of a water sample along a line (e.g. the GMWL) with a slope of 8, whilst kinetic (non-equilibrium) evaporation, at h < 100% causes water samples to shift in composition along an evaporation line to the right of the MWL (Fig. 6.1). d decreases with progressive evaporation but also depends on the conditions under which evaporation occurs (Fig. 6.1). Hence, the single parameter, d, can be representative of the degree of evaporation of a water sample, as well as the conditions under which evaporation occurred (e.g. humidity, temperature, TDS). For example, increasingly negative d values could represent more evaporated samples, or evaporation at a lower humidity. It is important to note that, based on the analytical uncertainties in $\delta^2H$ and $\delta^{18}O$ (1 ‰ and 0.1 ‰ respectively), the uncertainty in deuterium excess values is 1.04.

Fractionation by evaporation leads to the occurrence of large ranges in $\delta^{2}$H and $\delta^{18}$O in salt lake and other evaporitic environments. Research into the application of $\delta^{2}$H and $\delta^{18}$O in salt lake studies has developed in five key areas:

a) Quantification of groundwater evaporation rates from dry lake beds. In one of the earliest studies of $\delta^{2}$H and $\delta^{18}$O in soil water, Zimmerman et al. (1967) showed that pore water isotope vs depth profiles formed by evaporation in a saturated medium have a predictable shape resulting from a balance between the upward evaporative flux and a downward diffusive flux. This discovery was extended by Barnes and Allison (1983, 1984), who derived equations for the $\delta^{2}$H and $\delta^{18}$O vs depth profiles in non-vegetated unsaturated soils, where the water content changes with depth. Allison and Barnes (1985) used this analytical model to estimate an evaporation rate of 63 mm/y from the normally “dry” Lake Frome, Australia, and Fontes et al. (1986) similarly estimated groundwater discharge rates in the Sahara. The same principle was applied at Raak Plain to $\delta^{2}$H vs depth profiles obtained from playa sediments during summer to estimate summer evaporation rates of between 10 mm/y and 100 mm/y (Howes, 1998).

b) Quantitative lake-scale water balances. This area of research has focused mainly on the isotopic mass balances of surface water lakes (e.g. Friedman et al., 1964; Craig and Gordon, 1965; Fontes and Gonfiantini, 1967; Dincer, 1968; Gat and Bowser, 1991). The basic mathematical model for estimating the isotopic composition of water evaporating from a well-mixed reservoir was derived by Craig and Gordon (1965). Dincer (1968) used $\delta^{2}$H and $\delta^{18}$O mass balances to quantify inflows to a series of lakes in southwestern Turkey, where losses via leakage were unknown. Kinetic enrichment factors for these lakes were estimated using an index lake of known water balance. Gat and Levy (1978) applied an $\delta^{18}O$ mass balance to determine that surface waters in a series of inland sabkhas in Sinai were derived from the drainage of meteoric waters from surrounding dunes. They took this further to estimate ratios of inflow to evaporation and hence, the degree of leakage to groundwater.

Fontes and Gonfiantini (1967) suggested that some of the above models and assumptions applicable to steady state surface water lakes may not apply to those undergoing desiccation. In addition, Friedman et al. (1976) showed, using the example of Owens Lake, California, that in a desiccating lake the effective isotope fractionation factor, $\alpha$, between the atmospheric water vapour and brine decreases with increasing TDS. However, they found that the relationship between $\delta^{2}H$ in the lake and atmospheric water vapour remains close to equilibrium and can be described by the Rayleigh distillation equation. All of the above case studies pertain to well-mixed surface water lakes. An isotope mass balance approach was applied to the subsurface brines of the dry Lake Malata - Lake Greenly playa complex in South Australia by Dutkiewicz et al. (2000) to estimate brine leakage into the regional groundwater system. Present day leakage, as a fraction of inflow, was estimated at 75 to 90 %, approximately 35 times higher than that estimated from $Cl^-$ and $Br^-$ mass balances.

c) Constraint of physical and geochemical models of brine evolution and mixing. A lack of increase in $\delta^{2}H$ and $\delta^{18}O$ values excluded evaporation as a possible cause for the evolution of Na-$HCO_3$ recharge water to a Na-Cl brine in the Smith Creek Valley playa, Nevada, where the TDS increase was attributed to dissolution of pre-existing evaporite deposits (Thomas et al., 1989). Barnes et al. (1990) explained increases in $\delta^2H$ of groundwater brines towards the centres of two large playas, Lakes Frome and Tyrrell (discussed in detail in Section 4.2.4), located in south-eastern South Australia and north-western Victoria respectively, as the result of lateral movement of evaporated brine towards the centre of the playa by density driven convection cells. The onset of instability, leading to convection, was demonstrated using an analytical advection-diffusion model. Inundation of the lakes was additionally shown to potentially enhance density-related instabilities and the release of the underlying brine to the regional groundwater system. Additionally, Herczeg et al. (1992) used $\delta^2H$ and $\delta^{18}O$ at Lake Tyrrell to identify a reflux brine that has undergone several cycles of evaporation and mixing, distinguishing this from meteoric-derived regional groundwaters in seepage zones and presently forming shallow brines. Simmons et al. (2002) combined $\delta^2H$ and $\delta^{18}O$ data with a numerical modelling approach to identify the vertical and lateral extent of groundwater brine leakage from the active saline disposal basin, Lake Mourquong, in the central Murray Basin.

### 6.2.2 Radiocarbon and $\delta^{13}C$

The radioactive isotope of carbon, $^{14}C$, is primarily produced in the atmosphere by cosmic ray secondary neutrons via the $^{14}N(n,p)^{14}C$ reaction. It quickly oxidizes to $CO_2$ and mixes with atmospheric $CO_2$, eventually entering the hydrosphere by dissolving in rainwater. $^{14}C$ activities are measured on dissolved inorganic carbon (DIC = $HCO_3^- + CO_{2(aq)}$) as percent modern carbon (pmC), with the $^{14}C$ activity of atmospheric $CO_2$ in the year 1950 AD defined as 100 pmC. Nuclear weapons testing since 1950 has increased the amount of $^{14}C$ in the atmosphere so that modern atmospheric $CO_2$ may have a $^{14}C$ activity slightly greater than 100 pmC. $CO_2$

dissolved in rainwater is in equilibrium with the atmosphere and hence has the same $^{14}C$ activity (~100 pmC).

When rainwater percolates through the unsaturated zone, its $[CO_{2(aq)}]$ increases due to the much higher $P_{CO2}$ in soil, a result of plant root respiration and organic matter oxidation. The subsequent speciation of $CO_{2(aq)}$ to $HCO_3^-{}_{(aq)}$ and $CO_3^{2-}{}_{(aq)}$ results in the production of protons, which can then react with minerals such as carbonates, by the following overall reaction:

$$Ca_xMg_{(1-x)}CO_{3(s)} + H_2O + CO_2 = XCa^{2+} + (1-X)Mg^{2+}{}_{(aq)} + 2HCO_3^- \qquad (6.3)$$

The infiltrating rainfall can continue to dissolve minerals, supplied with $CO_2$ by the large soil gas reservoir, until it either becomes saturated with respect to that mineral or reaches the water table. In the absence of oxidation of old soil organic matter, DIC in the unsaturated zone continuously re-equilibrates with soil $CO_2$, preserving its atmospheric $^{14}C$ signature. When it enters the "closed" groundwater system, in the absence of complicating chemical reactions, the $^{14}C$ activity of the DIC decreases according to the general law of radioactive decay:

$$A = A_0e^{-\lambda t} \qquad (6.4)$$

Where:

A is the $^{14}C$ activity after time, t since isolation from the atmosphere; and

$A_0$ is the initial $^{14}C$ activity prior to radioactive decay;

$\lambda$ is the decay constant of the isotope, $^{14}C$ ($\lambda = 1.2097 \times 10^{-4}\ yr^{-1}$).

The "age", t, of the groundwater can then be calculated by rearranging the decay equation:

$$t = -8270.\ln\left(\frac{A}{A_0}\right) \tag{6.5}$$

Several processes can reduce the initial $^{14}$C activity ($A_0$) of groundwater to below 100 pmC, and calculations of meaningful residence times require correction of $A_0$ for these using other isotopic or hydrochemical tracer information. The two most common processes that cause this problem are the oxidation of old soil organic matter and dissolution of carbonate minerals. Microbial oxidation of organic matter that has been deposited for a long time (> several thousand years) releases $CO_2$ that has a $^{14}$C activity < 100 pmC. If infiltrating rainwater cannot re-equilibrate with atmospheric $CO_2$, mixing with this $CO_2$ can reduce its $^{14}$C activity. As described earlier, the dissolution of carbonate minerals occurs by the action of dissolved $CO_2$ (Eq. 6.3). This results in the formation of two moles of $HCO_3^-$ for every mole of $CO_2$ consumed. Most carbonate minerals are usually > 30,000 years old, and provide at least half of the dissolved carbon atoms. Re-equilibration with atmospheric $CO_2$ is slow below the water table and, therefore, the groundwater system can be interpreted as a closed system for $^{14}$C. Reactions below the water table will therefore dilute $^{14}$C and alter apparent $^{14}$C ages.

The ratio of the less abundant stable isotope of carbon, $^{13}$C, to the more abundant $^{12}$C in a sample is expressed in delta notation ($\delta^{13}$C) as per mil (‰) relative to a standard, according to Equation 6.1. The standard for $\delta^{13}$C is the Pee Dee Belemnite (PDB), the internal calcite structure from fossil *Belemnitella americana* from the Cretaceous Pee Dee Formation, South Carolina. $\delta^{13}$C can often be useful, along with other chemical and isotopic tracers, for correcting $A_0$ in the determination of groundwater residence times using $^{14}$C. Processes that reduce the $^{14}$C activity of groundwater DIC often involve end members with very distinct $\delta^{13}$C signatures (Table 6.2). Trends in

$\delta^{13}C$ can therefore be used to identify and quantify groundwater interactions with these reservoirs and hence to correct $A_0$.

A number of models exist for the estimation of initial $^{14}C$ activity ($A_0$) from $\delta^{13}C$. These are discussed in detail by Fontes (1983) and Kalin (2000). The models vary in their complexity and the processes they account for, ranging from the empirical approach of Vogel (1967) to chemical mass balances that include isotope exchange (e.g. Mook (1980) and Fontes and Garnier (1979)). The choice of the appropriate model depends on the physical situation, and hydrological and geochemical processes occurring within the land, soil and groundwater system of interest.

Table 6.2. $\delta^{13}C$ values for various carbon reservoirs in the environment (Clark and Fritz, 1999; Herczeg, 2000).

| | $\delta^{13}C$ (‰ vPDB) |
|---|---|
| Atmospheric $CO_2$ | -8 ± 1‰ |
| Soil $CO_2$ | -26 to -9 |
| Organic Matter | -30 to -10 |
| $CaCO_3$ | -6 to +1 |
| Biogenic Methane ($CH_4$) | <-50 |
| Soil Water and Groundwater DIC | -25 to +2 |

### 6.2.3 Chlorine-36

The chloride anion ($Cl^-$) is used extensively as a tracer of water and solute movement in hydrogeological studies. $Cl^-$ is extremely stable and has a negative charge that discourages adsorption onto silicate surfaces. Therefore, once it enters the hydrological system, it is usually advected at the same rate as the water and is removed by few geochemical processes. The long-lived radioisotope of chloride, $^{36}Cl$, with a half-life of 301 000 ± 4 000 years (Endt and Van der Leun, 1973;

Bentley et al., 1986b), can be used to date groundwaters with residence times up to approximately 1 million years. It also has a number of applications for tracing subsurface waters with short residence times (decades) due to the thermonuclear production of $^{36}$Cl during atomic bomb testing in the mid-1950s.

Most natural $^{36}$Cl is formed in the stratosphere and troposphere by cosmic ray interactions with atmospheric argon by the $^{40}$Ar(p, $n\alpha$) $^{36}$Cl and $^{36}$Ar($n$, p) $^{36}$Cl reactions (Lal and Peters, 1967). This cosmogenic $^{36}$Cl then mixes with atmospheric chlorine salts of marine and terrestrial origin, which typically contain only small amounts of $^{36}$Cl relative to the cosmogenic component. The $^{36}$Cl reaching the ground as rainfall is therefore diluted, particularly in near-coastal regions, where the addition of marine chloride is greater (Hutton, 1976; Hutton and Leslie, 1958; Blackburn and McLeod, 1983). The variation in $^{36}$Cl between coastal and inland areas can be from a few to several hundred parts in $10^{15}$ Cl atoms (Chivas et al., 1996). $^{36}$Cl contents are usually expressed as the number of $^{36}$Cl atoms per litre of water (N) or as the atomic ratio (R) of $^{36}$Cl with respect to the total chloride ($^{36}$Cl/Cl). The conversion factor between these two scales is:

$$N = 1.7 \times 10^{19} RC \qquad (6.6)$$

Where C is the chloride content of the water in mg/L.

On entering the groundwater cycle, $^{36}$Cl decays to $^{36}$Ar by $\beta^-$ emission (98%) and to $^{36}$S by electron capture (2%). The development of measurement techniques using Accelerator Mass Spectrometry (AMS) has meant that $^{36}$Cl can now be used practically as a dating tool for very old groundwaters (> 50 ka). Good reviews of this application of $^{36}$Cl distributions are presented by Bentley et al. (1986a), Andrews and Fontes (1992) and Phillips (2000). However, similarly to $^{14}$C, the use of $^{36}$Cl decay as an absolute dating tool requires a detailed knowledge of all processes influencing the $^{36}$Cl content of water within the hydrological cycle. Any mixing with other chloride sources must be quantified and the effect of in situ $^{36}$Cl production must be estimated. The latter can occur in the lithosphere by spallation of K, Ca and Ar (most commonly) by residual fluxes of fast protons and secondary particles at sea level. However, most importantly for high $Cl^-$ environments like Raak Plain, substantial amounts can also be produced by neutron capture on $^{35}$Cl by the $^{35}Cl(n, \gamma)^{36}Cl$ reaction. This can occur near the surface, as a result of cosmic neutrons, or at large depths as a result of natural radioactivity from the spontaneous fission of $^{238}$U in the aquifer matrix (Feige et al., 1968; Kuhn et al., 1984). Eventually, $^{36}$Cl/Cl will asymptotically approach a secular equilibrium value for in-situ production characteristic of the aquifer environment.

Water-rock interactions along groundwater flow paths liberate chloride that is contained in minerals, fluid inclusions and as intergranular saline pore fluids. By this mechanism, the chloride content of groundwater often increases along a flow path and the $^{36}$Cl/Cl ratio again tends towards the secular equilibrium value of the aquifer. The Great Artesian Basin in Australia (Bentley et al., 1986b; Torgersen et al., 1991; Love et al., 2000) and the Milk River Aquifer in Canada (Hendry and Schwartz, 1988) are some examples where this has been shown to occur.

Finally, the evolution of $^{36}$Cl/Cl in groundwater can be described using the following mass balance equation, including terms for (1) decay of the atmospheric (input) contribution, (2) underground production, and (3) additional chloride derived from the rock (by water rock interaction) (Phillips et al., 1986a; Bentley et al., 1986a):

$$RC = \underbrace{R_0C_0e^{-\lambda t}}_{(1)} + \underbrace{R_{eq}\, C_0\cdot(1-e^{-\lambda t})}_{(2)} + \underbrace{R_{eq}\,(C- C_0)}_{(3)}, \qquad (6.7)$$

where: R = $^{36}$Cl/Cl ratio at the point of sampling, C = Cl$^-$ concentration at the point of sampling, $R_0$ = input ratio, $C_0$ = input concentration of chloride (mg/L), $R_{eq}$ = secular equilibrium $^{36}$Cl/Cl ratio of dissolved chloride, $\lambda$ is the $^{36}$Cl decay constant ($2.3 \times 10^{-6}$ yr$^{-1}$) and t is the residence time of the sample [yr]. Equation 6.7 can be solved for residence time:

$$t = \frac{-1}{\lambda} \ln\left(\frac{C(R-R_{eq})}{C_0(R_0-R_{eq})}\right) \qquad (6.8)$$

Some of the very first applications of $^{36}$Cl dating of groundwater focused on the accumulation times of chloride in saline closed-basin lakes (Davis and Schaeffer, 1955; Bagge and Wilkom, 1966; Tamers et al., 1969). Because of the long half-life of $^{36}$Cl and the dominance of Cl$^-$ in evaporitic environments, there was a lot of potential for studying the origins and residence times of brines in slowly evolving closed salt lake systems. For example, Carlson et al. (1990) and Lyons et al. (1998) used the $^{36}$Cl/Cl ratios of saline surface waters of a system of lakes in the McMurdo Dry Valley, Antarctica to show variable sources of chloride for individual lakes. Kaufman et al. (1990) showed that most of the brines in the Lake Magadi/Natron basins and surrounding aquifers of the East African Rift are derived entirely from the evapo-concentration of meteoric Cl$^-$, and estimated an accumulation time of approximately 760 kyr for the salt inventory of these basins. Rogers (1993) and Phillips et al. (1995) estimated a range of Cl$^-$ accumulation times in Mono Basin, California of between 100 and 450 k yr, linking the onset of basin closure to long-term aridity in the region..

$^{36}$Cl/Cl ratios of halite from playa lakes in the western two thirds of the Australian continent range between 28 x $10^{-15}$ and 150 x $10^{-15}$ and increase towards the centre of the continent, mimicking an increase in rainfall $^{36}$Cl/Cl (Chivas et al., 1996). Rainfall ratios range between 8 x $10^{-15}$ at the coast and 400 x $10^{-15}$ inland, being lower near the coast due to dilution by marine chloride. A meteoric origin for surface chloride deposits, with an integrated residence time of approximately 1 Ma was inferred (Chivas et al., 1996). Mean $^{36}$Cl fallout in eastern Australia ranges between 35 atoms $^{36}$Cl/m$^2$/s at the coast to 13 atoms $^{36}$Cl/m$^2$/s in central Australia (Chivas et al., 1996). Keywood et al. (1998) showed a weak correlation between $^{36}$Cl fallout and rainfall, which possibly explains this variation. Davie et al. (1989) produced contours of estimated $^{36}$Cl/Cl ratios in precipitation for south-eastern Australia by combining the predicted latitude dependence of atmospheric $^{36}$Cl production with literature values of total chloride in precipitation.

The first published $^{36}$Cl measurements of groundwater in the Murray Basin, Australia were provided by Davie et al. (1989) for the Victorian and South Australian Mallee regions in the south-west of the basin. Groundwater $^{36}$Cl/Cl values ranged between 13 x $10^{-15}$, in the Parilla Sand aquifer below Raak Plain, and 43 x $10^{-15}$ in the Murray Group aquifer approximately 150 km to the west of Raak Plain (most of the measurements made in the Murray Group aquifer). The results of this study suggested that, with the exception of the groundwater discharge complexes, the major source of salts to the Murray Group aquifer was recent (compared with the half-life of $^{36}$Cl) atmospheric accessions via recharge. Groundwater $^{36}$Cl/Cl ratios below several groundwater discharge complexes varied considerably, suggesting that $^{36}$Cl could potentially be a useful tool for studying groundwater discharge in the Murray Basin. Subsequent to the study of Davie et al. (1989), a contour map of

$^{36}$Cl/Cl ratios in the regional unconfined aquifers (the Parilla Sand) across the entire Murray Basin has been produced (Kellett et al., unpublished). This shows $^{36}$Cl/Cl ratios decreasing steadily from 90 x $10^{-15}$ and 170 x $10^{-15}$ in the northern and eastern margins of the basin respectively to < 30 x $10^{-15}$ in the vicinity of the groundwater discharge complexes at the centre.

## 6.3 Results

### 6.3.1 $\delta^2$H and $\delta^{18}$O

#### 6.3.1.1 Parilla Sand Groundwater and Local Recharge (Low $\delta^2$H and $\delta^{18}$O End-Members)

Groundwater samples from below Raak Plain have $\delta^2$H and $\delta^{18}$O values that range from –39.7 ‰ and –5.1 ‰ respectively for the inflowing Parilla Sand groundwater to +29.2 ‰ and +9.6 ‰ for the shallowest subsurface pore water brines (Table 6.3). On a $\delta^2$H vs $\delta^{18}$O graph, all of the samples plot to the right of the meteoric water line (MWL) for Adelaide, $\delta^2H = 7.7\delta^{18}O + 13$, (J. Dighton, CSIRO Land and Water, unpublished data), approximately along the line $\delta^2H = 4.85\delta^{18}O - 8.2$ (Fig. 6.2).

The most negative $\delta^2$H and $\delta^{18}$O end-members of the linear trend in Figure 6.2 represent groundwater from the Parilla Sands, shallow local groundwater from the dunes and plains between the playas, and rainfall samples (Fig. 6.3). The most negative of these ($\delta^2$H = -39.7 ‰ and $\delta^{18}$O = -5.1 ‰ respectively) were recorded in the Parilla Sand aquifer in groundwater flowing into Raak Plain at the eastern margin of the discharge complex (bore 26240; Fig. 1.6). Slightly less negative values ($\delta^{18}$O ~ -3.8 ‰ and $\delta^2$H ~ -29.3 ‰) occur in the Parilla Sand below the Main Salina, where

Table 6.3 Isotopic compositions of groundwaters and brines at Raak Plain. Data is from April 2001, unless otherwise stated. Data from other sampling dates are included in Appendix H. *m bgl = metres below ground (numbers in brackets indicate m below water table). d-excess is calculated using equation 6.2.

| PIEZOMETER/ SITE NAME | SAMPLE DEPTH | TDS | $Cl^-$ | $Br^-$ | Alkalinity | pH | $\delta^{18}O$ | $\delta^{2}H$ | d-excess | $\delta^{13}C$ | $^{14}C$ | $^{36}Cl/Cl$ |
|---|---|---|---|---|---|---|---|---|---|---|---|---|
| Parilla Sand Groundwater Bores | m bgl* (m below water table) | g/kg | moles/kg | mmoles/kg | | | ‰ V-SMOW | | ‰ | ‰ V-PDB | pmC | x $10^{-15}$ |
| 26240 | 50 | 41.4 | 0.652 | 0.78 | 0.88 | 5.92 | -5.10 | -39.68 | 1.1 | | | 30.5 |
| 81945 | 37-43 | 53.1 | 0.857 | 1.13 | - | 5.53 | -4.46 | -32.57 | 3.1 | | | |
| 98347 | 38-42 | 51.0 | 0.763 | 0.71 | 0.82 | 6.07 | -3.98 | -28.80 | 3.0 | | | |
| 98349 | 68-74 | 49.0 | 0.729 | 0.60 | 0.91 | 6.21 | -3.83 | -28.57 | 2.1 | -5.0 | 14.9 | |
| 98351 | 37-48 | 51.2 | 0.768 | 0.71 | 0.89 | 5.95 | -3.82 | -29.39 | 1.2 | | | |
| 50073 | 36 | 65.3 | 0.999 | 1.28 | 0.90 | 6.28 | -4.21 | -33.04 | 0.6 | | | |
| 50074 | 54-57 | 82.1 | 1.297 | 1.64 | 0.19 | | -3.56 | -30.21 | -1.7 | 0.0 | 8.7 | |
| 50075 | 55-60.5 | 66.5 | 1.016 | 1.23 | 1.94 | 6.59 | -4.15 | -31.46 | 1.7 | -8.0 | 5.4 | |
| | | | | | | | | | | | | |
| Dune/Plain Groundwater | | | | | | | | | | | | |
| R1 | 13.3-13.8 (7.8) | 76.4 | 1.123 | 1.27 | 2.36 | 6.87 | -2.00 | -18.02 | -2.0 | -9.1 | 6.3 | |
| R2 | 1.5-2.0 (0.24) | 45.2 | 0.613 | 0.72 | 0.60 | 6.68 | -3.79 | -30.31 | 0.0 | -21.1 | 47.3 | |
| R3 | 5.3-5.8 (0.17) | 24.3 | 0.322 | 0.34 | 1.15 | 7.37 | -4.33 | -30.54 | 2.8 | -10.7 | 100.0 | |
| R4 | 4.8-5.3 (0.7) | 54.4 | 0.769 | 0.95 | 0.86 | 6.72 | -3.60 | -25.15 | 3.7 | | | |
| | | | | | | | | | | | | |
| Western Salina | | | | | | | | | | | | |
| West1 Profile | 2-4 cm | 242.5 | 3.793 | 4.08 | 3.15 | 7.42 | 7.59 | 29.25 | -31.4 | | | |
| (Jan 1998) | 8-10 cm | 216.7 | 3.442 | 3.53 | - | 7.09 | 5.12 | 20.05 | -20.9 | | | |
| | 20-25 cm | 199.1 | 3.136 | 3.71 | 1.59 | 7.05 | 1.85 | 9.40 | -5.4 | | | |
| | 60-70 cm | 193.7 | 3.070 | 2.93 | 0.83 | 6.81 | 2.28 | 7.43 | -10.8 | | | |
| | 80-90 cm | 194.7 | 3.073 | 3.02 | - | 7.12 | 2.68 | 7.42 | -14.0 | | | |
| | 153-160 cm | 192.8 | 3.081 | 3.13 | 0.79 | 6.51 | 2.71 | 6.71 | -15.0 | | | |
| | 166-177 cm | 193.1 | 3.05 | 3.13 | - | 6.99 | 2.38 | 6.64 | -12.4 | | | |
| | 274-292 cm | 193.1 | 3.079 | 2.83 | - | 6.95 | - | 7.33 | 9.0 | | | |
| West1a | 2.6-3.1 (2.6) | 180.5 | 2.654 | 2.05 | 0.148 | 5.75 | 2.07 | 3.33 | -13.3 | | 92.4 | 33.3 |
| West1b | 0.7-1.2 (0.75) | 186.7 | 2.758 | 2.34 | 0.08 | 6.41 | 1.74 | 2.32 | -12.1 | | 77.8 | |

Table 6.3 (continued)

| PIEZOMETER/ SITE NAME | SAMPLE DEPTH | TDS | $Cl^-$ | $Br^-$ | Alkalinity | pH | $\delta^{18}O$ | $\delta^{2}H$ | d-excess | $\delta^{13}C$ | $^{14}C$ | $^{36}Cl/Cl$ |
|---|---|---|---|---|---|---|---|---|---|---|---|---|
| | m bgl* (m below water table) | g/kg | moles/kg | mmoles/kg | | | ‰ V-SMOW | | ‰ | ‰ V-PDB | pmC | x $10^{-15}$ |
| West5 Profile | 0-2 cm | 264.2 | 3.507 | 4.62 | - | - | 1.75 | 0.41 | -13.6 | | | |
| (Apr 1998) | 2-4 cm | 234.5 | 3.218 | 5.15 | - | - | 1.76 | 2.43 | -11.7 | | | |
| | 6-8 cm | 212.6 | 3.091 | 4.45 | - | - | 1.09 | -1.11 | -9.9 | | | |
| West2a | 2.2 | 90.2 | 1.296 | 1.25 | - | 7.4 | -2.00 | -16.42 | -0.4 | | | |
| West2b | 1.6 | 92.7 | 1.357 | 1.25 | 1.65 | 7.28 | -1.85 | -27.15 | -12.3 | | | |
| West2c | 1.9 | 110.3 | 1.584 | 1.56 | 1.44 | 7.11 | -1.05 | -15.85 | -7.4 | | | |
| West2d | 1.8 | 104.4 | 1.539 | 1.68 | 1.45 | 6.95 | -1.34 | -12.26 | -9.5 | | | |
| West2e | 0.9 | 152.5 | 2.266 | 2.33 | 0.68 | 7.05 | 1.29 | -2.43 | -18.5 | | | |
| West2f | 2.2 | 131.5 | 1.854 | 1.63 | 0.43 | 6.95 | 1.78 | 5.91 | -8.3 | | | |
| West3 | 3.3-3.8 (2.7) | 153.1 | 2.243 | 2.65 | 0.24 | 6.43 | 2.32 | -3.97 | -22.5 | -7.6 | 80.8 | 29.1 |
| West4 | 11-12 (10) | 85.9 | 1.238 | 1.37 | 1.80 | 6.67 | -2.23 | -21.23 | -3.4 | -7.4 | 6.2 | 33.5 |
| | | | | | | | | | | | | |
| <u>Main Salina</u> | | | | | | | | | | | | |
| Main1 Profile | 0-2 cm | 232.4 | 3.221 | 3.00 | 81.36 | - | 6.22 | - | - | | | |
| (Jan 1998) | 2-4 cm | 243.8 | 3.640 | 2.86 | 109.83 | | - | - | - | | | |
| | 13-16 cm | 212.4 | 3.169 | 3.11 | 65.55 | | 3.67 | - | - | | | |
| | 30-35 cm | 206.1 | 3.060 | 3.02 | 107.57 | | 4.85 | - | - | | | |
| Main1 | 1.5-2.0 (1.5) | 187.1 | 2.762 | 2.63 | 0.26 | 4.57 | 2.56 | 4.36 | -11.1 | | | |
| Main2 | 0.4-0.5 (0.1) | 190.9 | 2.708 | 3.01 | 0.28 | 6.87 | 1.73 | 1.69 | -14.5 | -9.0 | 95.6 | |
| Main3 | 14-15 (14.5) | 50.7 | 0.743 | 0.83 | 0.92 | 6.07 | -4.22 | -30.60 | 5.8 | -5.0 | 15.7 | |
| Main4 | 6.5-7.0 (6.2) | 50.9 | 0.748 | 0.83 | 0.45 | 5.77 | --4.04 | -29.37 | 3.0 | 0.0 | 17.4 | |
| 98348 | 0.5-3.5 (2.0) | 51.3 | 0.779 | 0.71 | 0.04 | 4.35 | -4.04 | -30.45 | 1.9 | | | |

Table 6.3 (continued)

| PIEZOMETER/ SITE NAME | SAMPLE DEPTH | TDS | $Cl^-$ | $Br^-$ | Alkalinity | pH | $\delta^{18}O$ | $\delta^{2}H$ | d-excess | $\delta^{13}C$ | $^{14}C$ | $^{36}Cl/Cl$ |
|---|---|---|---|---|---|---|---|---|---|---|---|---|
| | m bgl* (m below water table) | g/kg | moles/kg | mmoles/kg | | | ‰ V-SMOW | | ‰ | ‰ V-PDB | pmC | x $10^{-15}$ |
| <u>Salt Lake</u> | | | | | | | | | | | | |
| Salt1 Profile | 0-2 cm | 259.2 | 3.873 | 5.74 | 3.36 | 6.14 | 9.64 | 25.87 | -51.2 | | | |
| (Jan 1998) | 2-4 cm | 258.0 | 3.893 | 5.65 | 1.82 | 7.09 | 5.82 | 23.88 | -22.7 | | | |
| | 4-6 cm | 255.9 | 3.974 | 5.19 | 0.65 | 6.56 | 5.75 | 23.13 | -22.9 | | | |
| | 50-55 cm | 235.3 | 3.651 | 3.10 | 0.04 | 6.03 | 2.93 | 10.77 | -12.65 | | | |
| | 100-110 cm | 235.9 | 3.725 | 2.64 | 0.13 | 6.02 | 3.70 | 11.86 | -17.7 | | | |
| | 255-263 cm | 203.9 | 3.034 | 2.37 | - | 5.88 | 3.00 | - | - | | | |
| Salt1a | 2.1-2.6 (2.4) | 199.5 | 2.701 | 1.91 | - | 5.2 | 3.05 | 9.45 | -15.0 | | | |
| Salt1b | 0.2-0.5 (0.3) | 236.5 | 3.454 | 2.83 | - | 5.2 | 1.34 | 0.87 | -9.9 | | | |
| Lake Water | | 242.2 | 3.703 | 1.19 | - | 4.96 | -2.63 | -17.56 | 3.5 | | | |
| | | | | | | | | | | | | |
| <u>Spectacle Lake</u> | | | | | | | | | | | | |
| SM1 Profile | 0.5-1.0 | 249.9 | 3.406 | 17.46 | - | | 3.02 | 4.53 | -19.6 | | | |
| (Jul 2001) | 1.0-1.1 | 251.8 | 3.482 | 17.51 | - | | 3.69 | 1.79 | -27.7 | | | |
| | 1.1-1.2 | 234.1 | 3.327 | 17.35 | - | | 3.63 | -0.88 | -29.9 | | | |
| | 2.2-2.3 | 238.1 | 3.396 | 6.74 | - | | 1.80 | -1.74 | -16.1 | | | |
| | 2.5-2.6 | 200.8 | 3.062 | 5.75 | - | | - | -11.93 | - | | | |
| | 3.9-4.0 | 191.6 | 2.801 | 3.01 | - | | -0.46 | -9.91 | -6.2 | | | |
| | 7.4-7.5 | 107.3 | 1.493 | 2.12 | - | | - | -22.32 | - | | | |
| | 8.1-8.2 | 85.6 | 1.210 | 1.31 | - | | -2.92 | -23.37 | 0.0 | | | |
| | 19.7-19.9 | 83.5 | 1.250 | 1.60 | - | | -2.78 | -23.33 | -1.1 | | | |
| | 19.9-20.0 | 81.8 | 1.227 | 1.72 | - | | - | -25.96 | - | | | |
| | 20.2-20.3 | 82.1 | 1.247 | 1.60 | - | | -3.05 | -25.68 | -1.3 | | | |
| | 21.2-21.3 | 83.0 | 1.182 | 1.54 | - | | -3.18 | -24.26 | 1.2 | | | |
| SM1 | 16.1-18.1 (16.9) | 99.5 | 1.435 | 1.80 | 1.71 | 6.61 | -2.52 | -21.38 | -1.2 | -7.5 | 13.2 | 40.9 |
| SM2 | 0.7-2.7 (1.9) | 226.6 | 3.330 | 4.60 | 0.44 | 6.17 | 1.20 | -2.94 | -12.6 | -3.4 | 68.6 | 37.9 |
| SM3 | 6.6-8.6 (7.8) | 85.2 | 1.232 | 1.60 | 1.49 | 6.96 | -3.00 | -25.58 | -1.6 | | 28.4 | 36.5 |
| SM4 | 5.5-7.5 (6.7) | 99.0 | 1.469 | 2.14 | 0.92 | 6.15 | -1.55 | -16.22 | -3.8 | | | 35.9 |

Table 6.3 (continued)

| PIEZOMETER/ SITE NAME | SAMPLE DEPTH | TDS | $Cl^-$ | $Br^-$ | Alkalinity | pH | $\delta^{18}O$ | $\delta^{2}H$ | d-excess | $\delta^{13}C$ | $^{14}C$ | $^{36}Cl/Cl$ |
|---|---|---|---|---|---|---|---|---|---|---|---|---|
| | m bgl* (m below water table) | g/kg | moles/kg | mmoles/kg | | | ‰ V-SMOW | | ‰ | ‰ V-PDB | pmC | x $10^{-15}$ |
| SM5 Profile (Mar 1999) | 2.0-2.1 | 250.2 | 3.624 | 4.22 | - | | 1.15 | -3.24 | -12.3 | | | |
| | 3.0-3.1 | 236.6 | 3.417 | 5.14 | - | | 1.94 | - | - | | | |
| | 3.7-3.8 | 209.5 | 3.025 | 4.44 | - | | 1.43 | -2.42 | -13.8 | | | |
| | 4.0-4.1 | 209.7 | 3.031 | 4.57 | - | | 0.46 | -6.21 | -9.9 | | | |
| | 5.1-5.2 | 148.5 | 2.183 | 8.10 | - | | 4.03 | -9.86 | -42.1 | | | |
| | 6.5-6.6 | 110.3 | 1.706 | 6.68 | - | | -0.87 | -14.96 | -10.3 | | | |
| | 7.2-7.3 | 105.7 | 1.617 | 2.15 | - | | -0.72 | -14.27 | -8.6 | | | |
| | 8.4-8.5 | 106.2 | 1.635 | 2.78 | - | | -1.98 | -17.48 | -1.6 | | | |
| SM5 | 5.5-6.0 (6.1) | 106.2 | 1.552 | 2.34 | 1.05 | 6.18 | -1.68 | -18.20 | -4.8 | -1.3 | 33.6 | |
| SM6 | 18-18.8 (18.8) | 72.0 | 1.076 | 1.39 | 0.74 | 6.07 | -2.9 | -26.48 | -3.3 | 1.7 | 21.0 | 26.6 |
| Pond 3 Lake Water | | 252.7 | 3.550 | 9.30 | - | 2.34 | 3.13 | 10.60 | -14.4 | | | |

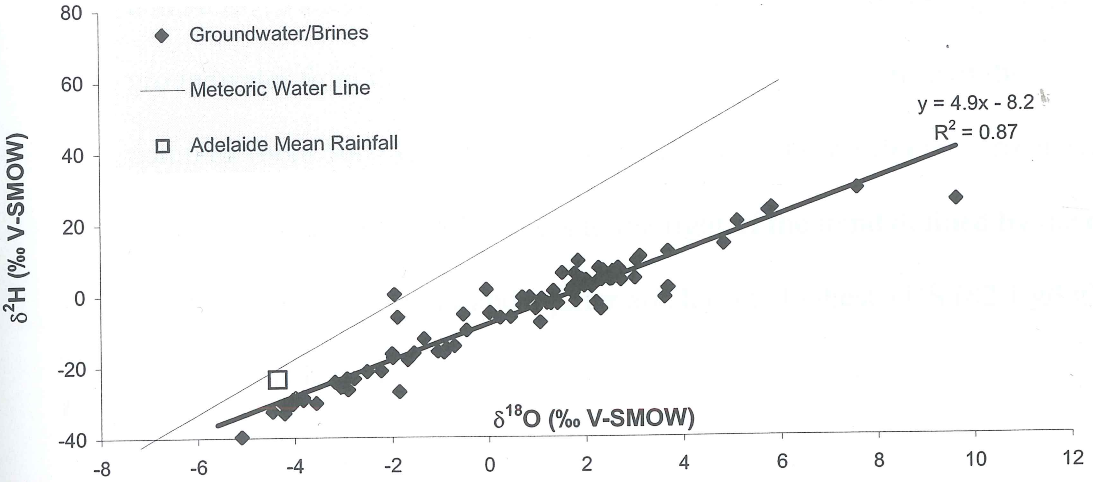

Figure 6.2. $\delta^2$H vs $\delta^{18}$O plot showing all groundwater and pore water data from Raak Plain. The data plot along the line y = 4.9x-8.2, to the right of the Meteoric Water Line due to evaporation.

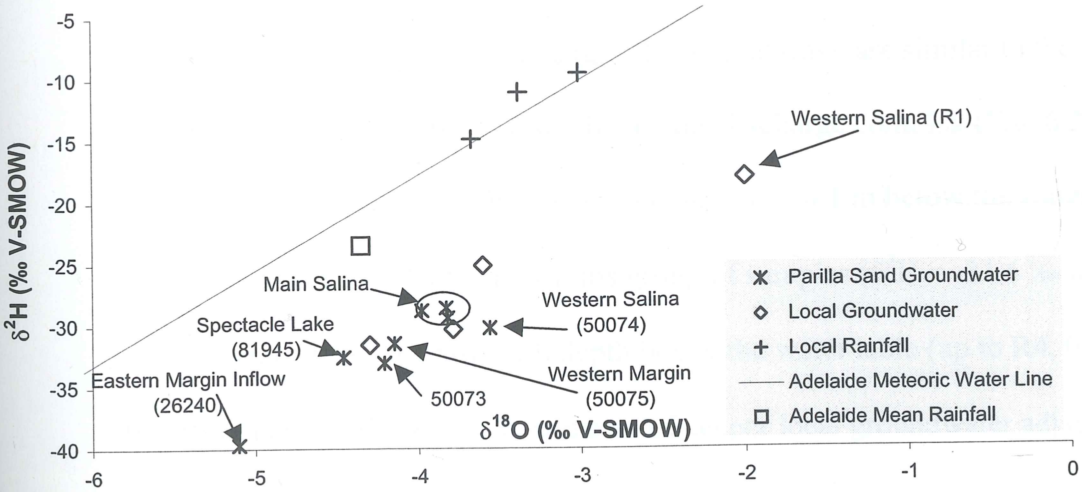

Figure 6.3. $\delta^2$H vs $\delta^{18}$O plot showing lower salinity, less isotopically enriched groundwaters only.

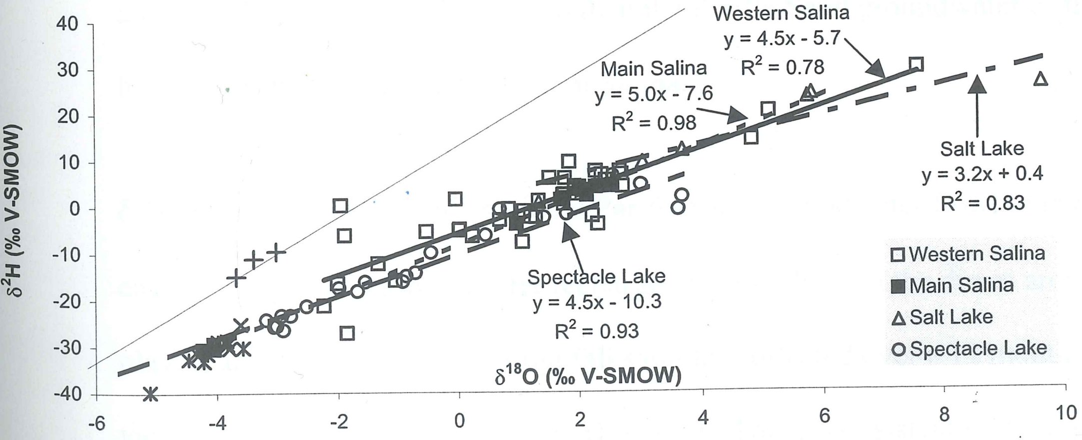

Figure 6.4. $\delta^2$H vs $\delta^{18}$O plot showing trend lines for individual playa lakes at Raak Plain. The similar linear trends are due to different degrees of evaporation of similar source waters

the signature is fairly constant at a range of depths in the aquifer (bores 98347, 98349 and 98351; Table 6.3). Intermediate to the above mentioned samples are groundwater from the western margin (bore 50075), the centre of the discharge complex (bore 50073) and below Spectacle Lake (bore 81945). Groundwater below Western Salina (bore 50074) plots to the right of the trend defined by the other samples from the Parilla Sand aquifer and has the highest TDS (82.1 g/kg) of these samples (Table 6.3).

$\delta^2$H and $\delta^{18}$O signatures of three shallow (< 1 m below water table) local groundwater samples, from below dunes and sand plains adjacent the Main Salina (piezometers R2, R3 and R4; see Fig. 2.1 for locations), are similar to those of the regional Parilla Sands groundwater below the discharge complex (Fig. 6.3). Groundwater sampled from below a sand dune (R3, 0.1 m below the water table) has the lowest $\delta^2$H and $\delta^{18}$O values of this group of samples ($\delta^2H = -31.6$ ‰ and $\delta^{18}O = -4.3$ ‰) and values increase with depth below the water table (up to R4, 0.7 m below the water table). $\delta^2$H and $\delta^{18}$O contents of deeper local groundwater adjacent Western Salina (piezometer R1, 8 m below the water table; see Fig. 2.2 for location) are much higher (-18.0 ‰, -2.0 ‰) than the Parilla Sand groundwater or the shallow local groundwater adjacent the Main Salina.

$\delta^2$H and $\delta^{18}$O values of this regional Parilla Sand groundwater flowing in at the eastern margin, and groundwater recharged locally through the dunes around the playas, are lower than those of rainfall samples collected over a 12 month period at various locations across Raak Plain (Fig. 6.3). This is consistent with groundwater recharge by only heavy rainfall events (i.e. the amount effect (Dansgaard, 1964)).

#### 6.3.1.2 $\delta^2$H and $\delta^{18}$O of Groundwater Brines Beneath the Playa Lakes

The $\delta^2$H and $\delta^{18}$O data for brines below each of the individual playa lakes at Raak Plain fall along straight lines with slopes ranging from 3.2 (Salt Lake) to 5.0 (Main Salina) (Fig. 6.4).

The linear trends are characteristic of different degrees of evaporation from a single source (see Section 6.2.1), but may also be due to a combination of evaporation and mixing between low and high $\delta^2$H and $\delta^{18}$O end-members. The Parilla Sand groundwater and local groundwater samples discussed in Section 6.3.1.1 lie at the low $\delta^2$H and $\delta^{18}$O ends of these lines.

$\delta^{18}$O values at Western Salina range between –2.2 ‰ and 9.5 ‰, and $\delta^2$H ranges between –27.1 ‰ and 32.1 ‰ (Fig. 6.5a). However, the very positive values occur only in the top few centimetres of the summer (Jan-98) pore water profile at the centre of the playa (site West1; see Fig. 2.1 for sample locations), and most samples are < 4 ‰ for $\delta^{18}$O and < 10 ‰ for $\delta^2$H. The exceptions to the linear trend are that some of the winter (July 2001) pore water samples from a transect at the edge of the playa (West2f) and the top 0-2 cm at the centre of the playa (West1) plot close to the local meteoric water line. Relatively low $\delta^2$H and $\delta^{18}$O values were measured 10 m below the water table, at the edge of the playa (West4). Groundwater samples in a shallow transect running from the playa margin towards the centre (West2(a-d)) also have low $\delta^2$H and $\delta^{18}$O values.

Few data points are available for the Main Salina (Fig. 6.5b) due to difficulties in extracting enough water for both $\delta^2$H and $\delta^{18}$O analyses from sediments at the centre of the playa (Main1; see Fig. 2.1 for sample locations). Pore water samples at this site were analysed for $\delta^{18}O$ only. $\delta^{18}O$ values at the Main Salina range between –4.2 ‰, at a depth of 14.5 m near the edge of the playa (Main3) and 6.2 ‰ in pore waters just below the surface at the playa centre (Main1; not shown on Fig. 6.5b). Observed $\delta^{2}H$ values ranged from –30.5 ‰, 4 m below the edge of the playa (bore 98348), to 4.3 ‰ at a depth of 1.7 m below the centre of the playa (Main1). Groundwater samples from depths greater than 2 m at the edge of the Main Salina (bore 98348, 2 m deep and piezometers Main3 and Main4, 15 m and 6.75 m deep) cluster with the regional Parilla Sands and local groundwaters (Fig. 6.5b). However, Main3 has a higher $\delta^{2}H$ value and plots closer to the meteoric water line.

$\delta^{18}O$ signatures of the shallow groundwater and pore waters sampled at the single site at the centre of Salt Lake range between 1.3 ‰ at 2.4 m below the playa surface (piezometer Salt1a) and 9.6 ‰ in the top 2 cm of the pore water profile (Fig. 6.5c). $\delta^{2}H$ values range between 0.9 ‰ and 25.9 ‰. Unlike Western Salina and the Main Salina, Salt Lake contains a layer of surface standing water up to 10 cm deep that only dries up in some parts of the lake during summer. The stable isotopic signature this water ($\delta^{2}H$ = -2.6 ‰ and $\delta^{18}O$ = -17.6 ‰, April 2001) plots closest to the regional and local groundwater samples on the evaporation / mixing line (Fig. 6.5c).

Groundwater $\delta^{18}O$ values at Spectacle lake range between –3.2 ‰ at a depth of 21.3 m below the edge of Pond 3 (pore water at SM1) and 3.7 ‰ at 1 m depth at the same site (Fig. 6.5d). $\delta^{2}H$ values range between –26.5 ‰ 18.5 m below the centre of Pond 2 (piezometer SM6) and 24.2 ‰ at the top of the pore water profile at the same site (SM5; not shown on Fig. 7.5d due to lack of $\delta^{18}O$ data). The deepest pore water and piezometer samples (between 18 m and 22 m depth in the Blanchetown Clay) have higher $\delta^{2}H$ and $\delta^{18}O$ values than all of the Parilla Sands groundwater samples. The

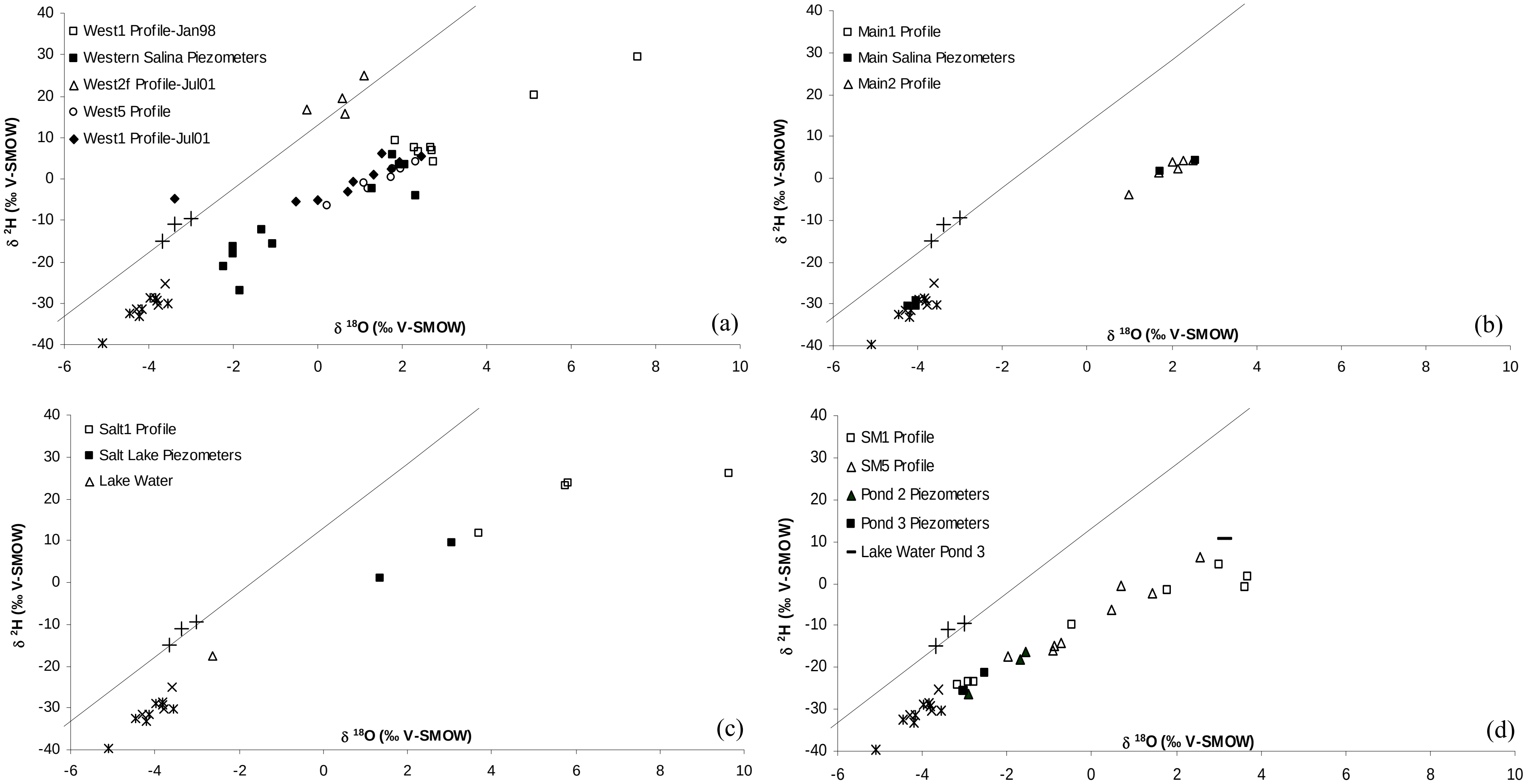

Figure 6.5. $\delta^2$H vs $\delta^{18}$O plots of groundwaters and pore waters from the individual playa lakes, (a) Western Salina, (b) The Main Salina, (c) Salt Lake and (d) Spectacle Lake at Raak Plain. Regional Parilla Sand groundwater, locally recharged groundwater from below sand dunes adjacent the playas (lower left corner) and local rainfall samples (crosses) are also shown for reference, along with the Meteoric Water Line for Adelaide.

very positive $\delta^2$H and $\delta^{18}$O values observed at the natural lakes were not observed at Spectacle Lake as detailed sampling was not carried out in the top 50 cm of the profiles. Surface water from Pond 3 ($\delta^2$H = 3.1 ‰ and $\delta^{18}$O = 10.6 ‰), sampled in April 2001, plots with the shallow groundwater brines on the groundwater evaporation / mixing line. This lake water is pumped from bores in the Parilla Sand aquifer adjacent the lake and evapo-concentrated in Ponds 1 and 2 before being pumped into Pond 3. It may also contain some rainfall and local recharge from the adjacent dunes.

### 6.3.2 Carbon Isotopes

Groundwater samples for carbon isotope ($\delta^{13}$C and $^{14}$C) analyses were selected from the three lakes along transect AA' (Fig. 1.6) to cover a range of depths within the Blanchetown Clay and playa sediments, as well as groundwater beneath the edges and the centres of the lakes. Samples of local (sand dune) and Parilla Sand groundwater were also included as the low TDS source waters for the brines. $\delta^{13}$C values ranged between –21.1 ‰ and 1.7 ‰, with the majority above -9‰ (Table 6.3). $^{14}$C activities ranged between 5.35 pmC for groundwater in the Parilla Sand (bore 50075) and 100 pmC for groundwater at the shallow sand dune site R3 (Fig. 2.1, Table 6.3). One sample of shallow local groundwater (site R2) had an anomalously low $\delta^{13}$C of –21.1 ‰, probably due to deposition and decay of organic matter and has been excluded from the present discussion.

$\delta^{13}$C signatures of the groundwater brines below the playas ranged between –9.0 ‰, just below the water table inside the edge of the Main Salina (Main2) and 1.7 ‰ at 18.8 m below the centre of the harvested Spectacle Lake (SM6) (Table 6.3; Fig.

6.6a). $^{14}$C activities below the playas ranged between 13.2 pmC at a depth of 16.9 m below the edge of Spectacle Lake (SM1) and 95.6 pmC just below the water table at the edge of the Main Salina (Main2) (Table 6.3; Fig. 6.6b).

Shallow (0.1 m below water table) groundwater beneath a sand dune adjacent the Main Salina (R3; cf. Fig. 2.1) was expected to represent the local recharge end member as it enters the groundwater system at Raak Plain. A modern $^{14}$C signature (> 100 pmC) is consistent with recent recharge, and the $\delta^{13}$C of –10.7 ‰ (Table 6.3) could be considered to be in equilibrium with soil $CO_2$ (–18.3 ‰) sampled below other mallee-vegetated and cleared sites in the Murray Basin (Leaney and Allison, 1986). For a pH of 7.37 (Table 6.3), the dominant dissolved carbon species in water are $CO_{2(aq)}$ (8%) and $HCO_3^-$ (92%). Once in the closed groundwater system (i.e. in isolation from the soil $CO_2$ reservoir), equilibrium fractionation between these species, with a fractionation factor of 7.0 ‰ at 25˚C (Deines et al., 1974) leads to a $\delta^{13}C_{DIC}$ of -11.3‰, close to that observed at R3 (Table 6.3).

The carbon isotope signature of the regional Parilla Sands groundwater end member is represented by samples from adjacent the Main Salina (bore 98347), adjacent Western Salina (bore 50074) and from the western margin of the discharge zone (bore 50075) (see Fig. 1.6 for locations). Samples from the eastern margin of Raak Plain (bore 26240) and adjacent Spectacle Lake (bore 81945) were contaminated by atmospheric $CO_2$ during sampling / storage (as indicated by $^{14}$C > 100 pmC) and could not be used. The $\delta^{13}C_{DIC}$ of Parilla Sands groundwater below Raak Plain varies considerably (Table 6.3; Fig. 6.6a). The highest $\delta^{13}$C value of 0 ‰ occurs below Western Salina (bore 50074), in conjunction with the lowest alkalinity (0.189 mmol/kg) and the highest TDS (82.1 g/kg). The lowest $\delta^{13}$C (-8 ‰) and the highest alkalinity (1.94 mmol/kg) occur at the western margin of Raak Plain (bore

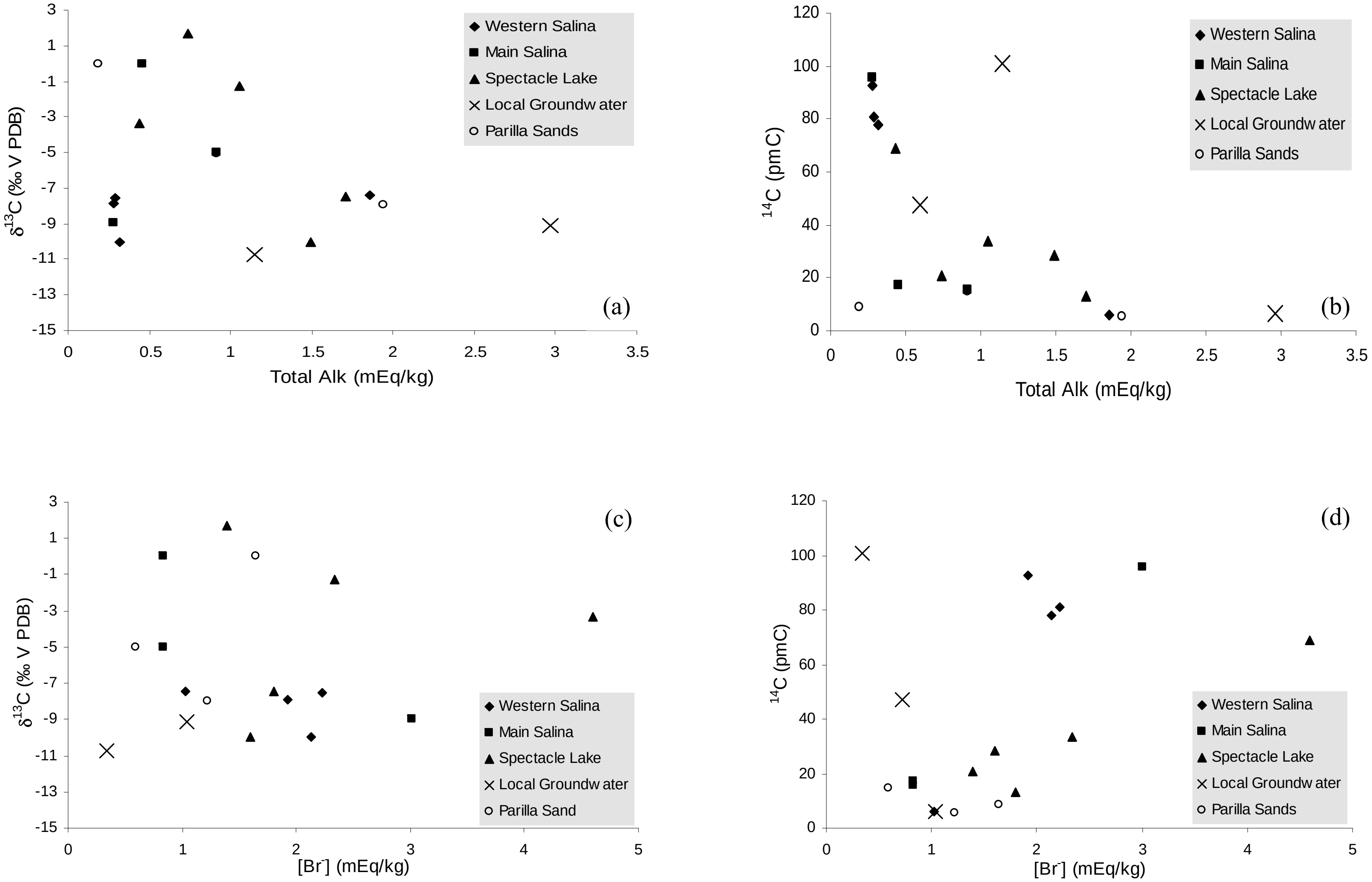

Figure 6.6. Carbon isotope data for selected groundwater samples at Raak Plain.

50075) and intermediate to these is the groundwater below the Main Salina (bore 98349), with an alkalinity of 0.912 mmol/kg and $\delta^{13}C$ of –5 ‰.

### 6.3.3 Chlorine-36

A range of groundwater / brine samples was analyzed for $^{36}Cl/Cl$ ratios, including samples from the Blanchetown Clay below the natural playa, Western Salina, the harvested Spectacle Lake, and from the Parilla Sand aquifer at the eastern margin of Raak Plain (Table 6.3; Fig. 6.7). Due to the presence of large numbers of $^{35}Cl$ atoms near the surface of the discharge complex, it was necessary to investigate the effects of in-situ cosmogenic production on the $^{36}Cl$ signatures of the brines. Estimates of in-situ production (Appendix J) suggested that this was only likely to be significant in brines with residence times ≥ 30 k yrs above 3 m depth. Even then, $^{36}Cl$ contributions by in-situ production are very low and can be excluded from interpretation of the data.

The $^{36}Cl/Cl$ ratio of Parilla Sand groundwater flowing into Raak Plain at the eastern margin is $31 \times 10^{-15}$ (bore 26240; Table 6.3, Fig. 6.7). This value is consistent with groundwater $^{36}Cl/Cl$ contours for the unconfined aquifer over the entire Murray Basin, produced by Kellett et al. (unpublished). The three measured $^{36}Cl/Cl$ ratios in the Blanchetown Clay below Western Salina range from $29.1 \times 10^{-15}$ at a depth of 2.7 m below the water table to $33.5 \times 10^{-15}$ at 10 m depth (Table 6.3, Fig. 6.7). Values below Spectacle Lake, range between $26.6 \times 10^{-15}$ in the deep piezometer at the centre of Pond 2 (SM6, 18.8 m deep) and $40.9 \times 10^{-15}$ in the deep piezometer at the edge of Pond 3 (SM1, 16.9 m deep) (Table 6.3, Fig. 6.7). Groundwater in the Parilla Sand aquifer below the Main Salina was sampled by Davie et al. (1989) and has a ratio of 13 x $10^{-15}$. Modern atmospheric precipitation in the vicinity of Raak Plain has a ratio of approximately 65 (± 5) x $10^{-15}$ (Davie et al., 1989).

Such low $^{36}$Cl/Cl values as those observed at Raak Plain have an analytical uncertainty of approximately 10% associated with them. When this is taken into consideration, it can be seen that differences in the ratios for many of the samples cannot be resolved (Fig. 6.7). No distinction can be made between shallow (< 4 m) and deep (> 6 m) samples based on their $^{36}$Cl/Cl ratios, and these groups can only be distinguished based on their $Cl^-$ concentrations (Fig. 6.7). The uncertainty of ± 10% translates into a residence time of approximately 90 k yrs, meaning that time scales of many of the processes occurring at Raak Plain may not be resolved by the $^{36}$Cl data (Section 5.5.4). The main outlier from the group is the Parilla Sand groundwater below the Main Salina (bore 98347, Fig. 6.7), with a $^{36}$Cl/Cl ratio of 13 x $10^{-15}$ (Davie et al., 1989). This low value was attributed to the recycling of salt within the groundwater discharge complex by Davie et al. (1989).

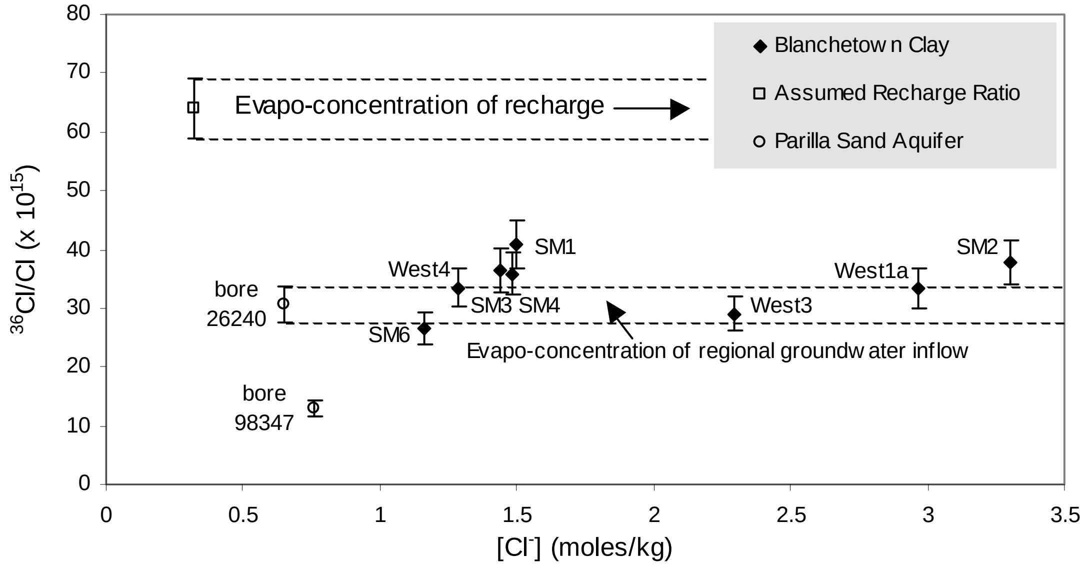

Figure 6.7. $^{36}$Cl/Cl vs [Cl$^-$] diagram for Raak Plain groundwaters and brines. Evapo-concentration has no effect on $^{36}$Cl/Cl ratios, but causes [Cl$^-$] to increase and groundwater compositions to move to the right on this diagram. Shallow brines and deeper groundwaters are indistinguishable based on their $^{36}$Cl/Cl ratios and are only separated by their $Cl^-$ concentrations.

## 6.4 Discussion

### 6.4.1 Major Controls on the Isotopic Signatures of the Groundwaters and Brines at Raak Plain

#### 6.4.1.1 Initial Signatures

A range of conceptual models derived in Chapter 5 (Figs. 5.2-5.12) suggest that the sources of salt and water to the hypersaline subsurface brines at Raak Plain are (a) regional Parilla Sand groundwater flowing in at the eastern margin, and/or (b) groundwater recharged locally through the dunes around the playas. The isotopic signatures ($\delta^2$H and $\delta^{18}$O, $\delta^{13}$C, $^{14}$C and $^{36}$Cl/Cl) of these two sources of solutes and water have been described systematically in Section 6.2, and are now summarized in Table 6.4. Although (a) and (b) have similar chemical characteristics (Chapter 3), their histories are vastly different. Regional groundwater in the Parilla Sand aquifer can originate up to 300 km away at the eastern margin of the Murray Basin, although recharge also occurs along the entire groundwater flow path (Evans and Kellett, 1989). Higher rainfall and lower potential evaporation at the Basin margin result in groundwater with more negative $\delta^2$H and $\delta^{18}$O signatures than that recharged in the Basin interior, near Raak Plain (Herczeg et al., 2001). However, the deuterium excess values of the two sources are similar (Table 6.4). Both end-members (a) and (b) lie along the inferred evaporation / mixing line (see Section 6.3.1.1) with the other groundwater and brine samples from Raak Plain (Fig. 7.2). Hence, the $\delta^2$H and $\delta^{18}$O signatures of the hypersaline brines below the playa lakes at Raak Plain may have originated from either or both of the two sources.

Table 6.4. Isotopic signatures of the potential low-TDS end-members to the brines at Raak Plain: (a) regional Parilla Sand groundwater and (b) locally recharged groundwater below the dunes around the playas.

| | (a) Parilla Sand Groundwater[1] | (b) Local Recharge[2] |
|---|---|---|
| $\delta^2$H (‰ V-SMOW) | -39.7 | -30.5 |
| $\delta^{18}$O (‰ V-SMOW) | -5.1 | -4.3 |
| "d-excess" (‰) | 1.1 | 2.8 |
| $\delta^{13}$C (‰ V-PDB) | -5.0[3] | -10.7 |
| $^{14}$C (pmC) | 14.9[3] | 100.0 |
| $^{36}$Cl/Cl (x $10^{15}$) | 31 | 65 (± 5)[4] |

[1] Unless otherwise stated, end-member (a) is represented by bore 26240 at the eastern margin of Raak Plain.

[2] Unless otherwise stated, end-member (b) is represented by piezometer R3, shallow groundwater below a sand dune adjacent the Main Salina.

[3] Values from bore 98349, below the Main Salina.

[4] Davie et al. (1989).

Regional groundwater at the eastern (up-gradient) margin of Raak Plain has a $^{36}$Cl/Cl ratio of 31 x $10^{-15}$ (Table 6.4, Fig. 6.7), whereas that of modern atmospheric deposition at the site is approximately 65 (± 5) x $10^{-15}$ (Table 6.4). The latter value is based on contours drawn for the Victorian and South Australian Mallee regions of the Murray Basin (Davie et al., 1989). The former is a result of a combination of (a) decay of $^{36}$Cl derived in the eastern high recharge zones of the Murray Basin ($^{36}$Cl/Cl $\cong$ 40 x $10^{-15}$), and (b) addition of Cl$^-$ with higher $^{36}$Cl/Cl along the 300 km groundwater flow path. Cl$^-$ added to the groundwater as recharge along the flow path has $^{36}$Cl/Cl ratios increasing towards the centre of the Basin (Davie et al., 1989).

Parilla Sand groundwater inflow below Raak Plain (bore 98349) has a more positive $\delta^{13}$C value ($\delta^{13}$C = -5 ‰) and a lower $^{14}$C activity ($^{14}$C = 14.9 pmC) than the locally and recently recharged groundwater source (Table 6.4, Fig. 6.8). This signature is similar to those of some comparatively fresh Parilla Sand groundwater samples from the Victorian and South Australian Mallee, south-west of Raak Plain, ($\delta^{13}$C = –7.7 ‰ to –5.5 ‰; $^{14}$C = 0 pmC to 14 pmC; Leaney and Herczeg, 1999), where measurable

$^{14}$C activities were attributed to recharge occurring only slightly up-gradient of the sampling location.

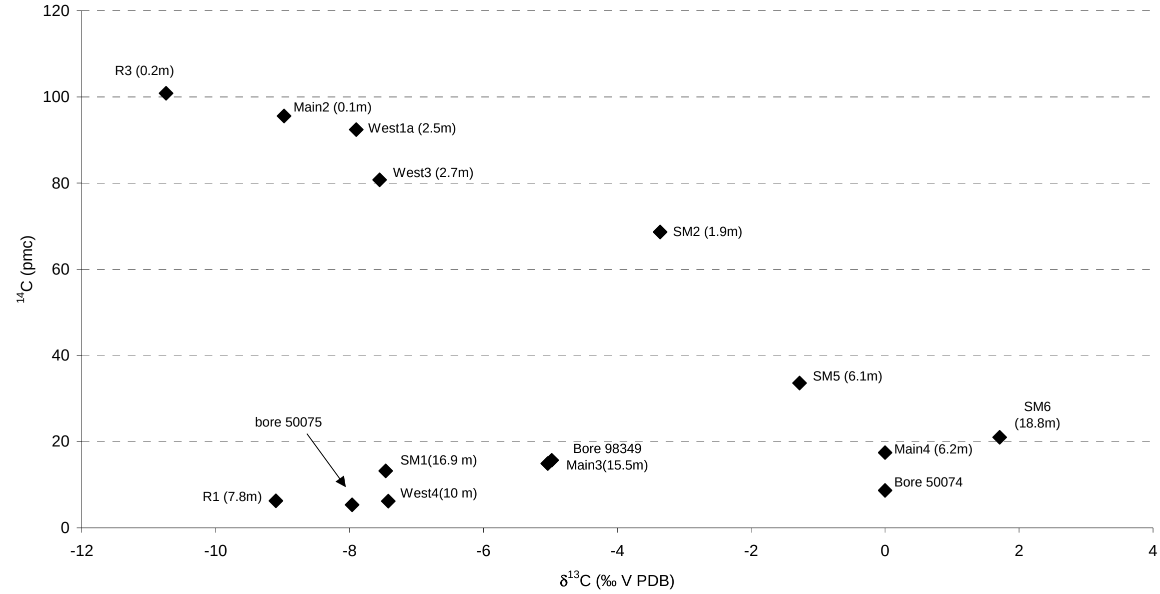

Figure 6.8. $^{14}$C activity vs $\delta^{13}$C of groundwater DIC from Raak Plain, showing the compositions of the modern recharge (R3) and regional groundwater inflow (bore 98349) sources. The samples can be divided into two groups based on their $^{14}$C activities, with the shallow brines having $^{14}$C > 60 pmC and most deeper groundwaters having $^{14}$C < 20 pmC. There are broad ranges in $\delta^{13}$C in both groups, however, indicative of interactions with carbonate minerals.

To understand the effect of recharge on groundwater $^{14}$C activities in the Parilla Sand, it must be considered that a 30 m thick layer of Blanchetown Clay overlies the Parilla Sand aquifer at Raak Plain and 25 km up-gradient (Fig. 1.5, Fig. 1.7). Assuming a recharge rate of 1 mm/y (a high value for mallee vegetated areas; Allison and Hughes (1978); Cook et al. (1994)), a porosity of 45% and no preferential vertical flow through the clay, a travel time of 13.5 k yr is estimated for local recharge to reach the aquifer. Assuming an initial activity of 100 pmC and simple radioactive decay, $^{14}$C activities of 20 pmC are possible in the Parilla Sand. However, for recharge rates ≤ 1 mm/y, diffusive transport of atmospheric $CO_2$ through the Blanchetown Clay can also increase $^{14}$C activities in unconfined aquifers (Walker and Cook, 1991). $^{14}$C activities of 10 pmC to 30 pmC are possible at 30 m depth for recharge rates between 0 mm/y (i.e. diffusion only) and 1 mm/y (Fig. 6.9). Based on Figure 6.9, the $^{14}C$ activity at bore 98349 (15 pmC) suggests recharge rates > 0.1 mm/y, and a residence time of 0 to 6 000 yrs in the Parilla Sand (assuming radioactive decay as the only process affecting $^{14}C$).

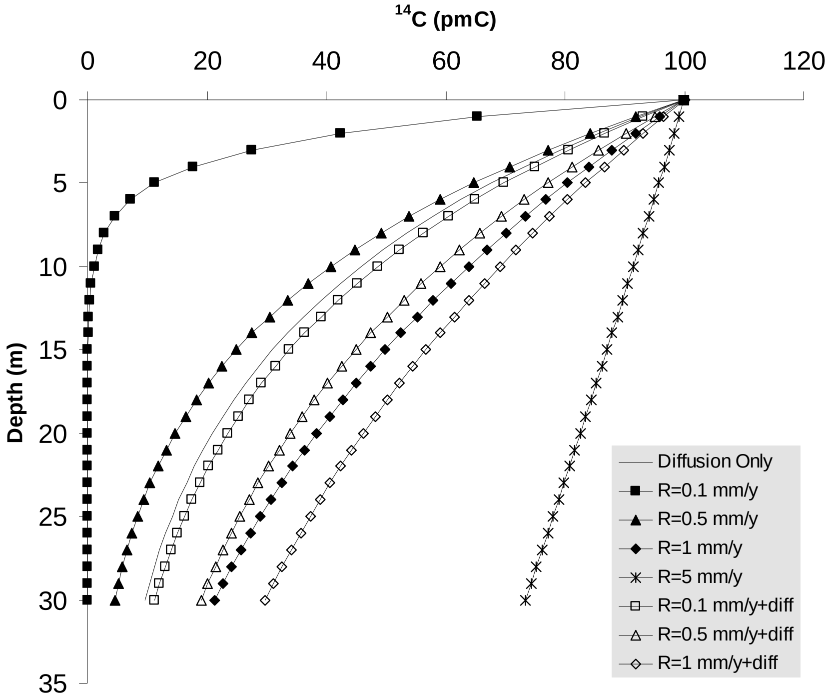

Figure 6.9. Theoretical $^{14}C$ vs depth profiles resulting from various recharge rates as well as the combination of recharge and diffusion from the atmosphere. The profiles were calculated using the steady-state model of Walker and Cook (1991), assuming an aquifer thickness of 90 m (30 m Blanchetown Clay + 60 m Parilla Sand) and an initial $^{14}C$ activity of recharge entering the aquifer of 100 pmC. The model also assumes that the only consumption of $^{14}C$ is via radioactive decay. The profiles show that groundwater in the Parilla Sand aquifer (i.e. at the base of the 30 m thick Blanchetown Clay) may have $^{14}C$ activities ranging from 10 pmC, under conditions of zero recharge and $^{14}C$ input via diffusion only, to 30 pmC, for a recharge rate of 1 mm/y, and with an additional input via diffusion.

In the absence of a groundwater discharge complex at Raak Plain, salinities and $\delta^{2}H$, $\delta^{18}O$, $\delta^{13}C$ and $^{36}Cl$ signatures of groundwater in the Blanchetown Clay and Parilla Sand would be equal to, or mixtures of the two end-members (a) and (b) defined above (Fig. 6.10a). Vertical distributions of $^{14}C$ in the Parilla Sand and Blanchetown

Clay would be consistent with diffusion of atmospheric $CO_2$ through the Blanchetown Clay, under low recharge conditions (Fig. 6.9). However, the current situation is one where discharge of regional and / or locally recharged groundwater occurs via evaporation at the surfaces of playa lakes (Fig. 4.9). The presence of shallow and saline groundwater has reduced the coverage of mallee vegetation, increasing recharge rates (Section 4.2.2). A broad range of groundwater isotopic signatures has developed at Raak Plain as a result (Fig. 6.10b-d). The large-scale trends in the isotopic data from across Raak Plain are the focus of this section and smaller scale processes will be discussed in sections 6.4.2 to 6.4.6.

#### 6.4.1.2 Evaporation and Mixing

The $\delta^2$H and $\delta^{18}$O data for pore waters and groundwaters at each of the lakes at Raak Plain lie on almost identical evaporation / mixing lines, with slopes of approximately 4.5 (Fig. 6.4). This suggests a similar process of evaporation across all of the playas, despite different physical conditions, such as the presence / absence of ponded surface water, presence / absence of a surface salt crust and differences in playa size and depths to water table (Section 1.3.5). An exception is Salt Lake, with a lower slope of 3.2 that is strongly influenced by a single pore water sample in the top 0-2 cm of the playa sediments (Fig. 6.5c). This will be discussed in Section 6.4.3.

As described in Section 6.2.1, the slope of an evaporation line on a $\delta^2$H vs $\delta^{18}$O diagram depends primarily on relative humidity. Theoretical curves for the progressive evaporation of a body of surface water, with a starting signature of Parilla Sand groundwater at bore 26240 ($\delta^2$H = -39.7 ‰, $\delta^{18}$O = -5.1 ‰) suggest that a slope as low as 4.5 can only be achieved with a relative humidity of ≤ 40% (Fig.

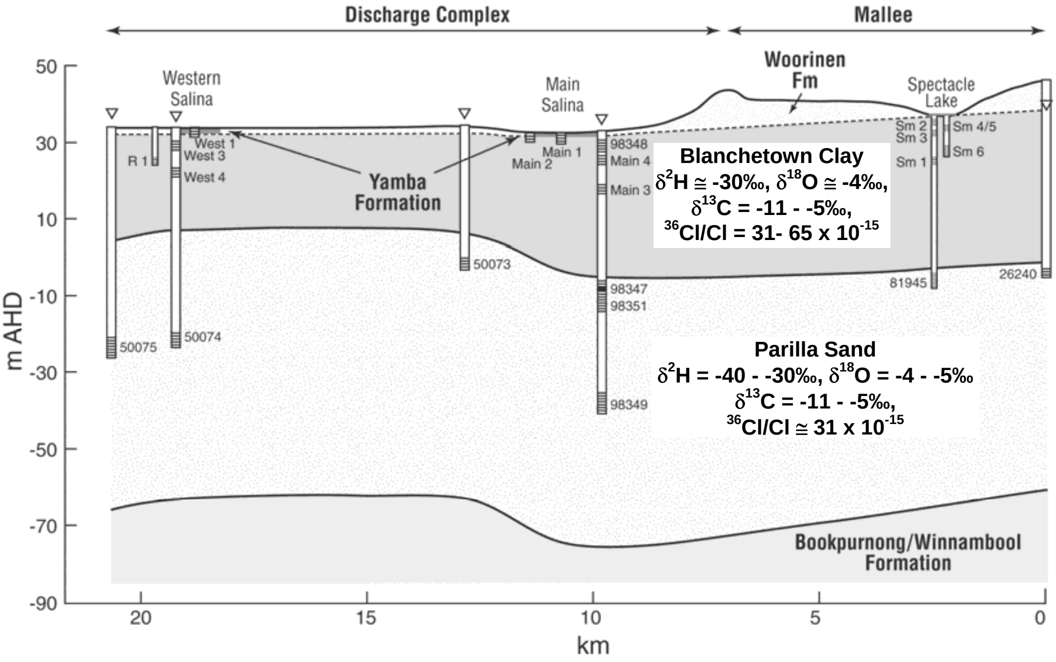

Figure 6.10a. Hypothetical isotopic signatures of groundwaters in the Blanchetown Clay and Parilla Sand aquifer below Raak Plain, in the absence of a groundwater discharge complex. $\delta^2$H, $\delta^{18}$O, $\delta^{13}$C and $^{36}$Cl/Cl would be similar to or mixtures of the regional groundwater or locally recharged groundwater end-members (Table 6.4). $^{14}$C would be influenced by diffusion from the atmosphere, as shown in Figure 6.9.

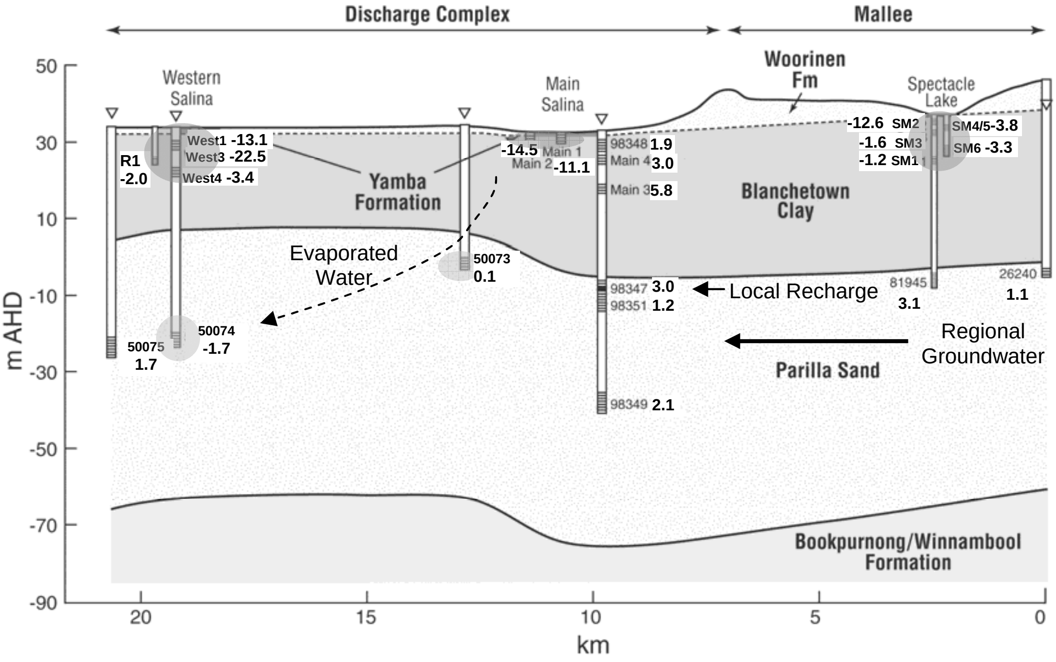

Figure 6.10b. Observed deuterium excess ("d") values in groundwaters at Raak Plain. The two potential sources, regional groundwater inflow (bore 26240) and locally recharged groundwater have deuterium excesses of 1.1 and 2.8 respectively. Shaded areas indicate sample points where negative "d" values suggest evaporated brine to be present.

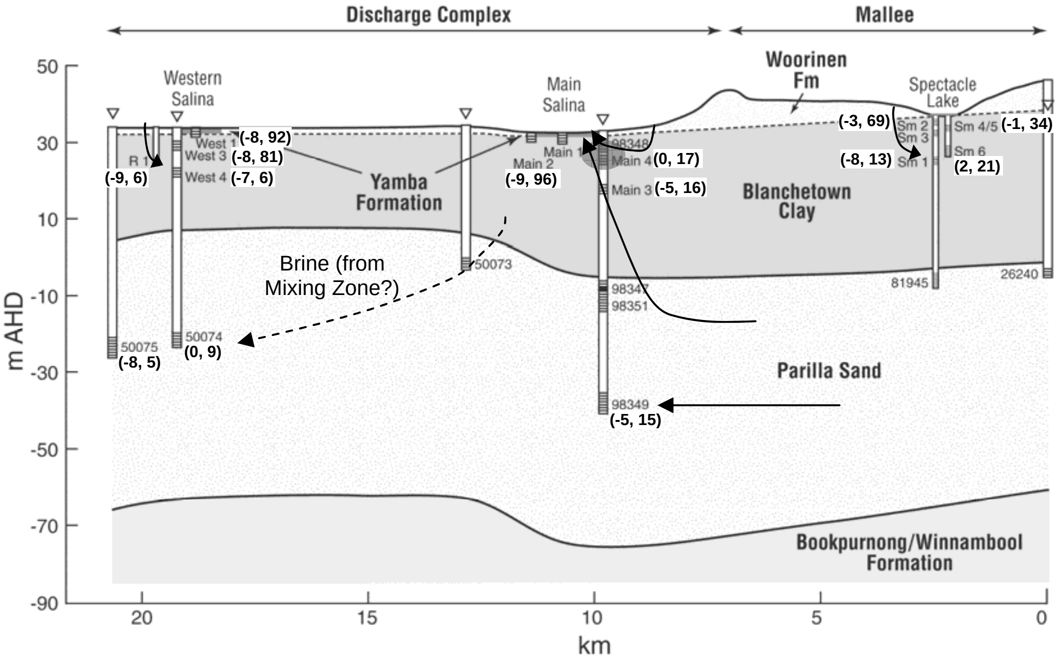

Figure 6.10c. Carbon isotope signatures of groundwaters at Raak Plain ($\delta^{13}C$, $^{14}C$). $^{14}C$ signatures are predominantly influenced by diffusion from the atmosphere. The identical signatures of the deep piezometer Main3 at the edge of the Main Salina and the underlying Parilla Sand groundwater suggest a regional groundwater source for Main3. More positive $\delta^{13}C$ values than those of the regional groundwater inflow and locally recharged groundwater sources ($\delta^{13}C$ = -5‰ and -11‰ respectively) are achieved by carbonate mineral dissolution, particularly incongruent dissolution, in mixing zones. This occurs at the up-gradient margin of the Main Salina (shaded region), where mixing between regional groundwater and locally recharged groundwater occurs. A similarly high $\delta^{13}C$ value observed in the Parilla Sand groundwater below Western Salina (bore 50074), suggests either leakage of brine from these mixing zones, or in-situ mineral dissolution due to mixing with brine at that location.

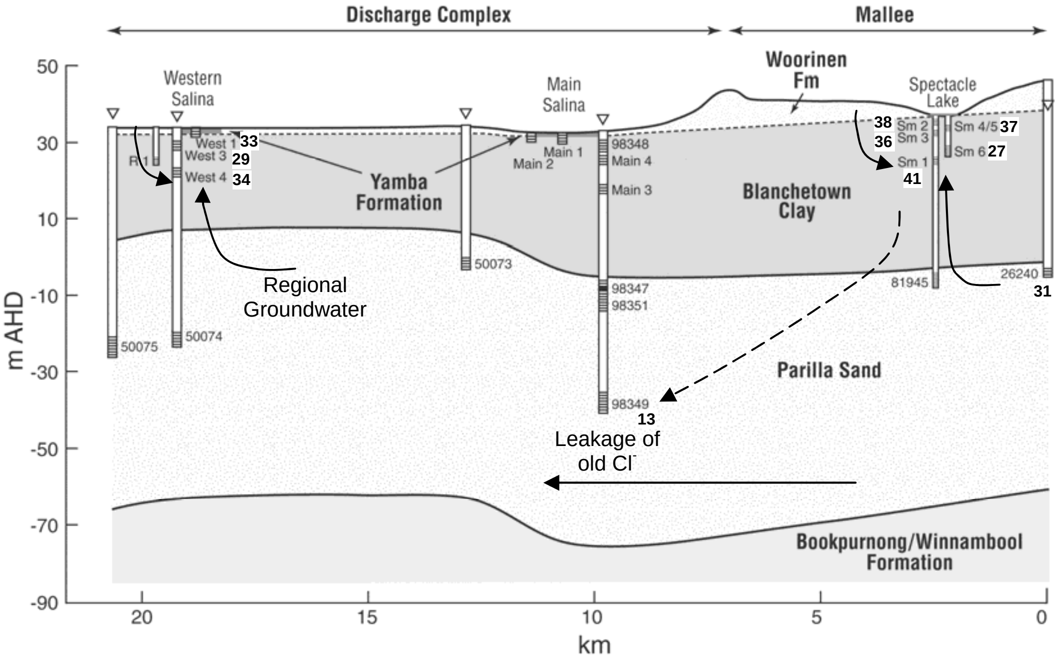

Figure 6.10d. $^{36}Cl/Cl$ ratios of groundwater at Raak Plain and the processes inferred from the interpretation of the $^{36}Cl$ data.

6.1). Mean annual humidities measured at Ouyen, 40 km south of Raak Plain, are 65% at 9 am and 39% at 3 pm, with an overall mean likely to be 55 ± 5%. Dividing this by 0.76, the apparent saturated relative humidity of brine at 300 g/L TDS, results in a relative humidity of 65% to 79% prevailing at Raak Plain. Hence, the linear trend in the $\delta^2$H and $\delta^{18}$O data is not the result of the evaporation of surface water ponded in the lakes. Allison (1982) showed that slopes as low as 2 can occur due to evaporation of water through a layer of dry soil, and Allison and Barnes (1985) observed a decrease in slope from 4.5 to 2 with increasing depth to water table at Lake Frome in South Australia. The fact that the brines at Raak Plain exhibit this trend is not surprising as the water tables in the playas can be up to tens of centimetres below the top of the soil profile, particularly in summer when evaporation is greatest and surface water is only present in winter when evaporation is at a minimum (Section 4.2.3). Hence, the brines and groundwaters at Raak Plain have been formed predominantly by evaporation of groundwater from a shallow water table rather than of the ponded surface water that occasionally accumulates in the playas.

The spread of data between the low $\delta^2$H and $\delta^{18}$O end-members and the most enriched brines at the playa surfaces (Fig. 6.5(a-d)) may be due to different degrees of evaporation from a single source. However, as discussed in Section 6.3.1.2, it may also be due to a combination of evaporation to the high $\delta^2$H and $\delta^{18}$O signatures at the evaporation front and re-mixing with one of the low $\delta^2$H and $\delta^{18}$O end-members. Because of the similarity of the $\delta^2$H and $\delta^{18}$O signatures of the regional groundwater inflow and locally recharged groundwater end-members (Fig. 6.4), such processes cannot be distinguished between based on $\delta^2$H and $\delta^{18}$O data alone.

Many of the brine samples from Raak Plain (SM6, West4, West3 and West1a) have $^{36}$Cl/Cl ratios very similar (within the limits of analytical uncertainty) to that of the regional groundwater end-member ($^{36}$Cl/Cl = 30 x $10^{-15}$) (Fig. 6.7). As evapo-concentration does not change the $^{36}$Cl/Cl ratio of a water sample, these brines may have formed simply by evapo-concentration of this source, rather than the local recharge end-member ($^{36}$Cl/Cl = 65 x $10^{-15}$). Other brine samples (SM1, SM2, SM3 and SM4) have $^{36}$Cl/Cl ratios slightly above that of the regional groundwater end-member, suggesting mixing with local recharge. If these higher $^{36}$Cl/Cl ratios were due to evapo-concentration of an entirely local recharge source, a $Cl^-$ residence time of at least 125 k yr is estimated from equation 7.8 (Fig. 6.7). In reality, however, the $^{36}$Cl signatures of these samples could be due to any combination of evapo-concentration, mixing and radioactive decay of the two potential sources. A discussion of how this can be better constrained by plotting [$^{36}$Cl] versus [Cl] is included in Section 6.4.2.

The carbon isotope signatures of the brines at Raak Plain do not specifically reflect evapo-concentration, with the exception that the brines that have been evaporated at the playa surfaces have also been re-equilibrated with atmospheric $CO_2$. Linear trends in the carbon isotope data may reflect mixing processes and these will be discussed in more detail in Sections 6.4.2 to 6.4.6.

#### 6.4.1.3 Carbonate Mineral Reactions

Carbonate mineral-solution reactions in or around the playa lakes at Raak Plain may explain the scatter in alkalinity (as $HCO_3^-$) with increasing concentration factor ([$Br^-$]), compared with the other ions in solution (Figs. 3.5-3.10). A number of groundwater samples collected during this study were at or near saturation with respect to calcite and dolomite, according to saturation index calculations performed with PHRQPITZ (Table 3.2). Precipitation and/or dissolution of the low solubility carbonate minerals (log K = -8.3 to -17) is likely, in principle, in an evaporitic environment, where large changes in ionic strength occur (due to evapo-concentration and mixing), and where groundwaters are brought into contact with the atmosphere (discharge), potentially causing degassing of $CO_2$.

Carbonate mineral precipitation and dissolution within the discharge complex have apparently caused a larger range of $\delta^{13}C$ signatures at Raak Plain than what would be expected in a non-discharge environment (Section 6.4.1.1; Fig. 6.10a). Brine / groundwater samples from various locations across Raak Plain can be grouped as shallow (< 3 m depth), with high $^{14}C$ activities (> 60 pmC), and deep (> 6 m depth), with low $^{14}C$ activities (< 40 pmC) (Fig. 6.8). There is a large range in $\delta^{13}C$ values in both of these groups, causing a two-armed distribution in Fig. 6.8. The shallow groundwaters and brines lie at the high $^{14}C$, low $\delta^{13}C$ end of the first arm, with $^{14}C$ decreasing as $\delta^{13}C$ tends towards zero. The second arm consists of the deeper groundwater samples, with a small range of $^{14}C$ activities (< 20 pmC), but a wide range of $\delta^{13}C$ values (-9.1 ‰ to 0 ‰). The two arms of the graph meet approximately at the composition of sample Main4 ($\delta^{13}C$ = 0 ‰, $^{14}C$ = 20 pmC), located 6.2 m below the water table at the edge of the Main Salina (see Fig. 2.1 for location).

In the absence of methanogenesis, $\delta^{13}C$ values as high as 0 ‰ (Main4 and bore 50074) and 1.7 ‰ (SM6) can only be achieved by the incongruent dissolution of Mg-carbonate minerals via the reaction (Wigley et al., 1978, 1979; Dogramaci and Herczeg, 2002):

$$Ca_xMg_{(1-x)}CO_{3(s)} \rightarrow xCaCO_{3(s)} + (1-x)Mg^{2+} + (1-x)CO_3^{2-} \quad (6.9)$$

Simple dissolution of calcite (Eq. 6.3) causes an increase in $\delta^{13}C$ and a reduction in the $^{14}C$ activity of groundwater DIC, but is limited by the fact that, of the two equivalents of $HCO_3^-$ produced, half of the carbon is derived from $CO_2$ dissolved in the water. Therefore, assuming a starting composition of recent local recharge (R3, $^{14}C > 100$ pmC, $\delta^{13}C = -10.7$ ‰), the $^{14}C$ activity of the DIC can be reduced, at most, to 50 pmC by this process, and $\delta^{13}C$ values near 0 ‰ could not be achieved. High-Mg-calcites, are slightly more soluble than low-Mg-calcites (Plummer and Mackenzie, 1974; Morse and Mackenzie, 1990), and incongruent dissolution (Eq. 6.9) is a continuous balance between the dissolution of the former, and re-precipitation of the latter. The continuous dissolution process causes the $\delta^{13}C$ signature of the DIC to approach that of the solid that is being dissolved (Smith et al., 1975), aided by a 1 ‰ fractionation during the re-precipitation of carbonate. The mineral that is re-precipitated is in isotopic equilibrium with the solution DIC. The effect of incongruent dissolution on the $\delta^{13}C$ of DIC has been discussed in detail by Smith et al. (1975), Wigley and Plummer (1976) and Wigley et al. (1978, 1979), and a correction of $^{14}C$ activities for this process is given by Wigley et al. (1978, 1979). High $\delta^{13}C$ values of groundwater DIC in the Murray Group aquifer system of the Murray Basin (Fig. 1.7), were found by Dogramaci and Herczeg (2002) to be due to incongruent dissolution of the carbonate aquifer matrix, based on $^{87}Sr/^{86}Sr$, Mg/Ca and Sr/Ca data. The linear trend of increasing $\delta^{13}C$ and decreasing $^{14}C$ between R3 and Main4 may represent evolution of groundwater in the near-surface groundwater system, by dissolving carbonate minerals either congruently (Eq. 6.3) or incongruently (Eq. 6.9).

### 6.4.2 Shallow Brine Formation

The shallow brines at Raak Plain are groundwaters with salinities > 100 g/kg, and were encountered in the top 3 m of the sediment profiles below the playa lakes and around their margins. They plot at the high $\delta^2$H and $\delta^{18}$O ends of the evaporation-mixing lines, with regional Parilla Sand groundwater and local groundwater below the dunes and plains adjacent the playas (the two potential sources) plotting as the low $\delta^2$H and $\delta^{18}$O end-members (Fig. 6.5 (a-d)). $\delta^2$H and $\delta^{18}$O values of the brines generally decrease away from the playa surface, probably due to back-diffusion between the highest $\delta^2$H and $\delta^{18}$O brines at the evaporation front, and the low $\delta^2$H and $\delta^{18}$O source. As described in Section 6.3.1.1, the origins of the brines as locally recharged or regional groundwater cannot be determined based on $\delta^2$H and $\delta^{18}$O alone.

The sources of the shallow brines also cannot be easily determined based on their carbon isotope signatures. They appear to be strongly affected by exchange with unsaturated zone $CO_2$, plotting close to the local recharge end-member (R3) on a $^{14}$C vs $\delta^{13}$C diagram (Fig. 6.8). The brines therefore may have originated as either modern, local recharge (similar to R3), or regional groundwater that has had a long residence time in the groundwater system, but has since re-equilibrated with atmospheric carbon near the surfaces of the lakes. By this process of re-equilibration, the DIC regains a modern $^{14}$C signature and a $\delta^{13}$C similar to that of unsaturated zone $CO_2$, and carbon isotopic evidence of its previous history in the saturated zone is erased.

The $^{36}$Cl data provides a better indication of the sources of the shallow brines. Those at Western Salina, (West1a and West3) have $^{36}$Cl/Cl ratios similar to that of the regional Parilla Sand groundwater ($^{36}$Cl/Cl = 31 x $10^{-15}$) (Fig. 6.7), and have therefore probably achieved their high salinities by simple evapo-concentration of this single source, with only a small or negligible input from locally recharged groundwater (Fig. 6.11a, Fig. 6.12a). This appears to be in contrast to the results of the numerical modelling (Chapter 5), which suggested that locally recharged groundwater becomes more important in the water balances of the playa lakes towards the western margin of the discharge complex. However, as discussed in Section 4.3.2.1, although this may be true for the water budget, the much greater TDS concentration of the regional groundwater means that a small volume of regional groundwater can still dominate the salt balance of the playa lakes, of which $^{36}$Cl/Cl is an indicator.

The shallow brine at Spectacle Lake (SM2; Fig. 6.13) has a higher $^{36}$Cl/Cl ratio (38 x $10^{-15}$) than both the shallow brines at Western Salina (West1a, $^{36}$Cl/Cl = 33 x $10^{-15}$; West3, $^{36}$Cl/Cl = 29 x $10^{-15}$) (Fig. 6.7). This signature is probably due to a mixed local recharge / regional groundwater source (Fig. 6.12b), which is consistent with the conclusions from Chapters 4 and 5. These suggested that locally recharged groundwater, following a shallow (and short time-scale) flow path into the lakes forms a large component of water balances of the playas at the up-gradient margins of the discharge complex. This is a phenomenon that would have more effect at the margins of the playas (i.e. at SM2) than at the centre. However, it should be noted that the $^{36}$Cl/Cl ratio is also very similar to that of a surface halite crust obtained from a salt lake in the same region of the Murray Basin as Raak Plain ($^{36}$Cl/Cl $\cong$ 40 x $10^{-15}$, Jake Turin, Los Alamos National Laboratory, pers. comm., 2002). Higher ratios in

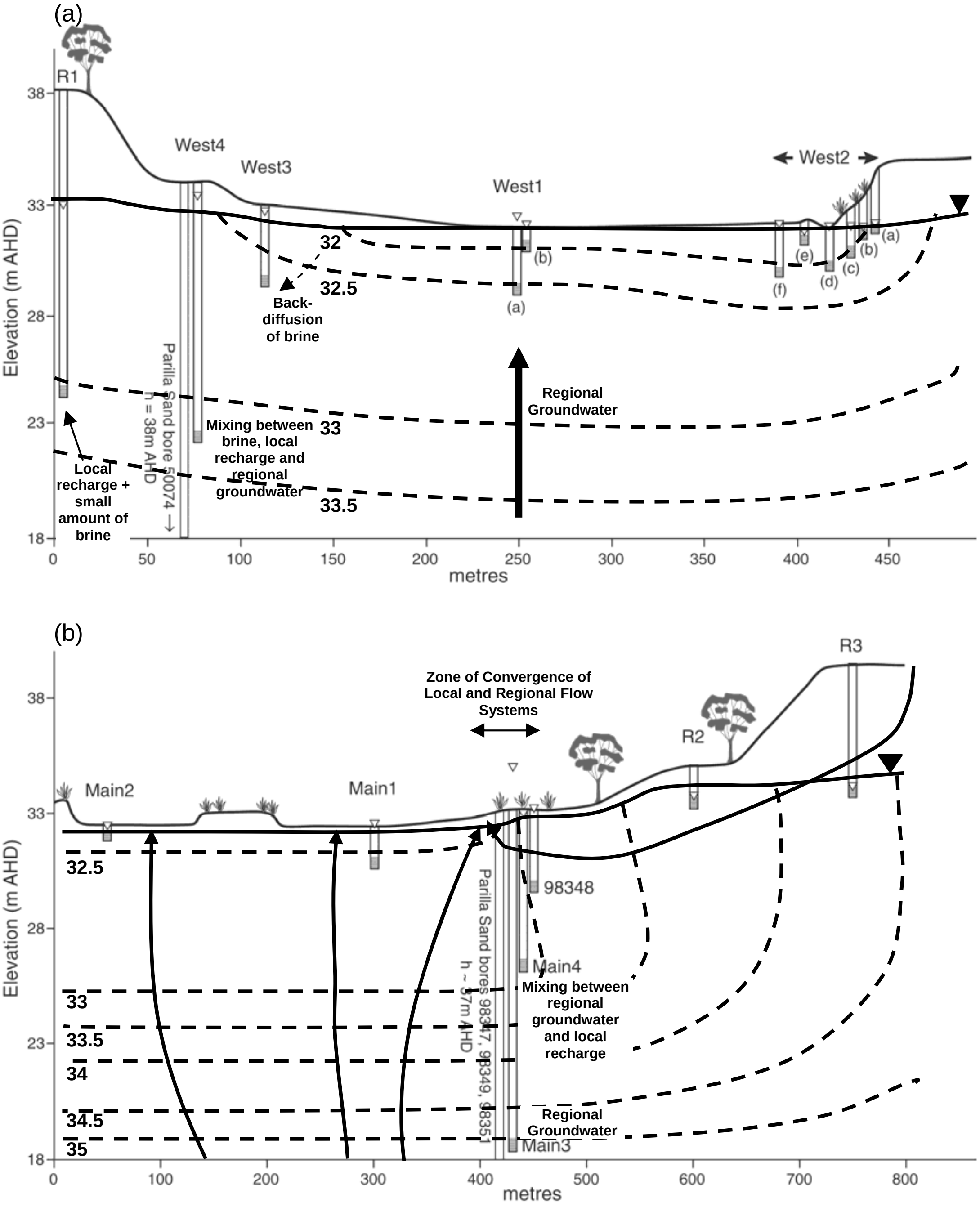

Figure 6.11. Cross-sectional conceptual models of (a) Western Salina and (b) the Main Salina, showing contours of equal hydraulic head and solute sources and mixing processes inferred from hydraulic and isotope data.

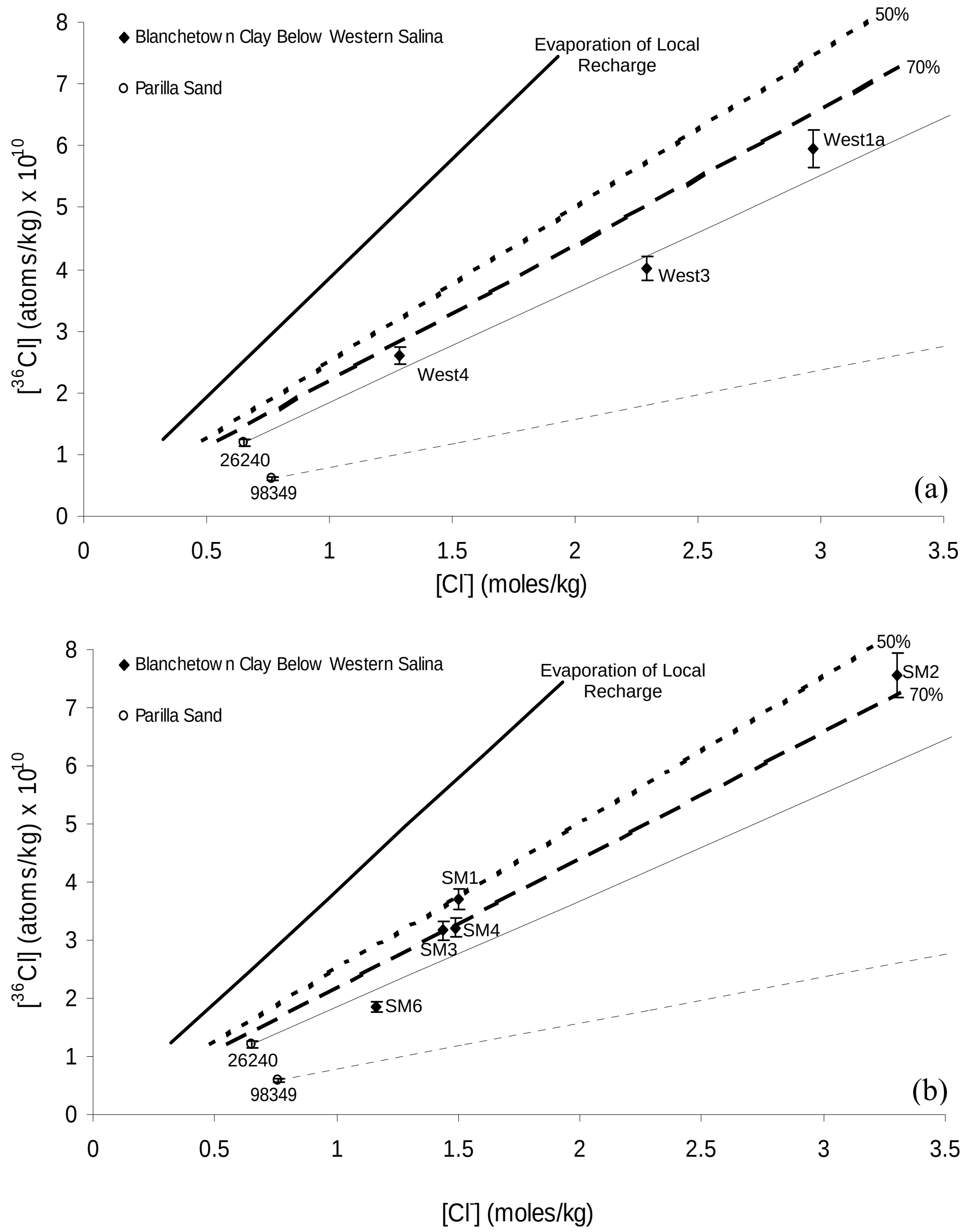

Figure 6.12. Graphs of $^{36}$Cl vs chloride concentrations for groundwaters in the Blanchetown Clay below (a) Western Salina and (b) Spectacle Lake. Two regional Parilla Sand groundwater samples from below Raak Plain (bores 26240 and 98349) are also shown for reference, along with evaporation lines for these (thin solid and dashed lines), locally recharged groundwater and mixtures of 50:50 and 70:30 regional groundwater : local recharge (solid broken lines labelled according to % regional groundwater). Based on the $^{36}$Cl data, brines at Western Salina have a predominantly regional groundwater source, with only small amounts of mixing with locally recharged groundwater. However, the brines at Spectacle Lake show more influence from locally recharged groundwater, particularly the deep (16-18 m) lake edge brine, SM1, which is comprised of 50% of each source. Low $^{36}$Cl regional groundwater found in the middle of the Parilla Sand aquifer below the Main Salina (bore 98349) is apparently not a source for the down-gradient shallow brines, indicating that solute recycling does not occur through the discharge complex.

surface halite crusts can be achieved via in-situ production of $^{36}$Cl according to the reaction $^{35}$Cl(n,$\gamma$) (See Appendix J), and dissolution of such a salt crust may therefore also be responsible for the high ratio in the near-surface brine.

The effects of back-diffusion and/or carbonate mineral dissolution on the shallow brines can be seen in a trend of decreasing $^{14}$C and increasing $\delta^{13}$C with depth below the water table (Fig. 6.8). A slightly lower $^{14}$C activity and higher $\delta^{13}$C at the edge of Western Salina (West3) than at the lake centre (West1a) can be explained by back-diffusion of brine into the regional groundwater source (e.g. bore 98349 or bore 50074; Fig. 7.8, Fig. 6.11a). The $^{36}$Cl signature of West3 is also consistent with back-diffusion of brine (West1a) with regional groundwater (bore 98349), supporting this hypothesis (Fig. 6.12a). These processes appear to occur to an even greater degree at Spectacle Lake (the harvested lake), where the shallow brine at the edge of Pond 3 (SM2, 1.9 m deep; Fig. 6.13) has a higher $\delta^{13}$C value and a lower $^{14}$C activity than the shallow brine samples at Western Salina, despite a shallower depth below the water table (Fig. 6.8). This may be due to a greater degree of mixing with groundwaters with low $^{14}$C and high $\delta^{13}$C values, or a greater influence of carbonate mineral dissolution as a result of salt harvesting and a change in the hydraulic balance of the lake. This will be discussed in more detail in Chapter 7.

Infiltration of rainfall that falls directly onto the surfaces of the playa lakes at Raak Plain has been considered in this study to have a negligible effect on the shallow brines. This assumption can be checked by comparing shallow $\delta^{2}$H and $\delta^{18}$O vs depth sediment pore water profiles collected at Western Salina in July 2001 (winter) and January, 1998 (summer) (Howes, 1998; Fig. 6.14). The shapes of the summer (Jan-98) profiles at the centre of Western Salina were characteristic of evaporation

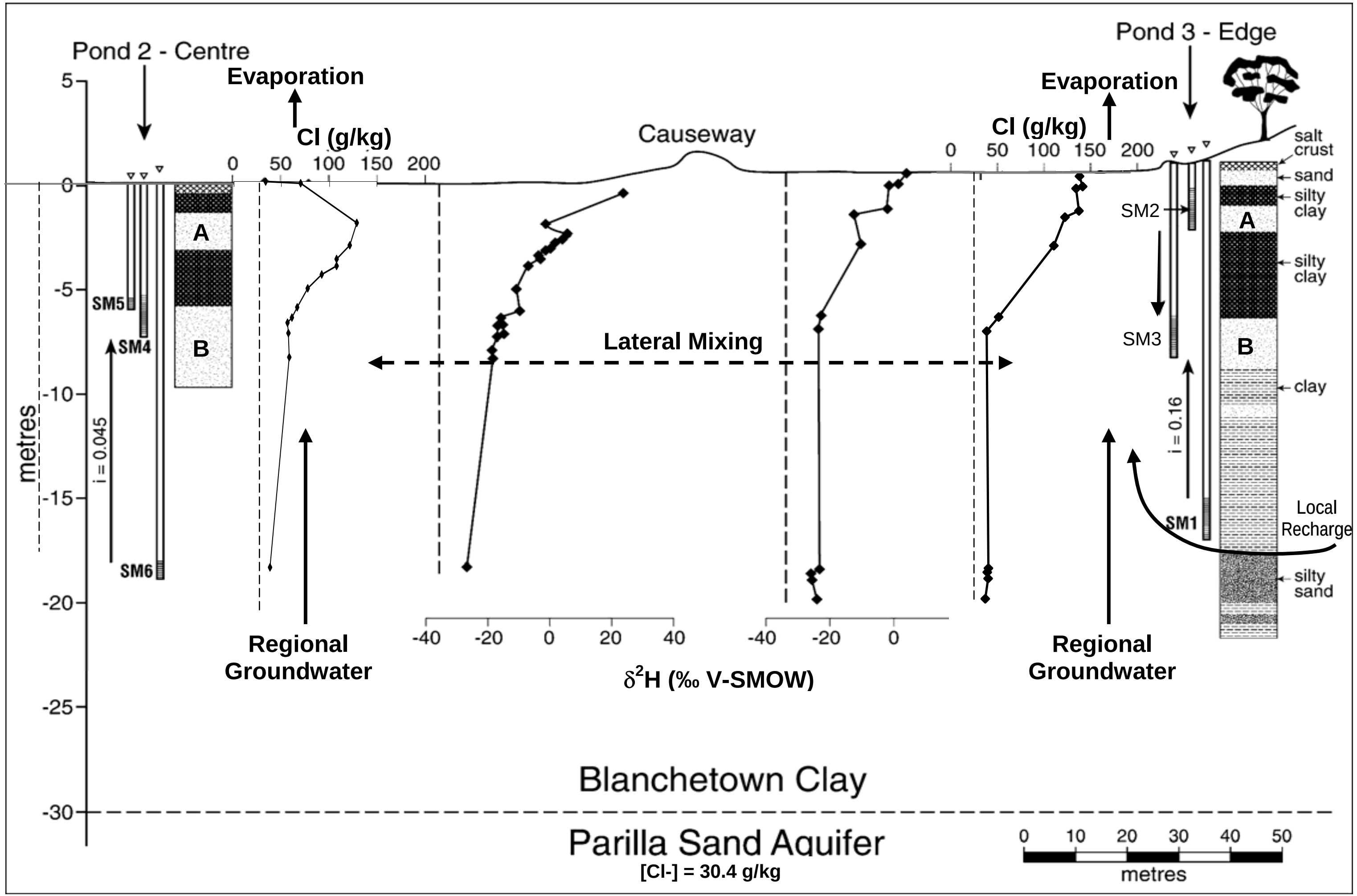

Figure 6.13. Cross-sectional conceptual model through Spectacle Lake, showing [Cl$^-$] and δ$^2$H vs depth profiles. The isotope data suggest a predominantly regional groundwater source, although mixing with up to 50% local recharge occurs at the lake edge. Diffusional back-mixing of the hypersaline near-surface brines with the source waters also occurs.

(Zimmerman et al., 1967), with $\delta^2$H and $\delta^{18}$O values above 20 cm depth increasing towards the surface, to maxima of 32.1 ‰ and 9.5 ‰ respectively (Fig. 6.14a). The values below 20 cm were fairly constant at 7.6 ‰ and 2.6 ‰ respectively, to a maximum sampling depth of 2.7 m. In contrast, the winter (Jul-01) profiles show decreases in $\delta^2$H and $\delta^{18}$O towards the surface, from 5.5‰ to –4.8‰ and 2.4‰ to –3.4‰ respectively. This difference in shape of the winter (Jul-01) profile above 20 cm is probably caused by infiltrating rainfall in the top 20 cm. This can be seen more clearly on a $\delta^2$H vs $\delta^{18}$O diagram (Fig. 6.14b), where the pore water and the regional (Parilla Sand) groundwater data lie on the same evaporation line. The summer (Jan-98) data is at the high $\delta^2$H vs $\delta^{18}$O end of this trend, with values increasing towards the surface and the winter (Jul-01) data lie below this, with values decreasing towards the surface. The two data sets coincide at approximately $\delta^{18}$O = 2 ‰ and $\delta^2$H = 7 ‰, where pore waters from below 20 cm cluster. The winter (Jul-01) profile above 6 cm tends towards the Meteoric Water Line, and more specifically the weighted mean isotopic composition of rainfall samples collected at Raak Plain over a one year period. This corresponds to an increase in water contents in the profile and suggests infiltration of rainwater to a maximum depth of 20 cm during the wetter winter season. Although the effect on solutes was not investigated, it can be assumed that a similar dilution effect occurs. At the onset of dry conditions, this water re-evaporates, restoring the $\delta^2$H and $\delta^{18}$O vs depth profiles to their original shape.

$\delta^2$H and $\delta^{18}$O contents in the profiles at Western Salina remain constant below 20 cm depth despite the infiltration of rainwater above this (Fig. 6.14a). This is probably due to the change in lithology observed at approximately 20 cm depth, from the

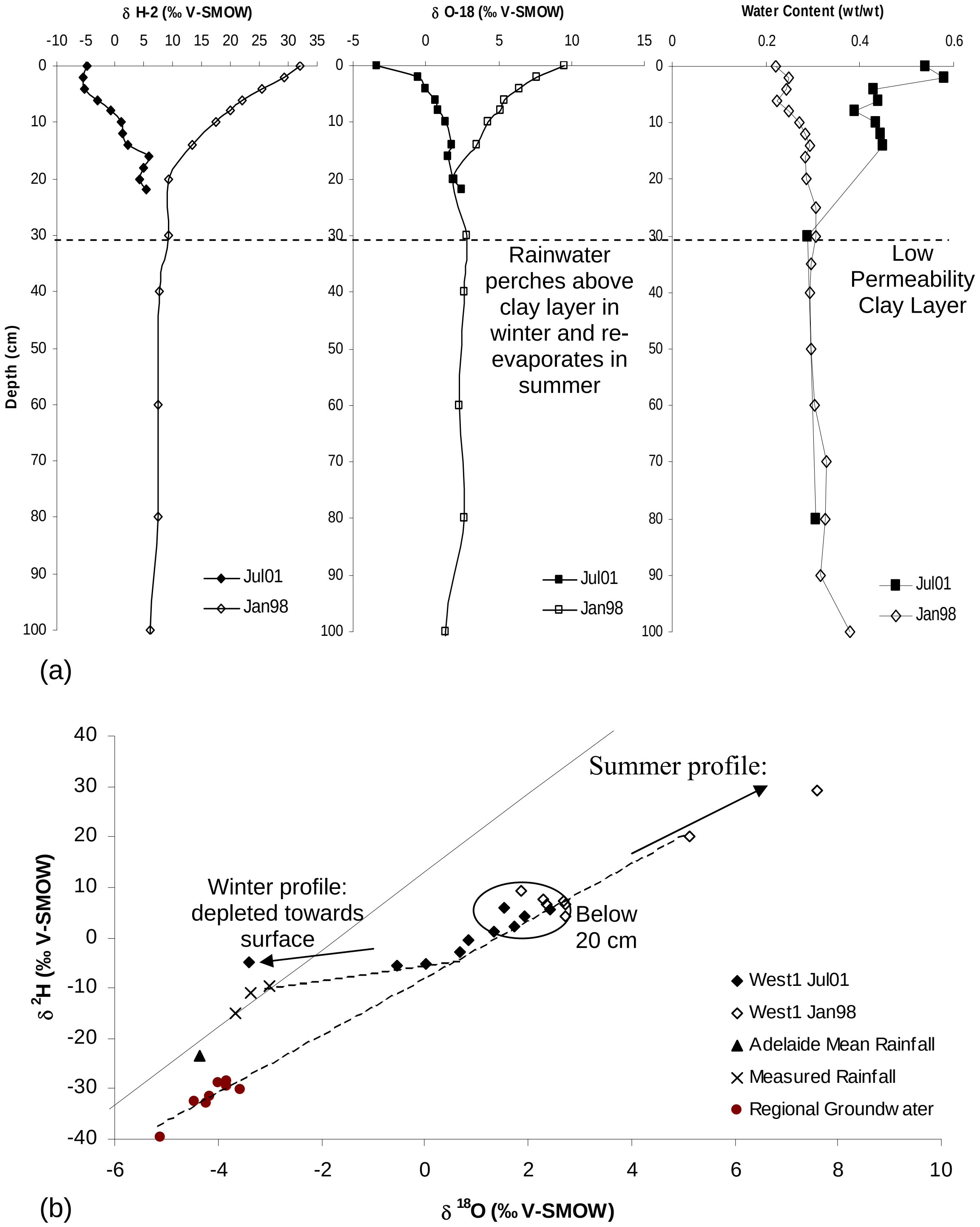

Figure 6.14. Summer (January 1998; Howes, 1998) and winter (July 2001) shallow pore water $\delta^2$H and $\delta^{18}$O and water content data from the centre of Western Salina. (a) $^2$H and $^{18}$O contents of the pore waters increase towards the surface in summer due to evaporation, but decrease towards the surface in winter due to infiltration of rainfall. The infiltrated water perches on top of a 20 cm deep low permeability clay layer during winter to be re-evaporated in summer, and does not affect $\delta^2$H and $\delta^{18}$O signatures below this depth. (b) On a $\delta^2$H vs $\delta^{18}$O plot, it can be seen that the summer (Jan98) data plot on an evaporation line for regional Parilla Sand groundwater whilst the winter data tend towards the compositions of rainfall samples collected at Raak Plain. This supports the theory that the brines are formed by the evapo-concentration of a predominantly regional groundwater source, and that infiltrating rainfall flushes the top approximately 20 cm of the profile on a seasonal basis.

sandy playa sediments, to a stiff, dry-textured sandy clay (See Appendix B). The characteristics of this clay (the top of the Blanchetown Clay) are such that, if a hole is dug into it, it would initially appear dry but water would seep from it after approximately half an hour. It is likely that the low hydraulic conductivity clay causes perching of infiltrating rain water, which evaporates before it can infiltrate to greater depths. Pore water below this is therefore relatively unaffected by seasonal wetting and drying cycles.

### 6.4.3 Processes Affecting Brines in the "Type D" (Surface-Water) Lakes

Salt Lake is the only natural lake included in this study that contains standing surface water for the majority of the year (Section 1.3.5.3; see Fig. 1.6 for location). This water only evaporates completely in some parts of the lake during the height of summer (January-February). It has $\delta^2$H and $\delta^{18}$O values (sampled in April-01) that are much lower than those of the shallow subsurface brines, but a TDS often in excess of 200 g/kg (Table 6.3). This suggests that the water is predominantly rainfall that falls on the lake, or drainage from the surrounding dunes that has evaporated slightly and partially dissolved the salt crust at the surface of the lake, leading to the high TDS. The water has a Cl/Br mass ratio of 2 500, characteristic of halite dissolution and may also have gained some solutes not present in the salt crust via diffusion from the subsurface brine.

The groundwater brine between 20 cm and 50 cm depth below Salt Lake (piezometer Salt1b) appears to have been influenced by downward advection of surface water. Although it has a higher TDS than that at 2.5 m depth (piezometer Salt1a) (Table 6.3), it is less enriched in $^2$H and $^{18}$O and has a higher d value, suggesting mixing with the surface water. A similar low conductivity dry textured clay layer to that observed at Western Salina occurring at 50 cm depth probably causes perching of infiltrating rainwater (that has accumulated solutes by partially dissolving the salt crust) and prevents it from interacting with the underlying brines.

A decrease in slope of the $\delta^2$H vs $\delta^{18}$O graph for Salt Lake groundwater and pore water samples in the top 2 cm of the profile (Fig. 6.5c, see Section 6.3.1.2) is probably an effect of the surface salt crust at this site. Although both $\delta^2$H and $\delta^{18}$O are expressed in this study as activities, having been corrected for fractionation by ion hydration (see Section 2.2.4.3), fractionation during incorporation of crystallization water into a precipitating surface salt crust has not been accounted for. The surface salt crust at Salt Lake is composed predominantly of halite (NaCl), but with trace amounts of gypsum ($CaSO_4 \cdot 2H_2O$) and bischofite ($MgCl_2 \cdot 6H_2O$) (Section 3.4.6). Crystallization of gypsum causes depletion in $\delta^{18}$O of the residual water by 3.5 ‰ and enrichment in $\delta^2$H by 14.9 ‰ (Gonfiantini and Fontes, 1963). Hence, gypsum precipitation is not the cause of the flattening of the graph in Figure 6.5c, although dissolution of some previously formed gypsum may be responsible.

The only other available empirical data for fractionation between the water of crystallization of an evaporite mineral and free water is for mirabilite ($Na_2SO_4 \cdot 10H_2O$) (Stewart, 1974), which causes depletion in the residual water body by 2 ‰ for $\delta^{18}$O and 19 ‰ for $\delta^2$H. The brine at Salt Lake is near saturation with respect to bloedite ($Na_2Mg(SO_4)_2 \cdot 5H_2O$), epsomite ($MgSO_4 \cdot 7H_2O$) and mirabilite, as is the case at Spectacle Lake, where a similar lowering of slope in $\delta^2$H vs $\delta^{18}$O is observed at the top of the profile, and a surface salt crust is also present (Table 1.1). Although data is not available for fractionation by crystallization of all of these hydrated minerals, it is possible that precipitation of one or a combination of them may be responsible for the changes in $\delta^{2}$H vs $\delta^{18}$O ratios.

### 6.4.4 Mixing With Locally Recharged Groundwater at the Edges of the Playas

Although $^{36}$Cl signatures suggest that regional groundwater is the dominant source of salt to the brines at Raak Plain, particularly at the centre of Western Salina (West1a), some influence of mixing with local recharge was also implied (Section 6.4.2). The large spread in $\delta^{13}$C values and the $^{36}$Cl signatures of the deeper groundwaters in the Blanchetown Clay at the edges of the playas, and the regional Parilla Sand groundwater, can provide insight into mixing processes occurring at the margins of the playas.

Groundwaters above 7.8 m depth at the edge of Spectacle Lake (SM2 and SM3; Fig. 6.13) have $^{36}$Cl signatures consistent with evaporation of a 70% regional groundwater, 30% locally recharged groundwater source (Fig. 6.12b). The evaporation line can also be considered a mixing line between the shallow saline brine (SM2) and the mixed groundwater source, with back-mixing along this line resulting in the signature at SM3 (Fig. 6.13). Groundwater below this (SM1; Fig. 6.13) has a different signature, more consistent with mixing between the brine (SM2) and locally recharged groundwater (Fig. 6.12b). The carbon isotope signature of SM1 supports this, with a more negative $\delta^{13}$C value than Parilla Sand groundwater (bore 98349), and any of the other samples from the Blanchetown Clay at Spectacle Lake, but closer to that of the local recharge end-member, suggesting that this is the dominant source (Figs. 6.8 and 6.13). Oxidation of organic matter is the only process that can move groundwater DIC towards a more negative $\delta^{13}$C, and very little organic matter has been observed in the Blanchetown Clay.

Based on this interpretation, a residence time for SM1 can be estimated for the local recharge source using the method of Walker and Cook (1991), and correcting for mixing with SM2. The latter results in an $A_0$ of 86 pmC, which becomes input for the $^{14}C$ diffusion model (Walker and Cook, 1991). Assuming a recharge rate below the mallee vegetated area around Spectacle Lake of between 0.1 mm/y and 0.5 mm/y, plus diffusion, a new $A_0$ of 25.2 to 34.6 pmC is derived (Fig. 6.15), which results in a calculated residence time of 5.6 k yr to 8.4 k yr for SM1 (Eq. 6.5). This is consistent with the shallow circulation and comparatively short residence times (<10 k yrs) of local recharge near Spectacle Lake predicted by the hydraulic modelling (Figure 5.2).

In contrast, groundwaters below the eastern margin of the Main Salina, even at a depth of 2 m, are apparently un-altered by mixing with the evaporated brines. They have similar $\delta^2H$ and $\delta^{18}O$ compositions to the Parilla Sand groundwater and locally recharged groundwater, and high deuterium excesses (between 1.9 and 5.8), similar to that of the Parilla Sand groundwater in the top of the aquifer, or local recharge (Figs. 6.5b and 6.10b). The $^{14}C$ and $\delta^{13}C$ signatures of groundwater 15.5 m below the water table (Main3; Fig. 6.11b) are also identical to those in the Parilla Sand aquifer below (bore 98349), suggesting an entirely regional groundwater source at this location (Fig. 6.10c). However, groundwater 6.2 m below the water table (Main4) has higher $\delta^{13}C$ and $^{14}C$ values than Main3 (0.0 ‰ and 17.4 pmC respectively; Fig. 6.8). In the absence of methanogenesis, such a high $\delta^{13}C$ value can only occur by incongruent carbonate mineral dissolution. If Main4 has evolved by incongruent dissolution, ultimately from a local recharge composition (R3, Fig. 6.8), this sample appears to be modern (Wigley et al., 1978, 1979). However, some $^{14}C$

has probably been added by diffusion from the atmosphere, meaning that this is an underestimate of residence time (Walker and Cook, 1991).

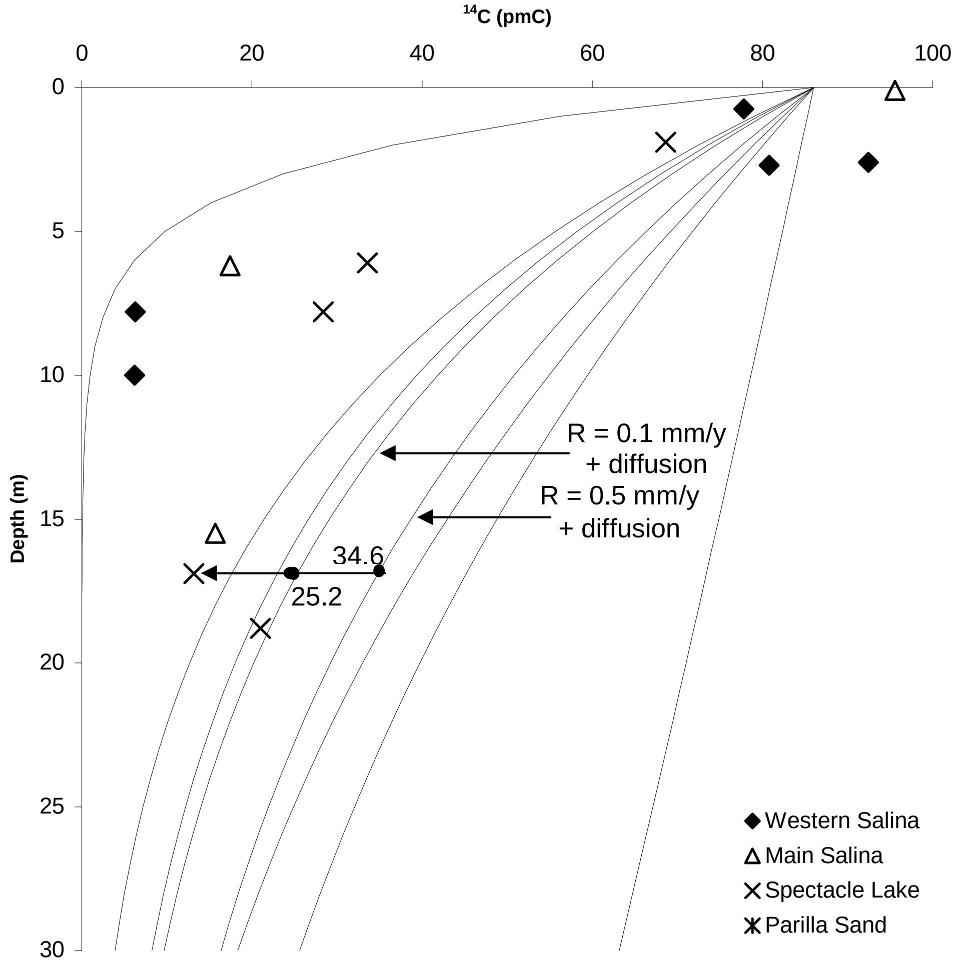

Figure 6.15. Illustration of the estimation of groundwater residence time for sample SM1, located approximately 17 m below ground at the edge of Pond 3, Spectacle Lake. The calculation is made, assuming mixing between a locally recharged groundwater source and the shallow brine at this site (SM2), with a resulting $A_0$ of 86 pmC. The curves shown are theoretical $^{14}C$ vs depth profiles through a 60 m thick aquifer, under the influence of various recharge rates and/or diffusion, and with an $A_0$ of 86 pmC (calculated using the method of Walker and Cook, 1991). The plotted points are $^{14}C$ activities of groundwater samples collected from Raak Plain, including SM1. For recharge rates between 0.1 and 0.5 mm/y around the margins of Spectacle Lake, $^{14}C$ activities between 25.2 and 34.6 pmC are estimated at the depth of SM1. $^{14}C$ decay to the activity of SM1 (13 pmC) results in an estimated residence time of 5.6 to 8.4 k yrs.

The reason for the positive $\delta^{13}C$ value at Main4 can be understood by looking at the conceptual hydraulic model for the Main Salina (Fig. 6.11b). Bore 98348, Main4 and Main3 are all located at the up-gradient margin of the playa, in a zone where the local and regional flow systems converge (Fig. 6.11b). Main4 lies right in this transition (or convergence) zone and Main3 and bore 98348 lie below and above it respectively. The zone of convergence will move backwards and forwards, towards and away from the playa, depending on the balance between local recharge and regional groundwater in the water budget of the playa (i.e. in response to changes in rainfall). The area around Main4 would therefore be a mixing zone, receiving different amounts of water from local recharge and the regional aquifer at different times. Such influxes of water with slightly different pH and alkalinities (Table 3.1) are favourable for incongruent dissolution of carbonates.

From the above discussion, the hydraulic model (Fig. 6.11b), which is supported by the carbon isotope data, suggests that brines at the centre of the Main Salina are formed by evapo-concentration of regional groundwater, whereas brines at the margin are dominated by local groundwater input. The sediments between the edge and centre of the playa probably contain brine formed from a mixture of local and regional groundwater, with the relative amounts of these changing over time.

Mixing of a predominantly regional groundwater source with locally recharged groundwater is also evident below the western (down-gradient) edge of Western Salina. The $^{36}$Cl signature of groundwater at 10 m depth (West4) is consistent with evapo-concentration of a predominantly regional groundwater source, as with the shallow brines (West1a and West3), but also with mixing between brine (West3) and the local recharge end-member (Fig. 6.12a). The $\delta^{13}$C signature also appears to be influenced by that of locally recharged groundwater, with a three end-member mixing process between the shallow brine, regional groundwater and locally recharged groundwater the most likely explanation for the signatures observed here.

### 6.4.5 Downward Movement of the Brines

Although a high [$Cl^-$] and $\delta^2H$ brine body appears to be confined above about 6.5 m to 8 m depth at both Spectacle Lake sites, the pore waters below this still have higher [$Cl^-$] and $\delta^2H$ than the underlying Parilla Sand groundwater, suggesting downward movement of salt. The concentration difference between the pore waters and the Parilla Sand groundwater is greater at the centre of Pond 2 than at the edge of Pond 3, where mixing between the brine and locally recharged groundwater has been shown to occur at 17 m depth (Section 6.4.4). It also has vastly different $^{36}Cl$ and carbon isotopic signatures from that at the edge of Pond 3 (SM1), despite being at a similar depth below the water table (Fig. 6.7, Fig. 6.8). The $^{36}Cl/Cl$ ratio of SM6 is consistent with simple evapo-concentration and subsequent back-mixing (diffusive or advective) of the brine with an entirely regional groundwater source, explaining the higher [$Cl^-$] and TDS here (Fig. 6.12b). If this is the case, very little $^{36}Cl$ decay is suggested, and hence a residence time for salt at SM6 of < approximately 100 k yrs is implied. This is consistent with the time scales of approximately 80 k yrs for regional groundwater flowing in at the eastern margin of Raak Plain to discharge at Spectacle Lake, predicted by the hydraulic modelling in Chapter 5.

Derivation of a residence time for SM6 based on $^{14}C$ is difficult as its carbon isotope signature appears to be a result of result of a complex combination of mixing of “modern” (re-equilibrated) brine with regional groundwater, $^{14}C$ decay and incongruent dissolution of carbonate minerals. When regional groundwater is transported near the surface under an upward hydraulic gradient, its DIC can re-equilibrate with unsaturated zone $CO_2$ by diffusion, resulting in a modern $^{14}C$ signature (e.g. the shallow brines in Fig. 6.8). Back-mixing (diffusive or advective) with regional groundwater, as indicated by the $^{36}$Cl data, would then reduce the $^{14}$C activity of the DIC. However, groundwater at SM6 has the most positive $\delta^{13}$C value observed at Raak Plain ($\delta^{13}$C = 1.7 ‰), suggesting incongruent dissolution of Mg-carbonate minerals, which also reduces the $^{14}$C activity of DIC.

Back-mixing via diffusion of $Cl^-$ between the shallow brines and a regional groundwater / local recharge end-member has been observed down to a depth of 10 m below the water table at Western Salina (West4), as already described in Section 6.4.4. This is also apparently the case at a similar depth approximately 50 m away from the playa edge (R1; Fig. 6.11a), where groundwater has a similar $\delta^{13}$C signature to that of modern, locally recharged groundwater (R3), but a much lower $^{14}$C activity and much higher TDS, $\delta^2$H and $\delta^{18}$O values (Table 6.3; Figs. 6.3 and 6.8). It has a d-excess of –2.0 ‰, similar to those of the Parilla Sand groundwater at this location (bore 50074; d = -1.7 ‰), but a more negative $\delta^{13}$C signature (Fig. 6.8). This groundwater, deep below a dune adjacent Western Salina, was probably recharged locally but, similarly to West4, has mixed with a small amount of brine from the playa, or the saline regional groundwater. Based on a conceptual model of mixing and decay, a residence time of approximately 23 k yrs is estimated for R1. However, $^{14}$C may have been added to the groundwater by diffusion from the atmosphere in the recharge area in which case the residence time may be greater than this.

### 6.4.6 Mixing of Brine in Horizontally Continuous Sand Layers

The potential for lateral movement of brine via horizontally continuous sand layers in the Blanchetown Clay was identified in Section 4.3.3. Groundwater sampled from SM4 at the centre of Pond 2 (Fig. 7.13) has an identical $^{36}$Cl signature to groundwater at a similar depth below the edge of Pond 3 (SM3; Fig. 6.12b).

However, the $^{36}$Cl signature at SM6 (some 13 m below SM4) is significantly different, which suggests that groundwater in the tight clay at SM6 has a different origin and evolution from that at SM4. Mixing over time scales less than 50 k yr (less than that resolved by $^{36}$Cl) in the top 8 m of the profile may explain the similarity between SM3 and SM4, and the presence of a laterally continuous 2-3 m thick sandy (high conductivity) layer at this depth could facilitate such mixing (Fig. 6.13). Groundwater sampled from just above this sandy layer (SM5) has a higher $^{14}$C activity and a more negative $\delta^{13}$C value than that at SM6 below it. The vertical distribution of $^{14}$C activities of these groundwaters are probably influenced by diffusion of atmospheric $CO_2$. However, an increase in the effect of incongruent carbonate mineral dissolution can be seen from SM5 to SM6, suggesting that the shallower groundwater (SM5) may be a precursor to the deeper groundwater sample (SM6).

### 6.4.7 Impact of Brine Leakage on Regional Groundwater Below Raak Plain

Increases in TDS of regional groundwater in the Parilla Sand aquifer below Raak Plain have been attributed to mixing with brine from the discharge complex (Sections 3.5.5 and 4.3.2.2; Fig. 4.9). If this theory is correct, it should be supported by the isotopic tracer data, and the time scale for brine leakage may be investigated using the radioactive tracers $^{36}$Cl and/or $^{14}$C. Groundwater flows into Raak Plain at the eastern margin (bore 26240). A slight increase in TDS of this groundwater occurs between the eastern margin and Spectacle Lake (bore 81945), and was attributed to mixing with salt from the subsurface brine below Spectacle Lake (Section 4.3.2.2; Fig. 4.9). The $\delta^2$H and $\delta^{18}$O values of the Parilla Sand groundwater also increase between these two points. However, the deuterium excess of the groundwater increases from 1.1 to 3.1 ‰ (Fig. 6.10b) and, as the evaporated brines have extremely negative deuterium excesses, this suggests that the increase is not due to mixing with evaporated water from the brine, but probably to a small increase in the influence of locally recharged groundwater (d = 2.8 ‰; Fig. 6.10b). Therefore, the TDS increase observed below Spectacle Lake does not occur as a result of downward advection (or convection) of evaporated brine, but is more likely to be the result of downward diffusion.

Groundwater below the up-gradient margin of the Main Salina (bores 98347, 98349 and 98351) has a slightly lower TDS, and slightly higher $\delta^2$H and $\delta^{18}$O values, than that below Spectacle Lake (Fig. 6.10b). The decrease in TDS ([$Cl^-$]) was attributed to either dispersion along the groundwater flow path, or increased mixing with recharge (Section 4.3.2.2; Fig. 4.9). The results of the numerical model of the discharge complex suggest that higher recharge rates through the dunes and plains of the discharge complex increase the importance of local flow systems so that the latter process is possible (Section 5.5.2). The carbon isotope signature of the groundwater below the Main Salina (bore 98349; Fig. 6.10c) is similar to those observed in other parts of the Victorian and South Australian Mallee (Section 6.3.1.1). However, the $^{36}$Cl/Cl ratio of groundwater in the same bore ($^{36}$Cl/Cl = 13 x $10^{-15}$; Fig. 6.7, Fig. 6.10d), is much lower than any other values measured as part of this study (Davie et al., 1989). Such low $^{36}$Cl/Cl values have only been found in the Mallee to occur below groundwater discharge zones, and have been interpreted as being due to the recycling of salt through these systems (Davie et al., 1989). If the difference in $^{36}$Cl/Cl between bores 26240 and 98349 is assumed to be due to simple radioactive decay of $^{36}$Cl along an east-west groundwater flow path, a residence time of approximately 370 kyr is estimated using equation 6.8. However, the hydraulic modelling in Chapter 6 suggests a groundwater travel time between bores 26240 and 98349 of the order of 80 kyrs. Other possible explanations for the low $^{36}$Cl/Cl ratio of groundwater in the Parilla Sand aquifer below the eastern edge of the Main Salina are:

a) Diffusion of old (low $^{36}$Cl/Cl) chloride from the overlying Blanchetown Clay aquitard. A travel time of 80 k yrs between the eastern margin of Raak Plain and the Main Salina would require a $R_0$ of 16 x $10^{-15}$ (Eq. 6.8). Based on an initial R of 31 x $10^{-15}$, this requires that 50% of $Cl^-$ in groundwater at bore 98349 be derived from regional groundwater inflow and 50% be "dead" $Cl^-$, with a residence time > 1.5 Ma ($^{36}$Cl/Cl = 0). Since evaporite deposits do not exist in the Parilla Sand aquifer, the most likely source of this additional chloride is diffusion from pore fluids in the overlying aquitard.

b) A longer residence time of groundwater in the upper Parilla Sand, due to disruption of flow by the discharge complex. Results of the numerical modelling (Chapter 5) suggested a combination of upward groundwater discharge from the Parilla Sand and deep local flow systems. Stagnation points may exist in the Parilla Sand, particularly at the up-gradient margins of the playas where these systems converge (Figs. 5.2-5.12). This can lead to long residence times for salt at these locations, and hence extremely low $^{36}$Cl/Cl ratios.

A combination of processes (a) and (b) may be responsible for the low $^{36}$Cl/Cl ratio of groundwater in bore 98349. A 25% increase in [$Cl^-$] occurs between the eastern margin of Raak Plain (bore 26240) and Spectacle Lake (bore 81945), with possibly a small amount added between this and the Main Salina. Assuming that this added $Cl^-$ has a $^{36}$Cl/Cl ratio (R) of 0 (i.e. a residence time > 1.5 Ma) and mixes with regional groundwater (R = 31 x $10^{-15}$), a $R_0$ value of 23 x $10^{-15}$ is implied, resulting in a residence time for chloride of 250 ka at bore 98349 (Eq. 6.8). However, there has been no evidence of such old $Cl^-$ in the Blanchetown Clay, so the implied residence time may be greater. As (a) the time scales for advection of chloride from the eastern margin of Raak Plain to the surfaces of Spectacle Lake and the Main Salina are estimated to be approximately 80 k yrs and 150 k yrs respectively (Section 5.5.4), and (b) back-diffusion of the resulting brines is considered to be a major mechanism causing groundwater TDS increases in the Parilla Sand, a residence time of the order of hundreds of thousands of years for $Cl^-$ in the Parilla Sand is possible. Despite the long residence time, a measurable $^{14}C$ activity can occur in bore 98349 due to diffusion of from the atmosphere (Section 6.3.1.1).

Significantly lower deuterium-excesses occur down-gradient of the Main Salina (bores 50073 and 50074), and can only be caused by entrainment of evaporated brines, which have deuterium excesses as low as –30 (Table 6.3, Fig. 6.10b). Western Salina bore 50074 also has the highest [$Cl^-$] and $\delta^2H$ and $\delta^{18}O$ values of all samples collected from the Parilla Sand aquifer (Fig. 4.9, Table 6.3). Its $\delta^{13}C$ signature (0.0 ‰) is about 5 ‰ more positive than groundwater 9.4 km up-gradient (bore 98349), and 10 ‰ more positive than locally recharged groundwater (R3). It has a similar $\delta^{13}C$ signature to groundwater in the Blanchetown Clay below the Main Salina (Main4) (Fig. 6.8, Fig. 6.10c). As described in Section 6.3.1.3, in the absence of methanogenesis, such a positive $\delta^{13}C$ signature can only be achieved by incongruent dissolution of Mg-carbonate minerals, a process that is likely to occur in or around the playas of the discharge complex. Hence, Parilla Sand groundwater arriving at Western Salina has undergone mixing (diffusive or advective) with solutes from the playa lakes to the east (Fig. 6.10c).

Bore 50075 is located slightly to the south of transect AA' (Fig. 1.6), at the south-western margin of the Raak Plain groundwater discharge complex. Its TDS and $\delta^2$H and $\delta^{18}$O values are slightly higher than those of groundwater at the eastern margin (bore 26240), but lower than those below Western Salina (bore 50074) (Table 6.3). Its $\delta^{13}$C value is much closer to that of locally recharged groundwater (R3) than Parilla Sand groundwater below the Main Salina (bore 98349). The signature of groundwater at this location has probably been derived from locally recharged groundwater, a result of the higher recharge rates (low vegetative cover) in the discharge complex. Because it is at the margin of the discharge complex, it has probably had little influence from the brines associated with the playa lakes.

## 6.5 Conclusions: Contribution of Isotopic Tracers to the Conceptual Model of a Groundwater Discharge Complex

In addition to information provided by hydraulic data and groundwater TDS information (Chapters 4 and 5), the isotopic tracers, $\delta^2$H and $\delta^{18}$O, $\delta^{13}$C and $^{14}$C, and $^{36}$Cl have assisted with the development of the conceptual model of the Raak Plain Groundwater Discharge Complex. $^{36}$Cl in particular has shown that, although there is an increase in the importance of local flow systems due to higher recharge rates across the discharge complex, regional groundwater is still the major source of salt to the playa lake brines, even at Western Salina (Fig. 6.10d). The isotopic tracers support back- of the brines with their sources (predominantly regional groundwater), leading to high TDS groundwater at depths of up to 10 m below the water table at Western Salina and 19 m at Spectacle Lake (Fig. 6.11 (a&b) and Fig. 6.13). Greater degrees of mixing of brine with locally recharged groundwater are observed at the down-gradient margins of the playas, particularly in the deeper groundwater samples at these locations (i.e. West4 and SM1) (Fig. 6.11b, Fig. 6.13).

An increase in TDS of Parilla Sand groundwater below Spectacle Lake (bore 81945) from the eastern margin of the discharge complex (bore 26240) was attributed to mixing with salt from the brine at Spectacle Lake. Apparent back-mixing to a depth of 19 m at the centre of Spectacle Lake supports this (Fig. 6.13). Lower [$Cl^-$] at a similar depth at the edge of Spectacle Lake is due to mixing with locally recharged groundwater (Fig. 6.13). A low $^{36}Cl/Cl$ ratio of Parilla Sand groundwater below the Main Salina is consistent with mixing with “old” chloride, from a regional groundwater source, that has been advected to the surfaces of the playa lakes and leaked back into the Parilla Sand. The time scale for this process is of the order of 300 k years. However, it is also important to note here that this low value may be due to old chloride leached from the underlying aquitard (the Bookpurnong Beds) as a result of the groundwater discharge occurring above. Additional work, including sampling of groundwater from the Bookpurnong Beds would be required to discount this process.

The carbon isotope data has shown that extensive incongruent dissolution of carbonate minerals occurs at the up-gradient edge of the Main Salina, where regional and local flow systems meet and groundwaters with subtle differences in their carbonate chemistry mix. Such a zone may also occur at the down-gradient margin of the playa, but sampling was not carried out there. In addition to a large increase in TDS, Parilla Sand groundwater in the western part of Raak Plain has a negative deuterium excess, suggesting an influence of water that has undergone evaporation in the playa lakes. It also has a $\delta^{13}C$ value of 0, similar to those observed at the edge of the Main Salina (at Main4) and at the centre of Spectacle Lake (SM6). This suggests solutes added to the regional groundwater below Western Salina have passed through zones of mixing between regional and local groundwater in and around the playas subsequent to evapo-concentration in the playas (Fig. 6.10c).

The $^{36}$Cl data has shown evapo-concentration and mixing processes occurring in the Blanchetown Clay below the playa lakes and their margins over time scales less than 100 k yrs, consistent with the results of the hydraulic modelling (Chapter 5). Estimates of residence times based on $^{14}$C data for groundwaters in the Blanchetown Clay at the playa edges suggest residence times of the order of thousands to tens of thousands of years within the playa systems.

# Chapter 7 The Influence of Salt Harvesting on a Natural Playa Lake (Spectacle Lake)

## 7.1 Introduction

As discussed in Section 1.1, the use of natural playa lakes as evaporation basins for disposal of saline groundwater, or for harvesting economically valuable evaporite minerals, is becoming more widespread in the Murray Basin of south-eastern Australia, and occurs in arid and semi-arid regions throughout the world. Both practices involve the impoundment of groundwater at the surface of a playa, and volume reduction by evaporation. For naturally dry playa lakes, this increase in hydraulic head at the playa surface has the potential to alter the hydraulic processes occurring below the playa and de-stabilize the naturally formed subsurface brine body (Barnes et al., 1990). Such a sudden imposition of high lake levels can be considered as a short time-scale analogue to climate-induced lake level fluctuations. An additional change to the natural status of the playa is the development of a thick surface salt crust as a result of enhanced evapo-concentration and, in the case of salt harvesting, progressive removal of this crust. Both processes are likely to alter the chemical evolution of subsurface brine bodies.

A few studies have investigated the effects of human intervention on natural playa lakes. Such examples in the Murray Basin include the Noora disposal basin in South Australia (Barnes et al., 1990) and the Mourquong disposal basin in New South Wales (Chambers et al., 1995; Simmons et al., 2002). At the Noora basin, irrigation wastewater is pumped onto the surface of a natural playa, where it quickly infiltrates into the sandy sediments underlying the basin and forms a relatively fresh lens on top of the saline regional groundwater (Barnes et al., 1990). Very little evapo-concentration of this inlet water occurs due to rapid infiltration into the basin sediments. Based on an analytical analysis of brine stability, and groundwater TDS measurements, Barnes et al. (1990) concluded that the increased hydraulic head in the basin, and the reduction in the stabilizing upward evaporative flux, had caused "relaxation", sinking and spreading of the natural brine body. The result is a cone of dense brine sitting at the base of the aquifer, under the lens of comparatively fresh disposal water. The processes believed to occur below this modified playa were compared with those below the natural groundwater discharge zones, Lakes Frome and Tyrrell, where horizontal influxes of regional groundwater and upward evaporative fluxes stabilize the brine bodies and restrict them to the areas below the playas.

In contrast to the Noora disposal basin, saline groundwater that is pumped into Lake Mourquong undergoes a high degree of evapo-concentration as it perches on top of the Blanchetown Clay aquitard (Simmons et al., 2002). The TDS of the disposal water is approximately 35 g/L and the surface brines can reach 350 g/L in some parts of the basin. Simmons et al. (2002) used a combination of chloride and $^{2}H/^{1}H$ and $^{18}O/^{16}O$, and numerical modelling to identify lateral migration of the brine body over at least 100 m. The numerical modelling showed that vertical transport through the clay layer was predominantly by diffusion but that, in an area where the clay aquitard was missing, very fast downward movement of the brine could occur by density-driven convection (see Section 4.1.2). It was also found that salt transport to the underlying aquifer was more sensitive to the TDS of the surface water rather than to increases in the hydraulic head within the basin.

Chambers et al. (1995) compared the chemical evolution of brines in two natural groundwater discharge complexes with that of brines in two disposal basins, Lake Mourquong and the engineered Wakool disposal basin, where salt harvesting is also carried out. The study showed that brines in both disposal basins, both underlain by clay aquitards, followed predictable evolutionary pathways. In contrast, brine evolution in the natural groundwater discharge complex, also underlain by a clay layer, was influenced by complex re-solution processes that may have been dependent on different inflow / leakage ratios in different parts of the lake. In the natural playa situated directly on top of a sandy aquifer, brine chemistry followed the predicted evolutionary path for simple evapo-concentration of inflow, possibly due to convective transport of salt away from the playa surface.

All of the studies described above showed that the presence / absence of an aquitard below natural or modified playa lakes is an important control over solute transport and brine chemistry. However, although they aimed to determine the factors controlling brine evolution in natural, modified and artificially engineered basins by comparing brine chemistries in each, the interpretation of Chambers et al. (1995) was complicated by differences in inflow water compositions and geological setting. Likewise, the comparison of Barnes et al. (1990) between hydraulic processes occurring at the Noora disposal basin and Lakes Tyrrell and Frome was also complicated by different geological settings. Unlike these previous studies, Raak Plain provides the opportunity to compare between the brines of natural playa lakes and one that has been hydraulically altered, all within the same hydrogeologic and climatic environment, and all underlain by a thick aquitard.

Groundwater from the Parilla Sand aquifer has been ponded at the surface of Spectacle Lake for salt harvesting since 1980 (Section 1.3.5.4). Such a recent change would only be expected to impact the brine to a few metres depth below ground. Hence, some hydraulic and hydrochemical data from Spectacle Lake has already been presented in previous chapters and discussed in the context of its natural playa characteristics. The objective of this chapter is therefore to:

- Identify how the harvesting operation has altered the chemical evolution and migration of the brine body by reviewing the data from Spectacle Lake (Chapters 3, 4 and 6) and comparing it with that from the natural playas.

## 7.2 Diffusional Back-Mixing of Salt Below a Salt Harvesting Operation

The vertical extents of the main brine bodies at Spectacle Lake, which are between 6.7 m and 7.5 m, are comparable with those observed at the edges of Western Salina and the Main Salina (Section 4.2.4; Fig. 4.6). Above these depths, a brine body with $Cl^-$ concentrations greater than 50 g/kg, and as high as 129 g/kg, occurs at both the edge of Pond 3 and the centre of Pond 2 (Fig. 4.2a). Below 7.5 m at the edge of Pond 3, $[Cl^-]$ then remains fairly constant at approximately 43 g/kg to a depth of 21.2 m where sampling stopped. Below 6.7 m at the centre of Pond 2, concentrations are fairly constant to the bottom of the core at 8.5 m, but still well above that of groundwater sampled at 18.8 m (piezometer SM6; $[Cl^-]$ = 382 g/kg). $\delta^2H$ and $\delta^{18}O$ display similar trends with depth to $[Cl^-]$ at both sites (Fig. 6.13 shows $\delta^2H$).

Unlike at the natural playa lakes, $Cl^-$ concentrations below the main brine body at the two Spectacle Lake sites remain well above that of the underlying regional Parilla Sand groundwater ($[Cl^-]$ = 30.4 g/kg) to at least 18 m depth (Fig. 4.6 (c&d)). Isotopic tracer data, particularly the $^{36}Cl$ signatures of the brines, have indicated that back-mixing between the shallow brines and their low-TDS sources (i.e. regional Parilla Sand groundwater or locally recharged groundwater) may be the reason for these higher salinities at depth below Spectacle Lake (Section 6.4.5). If this interpretation is correct, a lack of evidence of $^{36}$Cl decay implies that the evaporation and mixing processes have occurred over time scales less than 100 k yrs. The carbon isotope signature of the deep groundwater at the edge of Pond 3 (SM1) can also be explained by mixing between locally recharged groundwater and shallow brine, with a time scale of 6 to 8 k yrs (Section 6.4.4). The signature of the deep groundwater at the centre of Pond 2 (SM6) appears to be influenced by carbonate mineral-solution reactions and it is hence difficult to obtain a time scale based on $^{14}$C for the mixing process at this location (Section 6.4.5).

The effects of diffusion can be seen above 8 m depth in the shapes of the ion vs depth graphs (Fig. 3.4), and in changes in the slopes of ion vs [$Br^-$] plots (Fig. 3.8-3.10), which are caused by different rates of diffusion of the various ions. Below 7.5 m, concentration gradients are much lower and diffusion would occur much more slowly, with the effects of differential diffusion between the ions being less obvious. The time scale of 6 to 8 k yrs described above for mixing at 16 m depth (SM1), derived from $^{14}$C data is consistent with the predicted time scale for diffusion across the entire Blanchetown Clay of 10 k yrs (Table 4.7). As the salt harvesting operation has only been active at Spectacle Lake for the last 20 years, it is unlikely that diffusive mixing at such great depths occurs as a result of it.

Based on the [$Cl^-$] vs depth profiles (Fig. 4.6 (c&d)), slow diffusion of brine through the Blanchetown Clay, with a time scale of the order of 10 k yrs may be the cause of a TDS increase in the Parilla Sand aquifer approximately below Spectacle Lake (Fig. 4.5). However, the greatest TDS increase in the Parilla Sand occurs to the west of the Main Salina, suggesting that brine leakage is not limited to the harvested lake. Although no evidence for mixing with brine was observed below the main brine bodies at the two lake-edge sites at Western Salina and the Main Salina, this does not rule out diffusion or some other process occurring below other parts of the playas. Further investigation would be required to determine whether downward diffusion of brine is limited to Spectacle Lake, and whether any other localized processes, for example preferential flow, cause brine leakage into the Parilla Sand aquifer.

## 7.3 Downward Displacement of the Brine

Differences in the shapes of the ion vs depth profiles and ion vs [Br$^-$] graphs between the centre and edge of Spectacle Lake were identified in Section 3.4.7. The shapes of the graphs for the edge of Pond 3 are similar to those for the natural playa lakes, despite slightly higher concentration factors (indicated by [Br$^-$]) of the shallow brines at the edge of Pond 3. However, there is a distinct break in the linear trend of the data around a depth of 5 m at the centre of Pond 2 (See Section 3.4.7; Fig. 3.9). Below 5 m depth, the trend is similar to those of the natural playa lakes, including the maximum concentration factor of the brine ([Br$^-$] < 0.01 Eq/kg; Figs. 3.5-3.7). However, between 2 m and 5 m below ground level, [Br$^-$] decreases towards the surface whilst [Na$^+$], [Cl$^-$], [Mg$^{2+}$] and [SO$_4^{2-}$] increase (Fig. 3.4b).

The different trends can be explained by taking into consideration the recent changes to the salt and water balance of the lake as a result of the salt harvesting operation. Prior to the salt harvesting operation, Spectacle Lake probably would have been similar to Salt Lake, i.e. with a thin film of “surface water” that only dries up in the driest summer and a seasonal salt crust, perhaps up to 5 cm thick (refer to Section 1.3.5.4). Water has been pumped from the Parilla sand aquifer since 1980, and ponded (20 to 50 cm above the playa floor) at the surface of the playa for most of the year, and a permanent thick (up to 20 cm) salt crust has formed (Section 1.3.5.4).

The brine at 5 m depth may represent the near-surface brine that would have been present before standing water was added to the lake surface and the salt crust began to build up. Under natural, dry lake conditions (or with only a seasonal thin film of surface water), evaporation from the shallow groundwater would have occurred, with simple evapo-concentration of solutes occurring (Fig. 7.1a). Hence the relatively high evaporation factor ([$Br^-$]), but comparatively low concentrations of the other solutes.

The addition of surface water to the lake probably caused evapo-concentration of the shallow groundwater to cease and exerted a downward pressure on the original subsurface brine, pushing it downwards and causing it to be replaced by evaporated surface water (Fig. 7.1b). Because this surface water is pushed down more quickly, it would undergo a lower degree of evaporation, with the evaporation factor ([$Br^-$]) also decreasing as the surface salt crust becomes increasingly thick. The development of this thick and permanent salt crust would provide a constant source for the diffusion of salts into the subsurface brine, so that diffusion profiles develop for the salts included in the salt crust (Fig. 7.1c). This explanation for the break in trend of the chemistry data for the centre of Pond 2 around 5 m depth suggests that the natural subsurface brine formed below the playa lake prior to the salt harvesting operation has been displaced downwards by approximately 5 m. The brine occurring above 5 m depth is the result of evaporation and diffusion processes occurring under the influence of the salt harvesting operation.

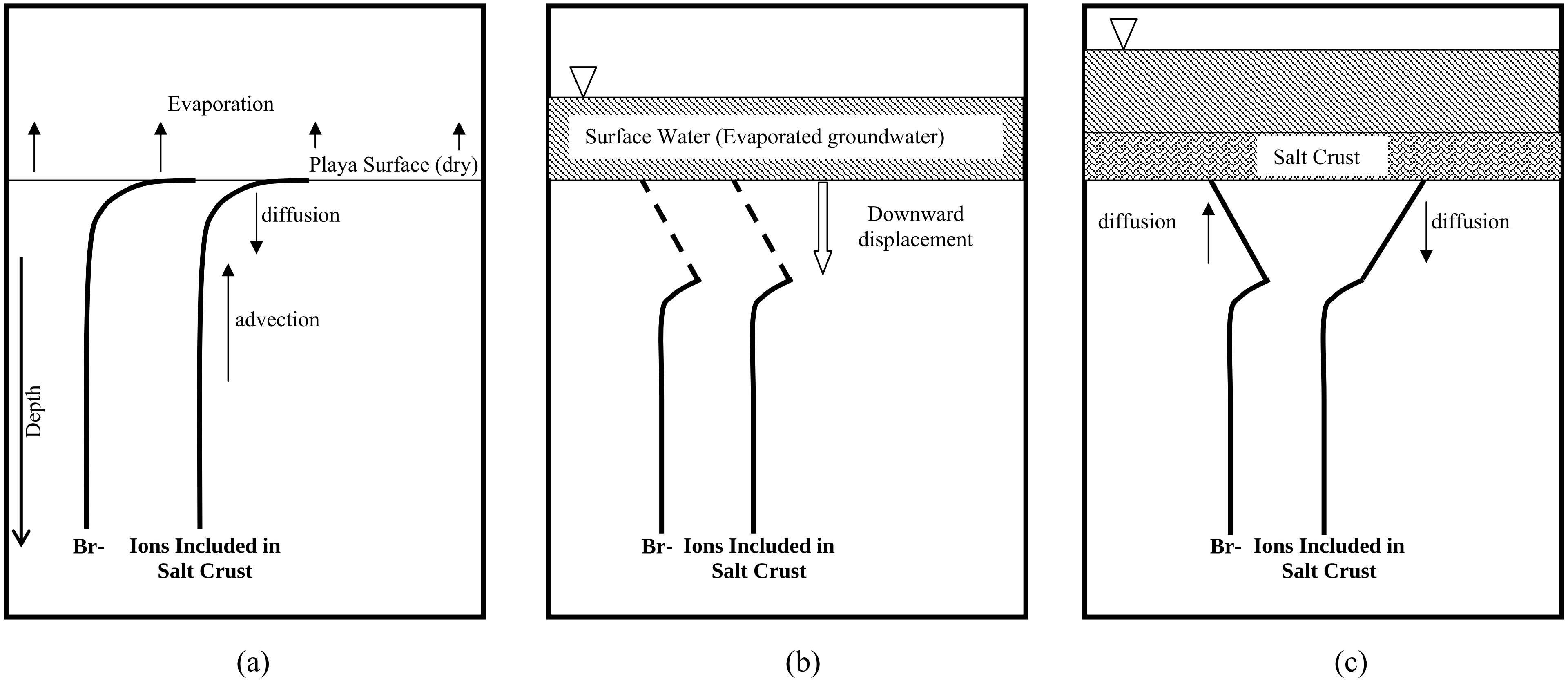

Figure 7.1. Conceptual diagram showing the formation of subsurface pore water solute vs depth profiles in a natural playa lake that is subsequently modified for salt harvesting. Profiles are shown for both the conservative Br$^-$ ion and for other solutes that may be incorporated into a surface salt crust (e.g. Na$^+$ and Cl$^-$). The scenarios shown are: (a) Formation of the steady state profile in a natural (normally dry) playa lake, (b) Addition of surface water (groundwater pumped from the regional aquifer), causing downward displacement of the natural brine body and evaporation of shallow groundwater to cease, (c) Formation of a surface salt crust as a result of the enhanced evapo-concentration of groundwater in the lake, causing diffusion of ions from the salt crust into the underlying brine.

Changes to the conditions under which water evaporates in Spectacle Lake would be expected to have an influence on the $\delta^2$H and $\delta^{18}$O signatures of the brine. However, the $\delta^2$H vs depth profile for the centre of Pond 2 has an approximately similar shape to the [Cl$^-$] vs depth profile, suggesting at first glance that this is not the case (Fig. 6.13; Fig. 7.2a). If the data are examined more closely, it can be seen that the situation is different for $\delta^{18}$O, with a break in the trend occurring at approximately 5 m depth, similar to the break in trend for the ion chemistry data (Fig. 7.2b). When deuterium excess values of the pore water brines for both the centre of Pond 2 and the edge of Pond 3 are plotted against depth, a particular trend can be seen for both sites (Fig. 7.3). Deuterium excesses at the centre of Pond 2 (site SM5) become more negative towards the surface to a depth of approximately 5.1 m, above which they become more positive. A similar situation occurs around a depth of 1.1 m below the playa floor at the edge of Pond 3 (site SM1). These transition points are probably the boundaries between the old and new brines, representing different evaporation rates. Downward displacement of the brine by about 1 m appears to have also occurred at the edge of Pond 3. The effect of the harvesting operation is smaller at this location, probably due to generally lower ponded water levels and a thinner (and often completely dissolved) surface salt crust.

The enhanced vertical movement of brine at Spectacle Lake may be the reason for an apparently greater influence of mixing and / or carbonate mineral dissolution on the shallow brine at this lake (SM2) compared with the shallow brines at the natural playa lakes (Section 6.4.2).

## 7.4 Lateral Mixing of Brine Along Horizontally Continuous Sand Layers

Two layers of sandy sediments were identified at both the centre of Pond 2 and the edge of Pond 3. The first, a thin (0.6 to 1 m thick) layer of fine – medium sand / silty sand occurs at a depth of 2 m (Sand Layer A, Fig. 6.13), and the second, thicker (2 to 2.5 m thick), medium – coarse sand layer occurs at a depth of approximately 6.1 m (Sand Layer B, Fig. 6.13). An additional 0.5 m thick sand layer (Sand Layer C) was identified at 11.6 m depth at the edge of Pond 3, but core was not collected to this depth at the centre of Pond 2 to confirm its continuity to that site.

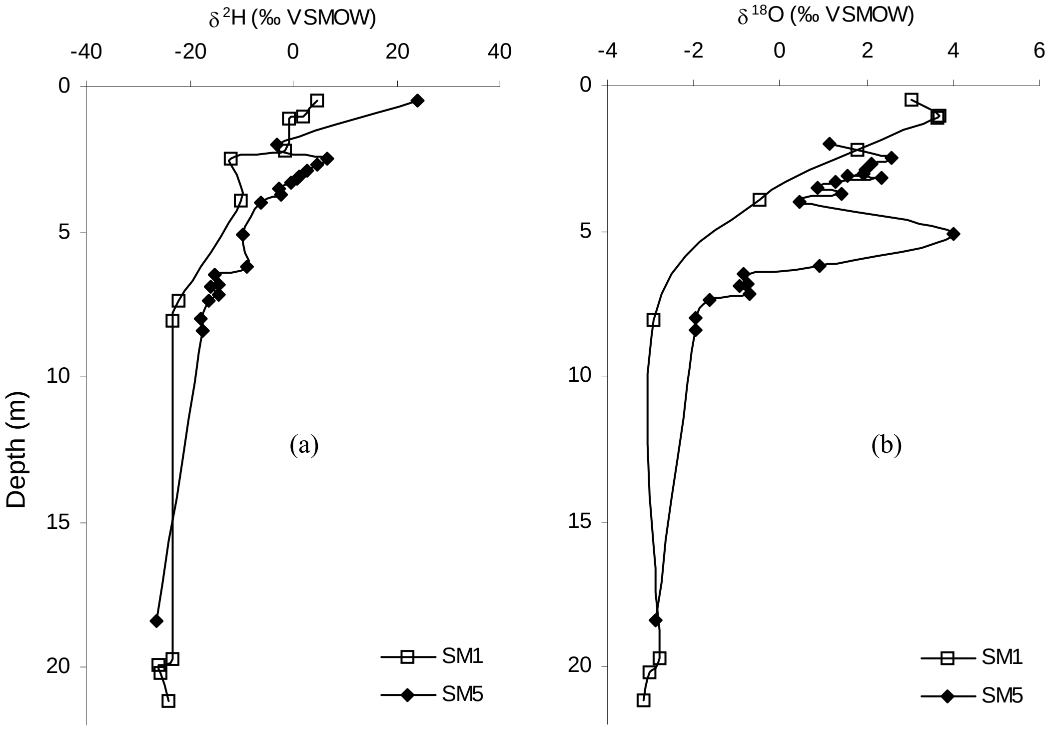

Figure 7.2. Pore water (a) $\delta^2$H and (b) $\delta^{18}$O vs depth profiles at the edge of Pond 3 (site SM1) and centre of Pond 2 (site SM5).

The possibility that these sand layers, with permeabilities up to 5 orders of magnitude greater than the clay, may provide preferential pathways for lateral transport of brine was raised in Section 4.3.3. They do appear to exert some control over the vertical distribution of Cl$^-$, $\delta^2$H and $\delta^{18}$O at Spectacle Lake, as indicated by distinct changes in these tracers at depths corresponding to Sand Layers A and B (Fig. 6.13 shows [Cl$^-$] and $\delta^2$H). At both the centre of Pond 2 and the edge of Pond 3, a distinct drop in $\delta^2$H can be observed at Sand Layer A, and this is mimicked by [Cl$^-$] at the latter site. A drop in [Cl$^-$] is not obvious at the centre of Pond 2 due to a lack of sample between the surface salt crust and Sand Layer A. The drop in [Cl$^-$] and $\delta^2$H in Sand Layer A may be due to mixing with fresher (lower [Cl$^-$]), lower $\delta^2$H groundwater flowing in from below the sand dunes directly adjacent Spectacle Lake.

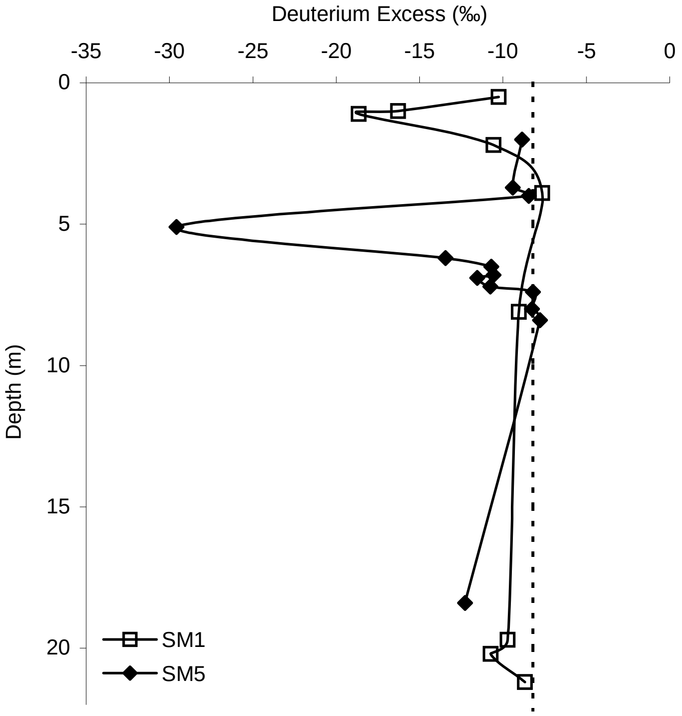

Figure 7.3. Pore water deuterium excess (“d”) vs depth profiles at the edge of Pond 3 (SM1) and the centre of Pond 2 (SM5). Dashed line indicates a deuterium excess of 0. Different deuterium excess values may indicate different degrees of evaporation (more negative d values indicate higher degrees of evaporation), or evaporation under different conditions (e.g. temperature, humidity, TDS). Distinct breaks in trend of the profiles are observed at depths of 5.1 m at the centre of Pond 2 (SM5) and 1.1 m at the edge of Pond 3 (SM1), signifying the boundary between the old (natural) brine body and the brine formed recently as a result of the salt harvesting operation.

The gradients in both [$Cl^-$] and $\delta^2H$ with depth at both Spectacle Lake sites decrease to zero at the top of the much thicker Sand Layer B. This is consistent with advective mixing with lower TDS groundwater and dispersion of salt in this layer. Lateral mixing along the sand layer between the edge of Pond 3 and the centre of Pond 2 is further supported by the almost identical $^{36}Cl$ signatures of groundwater in the sand layer at these locations (piezometers SM3 and SM4). This similarity occurs despite apparently different origins of the brines at these locations, implied by differences in $^{36}Cl$ and carbon isotope signatures of the deeper brines (Section 6.4.5). Although the shallow brines formed as a result of the salt harvesting operation would have similar origins across the playa (i.e. evapo-concentration of a purely regional groundwater source), the effect of this is unlikely to be seen as deep as 6 m in the sand layer. Therefore, lateral mixing rather than a common source is the most likely explanation for the similarities in isotopic composition in the sand layer, which may also provide a pathway for lateral movement of brine that has been displaced downwards (Section 7.3).

## 7.5 Conclusions

The following main conclusions can be drawn about the effects of salt harvesting on a natural playa:

- Downward diffusion of brine occurs below both the centre and edge of Spectacle Lake, at least to a depth of approximately 20 m and may be the reason for an increase in TDS of Parilla Sand groundwater in the vicinity of this playa. Because of the large time-scales required for diffusion to these depths (of the order of 10 k yrs), this is unlikely to be a result of the salt harvesting operation. Although evidence for diffusion below the main brine body was not observed at the natural playas, further investigations would be required to determine whether this process is specific to Spectacle Lake.

- Downward displacement of brine by 5 m at the centre of Pond 2 and 1 m at the edge of Pond 3 has occurred as a result of ponding of regional groundwater at the surface of the playa over a 20 yr period. This implies a displacement of brine by up to 0.25 m per year of operation of the evaporation ponds, although this displacement may not occur at a constant rate. The significance of this is that an aquitard such as the Blanchetown Clay that has some laterally extensive sand lenses may not be a perfect barrier to brine leakage in the case of salt disposal and salt harvesting operations. Therefore, such an aquitard must be sufficiently thick to be an effective buffer for underlying aquifers.

- Lateral flow along horizontally continuous sand layers disperses salt that diffuses into these layers. This process may not be limited to the harvested lake, but may provide a pathway for lateral flow of brine that has been displaced downward by ponding of water at the surface.

# Chapter 8 Summary and Conclusions

## 8.1 Overview

Regional groundwater discharge zones can accumulate large quantities of salt in the form of hypersaline subsurface brines by evapo-concentration of groundwater in arid and semi-arid environments. There have been numerous studies of single large playa lakes and man-made saline groundwater disposal basins, but relatively little is known about the links between hydraulic and hydrochemical processes that affect water and solute behaviour below complexes of numerous small playa lakes. This thesis has investigated the spatial variability in hydrochemical and hydraulic processes at a range of scales ($10^{-2} – 10^{3}$ m) in the Raak Plain groundwater discharge complex, located in the central Murray Basin of south-eastern Australia. A combination of hydraulic, hydrochemical and isotopic methods has been used to develop conceptual models for brine evolution and hydraulic and solute fluxes below the discharge complex.

## 8.2 Mechanisms of Brine Formation and Chemical Evolution

By the time groundwater in the regional Parilla Sand aquifer reaches Raak Plain, it has obtained a seawater-like chemical composition due to accessions of marine aerosols and the evaporative concentration of input waters along the flow path from the margins of the Murray Basin (Macumber, 1991; Herczeg et al., 2001). Upward leakage of this groundwater, through the 30 m thick Blanchetown Clay, is the dominant source of solutes to the subsurface brines, which are essentially evapo-concentrated versions of the seawater-like inflow. However, groundwater recharged locally through the dunes and plains between the playas also has a similar composition to that of the regional groundwater and can be a major source of solutes to the brines, particularly at the edges of the playas.

The pore water brines below the playas can reach salinities up to 260 g/kg (TDS) in the top 5 cm of the sediment profile, although this concentration decreases by up to 50 g/kg within the top 1 m. Brine chemistry is fairly constant across the playa lakes, and generally follows a seawater evaporation curve with increasing brine concentration factor (indicated in this study by [$Br^-$]). In fact, despite the range of salinities (30 – 350 g/kg), the chemical signatures of all waters at Raak Plain are relatively uniform. With the exception of the mineral-solution reactions described below, most major ions are conserved during the evapo-concentration of the regional / locally recharged groundwater sources, with little loss by deflation from the playa surfaces. Minor differences in Cl/Br and other ionic ratios within the top few metres of the sediment profiles can generally be explained by different rates of back-diffusion of the various ions across the steep concentration gradients that occur in this depth interval.

Chemical compositions of the most saline brines in the top few centimetres of some profiles indicate precipitation of halite (NaCl) and epsomite ($MgSO_4 \cdot 7H_2O$). However, this process appears to be seasonal, and the minerals are re-dissolved by the next rainfall. These highly soluble salts are therefore generally conserved in solution over long time scales. Precipitation of gypsum ($CaSO_4 \cdot 2H_2O$), however, observed in the sediment profiles around the zone of water table fluctuation, universally causes $Ca^{2+}$ concentrations to diminish relative to the other ions and $SO_4^{2-}$ to build up in the brines, all of which are at equilibrium with respect to this mineral. Carbonate mineral – solution reactions also cause large variability in the alkalinities of the brines (from 0 mEq/kg to 7 mEq/kg).

The presence of a thin layer of surface water in some of the playas, the origin of which is discussed in the next section, causes precipitation of a surface salt crust as this water evapo-concentrates in the semi-arid conditions. Initially, the comparatively fresh surface water may also obtain solutes by diffusion from the hypersaline subsurface brine. As the brine evapo-concentrates, halite, with minor gypsum and possibly trace amounts of bischofite ($MgCl_2 \cdot 6H_2O$), precipitates whilst the rest of the bittern solution sinks back into the playa sediments. Seasonal precipitation of the salt crust causes, for example, high Br/Cl and low $Ca/SO_4$ ratios in the shallow brines.

## 8.3 Development of a Conceptual Model for Recharge and Groundwater Flow

### 8.3.1 Groundwater Flow Patterns and Fluxes Below a Regional Groundwater Discharge Complex

Simple hydrological conceptual and numerical modelling showed that the groundwater flow pattern below Raak Plain is controlled predominantly by the vertical hydraulic conductivity ($K_{VB}$) of the underlying 30 m thick aquitard (the Blanchetown Clay), the horizontal hydraulic conductivity ($K_{HP}$) of the regional aquifer and the recharge rate (R) across the discharge complex. Variation of these parameters within reasonable ranges caused groundwater flow patterns predicted by numerical modelling to range from very little regional groundwater discharge (local flow systems dominating) to all regional groundwater inflow being discharged by the playas (regional groundwater flow systems dominating).

A fairly constant vertical hydraulic gradient of $10^{-1}$ between the Parilla Sand aquifer and the playa lakes implies upward groundwater fluxes through the Blanchetown Clay between 0.4 mm/y and 40 mm/y for a $K_{VB}$ between 5 x $10^{-4}$ and 5 x $10^{-6}$ m/d. An intermediate $K_{VB}$ of 5 x $10^{-5}$ m/d was found using the numerical model to best simulate field measurements of hydraulic head across the discharge complex, narrowing the flux estimates to approximately 3-4 mm/y. The numerical model also showed that all horizontal and vertical advective groundwater flow below the discharge complex, from the eastern margin and recharge areas to the western margin and the discharge areas is generally at time scales less than 300 k yrs. Simple chloride mass balances of the playas, based on broad assumptions of brine extents and the parameters described above suggest brine residence times of the order of 2 k yrs.

The hydraulic modelling showed that higher recharge rates, due to less coverage of native mallee vegetation across the discharge complex, may increase the importance of local groundwater flow systems, particularly west (down-gradient) of the Main Salina. In some scenarios (varying $K_V$ and R), locally recharged groundwater infiltrated the Parilla Sand aquifer through the Blanchetown Clay, before either being captured by the next playa lake along the flow path or flowing out of the system at the down-gradient margin. If brine is able to move laterally from the below the playa lakes into these recharge zones, this large downward flux provides a pathway for downward advection of salt into the Parilla Sand aquifer. The deeply penetrating local flow systems may also cause the source for the brines to be a mixture of locally recharged and regional groundwater.

Sandy layers of various thicknesses that were horizontally continuous over at least hundreds of metres were observed in the Blanchetown Clay at Raak Plain. These provide potential pathways for the lateral movement of brine away from the playas, particularly when horizontal hydraulic gradients are negligible or away from the playa. Occurrences of lateral mixing and dispersion along these layers at Spectacle Lake were suggested by trends in environmental tracer signatures. However, confirmation that lateral movement of brine occurs along these layers would require a more detailed hydraulic and hydrochemical investigation centred around them.

### 8.3.2 Hydraulic Processes Below Surface Water Lakes vs Dry Playas

Hydrological conceptual and numerical modelling helped to determine the reason for the presence of two types of discharge feature at Raak Plain: (1) bare playa lakes (clay surfaces with occasional minor salt efflorescences), and (2) those with 2-10 cm salt crusts and surface water for most of the year. The former are the dominant discharge feature at Raak Plain, whilst the latter tend to occur around the margins of the discharge complex. The difference between the two can be explained by the change in the balance between regional and local flow systems across the discharge complex. At the up-gradient margin of Raak Plain, hydraulic heads in the Parilla Sand aquifer are 2-3 m higher than at the centre and down-gradient margin of the discharge complex, and recharge rates are lower due to the dominance of native mallee vegetation. A lower hydraulic head difference between the dunes and the regional aquifer at the up-gradient margin of the discharge complex causes recharge in the dunes around the playas to follow a shallow flow path along the top of the Blanchetown Clay before draining into the playa lakes. Here, the water continues to perch above the Blanchetown Clay, which is approximately 50 cm below the playa surface. With rainfall occurring throughout the year, this surface water body can be maintained into the height of summer. In contrast, in the main part of the discharge complex, hydraulic heads in the Parilla Sand are lower and recharge is higher, meaning that locally recharged groundwater can circulate deeply through the Blanchetown Clay before being discharged upwards again and evaporating in the playas. This leads to less water becoming perched on top of the Blanchetown Clay and the occurrence of dry playa lakes.

## 8.4 Methodology for Testing Conclusions From the Numerical Model Using Environmental Tracers

A limited amount of hydraulic data on which to base the conceptual model led to only broad conclusions from the numerical model about the groundwater flow pattern below a groundwater discharge complex. The applicability of this simplified discharge zone scale model to Raak Plain was tested against the interpretation of environmental tracer signatures of various groundwater samples. The tracers could be interpreted at the discharge complex ($10^3$ m), playa lake ($10^2$-$10^3$ m) and point profile ($10^{-2}$-$10^0$ m) scales. The combination of these two methodologies provided a great deal of understanding of this complex system for which little data was available. This level of understanding could not have been achieved through the interpretation of one data set alone. Information provided by the environmental tracers allowed the hydraulic conceptual model to be refined, whereas the hydraulic conceptual model assisted in the interpretation of the environmental tracers, particularly where more than one explanation for their signature was available. This methodology could be more widely used in systems where:

- Groundwater flow patterns are complex.
- The chemical compositions of end-member water types are similar.
- Diffusion is suspected to be a significant process affecting solute distributions (i.e. solutes move independently of the water).

At the discharge complex scale, $\delta^2$H and $\delta^{18}$O signatures of all of the waters at Raak Plain confirmed that the process of evapo-concentration is fairly constant across the wide variety of playa lakes, consistent with the constant upward hydraulic gradients discussed in Section 9.3.1. The results of the numerical model showed that local groundwater flow patterns may become increasingly important in the west of Raak Plain, whilst groundwater $^{36}$Cl signatures indicated that the major source of solutes to the brines remains regional Parilla Sand groundwater similar to that flowing in at the eastern margin of Raak Plain. The greatest variability at the discharge complex scale is the occurrence of both dry playas and surface water lakes. $\delta^2$H and $\delta^{18}$O data combined with hydrochemistry confirmed the hypothesis derived from hydraulic data that the shallow film of surface water in the latter is direct rainfall or drainage from the surrounding dunes, rather than a surface expression of the saline groundwater brine body.

Playa lake and point scale processes have caused great variability in TDS and hydrochemistry within individual playa lakes. Isotopic data was used to identify mixing between brine, regional and locally recharged groundwater at the margins of the playas and vertical back-mixing, predominantly by diffusion, between the most saline near-surface brines and their source waters. The latter process causes the formation of intermediate compositions down to depths of up to 10 m across an entire playa lake.

An extremely low $^{36}$Cl/Cl ratio of 13 x $10^{-15}$ was observed by Davie et al. (1989) in the Parilla Sand groundwater below Raak Plain, suggesting a residence time for salt of at least 300 k yr. However, no other evidence for brine recycling, via leakage from one playa and capture by those down-gradient, has been found during the present study. $^{36}$Cl signatures of all brine samples, even in the western part of the discharge complex are consistent with simple evapo-concentration of the regional groundwater source, and possibly some mixing with locally recharged groundwater with a higher $^{36}$Cl/Cl ratio. This suggests time scales for formation of the brines, and subsequent mixing processes less than those resolved by $^{36}$Cl decay (< approximately 100 k yr), consistent with the results of the hydraulic modelling. The low $^{36}$Cl/Cl value of $13 \times 10^{-15}$ in the Parilla Sand is consistent with time scales estimated from the hydraulic modelling for mixing with brines formed by evapo-concentration of regional groundwater at the surfaces of the playas. However, a further investigation of $^{36}$Cl in the underlying Bookpurnong Formation would be required to discount leaching of chloride from this formation as another process that could be responsible for the low ratio.

## 8.5 Mechanisms of Salt and Water Exchange Between Brines and the Regional Groundwater

A two-fold increase in TDS of groundwater in the Parilla Sand aquifer below Raak Plain suggests leakage of salt from the subsurface brines of the overlying discharge complex. However, drilling at the edges of the natural playas indicated vertical extents of the brine bodies to be less than 10 m. Only at Spectacle Lake (the harvested lake) were pore water concentrations greater than that in the underlying Parilla Sand aquifer found below 10 m at both the centre and edge of the lake. As drilling at the natural playas was limited to the playa edges, it is possible that the brine bodies extend to greater depths at other locations. Because this question remains, information on the extent of the brine body below the playa lakes themselved is still essential to fully understanding the interaction between the playa lakes of groundwater discharge complexes and the underlying groundwater systems.

Development of a good methodology for sampling the brine bodies at depth in playa lakes is required to investigate this, both at Raak Plain and in other groundwater discharge zones.

In a number of groundwater discharge zones, the movement of brine over large distances has been attributed to density-driven convection. However, the extremely low conductivity clay layers that occur in the Blanchetown Clay aquitard at Raak Plain limit the possibility of this process occurring. Calculations of two Rayleigh numbers for brine stability in the playa lakes suggested that density-driven convection can occur only in the sandier (higher conductivity) layers of the Blanchetown Clay, under evaporation rates (upward groundwater fluxes) < 10 mm/y. Therefore, this process may occur in the top few metres of the Blanchetown Clay, before being damped out by the lower hydraulic conductivity clay layers.

Two mechanisms are proposed for the movement of salt from the brine bodies below the playa lakes into the Parilla Sand aquifer. Downward diffusion may occur at the centre of the playas, where sampling was not carried out. In the absence of an upward advective flux, the time scale for transport of salt across the Blanchetown Clay by this process is approximately 10 k yr. However, in the presence of even low competing advective fluxes, diffusion cannot transport salt over distances greater than approximately 1 m (Allison and Barnes; 1983, 1985). Alternatively, laterally continuous sandy layers in the Blanchetown Clay can provide potential pathways for lateral flow and mixing of brine beyond the margins of the playas to where net recharge (downward groundwater movement) is occurring. Changes in TDS and $\delta^2$H and $\delta^{18}$O of pore waters around these layers suggest that this may be occurring. Downward advection or diffusion of salt can occur most effectively in regions where net recharge is occurring, with time scales for transport across the 30 m thick

Blanchetown Clay to the Parilla Sand aquifer of $10^3$ to $10^4$ years. Results of the numerical modelling (Chapter 6) suggest a time scale of 40 k yrs.

This conclusion has highlighted the possibility that heterogeneity in the sediments below evaporation basins where large quantities of salt have accumulated may be important in the redistribution of salt. Hence, any study of the impacts of operations, such as saline groundwater disposal basins or salt harvesting, on underlying groundwater systems should:

- Determine the presence of permeable layers in the underlying sediments.
- Monitor groundwater quality in these layers.
- Consider the lateral movement of brine away from the site of the operation, as well as downward movement.

## 8.6 The Effect of a Salt Harvesting Operation on Brines Below Natural Playa Lakes

Solute and $\delta^2$H and $\delta^{18}$O vs depth profiles were obtained at both the centre and the edge of a playa lake that is now being used as an evaporation pond for salt harvesting (Spectacle Lake). Changes in Br/Cl ratios and deuterium excess values with depth indicate downward displacement of the natural brine body by up to 3 to 5 m at the centre of the playa and by 1 m at the edge. This natural brine has been pushed down by a brine body associated with the harvesting operation that has a lower evaporation factor, but has obtained higher concentrations of solutes such as $Na^+$ and $Cl^-$ by diffusion from the thick salt crust that is now present at the playa surface. Back-diffusion of brine below both the centre and edge of Spectacle Lake, at least to a depth of approximately 20 m may be the reason for an increase in TDS of Parilla Sand groundwater in the vicinity of this playa. Diffusion may be more effective in redistributing brine below the centre of this playa lake, due to the fact that the upward hydraulic gradient in the Blanchetown Clay is approximately half that below the lake edge.  This may also be the case below the natural playas, but data was not available at their centres to confirm this.  Diffusion through the Blanchetown Clay could not be a direct result of the salt harvesting operation at Spectacle Lake as the time scale of 10 k yrs required for this to occur is orders of magnitude greater than the period over which the playa has been used as an evaporation pond. Although evidence for this process was not observed at the natural playas, further investigations would be required to determine whether it is specific to the “surface water lakes” that occur at the up-gradient margin of the discharge complex.

The change in the hydraulic balance of natural playa lakes by ponding of groundwater at the playa surface for salt harvesting or saline groundwater disposal has the potential to vertically displace the original brine body.  However, the presence of a 30 m thick clay aquitard below Spectacle Lake appears to have effectively limited this displacement to a maximum of 5 m over the 20 years of operation of the evaporation ponds.  Based on this, it can be said that brine leakage from evaporation ponds is minimized by the presence of a thick aquitard, but whether the processes of back-diffusion of brine and lateral flow along horizontal sandy layers in heterogeneous formations is enhanced by such operations requires further investigation.

# Chapter 9 References

Allison, G.B. and Hughes, M.W., 1978, The Use of Environmental Chloride and Tritium to Estimate Total Recharge to an Unconfined Aquifer., *Aust. J. Soil Res.*, 16: 181-195.

Allison, G.B., 1982, The relationship between $^{18}$O and deuterium in water in sand columns undergoing evaporation., *J. Hydrol.*, 55: 163 – 169.

Allison, G.B. and Barnes, C.J., 1983, Estimation of evaporation from non-vegetated surfaces using natural deuterium., *Nature*, 301: 143-145.

Allison, G.B. and Barnes, C.J., 1985, Estimation of evaporation from the normally "dry" Lake Frome in South Australia., *J. Hydrol.*, 78: 229-242.

Allison, G.B., Stone, W.J. and Hughes, M.W., 1985, Recharge in Karst and Dune Elements of a Semi-Arid Landscape as Indicated by Natural Isotopes and Chloride., *J. Hydrol.*, 76: 1-25.

Allison, G.B., Cook, P.G, Barnett, S.R., Walker, G.R., Jolly, I.D., Hughes, M.W., 1990, Land clearance and river salinisation in the Western Murray Basin, Australia., *J. Hydrol.*, 119(1-4):1-20.

Andrews, J.N., Fontes, J.-Ch., Michelot, J.L. and Elmore, D., 1986, In-situ neutron flux, $^{36}$Cl production and groundwater evolution in crystalline rocks at Stripa, Sweden., *Earth Planet. Sci. Lett.*, 77: 49-58.

Andrews, J.N and Fontes, J.-C., 1992, Importance of the in situ production of $^{36}$Cl, $^{36}$Ar and $^{14}$C in hydrology and hydrogeochemistry., *Proc. Int. Symp. on Isotope Techniques in Water Resources Development, Vienna*, 11-15 March 1991. IAEA-SM-319/12.

Appelo, C.A.J. and Postma, D., 1999, Geochemistry, groundwater and pollution., Balkema, Rotterdam, 536 pp.

Bagge, E. and Wilkom, H., 1966, Geologic age determination with $^{36}$Cl., *Atomkernenergie*, 11: 176-184.

Barnes, C.J. and Allison, G.B., 1983, The distribution of deuterium and oxygen-18 in dry soils: I. Theory., *J. Hydrol.*, 60: 141 – 156.

Barnes, C.J. and Allison, G.B., 1984, The distribution of deuterium and oxygen-18 in dry soils: III. Theory for non-isothermal water movement., *J. Hydrol.*, 74: 119 – 135.

Barnes, C.J., Chambers, L.A., Herczeg, A.L., Jacobson, G., Williams, B.G. and Wooding, R.A., 1990, Mixing processes between saline groundwater and evaporation brines in groundwater discharge zones., *Int. Conf. on Groundwater in Large Sedimentary Basins*.

Bentley, H.W., Phillips, F.M., Davis, S.N., 1986a, Chlorine-36 in the terrestrial environment., In: Handbook of Environmental Isotope Geochemistry: The Terrestrial Environment (Fritz, P., Fontes, J.-C., Eds.), Vol. 2b, Elsevier, Amsterdam, pp 427-480.

Bentley, H.W., Phillips, F.M., Davis, S.N., Habermehl, M.A., Airey, P.L., Calf, G.E., Elmore, D., Grove, H.E., and Torgersen, R.T., 1986b, Chlorine-36 dating of very old groundwater 1. The Great Artesian Basin, Australia., *Water Resour. Res*., 22: 1991-2000.

Berner, R., 1980, Early Diagenesis: A Theoretical Approach., Princeton Univ. Press, 241 pp.

Bird, J.R., Davie, R.F., Chivas, A.R., Fifield, L.K. and Ophel, T.R., 1991, Chlorine-36 production and distribution in Australia, *Palaeogeogr., Palaeoclim., Palaeoecol*., 84: 299-307.

Blackburn, G. and McLeod, S., 1983, Salinity of Atmospheric Precipitation in the Murray-Darling Drainage Division, Australia., *Aust. J. Soil Res*., 21: 411-434.

Blum, D., 1993, Nuclear Detectives., *Discover,* 14(4): 31-37.

Bowler, J.M. and Wasson, R.J., 1984, Glacial age environments of inland Australia. In: Vogel, J.C., Late Cainozoic palaeoclimates of the Southern Hemisphere. A.A. Balkema, Rotterdam, pp 183-208.

Bowler, J.M., 1986, Spatial variability and hydrologic evolution of Australian lake basins: analogue for pleistocene hydrologic change and evaporite formation., *Palaeogeogr., Palaeoclim., Palaeoecol*., 54: 21-41.

Brown, C.M., 1989, Structural and stratigraphic framework of groundwater occurrence and surface discharge in the Murray Basin, southeastern Australia., *BMR J. Aust. Geol. And Geophys*., 11: 127-146.

Brown, C.M. and Radke, B.M., 1989, Stratigraphy and sedimentology of mid-Tertiary permeability barriers in the subsurface of the Murray Basin, southeastern Australia., *BMR J. of Aust. Geol. and Geophys*., 11: 367-385.

Bureau of Meteorology, Australia, 2002, Climate information website, www.bom.com.au, Bureau of Meteorology, G.P.O. Box 1289K MELBOURNE VIC 3001 Telephone: (03) 9669 4000 Fax: (03) 9669 4699.

Carlson, C.A., Phillips, F.M., Elmore, D. and Bentley, H.W., 1990, Chlorine-36 tracing of salinity sources in the Dry Valleys of Victoria Land, Antarctica., *Geochim. et Cosmochim. Acta*, 54: 311-318.

Chambers, L.A., White, I., Ferguson, J., Radke, B.M., Evans, W.R., 1995, Brine Chemistry of groundwater discharge zones in the Murray Basin, Australia.,*Water Resour. Res.*, 31( 5): 1343-1353.

Chivas, A.R., Keywood, M.D., Fifield, L.K. and Allan, G.L., 1996, Chlorine-36 in Australian rainfall and playas and the residence time of chloride in the Australian landscape., *Geological Society of Australia, Abstracts*.

Clark, I. And Fritz, P., 1997, Environmental Isotopes in Hydrogeology., CRC Press, 328 pp.

Cochran, G.F., Lopes, T.J., Mihevic, T., Tyler, S.W., 1988, Study of salt crust formation mechanisms on Owens (Dry) Lake, CA., *Water Resources Publ. 41108*., Desert Research Institute, Reno, NV.

Collins, A.G., 1975, Geochemistry of oilfield waters., Developments in Petroleum Science, 1., Elsevier, Amsterdam.

Conard, N.J., Elmore, D., Kubik, P.W., Gove, H.E., Tubbs, L.E., Chrunyk, B.A. and Wahlen, M., 1986, The chemical preparation of AgCl for measuring $^{36}$Cl in polar ice with accelerator mass spectrometry., *Radiocarbon*., 28: 556-560.

Connell, T.L. and Dreiss, S.J., 1995, Chemical evolution of shallow groundwater along the northeast shore of Mono Lake, California., *Water Resour. Res*., 31(12): 3171-3182.

Cook, P.G., Jolly, I.D., Leaney, F.W., Walker, G.R., Allan, G.L., Fifield, L.K., Allison, G.B., 1994, Unsaturated zone tritium and chlorine-36 profiles from southern Australia: Their use as tracers of soil movement., *Water Resour. Res*., 30(6): 1709-1719.

Cook, P.G., Kennett-Smith, A.K., Walker, G.R., Budd, G.R., Williams, R.M. and Anderson, R., 1996, Impact of dryland agriculture on land and river salinisation in the Western Lands, New South Wales., *CSIRO Div. of Water Resources Technical Memorandum* 96.16.

Craig, H., 1961, Isotopic variations in meteoric waters., *Science*, 133: 1702-1703.

Craig, H. and Gordon, L., 1965, Deuterium and oxygen-18 variation in the ocean and the marine atmosphere. In: E. Tongiorgi (Ed.), *Stable Isotopes in Oceanographic Studies and Paleotemperatures, Spoleto 1965*, pp. 9-130.

Dansgaard, W., 1964, Stable isotopes in precipitation., *Tellus*, 16: 436-468.

Davie, R.F., Kellett, J.R., Fifield, L.K., Evans, W.R., Calf, G.E., Bird, J.R., Topham, S. and Ophel, T.R., 1989, Chlorine-36 measurements in the Murray Basin: preliminary results from the Victorian and South Australian Mallee region., *BMR J. Aust. Geol. and Geophys*., 11: 261-272.

Davis, R.J. and Schaeffer, O.A., 1955, Chlorine-36 in nature., *Ann. N.Y. Acad. Sci.*, 62: 105-122.

Deines, P., Langmuir, D and Harmon, R.S., 1974, Stable carbon isotope ratios and the existence of a gas phase in the evolution of carbonate ground waters., *Geochim. et Cosmochim. Acta.*, 38: 1147-1164.

Dincer, T., 1968, The use of oxygen-18 and deuterium concentrations in the water balance of lakes., *Water Resour. Res.*, 4(6): 1289-1306.

Dogramaci, S.S. and Herczeg, A.L., 2002, Strontium and carbon isotope constraints on carbonate-solution interactions and inter-aquifer mixing in groundwaters of the semi-arid Murray Basin, Australia., *J. Hydrol.*, 262: 50-67.

Draper, J.J. and Jensen, A.R., 1976, The geochemistry of Lake Frome, a playa lake in South Australia., *BMR J. Aust. Geol. Geophys.*, 1: 83-104.

Drever, J.I. and Smith, C.L., 1978, Cyclic wetting and drying of the soil zone as an influence on the chemistry of ground water in arid terrains: *Am. J. Sci.*, 278: 1448-1454.

Drever, J.I., 1982, The Geochemistry of Natural Waters., Prentice-Hall Inc., U.S.A., 388 pp.

Duktiewicz, A., Herczeg, A.L. and Dighton, J.C., 2000, Past changes to isotopic and solute balances in a continental playa: clues from stable isotopes of lacustrine carbonates., *Chem. Geol.*, 165: 309-329.

Duffy, C.J. and Al-Hassan, S., 1988, Groundwater circulation in a closed desert basin: topographic scaling and climatic forcing., *Water Resour. Res.*, 24(10):1675-1688.

Ehalt, D., Knott, K., Nagel, J.F. and Vogel, C., 1963, Deuterium and oxygen-18 in rain water., *J. Geophys. Res.*, 68: 3775-3780.

Endt, P.M. and Van der Leun, C., 1973, Energy levels of A = 21-44 nuclei., *V. Nucl. Phys.* A214: 1-625.

Epstein, S. and Mayeda, T., 1953, Variations of O-18 content of water from natural sources., *Geochim. et Cosmochim. Acta*, 4: 213-224.

Eugster, H.P., 1970, Chemistry and origin of the brines of Lake Magadi, Kenya., *Mineral. Soc. Am. Spec. Pap.*, 3: 215-235.

Eugster, H.P. and Hardie, L.A., 1978, Saline Lakes. In: A. Lerman (ed.), Lakes: Chemistry, Geology, Physics, Springer-Verlag, New York, pp 237-293.

Eugster, H.P, and Jones, B.F., 1979, Behaviour of major solutes during closed-basin brine evolution., *Am. J. Sci.*, 279: 609-631.

Evans, W.R. and Kellett, J.R., 1989, The hydrogeology of the Murray Basin, southeastern Australia., *BMR J. Aust. Geol. and Geophys*., 11: 147-166.

Fan, Y., Duffy, C.J. and Oliver, D.S. Jr., 1997, Density-driven groundwater flow in closed desert basins: field investigations and numerical experiments., *J. Hydrol*., 196:139-184.

Feige, Y., Oltman, B.G. and Kastner, J., 1968, Production rates of neutrons in soils due to natural radioactivity., *J. Geophys. Res*., 73: 3135-3142.

Ferguson, J., Radke, B.M., Jacobson, G.J., Evans, W.R., Chambers, L., White, I.A. and Wooding, R.A., 1995, The Mourquong Discharge Complex and Disposal Basin, Murray Basin, SE Australia., *AGSO Record, 1995/9.* Australian Geological Survey Organisation, Canberra.

Fetter, C.W., 1994, Applied Hydrogeology, 3rd Edition., Prentice-Hall, Inc., New Jersey, 691 pp.

Fontes, J-C. and Gonfiantini, R., 1967, Fractionnment isotopique de l'hydrogene dans l'eau de crystallization du gypse., *Compes. Rend. Acad. Sci. Paris*, 265: 4-6.

Fontes, J-C. and Garnier, J-M., 1979, Determination of the Initial C-14 Activity of the Total Dissolved Carbon: A Review of the Existing Models and a New Approach., *Waer Resour. Res*., 15(2): 399-413.

Fontes, J-C., 1983, Radiocarbon (Carbon-14). In: Guidebook on Nuclear Techniques in Hydrology., *IAEA Technical Reports Series* No. 91, Vienna.

Fontes, J.-Ch., Brissaud, I., Michelot, J.L., 1984, Hydrological implications of deep production of chlorine 36., *Nucl. Instrum. Methods Phys. Res*., B5: 303-307.

Fontes, J. Ch., Yousfi, M. and Allison, G.B., 1986, Estimation of long-term, diffuse groundwater discharge in the northern Sahara using stable isotope profiles in soil water., *J. Hydrol*., 86: 315-327.

Freeze, R.A. and Witherspoon, P.A., 1967, Theoretical analysis of regional groundwater flow: 2. Effect of water table configuration and subsurface permeability variation., *Water Resour. Res*., 3: 623-634.

Freeze, R.A. and Cherry, J.A., 1979, Groundwater., Prentice-Hall, New Jersey, 604 pp.

Friedman, I., Redfield, A.C., Schoen, B. and Harris, J., 1964., *Rev. Geophys*., 2(1): 177-224.

Friedman, I., Smith, G.I. and Hardcastle, K.G., 1976, Studies of Quaternary saline lakes-II. Isotopic and compositional changes during desiccation of the brines in Owens Lake, California, 1969-1971., *Geochim. et Cosmochim. Acta*, 40: 501-511.

Friedman, I. and O’Niel, J.R., 1977, Data of Geochemistry (6th Ed.).,Chapter KK: Compilation of stable isotope fractionation factors of geochemical interest., *U.S. Geol. Surv. Prof. Paper*, 440-KK.

Garrels, R.M. and Mackenzie, F.T., 1967, Origin of the chemical compositions of some springs and lakes., In: Equilibrium Concepts in Natural Water Systems, R.F. Gould (ed.), *Adv. Chem. Ser*., 67: 222-242.

Garrels, R.M. and Mackenzie, F.T., 1971, Evolution of Sedimentary Rocks., Norton, NY, 397 pp.

Gat, J.R., 1971, Comments on the stable isotope method in regional groundwater investigations., *Water Resour. Res*., 7: 980-993.

Gat, J.R. and Levy, Y., 1978, Isotope hydrology of inland sabkhas in the Bardawil area, Sinai., *Limnol. Oceanogr*., 23(5): 841-850.

Gat, J.R., 1981, Isotopic Fractionation., In: Stable Isotopes in Hydrology, Deuterium and Oxygen-18 in the Water Cycle., *Technical Reports Series No. 210*, IAEA, Vienna, pp 21-34.

Gat, J.R. and Bowser, C., 1991, The heavy isotope enrichment of water in coupled evaporative systems., *The Geochemical Society, Special Publication* No. 3, 1991: 159-168.

Gat, J.R., 1995, Stable Isotopes of Fresh and Saline Lakes, In: Physics and Chemistry of Lakes, Springer-Verlag, pp 139-165.

Gonfiantini, R. and Fontes, J.C., 1963, Oxygen isotopic fractionation in the water of crystallization of gypsum., *Nature*, 200: 644 – 646.

Gonfiantini, R., 1965, Effetti isotopici nell'evaporazione di acque salate., *Atti Soc. Toscana Sci. Nat. Pisa*, Ser. A, 72: 550-569.

Gonfiantini, R., 1986, Environmental Isotopes in Lake Studies. In: Fritz, P., Fontes, J-Ch. (Eds), Handbook of Environmental Isotope Geochemistry. Vol. 2. The Terrestrial Environment. Elsevier, Amsterdam, pp. 113-168.

Greenberg, A.E., Eaton, A.D. and Cleseri, L.S., 1999, Standard Methods for the Examination of Water and Wastewater, 20th Edition., Amer Public Health Assoc., 1220 p.

Hahl, D.C. and Mitchell, C.G., 1963, Dissolved-mineral inflow to Great Salt Lake and chemical characteristics of the Salt Lake brine. Part I: Selected hydrologic data., Utah Geol. Mineral Survey, *Water Resour. Bull.* 3. 40 pp.

Hahl, D.C. and Langford, R.H., 1964, Dissolved-mineral inflow to Great Salt Lake and chemical characteristics of the salt lake brine; Part II., Utah Geol. Mineral Survey, *Water Resour. Bull.* 3. 40 pp.

Hahl, D.C., Wilson, M.T. and Langford, R.H., 1965, Physical and Chemical Hydrology of Great Salt Lake, Utah., US Geol. Survey Prof. Paper 525-C, pp 181-186. Reprinted in: Playas and Dried Lakes, J.T. Neal (ed.), Benchmark Papers in Geology, 20, Dowden, Hutchison & Ross, Inc., 1975.

Hahl, D.C. and Handy, A.H., 1969, Great Salt Lake, Utah: Chemical and physical variation of the brine, 1963-1966. *Utah Geol. Mineral Survey, Water Resour. Bull.* 12., 33 pp.

Hardie, L.A. and Eugster, H.P., 1970, The evolution of closed-basin brines., *Mineral Soc. Am. Spec. Paper.*, 3: 273-290.

Harvie, L.A. and Weare, J.H., 1980, The prediction of mineral solubilities in natural waters: The Na-K-Mg-Ca-Cl-SO4-H2O system from zero to high concentration at 25C., *Geochim. et Cosmochim. Acta*, 44: 981-998.

Hendry, M.J. and Schwartz, F.W., 1988, An alternative view on the origin of chemical and isotopic patterns in groundwater from the Milk River aquifer, Canada., *Water Resour. Res.*, 24: 1747-1763.

Herczeg, A.L., 1977, Geochemistry of groundwaters from the southern Murray Basin, Australia., Unpublished Honours Thesis, La Trobe University, Australia.

Herczeg, A.L. and Berry Lyons, W., 1991, A chemical model for the evolution of Australian sodium chloride lake brines., *Palaeogeogr., Palaeoclim., Palaeoecol.*, 84: 43-53.

Herczeg, A.L., Barnes, C.J., Macumber, P.G. and Olley, J.M., 1992, A stable isotope investigation of groundwater-surface water interactions at Lake Tyrrell, Victoria, Australia., *Chem. Geol.*, 96: 19-32.

Herczeg, A.L., 2000, Environmental Isotopes in Groundwater., In: Australian Groundwater School Notes: Fundamentals of Groundwater Science, Technology and Management., Vol. 1 (Science)., Centre for Groundwater Studies, Australia.

Herczeg, A.L., Dogramaci, S.S. and Leaney, F.W., 2001, Origin of dissolved salts in a large, semi-arid groundwater system: Murray Basin, Australia., *Marine Freshw. Res.*, 52: 41-52.

Hillel, D.J., 1991, Out of the Earth: Civilization and the Life of the Soil., The Free Press, USA.

Hines, M.E., Lyons, Wm. Berry, Lent, R.M., Long, D.T., 1992, Sedimentary biogeochemistry of an acidic, saline groundwater discharge zone in Lake Tyrrell, Victoria, Australia., *Chem. Geol.*, 96: 53-65.

Homsy, G.M. and Sherwood, A.E., 1976, Convective instabilities in porous media with through flow., *Am. Inst. Chem. Eng.*, 22: 168-174.

Horita, J., 1989, Analytical aspects of stable isotopes in brines., *Chem. Geol. (Isotope Geosciences Section)*, 79: 107-112.

Horita, J. and Gat, J.R., 1989, Deuterium in the Dead Sea: Remeasurement and implications for the isotopic activity correction in brines., *Geochim. et Cosmochim. Acta*, 53: 131-133.

Howes, N.M., 1998, Geochemistry and hydrologic processes in the evolution of hypersaline brines at a groundwater discharge area, Raak Plain, Murray Basin, Australia., unpublished Honours Thesis, Flinders University, South Australia.

Hutton, J.T. and Leslie, T.I., 1958, Accession of non-nitrogenous ions dissolved in rainwater to soils in Victoria., *Aust. J. Agric. Res.*, 9: 492-507.

Hutton, J.T., 1976, Chloride in rainfall in relation to distance from coast., *Search*, 7: 207-208.

Hvorslev, M.J., 1951, Time lag and soil permeability in groundwater observations., *U.S. Army Corps of Engineers Waterway Experimentation Station, Bulletin 36*.

Ingerson, E. and Pearson, F.J. Jr., 1964, Estimation of age and rate of motion of ground-water by the $^{14}$C-method., In: Y Miyake and T. Koyama (eds.), Recent Researches in the Fields of Hydrosphere, Atmosphere and Nuclear Chemistry., Maruzen, Japan, pp 263-283.

Jacobson, G. and Jankowski, J., 1989, Groundwater-discharge processes at a central Australian playa., *J. Hydrol.*, 105: 275-295

Johnson, A.I., 1967, Specific yield - Compilation of specific yields for various materials. *U.S. Geol. Survey Water-Supply Paper 1662-D.*

Jones, B.F. and Van Denburgh, A.S., 1966, Geochemical influences on the chemical character of closed lakes., *Int. Assoc. Sci. Hydrol.*, 70: 435-446.

Jones, B.F., VanDenbergh, A.S., Truesdell, A.H. and Rettig, S.L., 1969, Interstitial brines in playa sediments., *Chem. Geol.*, 4: 253-262.

Jones, B.F., Hanor, J.S. and Evans, W.R., 1994, Sources of dissolved salts in the central Murray Basin, Australia., *Chem. Geol.*, 111: 135-154.

Kalin, R.M., 2000, Radiocarbon Dating of Groundwater Systems., In: Cook, P.G and Herczeg, A.L. (eds), Environmental Tracers in Subsurface Hydrology, Kluwer Academic Publishers, Massachusetts, pp 111-144.

Kaufman, A., Margaritz, M., Paul, M., Hillaire-Marcel, C., Hollus, G., Boaretto, E. and Taieb, M., 1990, The $^{36}$Cl ages of the brines in the Magadi-Natron basin, East Africa., *Geochim. et Cosmochim. Acta,* 54: 2827-2834.

Keywood, M.D., Fifield, L.K., Chivas, A.R. and Cresswell, R.G., 1998, Fallout of chlorine 36 to the Earth's surface in the southern hemisphere., *J. Geophys. Res.*, 103 (D7): 8281-8286.

Kuhn, M.W., Davis, S.N. and Bentley, H.W., 1984, Measurements of thermal neutrons in the subsurface., *Geophys. Res. Lett.*, 11: 607-610.

Lal, D. and Peters, B., 1967, Cosmic ray produced radioactivity on the earth., In Handbuch der Physik., Vol. 46, ed. K. Sitte, pp 551-612. Springer-Verlag, Berlin.

Lal, D. and Arnold, J.R., 1985, Tracing quartz through the environment., Proc. Indian Acad. Sci. (Earth Planet Sci.), 94: 1-5.

Lal, D., 1988, In situ-produced cosmogenic isotopes in terrestrial rocks., *Ann. Rev. Earth Planet. Sci.*, 16: 355-388.

Langbein, W.B., 1961, Salinity and Hydrology of Closed Lakes., U.S. Geol. Survey Prof. Paper 412, pp 1-20. Reprinted in: J.T. Neal (ed.), Playas and Dried Lakes, Benchmark Papers in Geology, 20, Dowden, Hutchison & Ross, Inc., 1975.

Lapwood, E.R., 1948, *Proc. Camb. Phil. Soc.*, 44: 508.

Lawrence, C.R., 1975, Geology, hydrodynamics and hydrochemistry of the southern Murray Basin., *Geol. Surv. Vicoria Mem.*, pp 450-494.

Lawson E.M., Elliott, G., Fallon, J., Hotchkis, M.A.C., Hua, Q., Jacobsen, G.E., Lee, P., Smith, A.M., Tuniz, C. and Zoppi, U., 2000, AMS at ANTARES -The first 10 years., *Nucl. Instruments and Methods in Phys. Res. Section B: Beam Interactions with Materials and Atoms*, 172, pp 95-99.

Leaney, F.W. and Allison, G.B., 1986, Carbon-14 and stable isotope data for an area in the Murray Basin: it's use in estimating recharge., *J. Hydrol.*, 88: 129-145.

Leaney, F.W. and Herczeg, A.L., 1999, The Origin of Fresh Groundwater in the SW Murray Basin and its Potential for Salinisation., CSIRO Land and Water Technical Report 7/99, April, 1999.

Lee, C.H., 1912, An intensive study of the water resources of a part of Owens Valley, CA., *U.S. Geol. Surv. Water Supply Paper* 294.

Lerman, A., 1979, Geochemical Processes: Water and Sediment Environments., John Wiley and Sons.

Levy, D.B., Schramke, J.A., Esposito, K.J., Erickson, T.A. and Moore, J.C., 1999, The shallow ground water chemistry of arsenic, fluorine, and major elements: Eastern Owens Lake, California., *Appl. Geochem.*, 14: 53-65.

Lewis, D.W., 1983, Practical Sedimentology. Hutchinson Ross, Pennsylvania.

Long, D.T., Fegan, N.E., Lyons, W.B., Hines, M.E., Macumber, P.G. and Giblin, A., 1992, Geochemistry of acid brines: Lake Tyrrell, Victoria, Australia., *Chem. Geol.*, 96: 33-52.

Lopes, T.J., 1986, Hydrology and water budget of Owens Lake, California., MSc. Thesis, University of Nevada, Reno, 116 pp.

Love, A.J., Herczeg, A.L., Sampson, L., Cresswell, R.G. and Fifield, L.K., 2000, Sources of chloride and implications for $^{36}$Cl dating of old groundwater, southwestern Great Artesian Basin, Australia., *Water Resour. Res.*, 36(6): 1561-1574.

Lyons, W.B., Carey, A.E., Herczeg, A.L., Huey, S., Font, K.R. and Jackson, R., 1995, Preliminary ages of groundwater from flowing wells in Owens Valley near Independence, California., *Proc. American Water Resources Assoc.: Water in the 21st Century: Conservation, Demand and Supply.*, April 1995.

Lyons, W.B., Tyler, S.W., Gaudette, H.E. and Long, D.T., 1995, The use of strontium isotopes in determining groundwater mixing and brine fingering in a playa spring zone, Lake Tyrrell, Australia., *J. Hydrol.*, 167: 225-239.

Lyons, W.B., Welch, K.A. and Sharma, P., 1998, Chlorine-36 in the waters of the McMurdo Dry Valley lakes, southern Victoria Land, Antarctica: Revisited., *Geochim. et Cosmochim. Acta*, 62(2): 185-191.

Macumber, P.G., 1973, Progress report on the groundwater survey of the Avoca and Loddon valleys., In: *Groundwater Investigation Program Report 1972*, 9., Dept. Mines, Vic.

Macumber, P.G., 1983, Interactions between groundwater and surface systems in northern Victoria., Ph.D. Thesis, University of Melbourne, Melbourne, Vic., 506 pp.

Macumber, P.G., 1991, Interaction Between Ground Water and Surface Systems in Northern Victoria., Victorian Department of Conservation and Environment, Australia, 345 pp.

Macumber, P.G., 1992, Hydrological processes in the Tyrrell Basin, southeastern Australia., *Chem. Geol*., 96: 1-8.

Maddocks, G.E., 1967, The geochemistry of surface waters of the western district of Victoria. *Aust. J. Marine Freshw. Res*., 15: 35-52.

Malek, E. and Bingham, G.E., 1993, Comparison of the Bowen ratio energy balance and the water balance methods for the measurement of evaporation., *J. Hydrol*., 146: 209-220.

McDonald, J.M. and Harbaugh, A.W., 1988, A modular three-dimensional finite-difference flow model., *Techniques of Water Resources Investigations of the U.S. Geological Survey*, Book 6., 586 pp.

Merlivat, L., 1970, L'Etude quantitative de bilans de lacs a l'aides des concentrations en deuterium et oxygene-18 dans l'eau. In: *Isotope Hydrology 1970, IAEA Symposium* 129, March 1970, Vienna, pp 89-107.

Mook, W.G., 1980, Carbon-14 in hydrogeological studies., In: P.Fritz and J. Ch. Fontes (Eds.), Handbook of Environmental Isotope Geochemistry, Vol. 1, The Terrestrial Environment, A, Elsevier, Amsterdam, pp 49-74.

Morse, J.W. and Mackenzie, F.T., 1990, Geochemistry of Sedimentary Carbonates: Developments in Sedimentology., Elsevier, Amsterdam.

Mundorff, J.C., 1971, Nonthermal springs of Utah., *Utah Geol. Mineral Survey, Water Resour. Bull.* 16., 70 pp.

Narayan, K. A. and Armstrong, D., 1995, Simulation of groundwater interception at Lake Ranfurly, Victoria, incorporating variable density flow and solute transport., *J. Hydrol*., 165: 161-184.

Nishiizumi, K., Elmore, D., Ma, X.Z. and Arnold, J.R., 1984, $^{10}$Be and $^{36}$Cl depth profiles in an apollo 15 drill core., *Earth Planet. Sci. Lett*., 70: 157-163.

Peter, P., Martin, R., Wright, M. and Nefiodovas, A., 2000, Soft sediment piston core sampler and rig., unpublished technical sheet, Minesite Rehabilitation Research group, CSIRO Land and Water, Adelaide, South Australia.

Phillips, F.M., Bentley, H.W., Davis, S.N., Elmore, D. and Swannick, G.B., 1986, Chlorine-36 dating of very old groundwater II: Milk River Aquifer, Alberta., *Water Resour. Res*., 22: 2003-2016.

Phillips, F.M., Rogers, D.B., Dreiss, S.J., Jannik, N.O. and Elmore, D., 1995, Chlorine-36 in Great Basin Waters: Revisited., *Water Resour. Res*., 31: 3195-3204.

Phillips, F.M., 2000, Chlorine-36., In: Cook, P.G and Herczeg, A.L. (eds), Environmental Tracers in Subsurface Hydrology, Kluwer Academic Publishers.

Pitzer, K.S., 1973, Thermodynamics of electrolytes. 1. Theoretical basis and general equations: *J. Physical Chem*., 77: 268-277.

Plummer, L.N. and Mackenzie, F.T, 1974, Predicting mineral solubility from rate data: application to the dissolution of magnesian calcite., *Am. J. Sci*., 274: 61-83.

Plummer, L.N., Parkhurst, D.L., Fleming, G.W., and Dunkle, S.A., 1988, A computer program incorporating Pitzer's equations for calculation of geochemical reactions in brines: *U.S. Geological Survey Water-Resources Investigations Report* 88-4153, 310 pp.

Revesz, K. and Woods, P.H., 1990, A method to extract soil water for stable isotope analysis., *J. Hydrol*., 115: 397 - 406.

Robinson, R.A. and Stokes, R.H., 1959, Electrolyte Solutions. 2nd Edition., Butterworths, London, 559 pp.

Rogers, D.B., Dreiss, S.J. and Groeneveld, D.P., 1992, Near-shore groundwater and salt flat processes at Mono Lake, California., In: Hall, C.A., Doyle-Jones, V. and Widawski, B. (eds.), The History of Water: East Sierra Nevada, Owens Valley, White-Inyo Mountains, Symp. Vol. 4, pp 367-395.

Rogers, D.B., 1993, Saline Groundwater Circulation and Solute Balance at Mono Basin, California., PhD Thesis, University of California.

Rogers, P.A., 1995, Continental Sediments of the Murray Basin., In: Drexel, J.F. and Preiss, W.V. (eds), The geology of South Australia. Vol. 2: The Phanerozoic., Mines and Energy South Australia, pp 252.

Rogers, D.B. and Dreiss, S.J., 1995a, Saline groundwater in Mono Basin, California 1. Distribution., *Water Resour. Res*., 31(12): 3131-3150.

Rogers, D.B. and Dreiss, S.J., 1995b, Saline groundwater in Mono Basin, California 2. Long-term control of lake salinity by groundwater., *Water Resour. Res*., 31(12): 3151-3169.

Rural Water Commission, 1991, Mildura Hydrogeological Map (1:250000 scale), Bureau of Mineral Resources, Geology and Geophysics, Canberra, Australia.

Sheet 7328, Nowingi, 1:100 000 (Edition 1) 1977 National Topographic Map Series, Commonwealth of Australia.

Shepherd, R.G., 1989, Correlations of permeability and grain size., *Ground Water*, 30(1): 21-28.

Simmons, C.T. and Narayan, K.A., 1997, Mixed convection processes below a saline disposal basin., *J. Hydrol*., 194: 263-285.

Simmons, C.T. and Narayan, K.A., 1998, Modelling density-dependent flow and solute transport at the Lake Tutchewop saline disposal complex, Victoria., *J. Hydrol*. 206(3-4): 219-236.

Simmons, C.T., Narayan, K.A., Woods, J.A. and Herczeg, A.L., 2002, Groundwater flow and solute transport at the Mourquong saline-water disposal basin, Murray Basin, southeastern Australia., *Hydrogeol. J*., 10: 278-295.

Sinclair Knight Merz, 1996, Lake Tutchewop Investigation, Lake Tutchewop Model Calibration Report, October, 1996.

Department of Natural Resources and Environment, 2002, Victorian Groundwater Database, www.nre.vic.gov.au/dnre/grndwtr/grndwtr.htm.

Smith, D.B., Otlet, R.L., Downing, R.A., Monkhouse, R.A. and Pearson, F.J., 1975, Stable carbon and oxygen isotope ratios of groundwater from the Chalk and Lincolnshire Limestone., *Nature*, 257: 783-784.

Socki, R.A., Karlsson, H.R. and Gibson, E.K. Jr., 1992, Extraction techniques for the determination of oxygen-18 in water using preevacuated glass vials., *Anal. Chem*., 64: 829-831.

Sofer, Z. and Gat, J.R., 1972. Activities and concentrations of oxygen-18 in concentrated aqueous salt solutions: analytical and geophysical applications. *Earth Planet. Sci. Lett*., 15: 232-238.

Sofer, Z. And Gat, J.R., 1975. The isotope composition of evaporating brines: effect on the isotopic activity ratio in saline solutions., *Earth Planet. Sci. Lett*., 26: 179-186.

Spencer, R.J., Eugster, H.P., Jones, B.F. and Rettig, S.L., 1985a, Geochemistry of Great Salt Lake, Utah. 1: Hydrochemistry since 1850., *Geochim. et Cosmochim. Acta*, 49: 727-737.

Spencer, R.J., Eugster, H.P. and Jones, B.F., 1985b, Geochemistry of Great Salt Lake, Utah. 2: Pleistocene-Holocene evolution., *Geochim. et Cosmochim. Acta*, 49,: 739-747.

Stewart, M.K., 1974, Hydrogen and oxygen isotope fractionation during crystallization of mirabilite in ice., *Geochim. et Cosmochim. Acta*, 38 (1): 167-172.

Stuiver, M. and Polach, 1977, Reporting of $^{14}$C data, *Radiocarbon* 19(3): 355-363.

Talsma, T., 1963, The control of saline groundwater., *Mededelingen van de Landbouwhogeschool te Wageningen*, 63 (19): 1-68.

Tamers, M.A., Ronzani, C. and Scharpenseel, H.W., 1969, Naturally occuring chlorine-36., *Atompraxis*, 15: 433-437.

Taube, H., 1954, Use of oxygen isotope effects in the study of hydration of ions., *J. Phys. Chem.*, 58: 523 – 528.

Teller, J.T., Bowler, J.M and Macumber, P.G., 1982, Modern sedimentation and hydrology in Lake Tyrrell, Victoria, *J. Geol. Soc. Aust.*, 29: 159-175.

Thomas, J.M., Welch, A.H. and Preissler, A.M., 1989, Geochemical evolution of ground water in Smith Creek Valley - a hydrologically closed basin in central Nevada, U.S.A., *Appl. Geochem.*, 4: 493-510.

Torgersen, T., Habermehl, M.A., Phillips, F.M., Elmore, D., Kubik, P., Jones, B.G., Hemmick, T. and Gove, H.E., 1991, Chlorine 36 dating of very old groundwater 3. Further studies in the Great Artesian Basin, Australia., *Water Resour. Res.*, 27 (12): 32

Toth, J., 1963, A theoretical analysis of groundwater flow in small drainage basins., *J. Geophys. Res.*, 68: 4795-4812.

Tyler, S.W., Kranz, S., Parlange, M.B., Albertson, J., Katul, G.G., Cochran, G.F., Lyles, B.A. and Holder, G., 1997, Estimation of groundwater evaporation and salt flux from Owens Lake, California, USA., *J. Hydrol.*, 200 110-135.

Ullman, W.J. and Aller, R.C., 1982, Diffusion coefficients in nearshore marine sediments., *Limnol. Oceanogr.*, 27(3): 552-556.

Ullman, W.J., 1985, Evaporation rates from a salt pan: estimates from chemical profiles in near-surface groundwaters., *J. Hydrol.*, 79: 365-373.

Ullman, W.J. and McLeod, L.C., 1986, The late-quaternary salinity record of Lake Frome, South Australia: evidence from $Na^+$ in stratigraphically-preserved gypsum., Palaeogeogr., Palaeoclim., Palaeoecol., 54, pp 153-169.

Ullman, W.J. and Collerson, K.D., 1994, The Sr-isotope record of late Quaternary hydrologic changes around Lake Frome, South Australia., *Aust. J. Earth Sci.*, 41: 37-45.

Ullman, W.J., 1995, The fate and accumulation of bromide during playa salt deposition: An example from Lake Frome, South Australia., *Geochim. et Cosmochim. Acta*, 59(11): 2175-2186.

Vengosh, A., 2002, Salinization., In: B. Sherwood-Lollard and K. Turekian (eds.), Environmental Geochemistry, Ch. 9 Vol. 9, Treatise on Geochemistry., in press.

Vogel, J.C., 1967, Investigations of groundwater flow with radiocarbon., In: Isotopes in Hydrology (Proc. Symp. Vienna, 1966), IAEA, Vienna, pp. 383-395.

Walker, G.R. and Cook, P.G., 1991, The importance of considering diffusion when using carbon-14 to estimate groundwater recharge to an unconfined aquifer., *J. Hydrol.*, 128: 41-48.

Walker, G.R., Cook, P.G., Jolly, I.D., Hughes, M.W. and Allison, G.B., 1992, Diffuse Groundwater Recharge in the Western Murray Basin, *CSIRO Div. of Water Resources, Water Resources Series* No. 6.

Waterloo Hydrogeologic Inc., 2000, Visual MODFLOW v.2.8.2.

Whelan, J.A., 1973, Great Salt Lake Utah: Chemical and physical variations of the brine, 1966-1972., *Utah Geol. Mineral Survey, Water Resour. Bull.* 17. 24 pp.

Wigley, T.M.L. and Plummer, L.N., 1976, Mixing of carbonate waters., *Geochim. et Cosmochim. Acta*, 40: 989-985.

Wigley, T.M.L., Plummer, L.N. and Pearson, F.J. Jr., 1978, Mass transfer and carbon isotope evolution in natural water systems., *Geochim. et Cosmochim. Acta*, 42, pp 1117-1139.

Wigley, T.M.L., Plummer, L.N. and Pearson, F.J. Jr., 1979, Errata (Mass transfer and carbon isotope evolution in natural water systems)., *Geochim. et Cosmochim. Acta*, 43: 1395.

Williams, W.D., 2001, Anthropogenic salinization of inland waters., *Hydrobiol.*, 466: 329-337.

Wood, W.W and Sanford, W.E., 1990, Ground-Water Control of Evaporite Deposition., *Economic Geol.*, 85: 1226-1235.

Wood, W.W and Sanford, W.E., 1995, Eolian transport, saline lake basins, and groundwater solutes., *Water Resour. Res.*, 31(12): 3121-3129.

Wooding, R.A., 1960, Rayleigh Instability of a thermal boundary layer in flow through a porous medium., *J. Fluid Mech.*, 9: 183-192.

Wooding, R.A., Tyler, S.W. and White, I., 1997a, Convection in groundwater below an evaporating salt lake: 1. Onset of instability., *Water Resour. Res.*, 33(6): 1199-1217.

Wooding, R.A., Tyler, S.W., White, I. and Anderson, P.A., 1997b, Convection in groundwater below an evaporating salt lake: 2. Evolution of fingers or plumes., *Water Resour. Res.*, 33(6): 1219-1228.

Yadav, D.N., 1997, Oxygen isotope study of evaporating brines in Sambhar Lake, Rajasthan (India)., *Chem. Geol*., 138: 109-118.

Yechiechi, Y. and Wood, W.W., 2002, Hydrogeologic processes in saline systems: playas, sabkhas and saline lakes., *Earth Sci. Revs*., 58: 343-365.

Zimmermann, U., Ehalt, D. and Mtnnich, K.O., 1967, Soil-water movement and evapotranspiration: changes in the isotopic composition of the water., In: *Proc. Symp. Isotopes in Hydrology, Vienna, 1966*. IAEA, Vienna, pp 567 – 584.

Zuber, A., 1983, On the environmental isotope method for determining the water balance components of some lakes., *J. Hydrol*., 61: 409-427.

# Appendix A

## Rainfall Information

## Climate Data: Ouyen (Bureau of Meteorology, Australia, 2002)

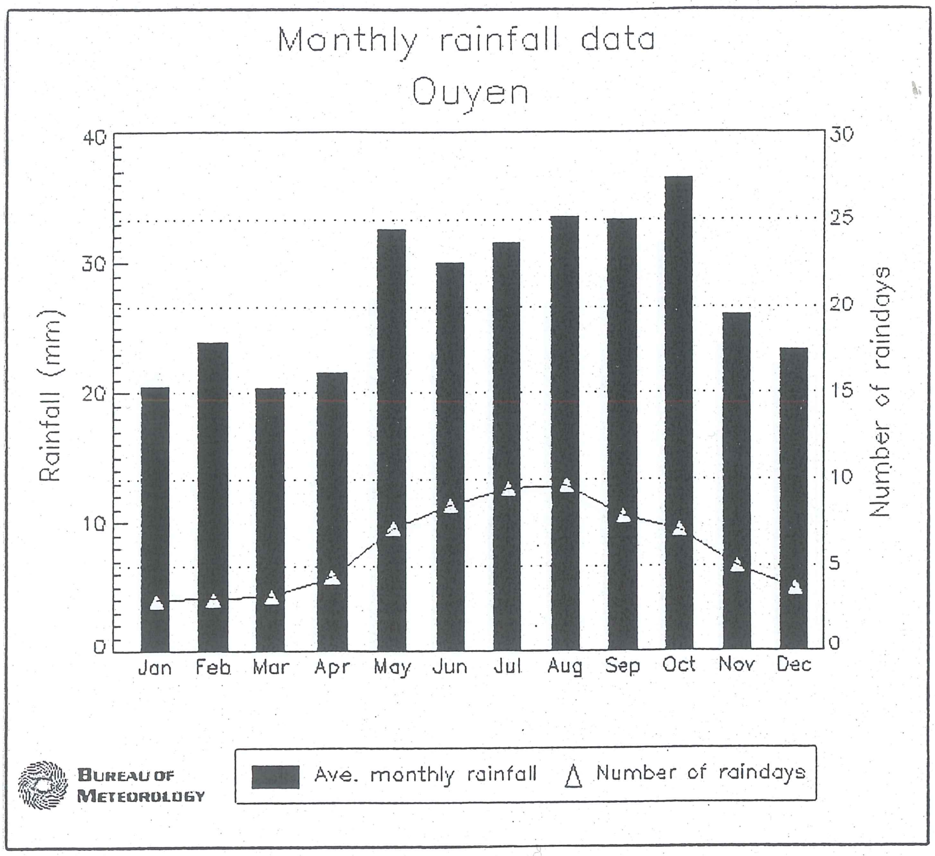

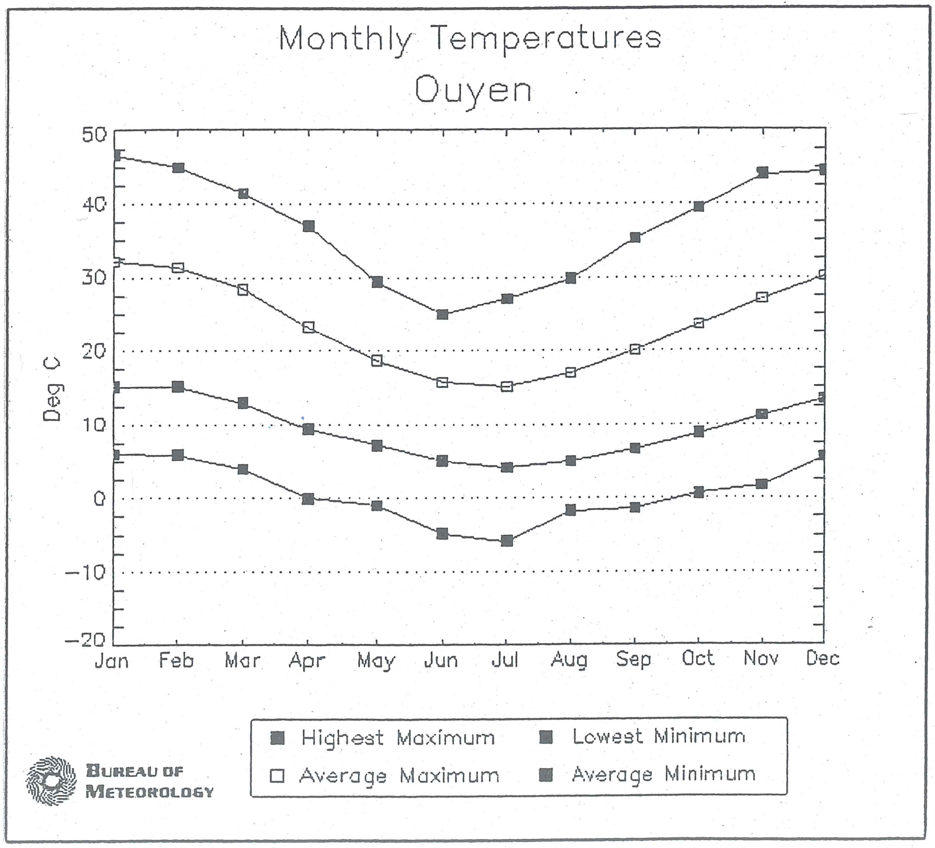

## Climate Data: Mildura (Bureau of Meteorology, Australia, 2002)

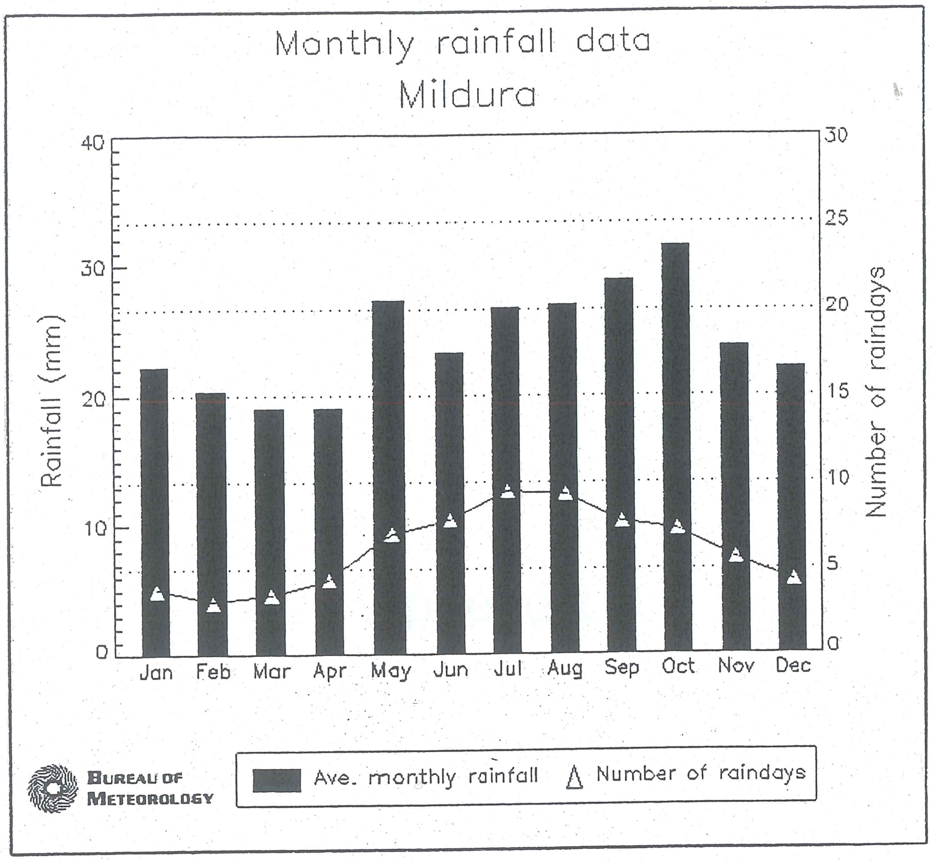

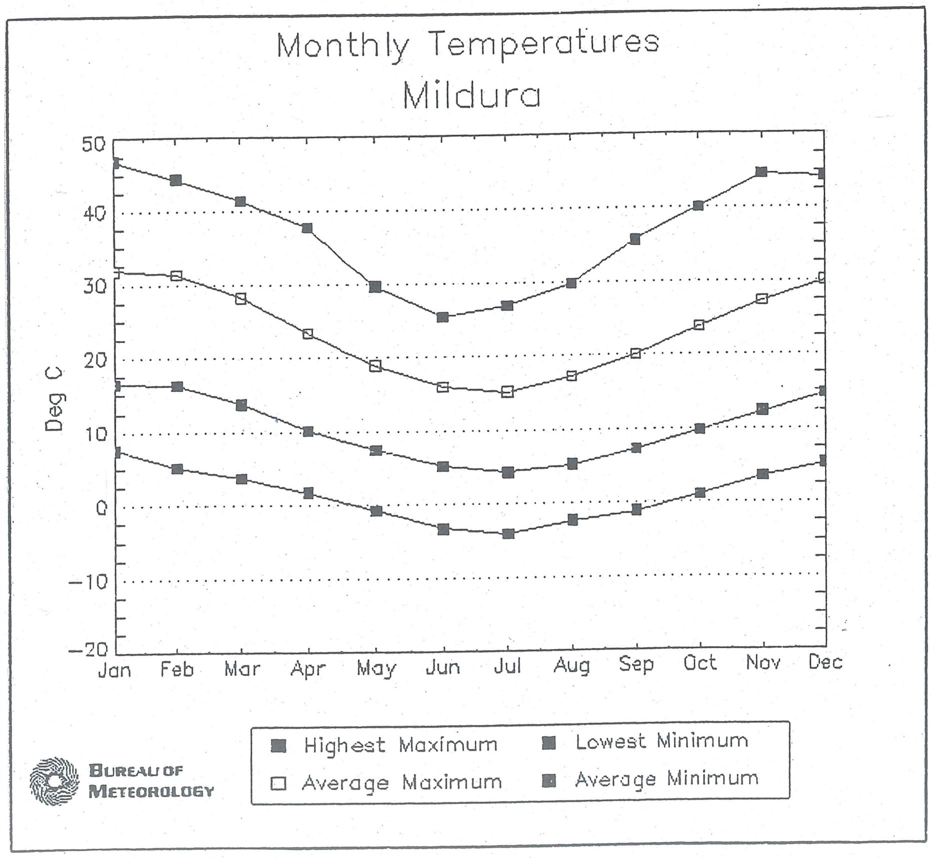

# Appendix B

## Shallow Sediment Profiles and Mineralogy Results

## Lake: Western Salina Site: West1

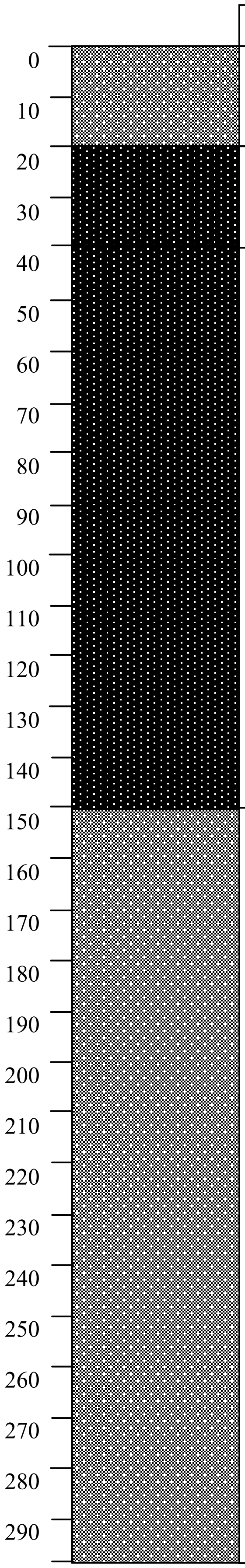

| Description | Mineralogy (XRF, XRD, SEM) |
|---|---|
| Silty SAND, minor clay. Fine-med. grained, light chocolate-brown with some red-brown nodules. Black nodules near the surface. | |
| Silty, clayey SAND, fine-grained, grey, damp. | |
| Silty clayey SAND, very dry texture, grey, increasing yellow iron staining with depth. | **40 cm**: Dominant quartz<br>Semi-dominant muscovite, kaolinite.<br>Minor albite, microcline<br>Trace halite<br>Normative calculations also predict Fe-oxy-hydroxide. |
| Silty SAND, fine-grained, alternating light brown/ yellow/ grey with hard yellow and grey nodules. | **153 cm:** Dominant quartz<br>Minor muscovite, albite, microcline<br>Trace halite, kaolinite<br>Normative calculations also predict Fe-oxy-hydroxide.<br>**166 cm:** Dominant quartz<br>Minor muscovite<br>Trace halite, albite, microcline, kaolinite.<br>Normative calculations also predict Fe-oxy-hydroxide.<br>SEM showed: Mainly quartz and halite<br>Some zircon, rutile, feldspar, biotite, barium mineral.<br>Cement between grains consists of clay, some Fe-oxy-hydroxide.<br>Narrow particle size distribution with large amount of infilling.<br>**197 cm:** Dominant quartz<br>Minor halite<br>Trace muscovite, albite, kaolinite, microcline.<br>Normative calculations also predict Fe-oxy-hydroxide.<br>SEM showed: Similar morphology to 166 cm sample.<br>Slightly smaller grainsize.<br>Orange zones consist of quartz grains coated with clay, and a little Fe. Some mica and feldspar.<br>In the grey zones, Fe approx. 25% lower, more mica. |

## Lake: Western Salina Site: West2

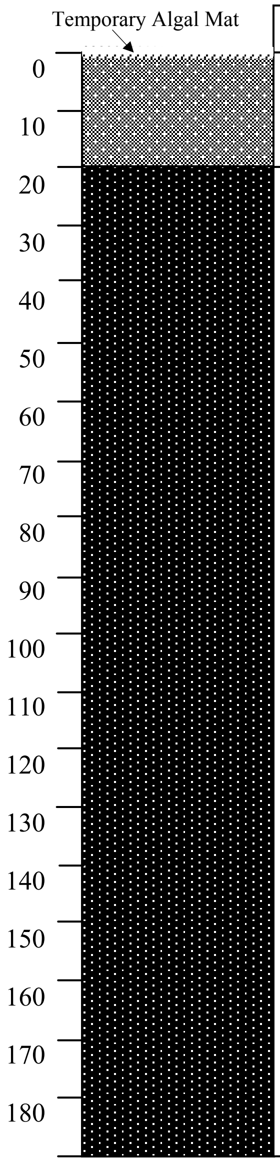

| Description | Mineralogy (XRF, XRD, SEM) |
|---|---|
| Silty SAND, minor clay. Fine-med. grained, light chocolate-brown, slushy (v. wet). | **10 cm**: Dominant quartz<br>Minor halite, muscovite<br>Trace kaolinite, microcline, celestite, albite.<br>Normative calculations also predict Fe-oxy-hydroxide.<br>SEM showed a similar morphology to the sediments at West1, but with prominent celestite crystals (Fig. 3.7). |
| Silty, clayey SAND, fine-grained, grey. Many hard iron nodules (ironstone). These can be chipped away with a spatula. The layer appears dry when a trench is dug, but water eventually seeps in through the bottom and sides. | |

## Lake: Main Salina Site: Main1

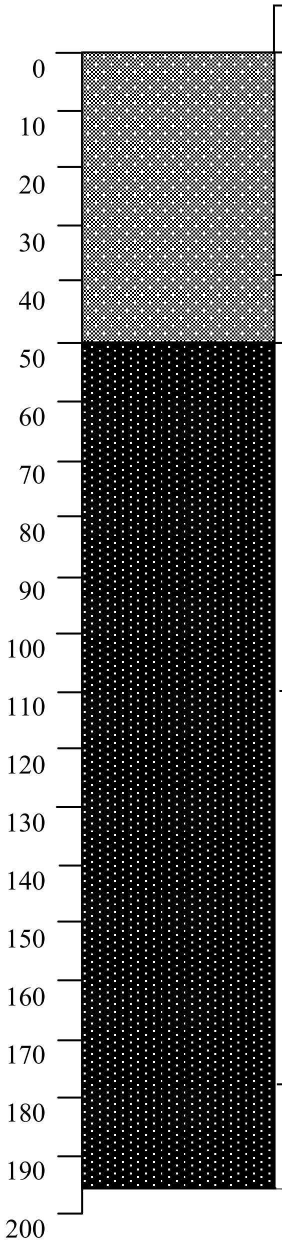

**Description**

Silty SAND. Fine-grained, dark brown. Small seed-like gypsum crystals between 2 and 30 cm.

Sediments developing a reddish colour. Hard red and yellow nodules present

Clayey SAND, fine-grained, red.

Becoming yellow in colour.

Hard red and grey nodules.

**Mineralogy (XRF, XRD, SEM)**

**4 cm**: Dominant quartz
Semi-dominant gypsum.
Minor halite
Trace muscovite, albite
Normative calculations also predict Fe minerals.

**83 cm:** Dominant quartz
Minor halite
Trace muscovite, hematite, albite, microcline, kaolinite.
SEM showed:
Coarser particle size than at Western Salina.
Dark grey areas had high Si, Al, Cl, Fe with some K and Na.
Quartz grains are covered in tiny Fe-oxy-hydroxide crystals.

**158 cm:** Dominant quartz
Minor halite
Trace hematite, microcline, gypsum, albite, muscovite.
SEM showed:
Cement between grains contained Mg and S.
Some regions with high Fe, S and Mg.
Small amounts of Al.

## **Lake: Main Salina** **Site: Main2**

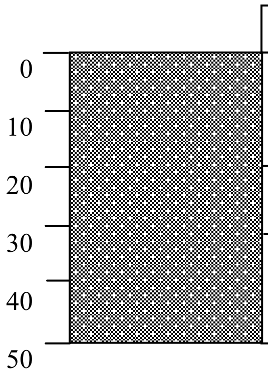

| Description | Mineralogy (XRF, XRD, SEM) |
|---|---|
| Silty SAND. Fine-grained, dark brown with some white zones. | |
| Increasing red/orange and cream-coloured mottles. Some black zones. | |
| More aggregated texture, some fine roots, lighter colour, black and orange mottles.<br>Seed gypsum between 35 and 40 cm. | **35 cm**: Dominant quartz<br>Minor halite<br>Trace muscovite, albite, microcline, kaolinite, celestite |

## Lake: Salt Lake Site: Salt1

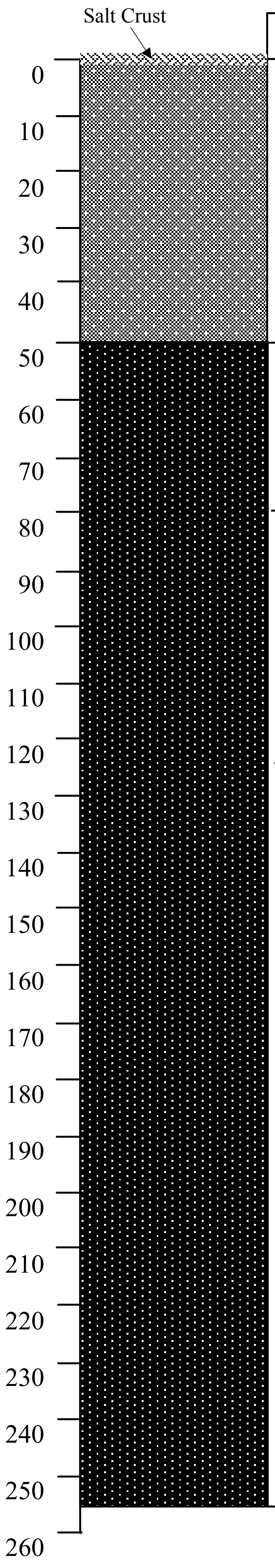

| Description | Mineralogy (XRF, XRD, SEM) |
|---|---|
| Silty SAND, 5% clay, brown. Some orange/yellow-coloured grains. | |
| Silty, clayey SAND, fine-grained, red-brown, plastic.<br>Red nodules (< 25 mm diameter).<br>Cream/grey colour, increasing yellow colour with depth. Grain-sized iron nodules, increasing in size with depth. | **60 cm**: Dominant quartz<br>Minor halite, muscovite, kaolinite.<br>Trace microcline, albite.<br>Normative calculations also predict Fe-oxy-hydroxide and jarosite.<br>SEM showed: Red nodules consist of quartz with some feldspar cemented with ilmenite ($FeTiO_3$) or rutile ($TiO_2$), Fe-oxy-hydroxide and clay. Grey zones also contained ilmenite and feldspar, but more biotite and quartz. Difference in colour due to dispersion of Fe-oxy-hydroxide minerals. More dispersed in orange zones and more localized in grey zones. Approximately double Fe in orange zones.<br>**100 cm:** Dominant quartz.<br>Minor halite.<br>Trace muscovite, kaolinite, microcline, albite.<br>Normative calculations also predict Fe-oxy-hydroxide.<br>SEM gave the same results as for the 60 cm sample with the following exceptions:<br>Scattered zircons in the white/grey zones.<br>Monazite ((Ce,La,Nd,Th)($PO_4SiO_4$)) and weathered mica in orange zones.<br>**125 cm:** Dominant quartz<br>Minor halite<br>Trace muscovite, kaolinite, microcline, albite.<br>Normative calculations also predict Fe-oxy-hydroxide and jarosite. |

## Lake: Spectacle Lake Site: SM1

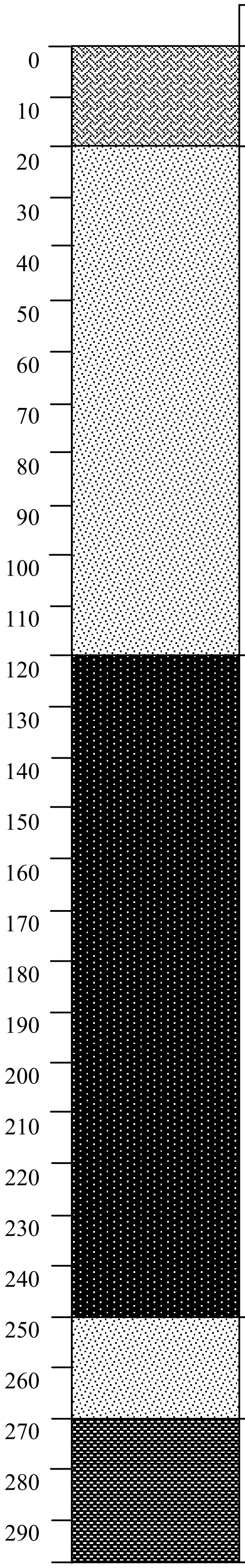

| Description | Mineralogy (XRF, XRD, SEM) |
|---|---|
| Salt Crust. | Salt Crust: Dominant halite<br>Trace gypsum and bischofite ($MgCl_2.6H_2O$) |
| SAND, med.-coarse-grained, cream/grey with red/brown mottles. | **50-100 cm**: Dominant quartz<br>Minor halite.<br>Trace calcite, illite/mica, albite, orthoclase, gypsum and hexahydrite. |
| Silty clayey SAND, fine-grained, stiff, grey/green, red/brown mottles, dry texture. | **120-130 cm:** Co-dominant quartz and probable interstratified smectite<br>Minor illite/mica, kaolinite and halite.<br>Trace albite, orthoclase, gypsum and calcite.<br>**160-170 cm:** Co-dominant quartz and probable interstratified smectite.<br>Minor illite/mica, kaolinite, halite.<br>Trace albite, orthoclase. |
| SAND, fine-med.-grained, wet, sloppy. | **240 cm-250 cm:** Dominant quartz<br>Minor probable interstratified smectite, illite/mica, kaolinite, halite.<br>Trace albite, orthoclase. |
| Silty CLAY, grey with brown mottles, dry, tight. | |

## Lake: Spectacle Lake Site: SM5

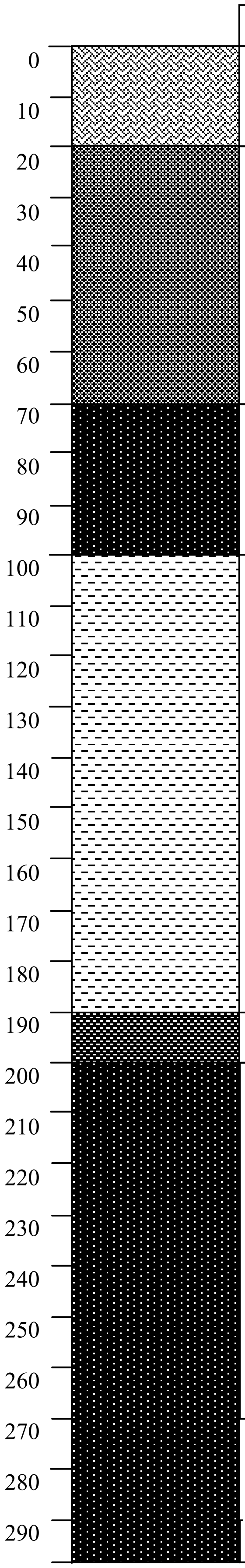

| Description | Mineralogy (XRF, XRD, SEM) |
|---|---|
| Salt Crust, iron stained. | **0-10 cm:** Dominant halite, trace gypsum, bischofite.<br>**10-20 cm:** Dominant halite, trace quartz, gypsum, bischofite and albite. |
| Black clayey sludge, containing halite crystals. | **20-30 cm**: Dominant halite<br>Trace quartz, gypsum, glauberite, rozenite and bischofite. |
| Clayey SAND, blue/grey. | |
| CLAY, grey, mottled, minor silt, becoming brown/grey and stiffer with some yellow/brown mottles. | |
| Silty CLAY, grey/brown, increased moisture. | |
| Silty SAND, fine, brown/grey. | **260 cm-270 cm:** Dominant quartz<br>Minor albite, orthoclase, illite/mica.<br>Trace halite, kaolinite. |
| Red/brown with 5% clay. | |
| Becoming grey with many red/brown mottles. | |

# Appendix C

## Site Photos

# Western Salina

Figure C1. View east over Western Salina from the top of a sand dune, showing recently ponded rainfall. This water blows across the playa surface with the prevailing wind until it is evaporated or infiltrates to the shallow water table. During extended rainy periods, this water body, only a few centimetres deep, can persist prompting the growth of algae at the playa surface.

Fig. C2. View of piezometer transect West2 at Western Salina (see Fig. 2.1 for location), showing temporary cover of ponded rainwater.

Fig. C3. Surface of Western Salina, showing location of piezometer West3 (see Fig. 2.1 for location).

Figure C4. View of Western Salina, looking east towards piezometers West1a and West1b near the centre of the playa. The vegetation around the rim of the playa is saltbush.

## The Main Salina

Fig. C5. View of the Main Salina, looking from the edge north-west towards piezometer Main1 at the centre. A thin film of water covers the playa surface due to recent rain. Recent expansion of the playa can be seen as it has encroached on an old fenceline.

Figure C6. View of piezometers Main3 and Main4 at the edge of the Main Salina (see Fig. 2.1 for locations), showing saltbush vegetation at the rim of the playa.

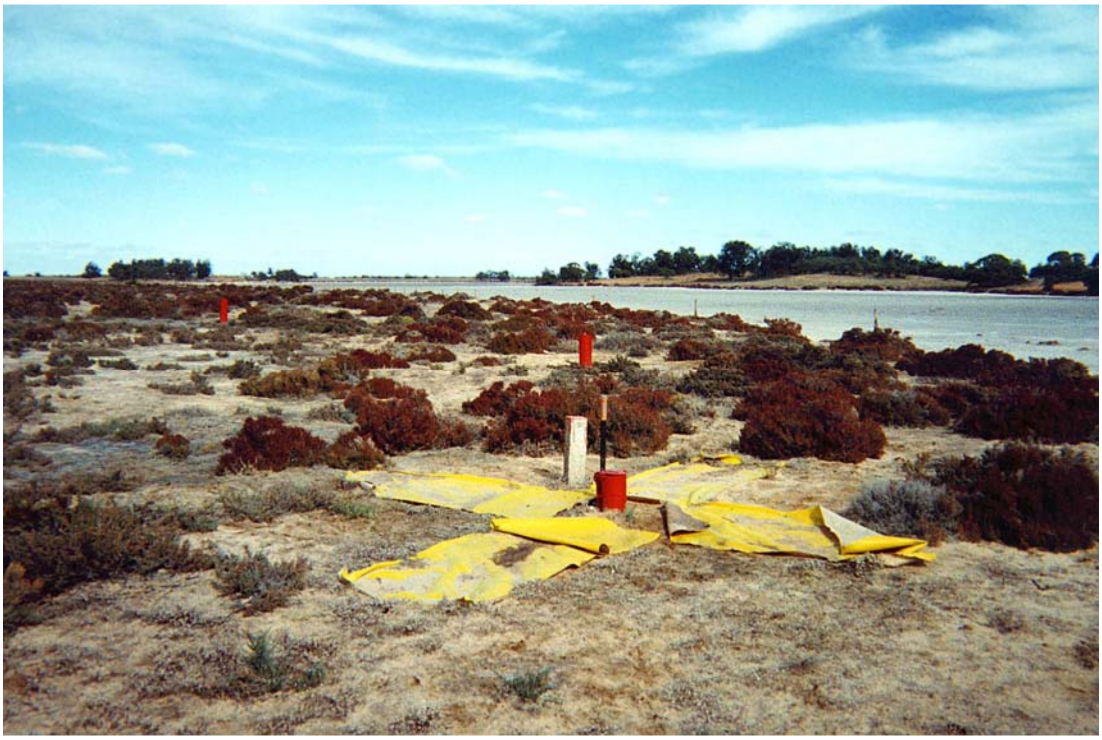

Fig. C7. Shallow bore 98348 (foreground with yellow plastic) and regional groundwater bores 98347 and 98349 (background) at the edge of the Main Salina (see Fig. 2.1 for locations).

Figure C8. Halite (NaCl) “strand-lines” observed on the playa surface, near the edge of the Main Salina in April 2001.

Figure C9. View of the Main Salina, looking north from the playa edge, towards piezometer Main2 (see Fig. 2.1 for location). Surface salt efflorescences (NaCl and $Na_2SO_4MgSO_4 \cdot 5H_2O$), formed after rain, can be seen on the playa surface. This was the most extensive efflorescence covering observed during the study.

Fig. C10. Close-up of surface salt efflorescences (NaCl and $Na_2SO_4MgSO_4 \cdot 5H_2O$) observed at site Main2 at the Main Salina (see Fig. 3.4e).

## Salt Lake

Figure C11. View of the edge of Salt Lake, showing border of mallee and sheoak trees.

Figure C12. View of the edge of Salt Lake, showing the sloping beach and border of mallee trees on the eastern (far) side of the lake. The surface water can be up to 15 cm deep.

Figure C13. View of the surface of Salt Lake, showing the surface salt crust, which can be up to 5 cm thick and surface water, which can be up to 15 cm deep.

Fig. C14. Large polygonal cracks observed in the salt crust at Salt Lake. The polygons are approximately 2-3 m wide.

## Spectacle Lake

Figure C15. The salt harvesting operation at Spectacle Lake, Pond 3. Groundwater from the Parilla Sand aquifer is pumped onto the surface of the playa lake, through a series of evaporation ponds. The ponded water in Pond 3 is usually < 40 cm deep. Infrastructure associated with the harvesting operation, as well as piles of harvested evaporite minerals, can be seen in the background. Spectacle Lake is situated at the eastern margin of the Raak Plain, and is hence surrounded by mallee vegetated sand dunes (background). Piezometers SM1, SM2 and SM3 can be seen inside the right hand margin of the evaporation pond.

Figure C16. Looking north-east over Spectacle Lake, Pond 3, showing piezometers SM1, SM2 and SM3 (see Fig. 2.2 for locations). Pond 1 and Pond 2 can be seen in the background right and left respectively.

Figure C17. Pumping of regional groundwater from the Parilla Sand aquifer onto the surface of Pond 1 at Spectacle Lake. Pond 2 can be seen in the background.

Figure C18. Piezometers SM4, SM5 and SM6 at the centre of Pond 2, Spectacle Lake. The water in this evaporation pond can be up to 50 cm deep. A 20 cm thick salt crust occurs below the water, on the floor of the pond. The mallee-vegetated bordering dunes can be seen in the background.

Figure C19. The salt-crusted surface of Pond 2, Spectacle Lake, when the evaporation pond has been allowed to dry out.

Figure C20. Small evaporation ponds for evapo-concentration of the bitterns formed in Pond 3. High value bittern minerals, such as epsomite ($MgSO_4 \cdot 7H_2O$), bischofite ($MgCl_2 \cdot 6H_2O$) and sylvite ($KCl$) are precipitated in these ponds.

## Recharge Sites

Figure C21. Piezometer R1, located amongst a grove of mallee trees on a dune adjacent the western margin of Western Salina (see Figure 2.1 for location). The water table is approximately 5.5 m below ground and the piezometer is screened approximately 8 m below the water table.

Figure C22. Piezometer R2, located on a grassy plain to the east of the Main Salina (see Fig. 2.1 for location). The Main Salina can be seen in the background of the photo. The water table at this site is between 1 m and 1.5 m below ground, and the piezometer is screened 0.35 m below the water table.

Figure C23. Piezometer R3, located on top of a sand dune to the east of the Main Salina (see Fig. 2.1 for location). The water table at this site is 5 m below ground, and the piezometer is screened approximately 0.1 m below the water table.

Figure C24. Piezometer R4, located amongst a grove of sheoak trees to the east of the Main Salina. The water table at this site is 4 m below ground, and the piezometer is screened 0.84 m below the water table.

# Appendix D

## Piezometer and Bore Details

Table D1. Summary of piezometer and regional bore details. See Figures 1.6, 2.1 and 2.2 for locations.

| Lake Setting | Site # | Location | Total depth (m bgl) | Screen Depth (m bgl) | Formation | P = pre-existing C = current study |
|---|---|---|---|---|---|---|
| Western Salina | West1a | Centre of playa - nested | 3.07 | 2.57-3.07 | Blanchetown | P |
| | West1b | | 1.2 | 0.7-1.2 | Yamba/ Blanchetown | P |
| | West2a | Edge of playa- transect | 3.07 | ? | Blanchetown | P |
| | West2b | | 2.2 | ? | Blanchetown | P |
| | West2c | | 1.88 | ? | Blanchetown | P |
| | West2d | | 1.55 | ? | Blanchetown | P |
| | West2e | | 2.05 | ? | Blanchetown | P |
| | West2f | | 1.26 | ? | Blanchetown | P |
| | West3 | Edge of playa – nested with bore 50074 | 3.8 | 3.3-3.8 | Blanchetown | P |
| | West4 | | 12 | 11-12 | Blanchetown | C |
| | R1 | Vegetated sand dune | 13.8 | 13.3-13.8 | Woorinen | P |
| Main Salina | Main1 | Centre of playa | 1.95 | 1.45-1.95 | Blanchetown | P |
| | Main2 | Edge of playa | 0.5 | 0.4-0.5 | Yamba | P |
| | Main3 | Edge of playa – nested, with bores 98347, 98349, 98351 and 98350. | 15 | 14-15 | Blanchetown | C |
| | Main4 | | 7 | 6.5-7 | Blanchetown | C |
| | 98348 | | 4 | 0.5-3.5 | Blanchetown? | P |
| | R2 | Inter-dunal plain | 2.0 | 1.5-2 | Woorinen / Blanchetown | P |
| | R3 | Sand dune | 5.75 | 5.25-5.75 | Woorinen | P |
| | R4 | Inter-dunal plain | 5.25 | 4.75-5.25 | Woorinen / Yamba | P |
| Salt Lake | Salt1a | Centre of playa - nested | 2.63 | 2.13-2.63 | Blanchetown | P |
| | Salt1b | | 0.5 | 0.2-0.3 | Yamba | P |
| Spectacle Lake | SM1 | Edge of playa - nested | 18.1 | 16.1-18.1 | Blanchetown | C |
| | SM2 | | 2.7 | 0.7-2.7 | Yamba / Blanchetown | C |
| | SM3 | | 8.6 | 6.6-8.6 | Blanchetown | C |
| | SM4 | Centre of playa - nested | 7.5 | 5.5-7.5 | Blanchetown | C |
| | SM5 | | 6 | 5.5-6 | Blanchetown | C |
| | SM6 | | 18.8 | 18-18.8 | Blanchetown | C |
| Regional Bores | 50073 | See Figure 2.1 for locations | 80.5 | | Parilla | P |
| | 50074 | | 75.5 | | Parilla | P |
| | 50075 | | 69.5 | | Parilla | P |
| | 98347 | | 52 | | Parilla | P |
| | 98349 | | 74 | | Parilla | P |
| | 98350 | | 466 | | Warina Sand (Renmark Group) | P |
| | 98351 | | 49 | | Parilla | P |
| | 81945 | | 50 | | Parilla | P |
| | 26240 | | 50.5 | | Parilla | P |

# Appendix E

## Deep Sediment Logs

Lake: Western Salina Site: West4 Method: Drill Cuttings

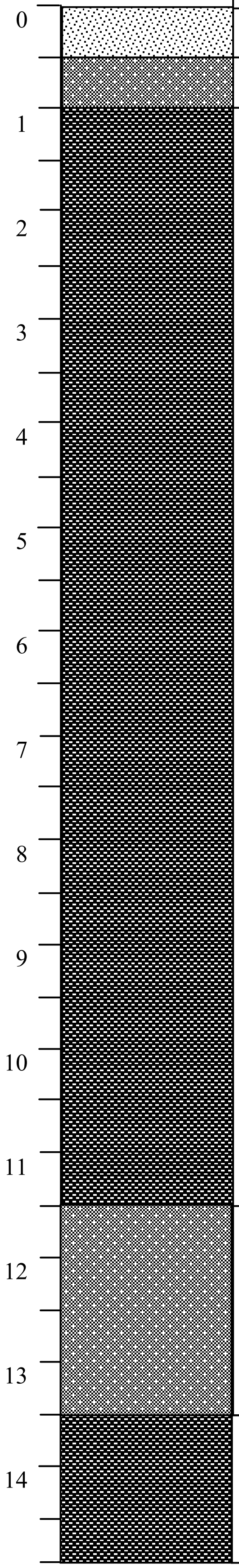

| Description |
|---|
| SAND |
| Silty SAND, grey (Playa Sediments). |
| Silty CLAY. |
| Silty SAND |
| Silty CLAY |

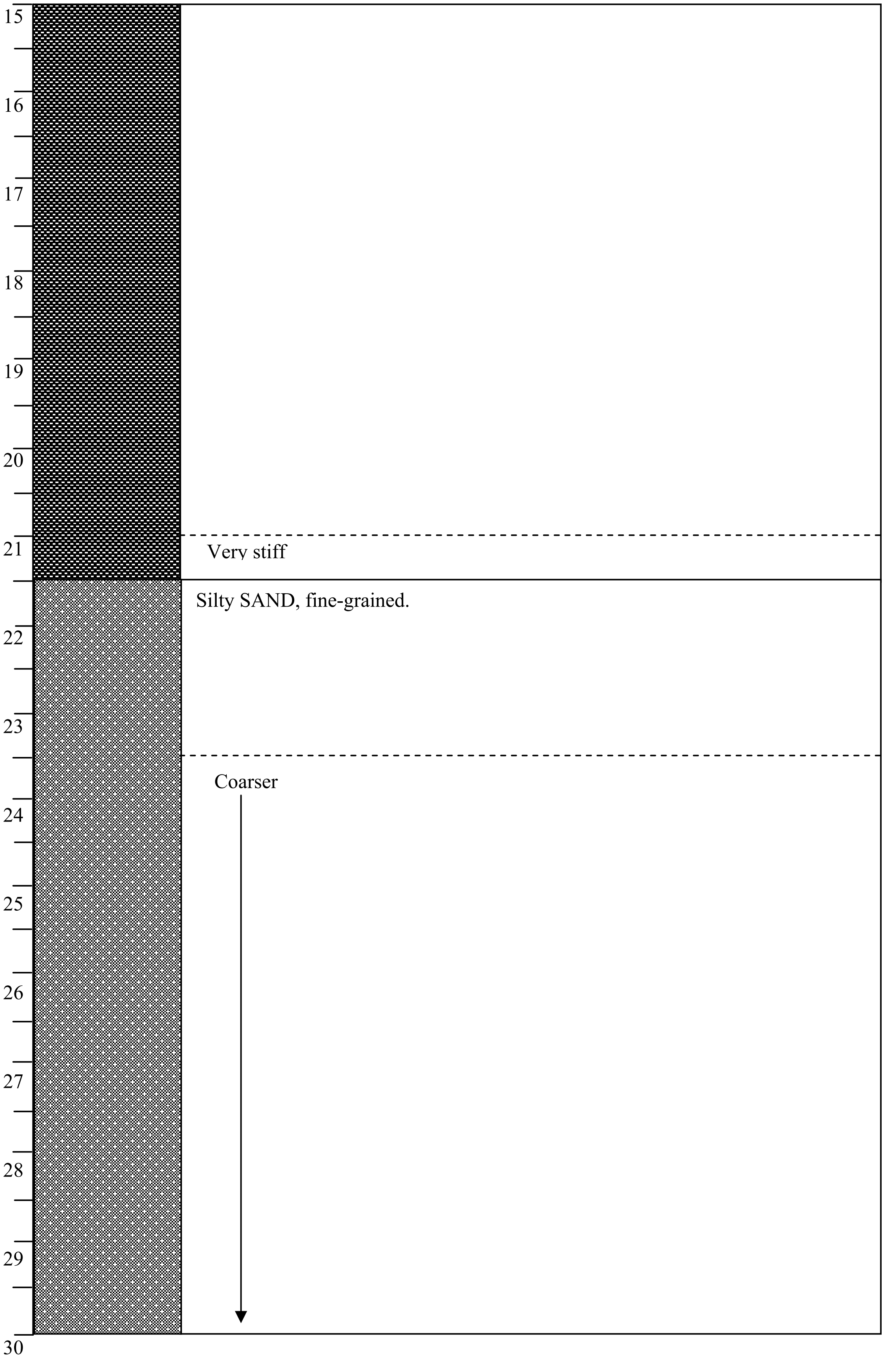
15
16
17
18
19
20
21
Very stiff
Silty SAND, fine-grained.
22
23
Coarser
24
25
26
27
28
29
30

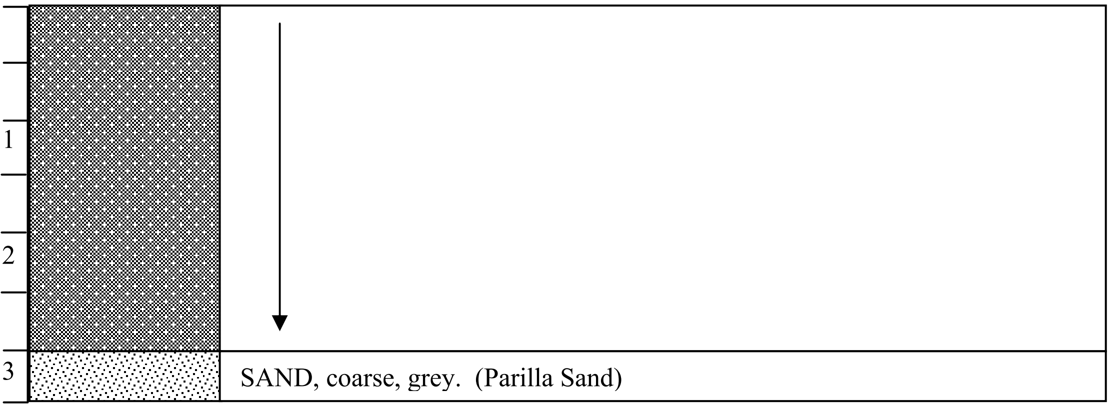

SAND, coarse, grey. (Parilla Sand)

## Lake: Spectacle Lake Site: SM1 Method: Continuous Core

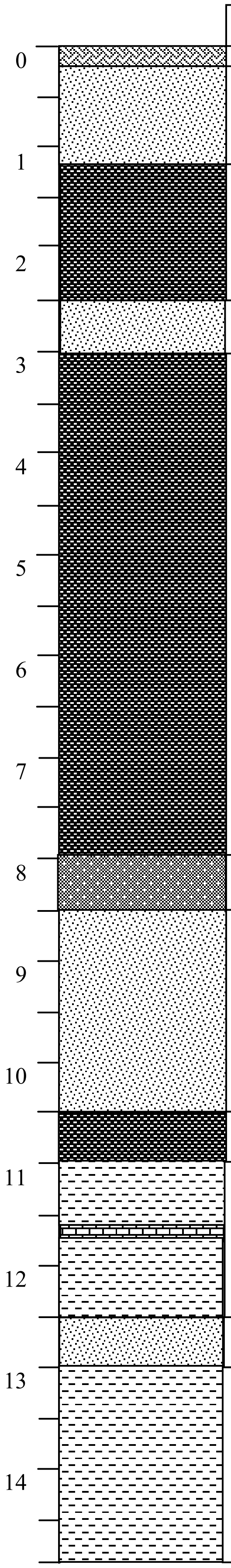

**Description**

Salt Crust.

SAND, med.-coarse-grained, cream/grey with red/brown mottles.

Silty CLAY, stiff, grey/green, red/brown mottles, dry texture.

SAND, fine-med.-grained, wet, sloppy.

Silty CLAY, grey with brown mottles, dry, tight.

Iron banding

Dark blue-grey with some yellow brown mottles

Very tight; yellow and brown mottles

Increasing fine sand; more sloppy

Becoming less mottled → grey

Silty SAND / Clayey silty SAND, fine, grey, 5% clay.

SAND, med.-coarse-grained, poorly sorted, grey.

Silty CLAY, grey, with some sandier bands.

CLAY, stiff, brown, some grey mottles, calcrete horizons.

Calcareous layer

SAND

CLAY, stiff, tight, chocolate brown.

Dry with calcrete horizons.
Sandy
“
“
CLAY, dry, brown with fine calcrete bands.

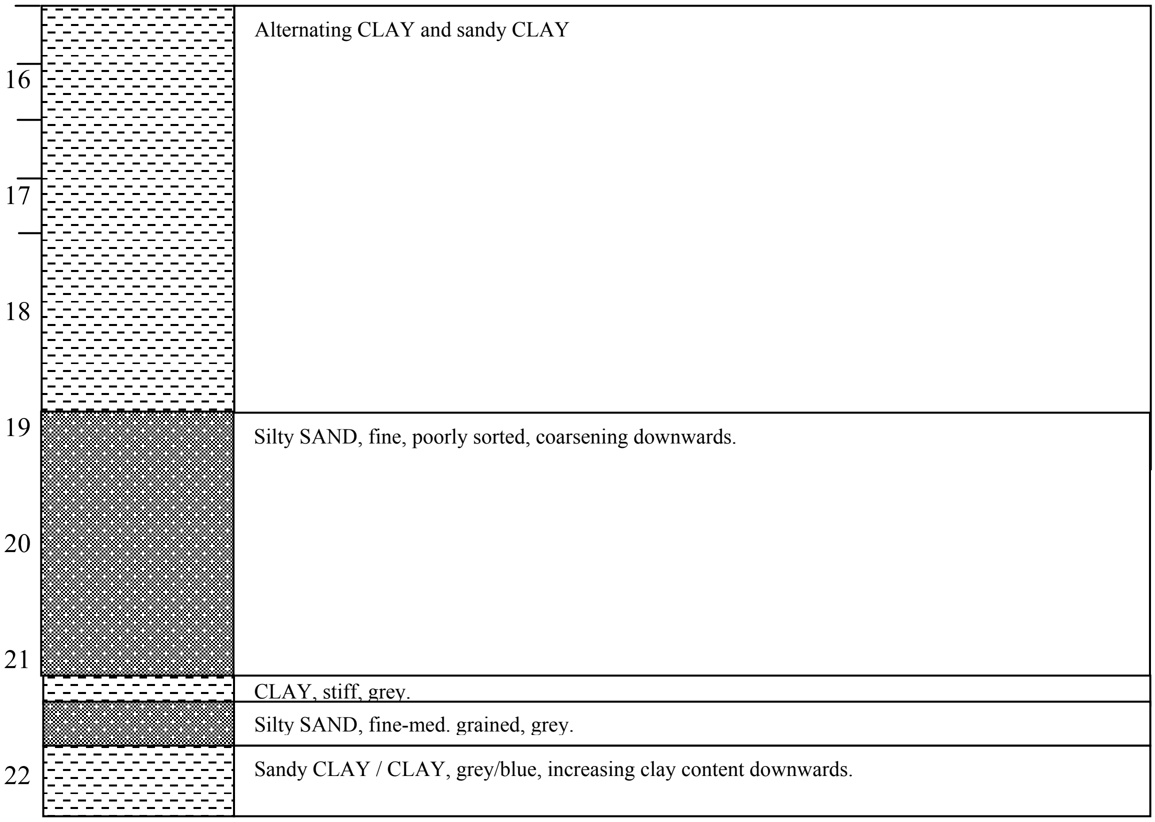

Alternating CLAY and sandy CLAY

Silty SAND, fine, poorly sorted, coarsening downwards.

CLAY, stiff, grey.

Silty SAND, fine-med. grained, grey.

Sandy CLAY / CLAY, grey/blue, increasing clay content downwards.

**Lake: Spectacle Lake** **Site: SM5** **Method: Continuous Core**

**Description**

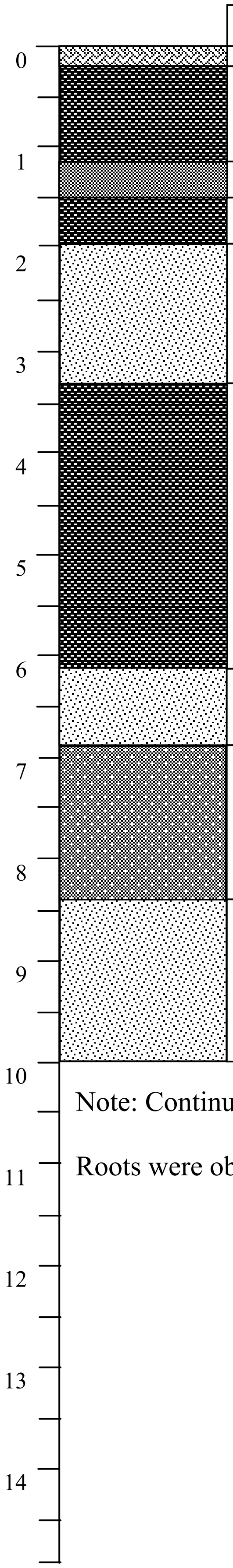

Salt Crust – iron stained.

Silty CLAY, wet, black, strong $H_2S$ smell.

Sandy CLAY, grey/blue.

Silty CLAY, grey, mottled, stiff.

SAND/ Silty SAND, fine, brown/grey, red and yellow mottles.

Silty CLAY, yellow/brown, becoming grey with red/brown mottles, minor fine sand.

SAND, fine-med.-grained, grey/brown, becoming med.-grained with yellow mottles.

Silty SAND, fine-med. grained, grey/brown with yellow mottles, becoming grey and less mottled.

SAND, medium-coarse grained, grey.

Note: Continuous core stopped at 8.5 m. Solid auger between 8.5 m and 20 m.

Roots were observed at 13.5 m.

# Appendix F

## Calculations and Results of Slug Tests

**Recovery Test: SM2**
**Depth of test: 0.7-2.7 m**
**Formation: Yamba**

T(0) = 3900 secs
r = 5 cm
Le = 200 cm
R = 15 cm

K = 4.15E-05 cm/sec
= 3.59 cm/day
= 0.04 m/day

Max. WL = 867 mm
Min. WL = 566 mm
Recovered WL = 775 mm
Drawdown = 301 mm
Recovery = 209 mm

Recovery = 69.44 %

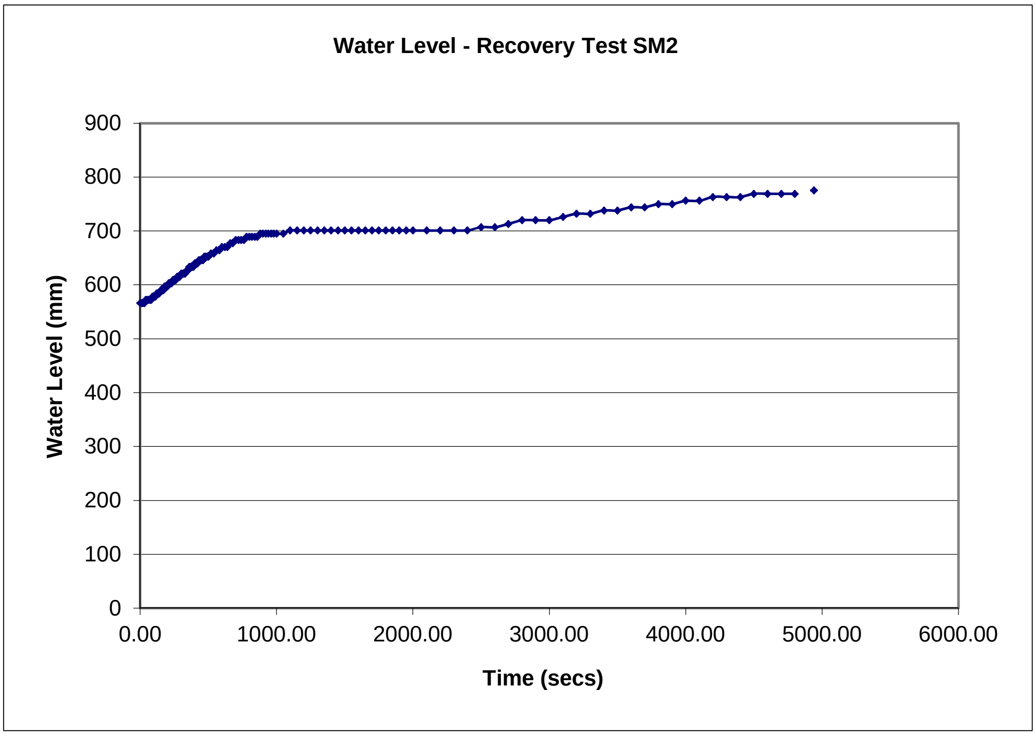

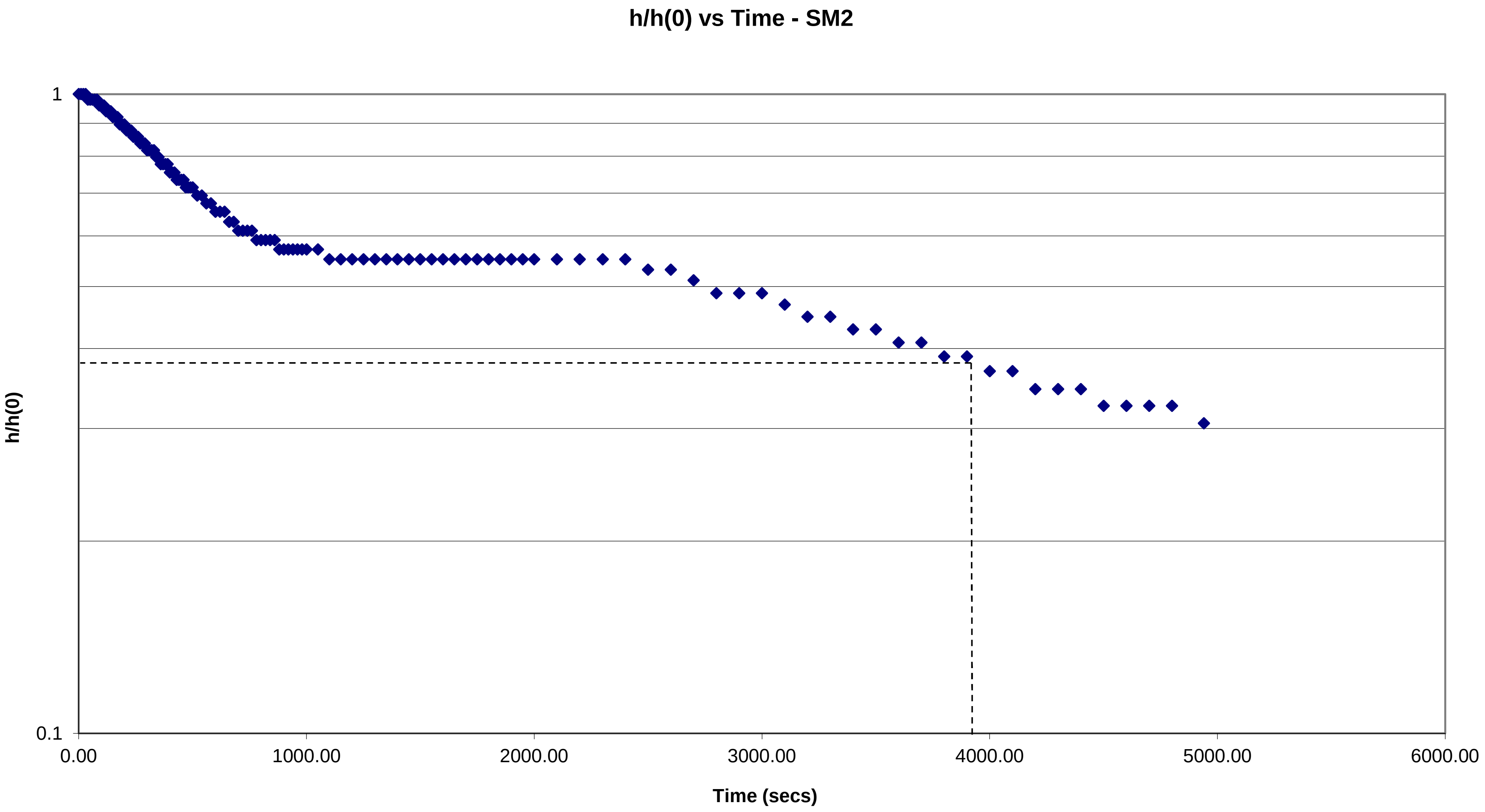
h/h(0) vs Time - SM2
1
0.1
h/h(0)
0.00
1000.00
2000.00
3000.00
4000.00
5000.00
6000.00
Time (secs)

**Recovery Test: SM4**
**Depth of test: 5.5-7.5 m**
**Formation:**

T(0) = 810 secs
r = 5 cm
Le = 200 cm
R = 15 cm

K = 0.0002 cm/sec
= 17.26845 cm/day
= 0.172684 m/day

Max. WL = 1056 mm
Min. WL = 644 mm
Recovered WL = 950 mm
Drawdown = 412 mm
Recovery = 306 mm

Recovery = 74.27184466 %

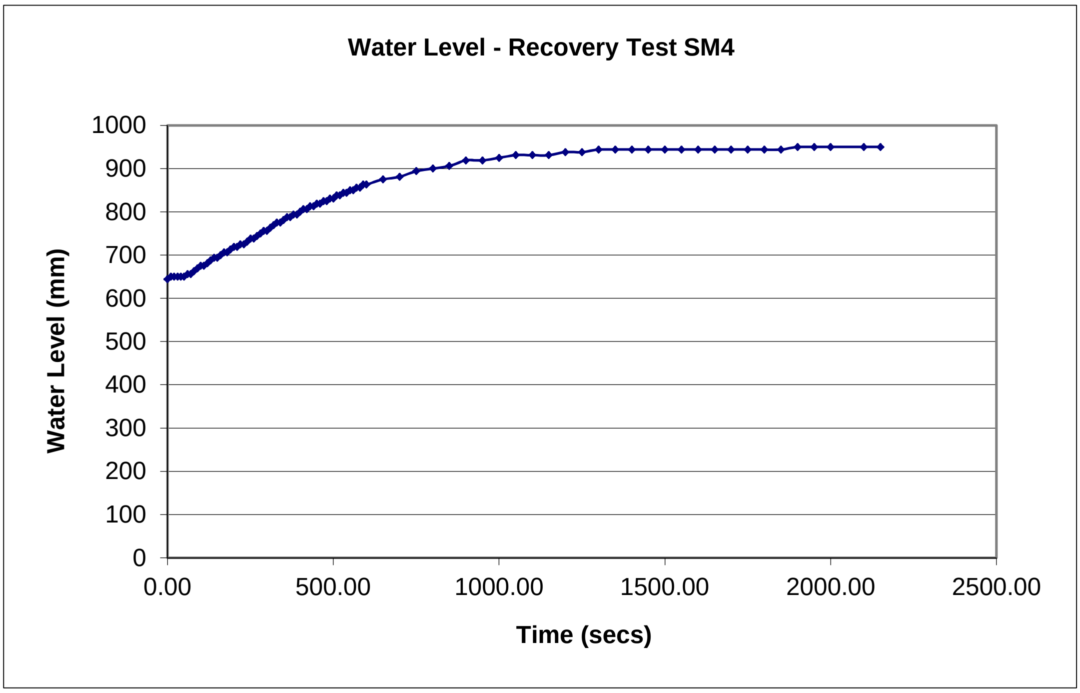

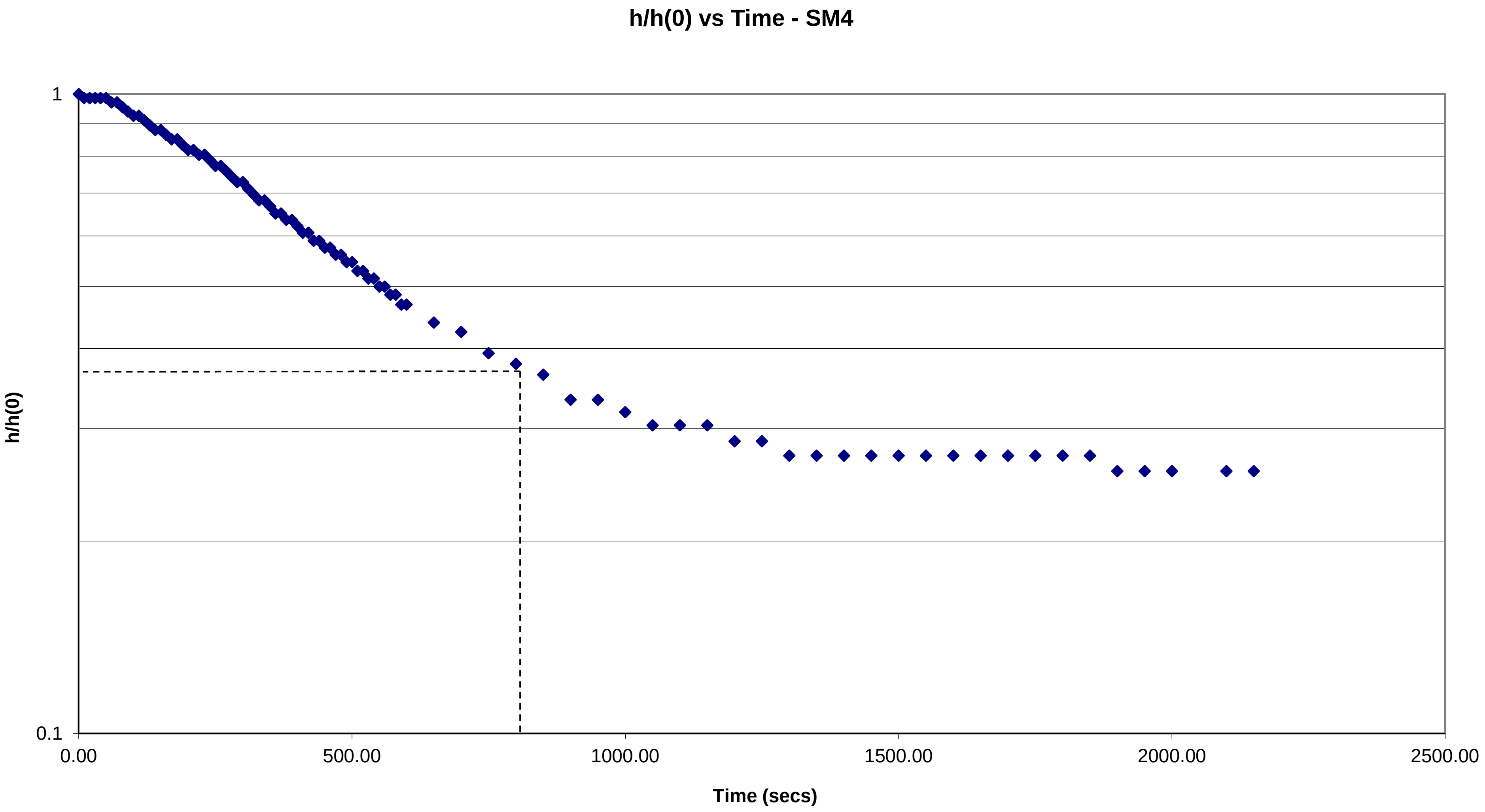
h/h(0) vs Time - SM4
1
0.1
h/h(0)
0.00
500.00
1000.00
1500.00
2000.00
2500.00
Time (secs)

**Recovery Test: SM3**
**Depth of test: 6.6-8.6 m**
**Formation:**

T(0) = 1650 secs
r = 5 cm
Le = 200 cm
R = 15 cm

K = 9.81E-05 cm/sec
= 8.477238 cm/day

Max. WL = 933 mm
Min. WL = 457 mm
Recovered WL = 826 mm
Drawdown = 476 mm
Recovery = 369 mm

Recovery = 77.52101 %

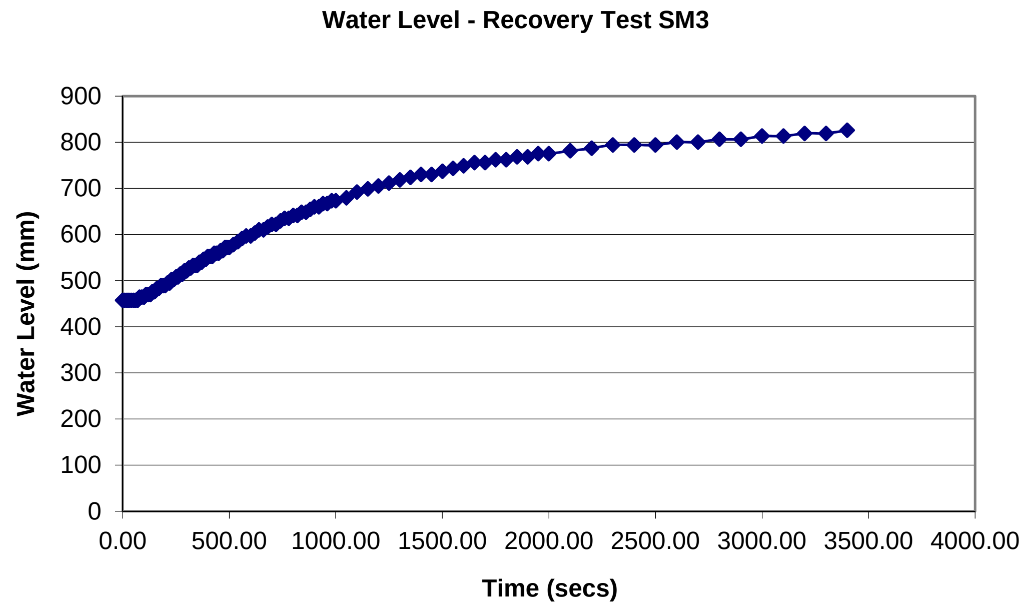

## h/h(0) vs Time - SM3

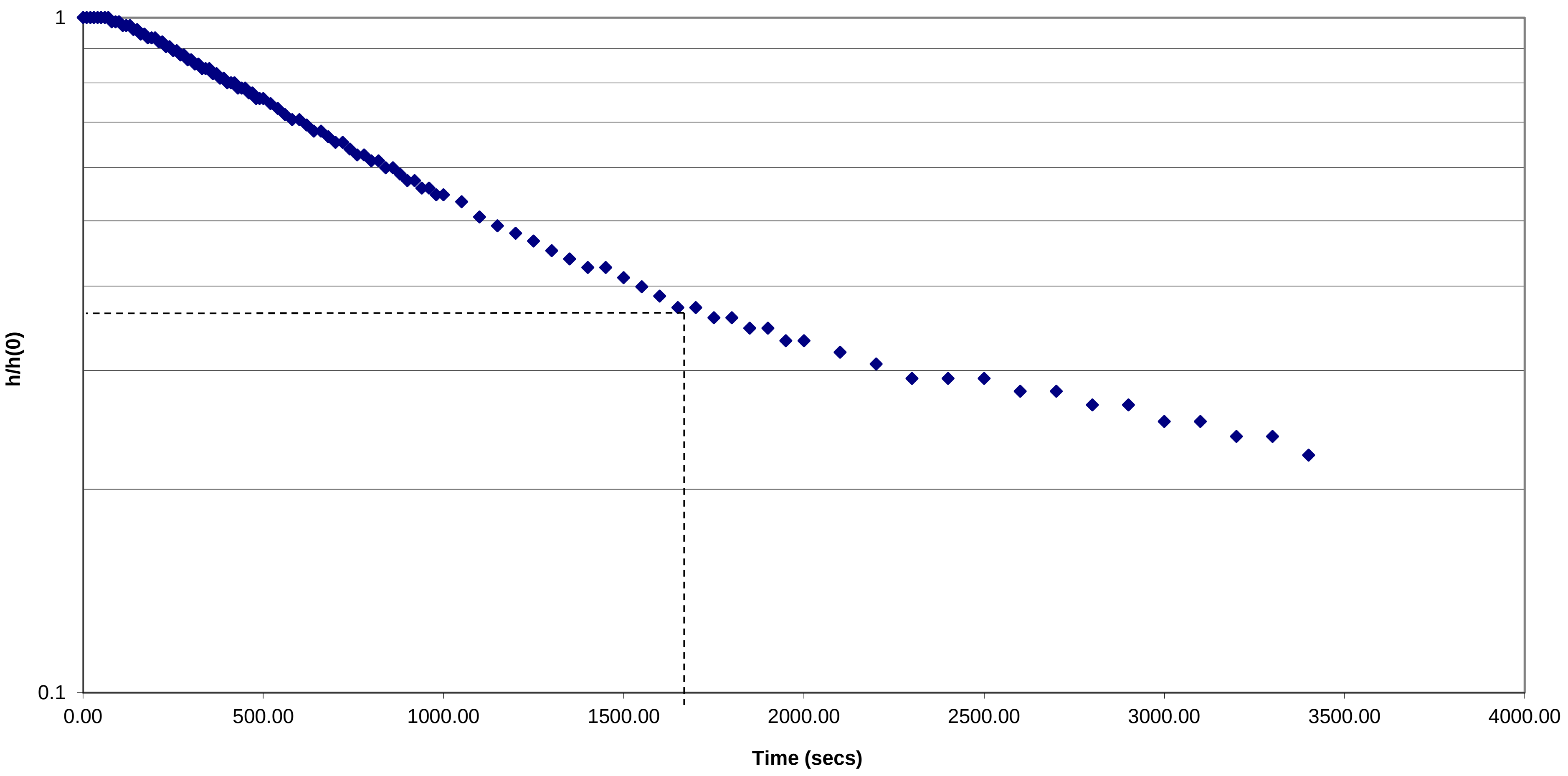

# Appendix G

## Shallow TDS vs Depth Profiles for the Natural Lakes

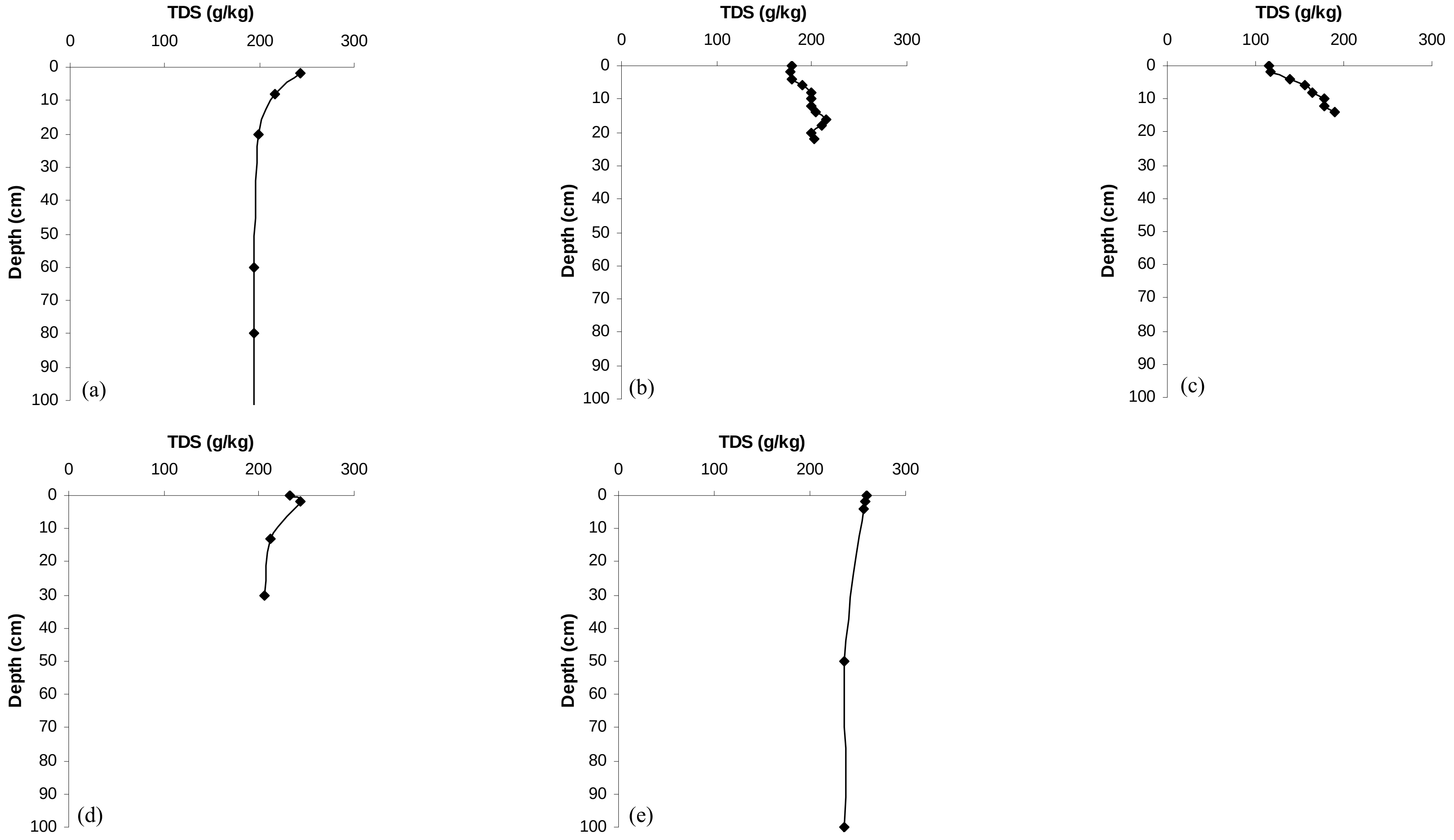

Appendix G. Summer (unless otherwise specified) TDS vs depth profiles for the natural playa lake sites: (a) West1, (b) West1 (winter 2001), (c) West2f, (d) Main1 and (e) Salt1. With the exception of the winter 2001 profile, all data was collected during the study of Howes (1998).

# Appendix H

## All Chemistry and Isotope Data

| WESTERN SALINA | | | | | | | | | | | | | | | | | delta | |
|---|---|---|---|---|---|---|---|---|---|---|---|---|---|---|---|---|---|---|
| **Site** | **Date** | **TDS** | **Cl** | **Ca** | **K** | **Mg** | **Na** | **$SO_4$** | **Sr** | **Fe** | **Br** | **$HCO_3$** | **pH** | **Eh** | **DO** | **T(C)** | **O-18** | **D** |
| | | **g/kg** | **Eq/kg** | | | | | | **mEq/kg** | | | | | **(mV)** | **(%sat)** | | **per mil** | |
| **West1(a)** | Apr-98 | 181.2 | 2.702 | 0.030 | 0.013 | 0.519 | 2.457 | 0.332 | 0.90 | 0 | 2.42 | 0.19 | 6.9 | | | 23.6 | 1.69 | -0.52 |
| | Oct-98 | 179.6 | 2.687 | 0.023 | 0.011 | 0.493 | 2.445 | 0.327 | 0.79 | 0 | 2.46 | 0.00 | 6.41 | 214 | | 17.3 | 2.18 | 0.89 |
| | Jun-99 | 196.4 | 2.855 | 0.035 | 0.018 | 0.540 | 2.782 | 0.360 | 0.61 | 0 | 2.70 | 0.12 | 5.1 | 280-300 | | 19 | 0.92 | -4.20 |
| | Sep-00 | 191.8 | 2.968 | 0.029 | 0.013 | 0.479 | 2.637 | 0.286 | 0.39 | 0 | 1.92 | 0.28 | 6.03 | 13-21 | 15.1 | 21.8 | 2.61 | -5.35 |
| | Apr-01 | 180.5 | 2.654 | 0.025 | 0.012 | 0.472 | 2.595 | 0.307 | 0.24 | 0 | 2.05 | 0.14 | 5.75 | 284 | 35.1 | 19.4 | 2.07 | 3.33 |
| | Jul-01 | 182.2 | 2.694 | 0.026 | 0.012 | 0.491 | 2.604 | 0.303 | 0.28 | 0 | 2.15 | 0.11 | 6.51 | 262 | 35.2 | 14.7 | 1.74 | 2.32 |
| **West1(b)** | Apr-98 | 189.7 | 2.869 | 0.032 | 0.015 | 0.524 | 2.552 | 0.335 | 1.08 | 0 | 2.53 | 0.26 | 7.23 | | | 22.5 | 0.85 | -2.80 |
| | Oct-98 | 184.1 | 2.782 | 0.024 | 0.012 | 0.490 | 2.513 | 0.321 | 0.82 | 0 | 2.50 | 0.00 | 7.05 | 213 | | 18.1 | 2.19 | 3.09 |
| | Jun-99 | 152.4 | 2.192 | 0.031 | 0.010 | 0.415 | 2.194 | 0.280 | 0.64 | 0 | 2.11 | 0.28 | 6.89 | 235-241 | | 15.5 | -0.54 | -8.04 |
| | Sep-00 | 188.0 | 2.726 | 0.026 | 0.013 | 0.521 | 2.684 | 0.345 | 0.32 | 0 | 2.13 | 0.31 | 5.82 | 158 | 16-21 | 21.3 | 2.16 | 2.40 |
| | Apr-01 | 186.7 | 2.758 | 0.023 | 0.012 | 0.495 | 2.650 | 0.322 | 0.22 | 0 | 2.34 | 0.08 | 6.41 | 202 | 48.4 | 20.1 | 1.95 | 3.48 |
| | Jul-01 | 185.0 | 2.736 | 0.023 | 0.011 | 0.510 | 2.616 | 0.316 | 0.26 | 0 | 2.35 | 0.04 | 5.67 | 248 | 35.2 | 16.2 | 2.22 | 2.76 |
| **West2(a)** | Apr-01 | 90.2 | 1.296 | 0.032 | 0.005 | 0.232 | 1.302 | 0.159 | 0.54 | 0 | 1.25 | 0.00 | 7.4 | -39 | 41.9 | 21.7 | -2.00 | -16.42 |
| | Jul-01 | 90.2 | 1.327 | 0.032 | 0.005 | 0.232 | 1.278 | 0.153 | 0.54 | 0 | 1.25 | 0.00 | 7.13 | -25 | 21.5 | 17.4 | -1.84 | -21.19 |
| **West2(b)** | Oct-98 | 109.1 | 1.696 | 0.039 | 0.006 | 0.264 | 1.411 | 0.189 | 1.44 | 0 | 1.68 | 0.00 | 7.04 | 194 | | 19.1 | -2.28 | -15.51 |
| | Sep-00 | 92.9 | 1.349 | 0.035 | 0.006 | 0.246 | 1.302 | 0.170 | 0.75 | 0 | 1.14 | 1.81 | 6.99 | 32-40 | 13.9 | 20 | -1.53 | -16.54 |
| | Apr-01 | 92.7 | 1.357 | 0.032 | 0.006 | 0.231 | 1.322 | 0.159 | 0.54 | 0 | 1.25 | 1.65 | 7.28 | 62 | 41.8 | 21.8 | -1.85 | -27.15 |
| | Jul-01 | 91.8 | 1.363 | 0.032 | 0.005 | 0.232 | 1.284 | 0.157 | 0.54 | 0 | 1.59 | 0.00 | 7.4 | 80 | 44.5 | 15.6 | 2.00 | -17.16 |
| **West2(c)** | Oct-98 | 102.3 | 1.610 | 0.030 | 0.006 | 0.244 | 1.355 | 0.157 | 1.43 | 0 | 1.78 | 0.00 | 7.11 | 187 | | 19 | 1.45 | -10.48 |
| | Apr-01 | 110.3 | 1.584 | 0.038 | 0.007 | 0.278 | 1.591 | 0.204 | 0.49 | 0 | 1.56 | 1.44 | 7.11 | -47 | 20.3 | 21.6 | -1.05 | -15.85 |
| | Jul-01 | 108.5 | 1.607 | 0.038 | 0.006 | 0.279 | 1.532 | 0.182 | 0.53 | 0 | 1.45 | 0.00 | 7.27 | -12 | 19.5 | 14.2 | -1.04 | -15.84 |
| **West2(d)** | Oct-98 | 150.4 | 2.372 | 0.032 | 0.008 | 0.357 | 2.010 | 0.228 | 1.28 | 0 | 2.36 | 0.00 | 6.96 | 186 | | 18.6 | -0.22 | 0.53 |
| | Sep-00 | 103.1 | 1.530 | 0.031 | 0.007 | 0.258 | 1.483 | 0.162 | 0.72 | 0 | 1.35 | 1.69 | 6.86 | -37 | 5.1 | 19.4 | 0.00 | -11.02 |
| | Apr-01 | 104.4 | 1.539 | 0.029 | 0.007 | 0.251 | 1.519 | 0.168 | 0.53 | 0 | 1.68 | 1.45 | 6.95 | 140 | 27.9 | 21.7 | -1.34 | -12.26 |
| | Jul-01 | 103.9 | 1.565 | 0.029 | 0.006 | 0.258 | 1.481 | 0.157 | 0.51 | 0 | 1.57 | 1.60 | 6.83 | 131 | 39.3 | 15.5 | -0.71 | -13.19 |
| **West2(e)** | Oct-98 | 118.0 | 1.781 | 0.031 | 0.009 | 0.305 | 1.515 | 0.237 | 1.13 | 0 | 1.74 | 0.00 | 7.39 | 168 | | 18.3 | -0.60 | -4.11 |
| | Sep-00 | 151.2 | 2.263 | 0.039 | 0.009 | 0.391 | 2.142 | 0.244 | 0.56 | 0 | 1.91 | 0.80 | 7 | -112 | 2.8 | 18.4 | 1.97 | 0.85 |
| | Apr-01 | 152.5 | 2.266 | 0.032 | 0.009 | 0.377 | 2.238 | 0.229 | 0.41 | 0 | 2.33 | 0.68 | 7.05 | 131 | 30 | 22.1 | 1.29 | -2.43 |
| | Jul-01 | 148.7 | 2.262 | 0.031 | 0.008 | 0.378 | 2.115 | 0.214 | 0.45 | 0 | 2.02 | 0.83 | 7.05 | 165 | 38.1 | 15.7 | 1.87 | 0.63 |

|  |  |  |  |  |  |  |  |  |  |  |  |  |  |  |  |  | delta |  |
|---|---|---|---|---|---|---|---|---|---|---|---|---|---|---|---|---|---|---|
| **Site** | **Date** | **TDS** | **Cl** | **Ca** | **K** | **Mg** | **Na** | **$SO_4$** | **Sr** | **Fe** | **Br** | **$HCO_3$** | **pH** | **Eh** | **DO** | **T(C)** | **O-18** | **D** |
|  |  | **g/kg** | **Eq/kg** |  |  |  |  |  | **mEq/kg** |  |  |  |  | **(mV)** | **(%sat)** |  | **per mil** |  |
| **West2(f)** | Apr-98 | 126.8 | 1.906 | 0.034 | 0.009 | 0.335 | 1.693 | 0.221 | 1.45 | 0 | 2.03 | 8.84 | 6.99 |  |  |  | 7.83 | -11.47 |
|  | Sep-00 | 137.2 | 1.986 | 0.040 | 0.011 | 0.369 | 1.914 | 0.264 | 0.59 | 0 | 1.62 | 0.62 | 7.02 | -249 | 14.8 | 20.6 | 0.97 | 1.82 |
|  | Apr-01 | 131.5 | 1.854 | 0.033 | 0.010 | 0.336 | 1.915 | 0.253 | 0.36 | 0 | 1.63 | 0.43 | 6.95 | 128 | 33.3 | 22.3 | 1.78 | 5.91 |
|  | Jul-01 | 118.1 | 1.729 | 0.029 | 0.010 | 0.290 | 1.692 | 0.200 | 0.36 | 0 | 1.32 | 0.57 | 7.1 | 159 | 41.7 | 15.1 | -0.28 | -5.34 |
| **West3** | Apr-98 | 155.7 | 2.358 | 0.040 | 0.013 | 0.437 | 2.124 | 0.251 | 1.60 | 0 | 2.84 | 2.03 | 6.55 |  |  |  | 0.04 | -13.70 |
|  | Oct-98 | 149.3 | 2.320 | 0.031 | 0.010 | 0.399 | 1.998 | 0.233 | 1.18 | 0 | 2.73 | 0.00 | 6.6 | 223 |  | 19.1 | 1.89 | -2.62 |
|  | Jun-99 | 154.9 | 2.298 | 0.045 | 0.016 | 0.430 | 2.191 | 0.249 | 0.96 | 0 | 2.90 | 0.32 |  | 215-220 |  | 13.6 | 1.37 | -21.21 |
|  | Sep-00 | 153.7 | 2.292 | 0.034 | 0.012 | 0.432 | 2.172 | 0.248 | 0.54 | 0 | 2.22 | 0.29 | 6.53 | 45-64.4 | 10.6 | 24.2 | 2.11 | -2.54 |
|  | Apr-01 | 153.1 | 2.243 | 0.031 | 0.012 | 0.418 | 2.236 | 0.247 | 0.39 | 0 | 2.65 | 0.24 | 6.43 | 125 | 40.5 | 22.5 | 2.32 | -3.97 |
|  | Jul-01 | 151.2 | 2.296 | 0.030 | 0.011 | 0.419 | 2.134 | 0.219 | 0.47 | 0 | 2.44 | 0.21 | 6.24 | 94 | 34.5 | 17.3 | 1.72 | -2.32 |
| **West4** | Jun-99 | 85.7 | 1.266 | 0.045 | 0.009 | 0.206 | 1.181 | 0.149 | 1.50 | 0 | 1.51 | 2.19 | 6.67 | 12 |  | 20.9 | -3.80 |  |
|  | Sep-99 | 89.3 | 1.351 | 0.045 | 0.009 | 0.205 | 1.212 | 0.149 | 1.54 | 0 | 1.47 | 0.00 |  |  |  |  | -3.82 | -31.85 |
|  | Sep-00 | 87.4 | 1.287 | 0.037 | 0.007 | 0.233 | 1.191 | 0.160 | 0.79 | 0 | 1.03 | 1.86 | 6.65 | -30 - 7 | 15.4 | 19.5 | -2.01 | -20.50 |
|  | Apr-01 | 85.9 | 1.238 | 0.034 | 0.007 | 0.218 | 1.237 | 0.150 | 0.65 | 0 | 1.37 | 1.80 | 6.67 | -14 | 32.5 | 21.9 | -2.23 | -21.23 |
|  | Jul-01 | 86.2 | 1.266 | 0.031 | 0.007 | 0.211 | 1.248 | 0.137 | 0.63 | 0 | 1.26 | 1.89 | 6.57 | -21 | 28 | 17.7 | -1.77 | -22.19 |
| **Ponded Water** | Sep-00 | 87.4 | 1.277 | 0.059 | 0.010 | 0.203 | 1.191 | 0.165 | 0.62 | 0 | 0.91 | 0.40 | 8.24 | -22 | 2.1 | 22.5 | 3.33 | 24.35 |
|  | Jul-01 | 92.1 | 1.355 | 0.054 | 0.008 | 0.217 | 1.276 | 0.163 | 0.44 | 0 | 1.25 | 0.40 | 8.64 | 161 | 73.5 | 20.4 | 1.57 | 9.28 |
| **R1** | Jun-99 | 74.9 | 1.112 | 0.042 | 0.009 | 0.192 | 1.014 | 0.128 | 0.00 | 0 | 1.38 | 2.68 | 6 | 40 |  | 23 | -2.47 | -19.99 |
|  | Sep-00 | 78.9 | 1.161 | 0.034 | 0.008 | 0.212 | 1.082 | 0.138 | 0.86 | 0 | 1.04 | 2.96 | 6.74 | -28 - -7 | 14.8 | 21.4 | -2.19 | -18.92 |
|  | Apr-01 | 76.4 | 1.123 | 0.030 | 0.008 | 0.205 | 1.065 | 0.129 | 0.61 | 0 | 1.27 | 2.36 | 6.87 | 82 | 32 | 20.7 | -2.00 | -18.02 |
|  | Jul-01 | 75.2 | 1.099 | 0.029 | 0.007 | 0.198 | 1.054 | 0.127 | 0.61 | 0 | 3.70 | 2.83 | 6.67 | -28 | 16.4 | 20.4 | -2.64 | -22.30 |

| **MAIN SALINA** | | | | | | | | | | | | | | | | | **delta** | |
|---|---|---|---|---|---|---|---|---|---|---|---|---|---|---|---|---|---|---|
| **Site** | **Date** | **TDS** | **Cl** | **Ca** | **K** | **Mg** | **Na** | **$SO_4$** | **Sr** | **Fe** | **Br** | **$HCO_3$** | **pH** | **Eh** | **DO** | **T(C)** | **O-18** | **D** |
| | | **g/kg** | **Eq/kg** | | | | | | **mEq/kg** | | | | | **(mV)** | **(% sat)** | | **per mil** | |
| **Main1** | Apr-98 | 187.1 | 2.844 | 0.024 | 0.017 | 0.591 | 2.561 | 0.392 | 0.96 | 0.01 | 2.85 | 0.02 | 4.7 | 106 | | 22.8 | 0.33 | -2.98 |
| | Oct-98 | 180.1 | 2.790 | 0.019 | 0.013 | 0.529 | 2.436 | 0.366 | 0.71 | | 2.84 | 0.00 | 4.36 | -206 | | 19 | 1.87 | 3.53 |
| | Jun-99 | 189.9 | 2.799 | 0.026 | 0.014 | 0.502 | 2.833 | 0.377 | | | 2.72 | 196.69 | | 194-206 | | 16.4 | 1.18 | 0.43 |
| | Sep-00 | 188.0 | 2.780 | 0.021 | 0.015 | 0.557 | 2.734 | 0.388 | | | 2.22 | 158.56 | 4.33 | -263 | 16.4 | 21.8 | 2.00 | 4.31 |
| | Apr-01 | 187.1 | 2.762 | 0.019 | 0.015 | 0.551 | 2.730 | 0.386 | 0.26 | | 2.63 | 0.26 | 4.57 | 201 | 29.1 | 21.4 | 2.56 | 4.36 |
| | Jul-01 | 181.3 | 2.770 | 0.017 | 0.013 | 0.515 | 2.539 | 0.362 | 0.24 | | 2.65 | 0.26 | 4.36 | 226 | 156.2 | 15 | 1.93 | 3.58 |
| **Main2** | Apr-98 | 187.2 | 2.749 | 0.025 | 0.012 | 0.563 | 2.593 | 0.457 | 0.77 | 0.01 | 3.35 | 0.01 | 6.92 | | | | 0.27 | -4.78 |
| | Oct-98 | 185.5 | 2.785 | 0.018 | 0.009 | 0.531 | 2.504 | 0.453 | 0.68 | | 3.22 | | 6.88 | 191 | | 20.4 | 1.60 | 0.98 |
| | Jun-99 | 185.9 | 2.718 | 0.027 | 0.012 | 0.511 | 2.643 | 0.441 | 0.46 | | 3.39 | | | 145-153 | | 15.4 | 1.92 | 0.48 |
| | Sep-00 | 189.2 | 2.703 | 0.020 | 0.011 | 0.555 | 2.725 | 0.477 | 0.13 | | 2.71 | 0.72 | 6.95 | -14 | 3.9 | 19.7 | 2.05 | 1.77 |
| | Apr-01 | 190.9 | 2.708 | 0.018 | 0.011 | 0.554 | 2.848 | 0.451 | 0.18 | | 3.01 | 0.28 | 6.87 | 140 | 25.9 | 19.2 | 1.73 | 1.69 |
| | Jul-01 | 184.5 | 2.689 | 0.017 | 0.009 | 0.526 | 2.620 | 0.449 | 0.18 | | 3.14 | 0.65 | 7.04 | 172 | 42.7 | 14.4 | 1.94 | -0.71 |
| **Main3** | Jun-99 | 49.7 | 0.741 | 0.021 | 0.007 | 0.145 | 0.685 | 0.104 | 0.71 | 2.17 | 0.96 | 0 | | 2 | | 15.4 | -5.12 | -35.06 |
| | Sep-99 | 52.0 | 0.809 | 0.021 | 0.007 | 0.143 | 0.687 | 0.102 | 0.67 | 2.20 | 0.97 | 0 | | | | | -3.87 | -28.81 |
| | Sep-00 | 53.4 | 0.826 | 0.017 | 0.007 | 0.156 | 0.703 | 0.107 | 0.33 | 5.48 | 0.71 | 0 | 6.03 | -36 | 16.9 | 20 | -3.89 | -28.06 |
| | Apr-01 | 50.7 | 0.743 | 0.016 | 0.007 | 0.148 | 0.734 | 0.099 | 0.30 | 5.09 | 0.83 | 0.92 | 6.07 | -5 | 48.9 | 19.7 | -4.22 | -30.60 |
| | Jul-01 | 50.0 | 0.763 | 0.014 | 0.006 | 0.140 | 0.689 | 0.097 | 0.28 | 4.08 | 0.87 | 0.45 | 5.72 | 39 | 41.2 | 15.3 | -4.23 | -25.67 |
| **Main4** | Jun-99 | 49.8 | 0.730 | 0.022 | 0.007 | 0.145 | 0.693 | 0.106 | 0.71 | 2.07 | 2.85 | 0 | | | | 15.8 | -5.52 | -38.18 |
| | Sep-99 | 50.4 | 0.778 | 0.021 | 0.007 | 0.141 | 0.668 | 0.102 | 0.69 | 2.07 | 0.95 | 0 | | | | | -6.01 | -41.17 |
| | Sep-00 | 50.9 | 0.756 | 0.018 | 0.006 | 0.157 | 0.704 | 0.107 | 0.33 | 4.23 | 0.60 | 0 | 5.65 | 17.2 | | 18 | -3.87 | -29.35 |
| | Apr-01 | 50.9 | 0.748 | 0.016 | 0.007 | 0.148 | 0.725 | 0.107 | 0.30 | 4.41 | 0.83 | 0.45 | 5.77 | 23.1 | | 21.6 | -4.04 | -29.37 |
| | Jul-01 | 49.0 | 0.739 | 0.014 | 0.006 | 0.141 | 0.677 | 0.099 | 0.28 | 4.08 | 0.86 | 0.61 | 5.81 | 27.3 | | 14.5 | -4.59 | -29.42 |
| **98348** | Nov-99 | 52.7 | 0.855 | 0.029 | 0.008 | 0.151 | 0.766 | 0.000 | 0.95 | 1.63 | 1.09 | 0 | 3.95 | | | 18.6 | -5.50 | -40.42 |
| | Sep-00 | 51.3 | 0.779 | 0.021 | 0.006 | 0.156 | 0.702 | 0.101 | 0.39 | 3.13 | 0.71 | 0.04 | 4.35 | -26 | 18.9 | 19.6 | -4.10 | -30.45 |
| | Jul-02 | 50.8 | 0.763 | 0.017 | 0.006 | 0.141 | 0.706 | 0.107 | 0.37 | 2.38 | 0.91 | 0 | 3.31 | 363 | 25.3 | 16.6 | -3.95 | -25.78 |
| **R2** | Oct-98 | 42.3 | 0.612 | 0.034 | 0.005 | 0.118 | 0.540 | 0.119 | 1.35 | | 0.80 | | 6.68 | 216 | | 19.3 | -5.06 | -36.26 |
| | Jun-99 | 42.9 | 0.593 | 0.037 | 0.006 | 0.123 | 0.578 | 0.123 | 1.26 | | 0.84 | | | 135-145 | | 17.2 | -5.22 | -38.72 |
| | Apr-01 | 45.2 | 0.613 | 0.035 | 0.006 | 0.125 | 0.642 | 0.127 | 0.59 | | 0.72 | 0.60 | 6.68 | 137 | 58.9 | 22.6 | -3.79 | -30.31 |
| | Jul-01 | 45.4 | 0.631 | 0.036 | 0.006 | 0.133 | 0.634 | 0.119 | 0.57 | | 0.68 | 0.56 | 6.43 | 122 | 57.5 | 17.3 | -4.33 | -26.24 |

| **Site** | **Date** | **TDS** | **Cl** | **Ca** | **K** | **Mg** | **Na** | **$SO_4$** | **Sr** | **Fe** | **Br** | **$HCO_3$** | **pH** | **Eh** | **DO** | **T(C)** | **O-18** | **D** |
|---|---|---|---|---|---|---|---|---|---|---|---|---|---|---|---|---|---|---|
|  |  | **g/kg** | **Eq/kg** |  |  |  |  |  | **mEq/kg** |  |  |  |  | **(mV)** | **(% sat)** |  | **per mil** |  |
| **R3** | Apr-98 | 23.28 | 0.312 | 0.035 | 0.003 | 0.067 | 0.285 | 0.079 | 1.90 | 0.01 | 0.42 | 0.75 | 7.48 |  |  |  | -4.76 | -33.30 |
|  | Oct-98 | 22.08 | 0.298 | 0.028 | 0.003 | 0.065 | 0.280 | 0.073 | 1.25 |  | 0.39 | 0.00 | 7.3 | 143 |  | 20.3 | -6.14 | -39.73 |
|  | Jun-99 | 23.03 | 0.314 | 0.030 | 0.003 | 0.063 | 0.284 | 0.076 | 1.23 |  | 0.42 | 0.00 |  | 167 |  | 18.5 | -4.71 | -32.14 |
|  | Apr-01 | 24.26 | 0.322 | 0.029 | 0.004 | 0.064 | 0.331 | 0.075 | 0.56 |  | 0.00 | 1.15 | 7.37 | 125 | 53.5 | 22.3 | -4.17 |  |
|  | Jul-01 | 23.52 | 0.314 | 0.029 | 0.003 | 0.064 | 0.318 | 0.071 | 0.51 |  | 0.34 | 1.15 | 7.15 | 136 | 59.8 | 21.2 | -4.33 | -30.54 |
| **R4** | Apr-98 | 206.1 | 0.788 | 0.021 | 0.006 | 0.155 | 0.739 | 0.135 | 1.64 | 0.01 | 0.97 | 81.36 | 6.64 |  |  |  | -4.32 | -30.69 |
|  | Oct-98 | 49.66 | 0.749 | 0.020 | 0.005 | 0.133 | 0.656 | 0.118 | 1.30 |  | 0.93 | 0.00 | 6.49 | 124 |  | 18.9 | -3.30 | -26.15 |
|  | Jun-99 | 52.45 | 0.755 | 0.018 | 0.006 | 0.142 | 0.749 | 0.123 | 1.01 |  | 0.98 | 0.00 |  | 84 |  | 18 | -3.18 | -26.39 |
|  | Apr-01 | 54.39 | 0.769 | 0.014 | 0.006 | 0.148 | 0.804 | 0.128 | 0.52 |  | 0.94 | 0.86 | 6.72 | 55 | 36 | 20.6 | -3.60 | -25.15 |
|  | Jul-01 | 53.65 | 0.767 | 0.013 | 0.006 | 0.148 | 0.793 | 0.120 | 0.50 |  | 0.90 | 0.79 | 6.7 | 41 | 35.2 | 19.2 | -3.64 | -27.37 |
| **Ponded Water** | Apr-01 |  | 1.005 | 0.002 | 0.001 | 0.004 | 1.035 | 0.006 | 0.02 |  | 0.00 | 0.00 |  |  |  |  |  |  |

| SALT LAKE | | | | | | | | | | | | | | | | | delta | |
|---|---|---|---|---|---|---|---|---|---|---|---|---|---|---|---|---|---|---|
| **Site** | **Date** | | **Cl** | **Ca** | **K** | **Mg** | **Na** | **$SO_4$** | **Sr** | **Fe** | **Br** | **$HCO_3$** | **pH** | **Eh (mV)** | **DO** | **T(C)** | **O-18** | **D** |
| | | **g/kg** | **Eq/kg** | | | | | | **mEq/kg** | | | | | | **(% sat)** | | **per mil** | |
| **Salt1(a)** | Apr-98 | 195.1 | 2.752 | 0.025 | 0.012 | 0.545 | 2.439 | 0.341 | 0.78 | 0 | 2.09 | | | | | | 2.90 | 9.31 |
| | Sep-00 | 210.3 | 2.947 | 0.015 | 0.011 | 0.599 | 2.787 | 0.391 | 0.12 | 0 | 1.73 | | 4.8 | -3 | 16.3 | 18.1 | 2.94 | 10.03 |
| | Apr-01 | 199.5 | 2.701 | 0.017 | 0.010 | 0.551 | 2.698 | 0.364 | 0.18 | 0 | 1.91 | 0.07 | 5.2 | 193 | 52 | 16.4 | 3.05 | 9.45 |
| | Jul-01 | 202.8 | 2.863 | 0.014 | 0.010 | 0.545 | 2.638 | 0.353 | 0.18 | 0 | 1.91 | | 5.7 | 35.9 | 78 | 12.6 | 3.09 | |
| **Salt1(b)** | Apr-98 | 189.0 | 2.649 | 0.019 | 0.011 | 0.545 | 2.344 | 0.322 | 0.73 | 0 | 0.98 | | | | | | 2.60 | 6.05 |
| | Sep-00 | 237.2 | 3.438 | 0.012 | 0.014 | 0.659 | 3.357 | 0.427 | 0.10 | 0 | 2.00 | | 4.8 | -35 | 27.5 | 19.6 | 2.20 | 5.78 |
| | Apr-01 | 236.5 | 3.454 | 0.009 | 0.015 | 0.833 | 3.145 | 0.455 | 0.17 | 0 | 2.82 | | 5.22 | 142 | 27.7 | 14.8 | 1.34 | 0.87 |
| | Jul-01 | 237.9 | 3.489 | 0.009 | 0.014 | 0.767 | 3.269 | 0.423 | 0.18 | 0 | 2.82 | | 5.69 | 52 | 38.7 | 11.9 | -1.00 | -6.25 |
| **Ponded Water** | Sep-00 | 227.8 | 3.395 | 0.017 | 0.012 | 0.389 | 3.357 | 0.268 | 0.18 | 0 | 1.28 | | 4.26 | -13 | 25.4 | 18.2 | 4.01 | 15.65 |
| | Apr-01 | 123.4 | 1.764 | 0.014 | 0.001 | 0.003 | 1.685 | 0.020 | 0.08 | 0 | | | 4.62 | 184 | 35 | 12.7 | | |
| | Apr-01 | 242.2 | 3.703 | 0.021 | 0.007 | 0.318 | 3.874 | 0.182 | 0.17 | 0 | 1.18 | | | | | | -2.63 | -17.56 |
| | Jul-01 | 237.0 | 3.744 | 0.017 | 0.007 | 0.222 | 3.576 | 0.180 | 0.23 | 0 | 1.18 | | 4.96 | 173 | 30.4 | 10.6 | -1.51 | -10.81 |

| SPECTACLE LAKE | | | | | | | | | | | | | | | | | delta | |
|---|---|---|---|---|---|---|---|---|---|---|---|---|---|---|---|---|---|---|
| **Site** | **Date** | **TDS** | **Cl** | **Ca** | **K** | **Mg** | **Na** | **$SO_4$** | **Sr** | **Fe** | **Br** | **$HCO_3$** | **pH** | **Eh** | **DO** | **T(C)** | **O-18** | **D** |
| | | **g/kg** | **Eq/kg** | | | | | | **mEq/kg** | | | | | **(mV)** | **(% sat)** | | **per mil** | |
| **SM1** | Sep-00 | 99.5 | 1.503 | 0.030 | 0.013 | 0.310 | 1.366 | 0.202 | 0.37 | 0.00 | 1.57 | 1.43 | 6.8 | -15 | 13.9 | 19.4 | -2.46 | -21.34 |
| | Apr-01 | 98.0 | 1.435 | 0.027 | 0.013 | 0.303 | 1.439 | 0.187 | 0.37 | 0.00 | 1.80 | 1.71 | 6.61 | -11 | 25.4 | 20.7 | -2.52 | -21.38 |
| | Jul-01 | 98.2 | 1.452 | 0.027 | 0.013 | 0.296 | 1.427 | 0.187 | 0.35 | 0.00 | 1.80 | 1.66 | 6.4 | -15 | 25.6 | 17.2 | -2.41 | -21.45 |
| **SM2** | Sep-00 | 222.2 | 3.306 | 0.012 | 0.030 | 0.824 | 3.048 | 0.481 | 0.09 | 0.00 | 4.63 | 0.31 | 6.13 | -151 | 13.3 | 23.2 | 2.03 | -1.42 |
| | Apr-01 | 226.6 | 3.330 | 0.012 | 0.025 | 0.762 | 3.214 | 0.494 | 0.14 | 0.00 | 4.60 | 0.44 | 6.17 | 60 | 22.4 | 19.7 | 1.20 | -2.94 |
| | Jul-01 | 219.1 | 3.213 | 0.012 | 0.022 | 0.700 | 3.215 | 0.444 | 0.12 | 0.00 | 4.26 | 0.28 | 5.85 | 126 | 23.3 | 15.7 | 1.10 | -5.09 |
| **SM3** | Sep-00 | 97.9 | 1.438 | 0.028 | 0.017 | 0.384 | 1.290 | 0.230 | 0.35 | 0.00 | 2.14 | 1.49 | 7.01 | -3 | 14 | 21.3 | -3.22 | -21.31 |
| | Apr-01 | 85.2 | 1.232 | 0.030 | 0.012 | 0.270 | 1.206 | 0.190 | 0.37 | 0.00 | 1.60 | 1.49 | 6.96 | -68 | 24 | 19.1 | -3.00 | -25.57 |
| | Jul-01 | 82.9 | 1.225 | 0.028 | 0.012 | 0.233 | 1.181 | 0.171 | 0.35 | 0.00 | 1.37 | 1.44 | 6.67 | -31 | 25.1 | 16 | -2.55 | -23.36 |
| **SM4** | Sep-00 | 97.2 | 1.488 | 0.020 | 0.021 | 0.326 | 1.331 | 0.174 | 0.33 | 0.00 | 1.91 | 0.88 | 6.32 | -76 | 14.1 | 24 | -2.19 | -17.63 |
| | Apr-01 | 99.0 | 1.469 | 0.017 | 0.023 | 0.333 | 1.422 | 0.181 | 0.35 | 0.00 | 2.14 | 0.92 | 6.15 | 42 | 35.9 | 20.1 | -1.55 | -16.22 |
| | Jul-01 | 92.6 | 1.409 | 0.017 | 0.021 | 0.290 | 1.322 | 0.153 | 0.31 | 0.00 | 2.04 | 0.85 | 6.06 | 58 | 34.4 | 15.5 | -1.91 | -18.95 |
| **SM5** | Jun-99 | 107.0 | 1.611 | 0.024 | 0.026 | 0.398 | 1.436 | 0.215 | 0.77 | 0.00 | 0.92 | 1.04 | | -16 | | 16.3 | -1.72 | -16.41 |
| | Sep-99 | 105.0 | 1.638 | 0.021 | 0.029 | 0.374 | 1.377 | 0.187 | 0.75 | 0.00 | 2.59 | 0.00 | | | | | -3.51 | -25.71 |
| | Sep-00 | 103.9 | 1.551 | 0.020 | 0.023 | 0.389 | 1.398 | 0.217 | 0.37 | 703.34 | 2.12 | 1.20 | 6.31 | -140 | 12.9 | 22.8 | -1.84 | -16.36 |
| | Apr-01 | 106.2 | 1.552 | 0.019 | 0.024 | 0.388 | 1.483 | 0.222 | 0.35 | 414.48 | 2.34 | 1.05 | 6.18 | 14 | 33.2 | 20 | -1.68 | -18.20 |
| | Jul-01 | 103.1 | 1.558 | 0.018 | 0.023 | 0.360 | 1.407 | 0.199 | 0.31 | 480.13 | 2.35 | 1.02 | 6.1 | 28 | 35.9 | 15 | 4.70 | -11.03 |
| **SM6** | Jun-99 | 87.3 | 1.296 | 0.025 | 0.018 | 0.439 | 1.064 | 0.208 | 0.00 | 276.85 | 3.13 | 0.91 | | -7 | | 17.7 | -2.57 | -21.63 |
| | Sep-99 | 115.6 | 1.825 | 0.021 | 0.020 | 0.380 | 1.556 | 0.189 | 0.80 | 378.76 | 2.42 | 0.00 | | | | | -1.80 | -24.16 |
| | Sep-00 | 76.4 | 1.159 | 0.021 | 0.011 | 0.250 | 1.042 | 0.150 | 0.42 | 2441.49 | 1.38 | 0.92 | 6.27 | -23 | 20.5 | 23 | -3.15 | -23.82 |
| | Apr-01 | 72.0 | 1.076 | 0.019 | 0.011 | 0.221 | 1.035 | 0.131 | 0.36 | 1989.36 | 1.39 | 0.74 | 6.07 | 4 | 35.5 | 20.4 | -2.90 | -26.48 |
| | Jul-01 | 71.9 | 1.089 | 0.019 | 0.010 | 0.213 | 1.031 | 0.123 | 0.34 | 2321.47 | 1.39 | 0.86 | 6.06 | 8 | 35 | 15.1 | -3.30 | -23.95 |
| **Pond 1** | Sep-00 | 186.5 | 2.816 | 0.025 | 0.027 | 0.645 | 2.600 | 0.358 | 0.29 | 1880.25 | 3.23 | 0.00 | 2.68 | -17 | 30 | 26.3 | 1.67 | 5.70 |
| | Jul-01 | 220.3 | 3.376 | 0.025 | 0.029 | 0.757 | 3.077 | 0.386 | 0.34 | 0.00 | 4.55 | 0.00 | 2.5 | 393 | 41 | 14.7 | | |
| **Pond 2** | Sep-00 | 204.4 | 3.153 | 0.018 | 0.026 | 0.650 | 2.887 | 0.345 | 0.18 | 1810.87 | 3.36 | 0.00 | 2.76 | -45 | 23.9 | | 3.55 | -20.33 |
| | Apr-01 | 247.1 | 3.720 | 0.010 | 0.036 | 0.956 | 3.406 | 0.481 | 0.39 | 4002.57 | 5.22 | 0.00 | 2.69 | 374 | 33 | 16.2 | | |
| | Jul-01 | 243.8 | 3.843 | 0.015 | 0.021 | 0.532 | 3.820 | 0.246 | 0.27 | 1346.39 | 3.58 | 0.00 | 2.62 | 395 | 38.3 | 14.1 | 1.39 | -14.44 |
| **Pond 3** | Sep-00 | 243.7 | 3.763 | 0.014 | 0.033 | 0.741 | 3.490 | 0.398 | 0.14 | 1718.78 | 4.13 | 0.00 | 2.64 | -9 | 25 | 23.5 | 1.72 | 6.36 |
| | Apr-01 | 252.7 | 3.550 | 0.006 | 0.066 | 1.586 | 2.953 | 0.750 | 0.40 | 5531.38 | 9.30 | 0.00 | 2.58 | 381 | 27.1 | 18.4 | 3.13 | 10.60 |
| | Jul-01 | 243.8 | 3.596 | 0.007 | 0.054 | 1.442 | 2.850 | 0.627 | 0.34 | 4271.64 | 9.14 | 0.00 | 2.34 | 375 | 27.1 | 13.5 | -2.12 | -7.97 |

# Appendix I

## Geological Logs of the Blanchetown Clay and Parilla Sand from Bores in the Vicinity of Raak Plain

## Geological Logs of the Parilla Sand from Bores in the Vicinity of Raak Plain (after Department of Natural Resources and Environment (NRE), Victoria)

| Bore ID: 50078 Date: ? | | |
|---|---|---|
| From (m) | To (m) | Description |
| 0 | 2 | Brown sand |
| 2 | 5 | Brown clay **(Blanchetown Clay)** |
| 5 | 30 | Grey clay |
| 30 | 33 | Grey sand **(Parilla Sand)** |
| 33 | 34 | Grey clay |
| 34 | 39 | Red sand |
| 39 | 42 | Brown sand |
| 42 | 62 | Grey sand |
| 62 | 66 | Clay and sand |

| Bore ID: 26241 Date: 30 / 9 1972 | | |
|---|---|---|
| From (m) | To (m) | Description |
| 0 | 0.5 | Brown fine sandy loam, dry |
| 0.5 | 1 | L brown-l yellow white silty clay, some med sand **(Blanchetown Clay)** |
| 1 | 2.5 | L brown-l grey silty clay, dry |
| 2.5 | 3 | Pale yellow-yellow brown silty clay, damp |
| 3 | 4 | Pale yellow brown silty clay, damp |
| 4 | 4.5 | L yellow grey silty clay damp |
| 4.5 | 5 | L grey-l red silty clay, damp |
| 5 | 5.5 | L grey-l red/orange silty clay, damp |
| 5.5 | 6 | Pale yellow grey silt, damp |
| 6 | 9 | White silt, damp |
| 9 | 10 | White/red silt, damp |
| 10 | 12 | Pale yellow grey silt, wet |
| 12 | 13 | L grey/yellow silty clay, wet |
| 13 | 17 | Grey silty clay wet |
| 17 | 19 | Brown silty clay, wet |
| 19 | 22 | L grey/brown silty clay, wet |
| 22 | 23 | L brown-l grey silty clay, wet |
| 23 | 27 | Brown-l grey silty clay, wet |
| 27 | 28 | Grey/brown medium sandy clay, wet |
| 28 | 30 | Grey brown/pale grey/purple silty clay |
| 30 | 32 | Yellow brown med sand, wet **(Parilla Sand)** |

| Bore ID: 26285 Date: 30 / 9 / 1973 | | |
|---|---|---|
| From (m) | To (m) | Description |
| 0 | 0.5 | Orange to orange brown fine sandy loam, dry. |
| 0.5 | 1.5 | Brown, some white inclusions fine sandy loam, some limestone, dry. |
| 1.5 | 2 | Brown, white, orange, yellow motley fine sandy silty clay, damp **(Blanchetown Clay)** |
| 2 | 2.5 | Grey, white, yellow and orange inclusions, silty clay, damp. |
| 2.5 | 4 | Grey, white small yellow inclusions, silty clay, damp. |
| 4 | 5 | Brown/grey silty clay, moist. |
| 5 | 5.5 | Grey brown small yellow and red inclusions, silty clay (some small hard clay nodules) |
| 5.5 | 6 | Brown grey, red, yellow motley silty clay (some small hard clay nodules). |
| 6 | 7 | Red, yellow, grey, white motley silty clay, moist to wet. |
| 7 | 8 | Grey brown with reddish tint silty clay, moist to wet. |
| 8 | 9 | Grey silty clay, moist to wet. |
| 9 | 10 | Grey yellow motley silty clay, moist to wet. |
| 10 | 11 | Yellow silty clay, saturated. |
| 11 | 13 | Dark yellow silty clay, wet. |
| 13 | 14 | Dark yellow with grey inclusions silty clay, wet. |
| 14 | 15 | Grey green silty fine sand, wet. |
| 15 | 18 | Dark grey green fsandy silty clay, moist. |
| 18 | 20 | Dark green some grey inclusions fine to coarse sand, saturated. |
| 20 | 22 | Grey black dark green motley fine to coarse sand, wet. |
| 22 | 23 | Brown with grey inclusions silty fine sand, moist to wet. |
| 23 | 25 | Dark brown fine sandy silty clay, moist. |
| 25 | 26 | Dark brown silty clay, moist. |
| 26 | 27 | Dark brown small dark grey inclusions silty clay, moist. |
| 27 | 28 | Dark grey green some brown silty clay, moist. |
| 28 | 29 | Dark grey and brown motley silty clay, moist. |
| 29 | 33 | Dark brown some grey inclusions, silty clay, moist. |
| 33 | 36 | Dark grey brown silty clay, moist. |
| 36 | 40 | Grey black silty clay, moist. |
| 40 | 44 | Dark green grey fine to med. silty sand, moist to wet **(Parilla Sand)** |
| 44 | 46 | Dirty green medium to coarse sand, saturated. |
| 46 | 48 | Yellow to bark orange brown med. To coarse sand, saturated. |

# Appendix J

## In-Situ Cosmogenic Production of $^{36}$Cl: Theory and Calculations for Raak Plain

## In-Situ Production of $^{36}$Cl

For the interpretation of $^{36}$Cl data in such a high Cl$^-$ environment as Raak Plain, the in-situ production of $^{36}$Cl according to the reaction $^{35}\mathrm{Cl}(n,\gamma)^{36}\mathrm{Cl}$ must be considered because of the large activation cross-section of $^{35}$Cl (44 x 10$^{-28}$ m$^2$) (Lal, 1988; Andrews and Fontes, 1992). $^{36}$Cl is produced from the more common $^{35}$Cl atoms by the capture of fast and thermal neutrons, which originate respectively from cosmic rays that penetrate the Earth's surface or from the decay of U and Th in the aquifer matrix. The latter was found to be important in groundwaters in a granite aquifer at Stripa, Sweden (Fontes et al., 1984; Andrews et al., 1986). At Raak Plain, Cl$^-$ is concentrated in groundwater at or near the surfaces of the playas, meaning that the absorption of cosmic neutrons by $^{35}$Cl may also be an important production mechanism.

The number of $^{36}$Cl atoms, $^{36}$N (atomsg$^{-1}$ soil), produced after time, T (sec), by irradiation with a constant neutron flux, $\phi$ (neutronsg$^{-1}$sec$^{-1}$) is (Bentley et al., 1986a):

$$^{36}N = \sigma_{35Cl}\ ^{35}N\ \phi\ (1-e^{-\lambda T})\ /\ \lambda\ \sigma_m \qquad \text{(J1)}$$

where $^{35}$N is the number of $^{35}$Cl atoms present (atoms g$^{-1}$ saturated porous media), $\sigma_{35Cl}$ is the neutron capture cross-section of $^{35}$Cl (44 barns), $\lambda$ is the disintegration constant for $^{36}$Cl (7.3 x 10$^{-14}$ sec$^{-1}$) and $\sigma_m$ is the macroscopic neutron absorption cross-section of the rock (mole barns g$^{-1}$). The flux of neutrons ($\phi$) decreases exponentially with depth below the Earth's surface, and can be calculated for depth, X (g cm$^{-2}$) using the following equation (Bird et al., 1991):

$$\phi = \phi_0 e^{-X/\beta} \qquad (J2)$$

where $\phi_0$ is the flux of neutrons at the surface and $\beta$ is the attenuation coefficient ($gcm^{-2}$).

By substituting equation J2 into equation J1, we obtain the equation for the number of $^{36}Cl$ atoms produced by the absorption of cosmic neutrons onto $^{35}Cl$ at depth, X (Lal and Arnold, 1985; Bentley et al., 1986a; Andrews and Fontes, 1992):

$$^{36}N(X) = \sigma\ ^{35}N\ \phi_0\ e^{-X/\beta}\ (1-e^{-\lambda T}) / \lambda\ \sigma_m \qquad (J3)$$

For $\beta$, a value of 190 g $cm^{-2}$ (Nishiizumi et al., 1984) is applied, as recommended by Bird et al. (1991). $^{35}N$ is calculated from brine chemistry data using the following equation (Bentley et al., 1986b):

$$^{35}N = 0.7577\ n\ [Cl^-]\ A / \rho_B \qquad (J4)$$

where n is the porosity of the aquifer material, $[Cl^-]$ is the $Cl^-$ concentration of the groundwater / brine (moles $cm^{-3}$), A is Avogadro's constant (6.022 x $10^{23}$ atoms / mole), $\rho_B$ is the bulk density of the sample (g $cm^{-3}$) and 0.7577 is the isotopic abundance of $^{35}Cl$.

Finally, $\phi_0$ is latitude and altitude dependent and must be estimated for Raak Plain. The sea-level surface capture rate for thermal neutrons from cosmic ray interactions was estimated by Lal and Peters (1967) to be 3 x $10^{-2}$ atoms $kg^{-1}$ $sec^{-1}$. An estimate for the surface capture rate, defined by $C = \sigma\ \phi_0 / \sigma_m$ can be obtained from the knowledge that playa surface halite deposits across eastern Australia have a fairly uniform $^{36}Cl/Cl$ ratio of 50 x $10^{-15}$ (Richard Cresswell, Bureau of Rural Sciences, pers. comm., 2002). Assuming a $^{36}$Cl/Cl ratio of 50 x $10^{-15}$ for a surface halite deposit (X = 0 m below ground surface, T = 1.5 Ma (time to reach isotopic equilibrium), [Cl$^{-}$] of 0.017 moles / g (1.0237 x $10^{22}$ atoms / g)), a value of 2.899 x $10^{-3}$ neutrons mole$^{-1}$ sec$^{-1}$ can be estimated for C. This value has been used in place of $\sigma\ \phi_0 / \sigma_m$ in equation J3 for estimation of the contribution of in-situ cosmogenic production of $^{36}$Cl to the observed $^{36}$Cl/Cl ratios (Table J1).

The additional assumptions made in these estimations of in-situ cosmogenic produced $^{36}$Cl are:

1) $^{35}$Cl is the dominant target element for cosmogenic in-situ production. It is assumed that production by the $^{39}$K(n,$\alpha$)$^{36}$Cl and $^{40}$Ca(n,p$\alpha$)$^{36}$Cl reactions is minor compared to that from the $^{35}$Cl(n,$\gamma$)$^{36}$Cl reaction.

2) $\sigma\ \phi_0 / \sigma_m$ is constant with depth, i.e. the value of this parameter is the same for a surface halite deposit as for groundwater in the Blanchetown Clay and Parilla Sand. In reality, this is not likely to be the case, as the macroscopic thermal neutron absorption cross-sections are likely to vary for these three units due to differences in abundance of other elements that can absorb neutrons.

As a first estimate, the above calculations provide an indication of whether in-situ production by cosmic neutron activation of $^{35}$Cl in the near-surface brines is important in the interpretation of the observed $^{36}$Cl/Cl ratios. The results of these calculations (Table J1) show that, for exposure times of 7 k yrs or less, in-situ cosmogenic production is negligible, even in surface halite crusts. However, for halite or halite-saturated brines at the playa surface, the process becomes significant at exposure times around 30 k yrs (contribution to $^{36}$Cl/Cl ~ 3 x $10^{-15}$). For exposure times around 1.5 Ma (3 half-lives of $^{36}$Cl), equilibrium is reached between decay and in-situ production of $^{36}$Cl (Andrews and Fontes, 1992). In this case, cosmogenic production in halite or halite-saturated brines at the playa surface can result in $^{36}$Cl/Cl of approximately 50 x $10^{-15}$ (assumption made from observed $^{36}$Cl/Cl of surface halite samples assumed to be in equilibrium with cosmogenic production (see above)). However, this is really only significant at depths < ~ 3 m, where an equilibrium $^{36}$Cl/Cl ratio up to 10 x $10^{-15}$ can result, depending on the [$Cl^-$] of the brine (Table J1). Based on the above calculations, and because brine residence times have been estimated to be < 20 k yrs (Section 4.3.2.1), it is unlikely that cosmogenic production of $^{36}$Cl in the brines near the surface of the playas is significant.

Below the depths of cosmogenic production, the irradiation of light nucleii by $\alpha$ particles emitted by natural radioelements in the aquifer matrix can also be an important production mechanism (Lal, 1988; Andrews and Fontes, 1992). In this case, typical secular equilibrium $^{36}$Cl/Cl ratios for sandstones and shales have been estimated at 4.7 x $10^{-15}$ and 12.5 x $10^{-15}$ respectively (Bentley et al., 1986a). The aquifer compositions, in terms of radioactive elements and their potential for in-situ production of $^{36}$Cl have not been assessed for Raak Plain, so the above values must be used as a guide.

TableJ1. Calculations of in-situ cosmogenic $^{36}$Cl production by neutron absorption on $^{35}$Cl (T = 7 ka, 30 ka and 1.5 Ma) for brine / groundwater with measured $^{36}$Cl/Cl values, as well as for a theoretical surface halite sample and a near-surface brine.

| Sample # | Depth (m below surface) | Depth (g cm$^{-2}$) | Assumed porosity | Solution density (g cm$^{-3}$) | Bulk density (g cm$^{-3}$) | [Cl-] (molesL$^{-1}$) | [Cl-] (x10$^{-20}$ atoms g$^{-1}$ soil) | [$^{35}$Cl] (x10$^{4}$ moles g$^{-1}$ soil) | Measured $^{36}$Cl/Cl x10$^{15}$ | $^{36}$Cl/Cl x10$^{15}$ T= 7 ka | $^{36}$Cl/Cl x10$^{15}$ T= 30 ka | $^{36}$Cl/Cl x10$^{15}$ T= 1.5 Ma |
|---|---|---|---|---|---|---|---|---|---|---|---|---|
| 26240 | 50.5 | 10950 | 0.3 | 1.043 | 2.168 | 0.68 | 0.566 | 0.713 | 30.5 | neg. | neg. | neg. |
| 98347 | 52 | 11290 | 0.3 | 1.054 | 2.171 | 0.80 | 0.669 | 0.842 | 13 | neg. | neg. | neg. |
| West1a | 2.82 | 508 | 0.6 | 1.237 | 1.802 | 3.67 | 7.357 | 9.257 | 33.3 | **0.05** | **0.23** | **3.4** |
| West3 | 3.55 | 628 | 0.6 | 1.182 | 1.769 | 2.71 | 5.535 | 6.965 | 29.1 | **0.03** | **0.12** | **1.8** |
| West4 | 11.5 | 1980 | 0.6 | 1.096 | 1.717 | 1.41 | 2.967 | 3.733 | 33.5 | neg. | neg. | neg. |
| SM1 | 17.1 | 2960 | 0.6 | 1.114 | 1.729 | 1.67 | 3.491 | 4.392 | 40.9 | neg. | neg. | neg. |
| SM2 | 1.7 | 313 | 0.6 | 1.299 | 1.839 | 4.29 | 8.428 | 10.605 | 37.9 | **0.15** | **0.64** | **9.6** |
| SM3 | 7.6 | 1310 | 0.6 | 1.113 | 1.728 | 1.6 | 3.346 | 4.210 | 36.5 | neg. | neg. | neg. |
| SM4 | 6.5 | 1120 | 0.6 | 1.111 | 1.727 | 1.65 | 3.453 | 4.345 | 35.9 | neg. | neg. | neg. |
| SM6 | 18.4 | 3150 | 0.6 | 1.085 | 1.711 | 1.26 | 2.660 | 3.347 | 26.6 | neg. | neg. | neg. |
| Surf. halite | 0 | 0 | | | | | 102.4 | 128.81 | - | **0.80** | **3.33** | **50.0** |
| West1(2-4cm) | 0.03 | 4.2 | 0.4 | 1.320 | 2.118 | 5.01 | 5.693 | 7.163 | - | **0.80** | **3.26** | **48.9** |